JULY 1982
ENVIRONMENTAL SCIENCE & TECHNOLOGY

ES&T

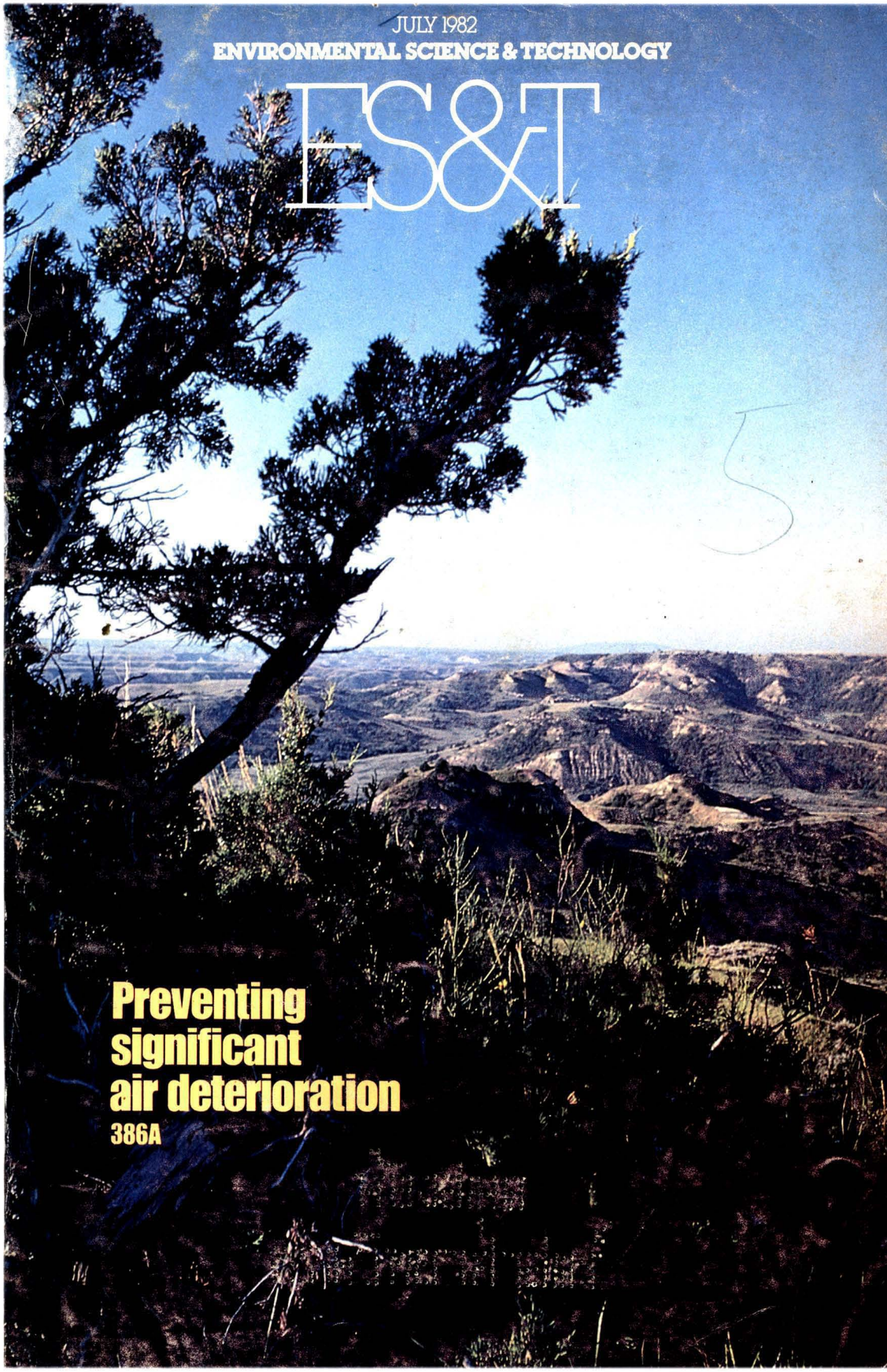

Preventing significant air deterioration

386A

ES&T
CONTENTS
Volume 16, Number 7, July 1982

373A

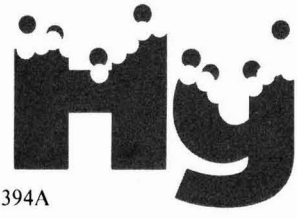

394A

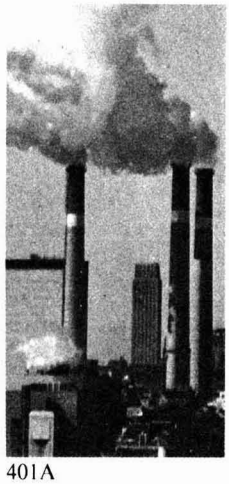

401A

OUTLOOK

REGULATORY FOCUS

FEATURES

CRITICAL REVIEW

RESEARCH

Environmental Science & Technology

"Environmental Science & Technology ES&T (ISSN 0013-936X) is published monthly by the American Chemical Society at 1155 16th Street, N.W., Washington, D.C. 20036. Second-class postage paid at Washington, D.C. and at additional mailing offices. POSTMASTER: Send address changes to Membership & Subscription Services, PO Box 3337, Columbus, OH, 43210."

SUBSCRIPTION PRICES 1982: Members, $19 per year; nonmembers (for personal use), $23 per year; institutions, $94 per year. Foreign postage, $8 additional per year/Air freight add $30; multiple year rates available on request. Single issues $8.00 for current year; $9.00 for prior years. Back volumes $96. Rates above do not apply to nonmember subscribers in Japan, who must enter subscription orders with Maruzen Company Ltd., 3-10 Nihon bashi 2-chome, Chuo-ku, Tokyo 103, Japan. Tel: (03) 272-7211.

SUBSCRIPTION SERVICE: Orders for new subscriptions, single issues, back volumes, and microfiche and microform editions should be sent with payment to Office of the Treasurer, Financial Operations, ACS, 1155 16th St., N.W., Washington, D.C. 20036. Phone orders may be placed, using Visa or Master Card, by calling toll free (800) 424-6747 from anywhere in the continental U.S. Changes of address, subscription renewals, claims for missing issues, and inquiries concerning records and accounts should be directed to Manager, Membership and Subscription Services, ACS, P.O. Box 3337, Columbus, Ohio 43210. Changes of address should allow six weeks and be accompanied by old and new addresses and a recent mailing label. Claims for missing issues will not be allowed if loss was due to insufficient notice of change of address, if claim is dated more than 90 days after the issue date for North American subscribers or more than one year for foreign subscribers, or if the reason given is "missing from files."

Credits: 373A Washington Public Power Supply System; 380A, 381A *ES&T's* Julian Josephson

Cover: Dean Hanson, North Dakota Tourism, Promotion Division

ESTHAG 16(7) 361A-424A
377-442 (1982)
ISSN 0013-936X

NOTES

CORRESPONDENCE

* To whom correspondence should be addressed.

■ This article contains supplementary material in microform. See ordering instructions at end of paper.

DEPARTMENTS

Published by the
AMERICAN CHEMICAL SOCIETY
1155 16th Street, N.W.
Washington, D.C. 20036
(202) 872-4600

BOOKS AND JOURNALS DIVISION
Director: D. H. Michael Bowen

Head, Journals Department: Charles R. Bertsch
Head, Production Department: Elmer M. Pusey
Head, Research and Development Department: Seldon W. Terrant
Head, Marketing and Sales Department: Claud K. Robinson
Manager, Circulation Development: Cynthia Smith
Associate, Circulation Development: Mary-Ellen Kirkbride
ADVERTISING MANAGEMENT
Centcom, Ltd.
For officers and advertisers, see page 424 A.
Please send *research* manuscripts to Manuscript Reviewing, *feature* manuscripts to Managing Editor. For author's guide and editorial policy, see the January 1982 issue, page 78A, or write Katherine I. Biggs, Manuscript Reviewing Office, *ES&T*. A sample copyright transfer form, which may be copied, appears on the inside back cover of the January 1982 issue.

Environmental concerns? We can help you comply— from planning to filing.

Whether you have one or many environmental concerns, we can help you. We're the Rockwell International Environmental Monitoring & Services Center (EMSC), a team of professionals addressing the full spectrum of environmental requirements. We have offices coast to coast, and are familiar with the national and regional issues that often influence your environmental programs.

During the many years the EMSC has been in business, we've built a reputation for service backed by expertise. Experience is our most important asset — and your assurance of thoroughness when we assist you in the planning, analysis, or implementation of your program. Since we understand not only the environmental, but the fiscal constraints of a project as well, we can act as an effective arm of your organization.

Whether yours is a current or future problem, whether you have a requirement for planning a new facility or for a generalized study, we can help. We are prepared to stand by you with proof that the requirements of cognizant agencies are met.

For full information on how we can service your needs, contact Marketing Department, Environmental Monitoring & Services Center, Environmental & Energy Systems Division, Rockwell International, 2421 West Hillcrest Drive, Newbury Park, CA 91320. Phone: (805) 498-6771.

Rockwell International

...where science gets down to business

CIRCLE 11 ON READER SERVICE CARD

ES&T
GUEST EDITORIAL

The Regulatory Reform Act of 1982

Congress will soon take action on the Regulatory Reform Act, S.1080. The bill provides an arguably needed requirement that regulatory agencies assess the costs and benefits of major regulations. However, this compromise bill and, in particular, its amendments raise issues that should provide serious concern regarding a potentially dangerous tendency to hand over unnecessarily extensive control to the executive branch without appropriate legislative or judicial checks. The legislation also exacerbates the already existing imbalance of access to government and the courts, disfavoring environmental and public interest groups. In addition, the bill opens the door for abuse of discretion by regulatory agencies and the executive branch, while deceptively appearing to offer more legislative guidance and control.

Once a rule is designated as major, a regulatory impact analysis is required, and the executive branch is given oversight responsibility to ensure compliance with the requirement to do analysis. In some cases the executive branch can hold up a rule indefinitely, and its activities are not reviewable in the courts under this legislation.

The proposed legislation places severe burdens upon the regulatory agencies to justify their regulations, and at the same time makes it difficult for the consumer, worker, and citizen to participate in governmental decision making. The legislation requires that courts reject agency rules not backed up by substantial support in the rule-making record. At the same time, there is no requirement that an opportunity for cross-examination of witnesses offering evidence be provided.

An agency hesistant in promulgating protective regulations can easily ensure that the record is weak by exercising its discretion to limit meaningful debate in the hearings on a rule. This legislation requires more facts and offers less opportunity to ensure that the record is balanced. Venue legislation seeking to disperse the locus of judicial challenges beyond the D.C. Circuit Court of Appeals to the other circuit courts further exacerbate the imbalance of opportunities for participation in governmental decision making that exists between industry on the one hand, and consumers, workers, and citizens on the other, because the latter groups do not have the resources to mount decentralized challenges.

One major uncertainty created by the legislation is the congressional veto, which can nullify regulatory actions taken by the agencies. This will invite intense industry lobbying and leave the future direction of health, safety, and environmental protection to the political arena. Power, and not better decision making, will determine the outcome of governmental protection measures.

One may have sympathy for requiring the agencies to give more thoughtful consideration to the costs and benefits of their regulations. However, it is very likely that the agencies will come to a full stop because there is a provision in the bill that permits the use of outside consultants to do little more than gather data in a time when the agency budgets have been cut drastically, and the agencies themselves have been emptied of the technical manpower to do the necessarily sophisticated analyses required. The laudable improvements in agency decision making contained in this legislation may still be retained without crippling the regulatory system. However, executive oversight must be limited and checked, the use of outside expertise must be allowed, burdens of proof that will be impossible to meet must not be placed on the agencies, and public participation must be encouraged.

Nicholas A. Ashford

Nicholas A. Ashford *is associate professor of technology and policy and assistant director of the Center for Policy Alternatives at the Massachusetts Institute of Technology. He is a public member and former chairman of the National Advisory Committee on Occupational Safety and Health, and serves on the EPA Science Advisory Board.*

0013-936X/82/0916-0365A$01.25/0

ES&T LETTERS

History of acid rain

Dear Sir: Comments were requested regarding the article "Acid precipitation in historical perspective" by Ellis B. Cowling, (*ES&T*, Vol. 16, No. 2, 1982, p. 110A). The feature article was timely, well written, and informative. The extensive compilation of references and the tabular presentation of important research certainly provides a basis for understanding the nature of the present problem. Thus the article is a valuable reference that will permit interested researchers or administrators to examine research data and methodology in greater depth if they desire. Such articles represent real accomplishments of the objectives of environmental education of the scientific community and interested public.

Robert L. Jolley
Advanced Technology Section
Chemical Technology Division
Oak Ridge National Laboratory
Oak Ridge, Tenn. 37830

Fermentation technology

Dear Sir: Scientists, engineers, technology managers, and corporate research and development executives from U.S. and European pharmaceutical, food, chemical processing, and biotechnology companies will have an opportunity to get a first-hand look at state-of-the-art fermentation technology in Japan during a 16-day June study mission organized by Technology Transfer Institute with assistance from the Division of Microbial and Biochemical Technology at the American Chemical Society.

Dr. Elmer Gaden, the Wills Johnson Professor of Chemical Engineering at the University of Virginia, will lead the mission. Dr. Gaden, active in fermentation technology since 1947, has served as editor of *Biotechnology and Bioengineering* since its establishment in 1959, and is credited with playing a major role in the development of "biochemical engineering" in the U.S.

Mission members will examine large-scale manufacturing of commercial chemicals, intermediates, enzyme and amino acids; recovery and purification fermentation technology; solid substrate fermentation and other novel fermentation techniques; as well

as taking an in-depth look at fermentation plant management, quality control, and automatically controlled systems.

Technology Transfer Institute is a Japanese management consulting firm with offices in New York, Los Angeles, London, Düsseldorf, and Singapore. Founded in Tokyo in 1969, TTI promotes the international exchanges of information and ideas among scientists, engineers, and businessmen and has conducted more than 800 forums, seminars, and study missions during the past 13 years.

For a brochure about the upcoming study mission, contact: Nancy A. Dyer, Project Manager, Technology Transfer Institute, One Penn. Plaza, Suite 1411, New York, N.Y. 10119; (212) 947-2648.

Biological diversity

Dear Sir: I am pleased to comment on the question of "Why maintain biological diversity?" and on why the question needs to be asked at all (*ES&T*, Vol. 16, No. 2, 1982, p. 94A). I agree with the positions taken by my friends and colleagues Ehrlich, Hubbs, Iltis, and Turner as to why diversity is significant for the survival of our species. However, I would go back one step and examine why this is a problem. The answer is simple. There are too many of us and we have evolved the technological capacity to alter the biospheric system of which we are a part but without, as a species, understanding the consequences.

It is useful to categorize the reasons why we are, or should be, concerned about the preservation of biological diversity on our planet. I see three main categories of reasons, each of which will appeal to different people to a lesser or greater degree.

- There are ethical and moral reasons. We, as the one species among the earth's millions that has evolved a culture, a science, and a technology, should accept the role of protector of biospheric diversity. Earth's biosphere has been evolving through hundreds of millions of years. Knowing this, it takes a callous, arrogant, egotistical human being to show no concern about terminating a component species that has evolved through millions of years. This ethical consideration appeals to those at least minimally knowledgeable about biospheric science, about biospheric history and function; unfortunately, most of us woefully lack such knowledge.
- There are selfish reasons for maintaining biological diversity relative to a monotonous vs. a diversified environment. Ask any birdwatcher if he or she would be content with a bird world inhabited solely by robins. Assume that we could replace all of our native vegetation with wheat fields to feed our population. Could we find such a planet esthetically and spiritually tolerable? I think not.
- Categories 1 and 2 will not appeal to everyone. Category 3 should, as it involves the very survival of our species. Every living species is potentially significant in one way or another for the survival of our own. The biosphere is not static; it is a dynamic, evolving system. Maintenance of the genetic diversity existent in the system maximizes our options for solving critical problems as they arise. Examples are so numerous (as cited in the Josephson article) as to make this set of reasons undebatable.

What are the prospects? I find myself only slightly less pessimistic than Turner. If he is right, the future of our species and even of the biosphere is predictably uncertain. I find the statement of Jones that "we also have the problem of feeding a burgeoning world population," to be symptomatic of the limitations of the bureaucratic mind. The burgeoning human population is our planet's greatest threat. Control of population growth is the only answer, not destruction of the biosphere to expand its carrying capacity for a few more generations.

Is there hope? There is some hope if the educational process can be tailored to give each person some understanding of basic biospheric science. After more than a third of a century of dealing with college students, I am aware that most of them graduate as functional illiterates insofar as biospheric science is concerned. The situation is even worse with high school graduates. The curriculum should include a *mandatory* course, at the appropriate level in each, dealing with biospheric science and our place in the biosphere. I am convinced that this would improve the quality of policy decisions at all levels of government and of industry relative to our survival in a livable environment. It might make the difference between survival and nonsurvival.

W. Frank Blair
Professor of Zoology
The University of Texas at Austin
Austin, Tex. 78712-7818

(Editor's Note: W. Frank Blair was chairman of the U.S. National Committee for IBP, The International Biological Program, which ended in 1974.)

INTERNATIONAL

The second United Nations conference on the global environment, held in Nairobi, Kenya, in May, urged that an independent commission be created to devise policies for protecting the environment beyond the year 2000. For the first time, the conference declared matters of war and peace to be of environmental concern. There was also a new concern that international trade in hazardous materials could pose a serious threat to the environment. At this conference the developing nations expressed the opinion that economic development and environmental protection must go hand-in-hand, unlike the first conference, when they seemed to fear that measures to protect the environment would prevent development.

Aquaculture and hydroponics are uses for geothermal water or steam condensate at Cerro Prieto, Mexico, as part of a project being conducted for the Mexican Federal Electricity Commission by Geología y Minería, S. A. Water condensed from steam and kept at about 28 °C is used to raise crayfish about 18 cm long, approximately commercial size. They will be frozen through refrigeration provided by heat exchange from hot geothermal fluids. Cooled, salt-rich water nourishes hydroponically grown tomatoes and cucumbers in a greenhouse 30 m long, providing two harvests per year of 8 tons of tomatoes and 12 tons of cucumbers. Team leader Gabriel Delgado expects to see expanded aquaculture and hydroponics enterprises using the "unique conditions" of the region.

WASHINGTON

At least one out of every 25 preschool children has unacceptably high blood lead levels, according to a study by the National Center for Health Statistics. This is "at least 50% more" children than expected, said Vernon Houk, environmental health services director at the U.S. Center for Disease Control. Low-level lead exposure has been linked to learning disabilities and lowered IQ levels. The 0.5 g per gallon limit of lead in gasoline now in effect for large refiners has been eased by 10%, and EPA is considering easing it further or rescinding it. A bipartisan group of congressmen has asked EPA administrator Anne M. Gorsuch not to ease the existing regulations and said: "While no single source of lead is responsible for the population's total exposure to this toxic metal, lead from gasoline continues to be one of the most significant and easily controllable sources."

"The large reductions in the (EPA) FY '83 budget represent real reductions in environmental protection," according to a study prepared by Sen. Patrick Leahy's (D-Vt.) staff. They compared the EPA's fiscal 1983 budget request to the Office of Management and Budget with the agency's budget report sent to Congress and found 70 instances in which EPA told Congress the cuts represented efficiency, delegation of effort, or completion of programs and told OMB these same cuts reflected a "reduction in effort" or total elimination of programs. Sen. Leahy concluded that EPA administrator Anne M. Gorsuch had been less than candid about her aims.

Haig: would export hazardous goods

Exporting hazardous goods that have been banned or restricted in this country will be much easier under a new plan approved by two Reagan cabinet members, Secretary of State Alexander M. Haig, Jr., and Commerce Secretary Malcolm Baldridge. The new policy eliminates almost all rules that require manufacturers to notify or obtain consent from foreign governments before they export banned or restricted goods such as DDT and tightly regulated chlorofluorocarbons. Drugs and other medical products not approved in this country can also be exported under the new plan. Haig and Baldrige say the present restrictions are too costly and hurt U.S. firms in international trade. A cabinet level committee is now reviewing the new policy; but administration officials doubt the policy will be changed before being sent to the president, because it was formulated by two top cabinet officials.

The amount of carbon monoxide permitted in the air would be substantially increased under a new rule proposed by EPA. The number of days that the standard of 9 ppm could be exceeded would be raised from one to five. Agency officials said the new rule would make it easier for many states to meet the carbon monoxide standard. A number of environmentalists and public health groups as well as congressmen from both parties called the proposal a serious step backward. Rep. Ron Wyden (D-Ore.) termed the new change "an example of voodoo environmental protection," and Rep. Toby Moffett (D-Conn.) said in a press conference that the relaxation could result in levels of carbon monoxide that are 15% higher than what current standards allow. Public comments are not legally required before the rule becomes final, but disagreements between the air staff and the R&D staff at EPA over the proposed change may hold up action on it.

A Department of Energy (DOE) plan to install the generators at the Clinch River Breeder Reactor (CRBR) before testing a prototype is hazardous and financially risky, a General Accounting Office report states. The report warned: "Small breeder reactors in this country and demonstration breeder reactors in foreign countries have

0013-936X/82/0916-0369A$01.25/0

experienced steam generator failures. Steam generators for the CRBR have also experienced a number of problems during their development," and noted that the French demonstration breeder reactor was shut down recently because sodium leaks in a steam generator caused a fire. Rep. John D. Dingell (D-Mich.) concurred with the GAO report when he said. "It is outrageous that DOE is taking advice from potential contractors who then refuse to warrant either the design or the performance of the steam generators they would construct." On May 17, the Nuclear Regulatory Commission declined to approve a request by the administration to waive normal licensing requirements for the CRBR.

STATE

Three Long Island towns–Islip, Babylon, and North Hempstead—plan to mine their landfills for methane gas. They have signed contracts with Getty Synthetic Fuels. If Getty finds that the gas can be recovered economically, it will be used to generate electricity. Mining the gas will reduce the horizontal pressure on the gas to escape to areas outside the landfills and will provide the towns with royalties from Getty. Already methane gas has been found in the basements of some homes near the landfills and has caused several minor explosions when oil burners ignited.

A Pennsylvania executive, Russell W. Mahler, has been fined $750 000 and sentenced to one year in prison for dumping toxic wastes in Pennsylvania. He was convicted of violations on 22 counts of the Clean Streams Act. His business was oil reclamation. Under as many as eight different corporate names, he collected oil wastes, treated them to separate the oil from the contaminants, and then sold the oil. The contaminants were dumped into city landfills, sewers, or any other convenient place, according to testimony in the Pennsylvania and New York investigations. One dumping spot was a bore hole leading into an abandoned mine near Wilkes-Barre, Pa. Hundreds of gallons of wastes overflowed the mine and spilled into the Susquehanna River, a source of drinking water for the city of Danville, Pa.

The administration is proposing that federal funding for 54 state water research institutes be terminated. No funds were requested for them in the fiscal year '83 budget of the Department of Interior. These institutes, which at present receive federal funds matched by other sources, are located at land-grant or state universities. Last year the administration tried to cut off funding for the institutes but Congress restored the support. There are indications that Congress may again override the administration's proposals by continuing that support in 1983.

A new report by the Council of State Governments says that terminating federal grants to states will cause "severe financial problems" for many state solid waste management programs. Cuts in federal grants may force some states to reduce their solid waste management activities to a minimum level and others to seek increased appropriations from the state legislatures. Those states with resource recovery programs, such as community recycling centers, are least affected by the federal cutbacks.

SCIENCE

Almost 39 million rural-area Americans may be drinking unsafe water, says "National Statistical Assessments of Rural Water Conditions," a report Cornell University prepared for EPA under Congressional mandate. For instance, 29% had enough bacteria for a possible health hazard; 17% had too much cadmium; 17%, too much lead; and 14%, too much selenium, as set forth by federal community water supply standards, the report warned. These standards are not legally binding for small, individually owned water systems. No pesticides or radionuclides were found in the 1978–1979 sampling of 2654 households in several regions. Most problems were with 2–14-household systems. For more information, contact Victor J. Kimm, U.S. EPA, Washington, D.C. 20460.

Another climatic warming threat has been found—soot in the Arctic. Particles of black soot, similar to those present in polluted urban atmospheres, have been discovered in the Arctic air over Barrow, Alaska, the northernmost U.S. village, by scientists from Lawrence Berkeley Laboratory. Because these particles absorb solar radiation, at the levels found in the Arctic, they could warm the atmosphere as much as doubling the carbon dioxide content, the laboratory says.

Extraction with *n*-hexane and methylene chloride is a first step in analyzing for organophosphorus pesticides in water samples, as reported by R. Fabbrini et al., of the Institute of Water Research (Rome). Typical pesticides being determined are TEPP, dichlorvos, parathion, and malathion. The organic phase is concentrated to dryness, and then analyzed by gas chromatography (GC). Detectors are selective for phosphorus, sulfur, and nitrogen. The organic phase is cleaned up with *n*-hexane/acetonitrile, and by chromatography on an alumina column.

TECHNOLOGY

One way to handle nuclear wastes is calcining. In this process, which Fluor Corp. says has been in use since 1963, spent fuel rods, mostly from submarines and research reactors, are dissolved in acid. Residual uranium and plutonium are recovered. Remaining liquid is atomized and sprayed into a vessel at up to 1100 °F, at which radioactive chemicals are oxidized and solidified. Vapors are "scrubbed" free of radioactive materials before discharge to the atmosphere. In Fluor's new system, most equipment needing maintenance can be remotely removed or replaced.

Calcining process

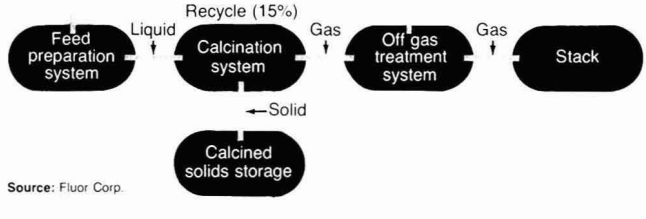

Source: Fluor Corp.

Also, a chrome/nickel/steel alloy resists corrosion much better. The new calciner is expected to have at least 25 more years of service.

Certain leachates generated from organic wastes can permeate clay liners at disposal sites, S. S. Iyengar et al., of D'Appolonia Consulting Engineers, Inc. (Pittsburgh) warn. They investigated four volatile and four nonvolatile chlorinated organics, plus Mirex and Kepone. Known concentrations of the 10 substances were equilibrated with clay samples for 48 h at the leachate's "natural" pH of about 8.5, and at pH 5. pH seemed to have no significant effect. Water solubility and octanol/water partition coefficients (K_{oc}) did seem to be factors. It may be, then, that the main interaction between the liner and chlorocarbons is hydrophobic, and that these compounds were adsorbed onto the organic fraction of clay liners.

Ozone will be the primary disinfecting agent at Los Angeles's first water treatment plant aimed at replacing the nearly 70-year-old aqueduct system. Expectations are that ozone use will save $4.5 million in capital costs, according to Camp Dresser & McKee, Inc. The city's project engineer says that the process will cost more than would chlorination, but will pay for itself through increased capabilities. It is anticipated that ozonation will help Los Angeles meet tighter California turbidity guidelines, as well as any federal standards of trihalomethanes.

For measuring PCBs in utility transformers, a low-cost, easily used device is being developed at Battelle (Columbus, Ohio) as part of a $300 000 study for the Electric Power Research Institute (EPRI). The instrument will use infrared (IR) to measure PCBs in transformer insulating oil to as low concentrations as 40 ppm. Oil with 50–500 ppm is "contaminated"; with more than 500 ppm, is considered to be a PCB. IR would be absorbed by any PCBs in the oil, and show up as a pattern on a recorder. Analysis of the pattern would give the PCB concentration. The device is to be small enough to fit into the back of a car.

Removal of cyanide from mining or electroplating wastewaters may be accomplished by adding very small amounts of ferrous sulfate and SO_2 (or sodium sulfite), E.T.C., Inc. (Redwood City, Calif.), says. Two simultaneous reactions take place: Prussian blue precipitates, and then reacts with sulfite or SO_2 to yield water, carbon dioxide, and ammonia in such trace amounts that they are environmentally harmless, the company says. According to the firm, cyanide is removed to environmentally acceptable levels.

INDUSTRY

To facilitate sample analysis in connection with Superfund priority waste sites, Mead CompuChem (Research Triangle Park, N.C.) has established the Disposal Site Screening (DSS) program. There would be a special two-step GC pre-analysis with a pre-extraction screen (to determine the right protocol), and a pre-analysis screen (to ensure that the extract is in the analysis range of the instrument). Next comes any necessary dilution or concentration and GC/mass spectrographic (MS) analysis. But if pre-screens are "below detectable limits," the GC/MS step can be eliminated. Also offered is analysis for specific metals, or for metal panels when contaminants may be unknown.

Farkas: *recession only* ***one*** *factor*

Major U.S. hazardous waste management firms raised prices and acquired new facilities in order to increase income by more than 20% in 1981 over the previous year, according to Alan Farkas, vice president of Booz Allen & Hamilton Inc. (Bethesda, Md.). He noted that last year those firms—at least, the nine largest—disposed of 3.6 million wet metric tons (wmt), while they disposed of 3.7 million wmt in 1980. They increased the number of facilities they own to 46 in 1981 from 36 in 1980. Farkas attributes some of the decline in disposed waste to the recession, but also to the fact that generators are reducing hazardous wastes through raw materials substitution, recycling, and on-site management. His figures come from a study done for EPA.

Biological treatment has been very successful in removing toxic organic pollutants from organic chemical plant wastewaters, according to a joint Chemical Manufacturers Association (CMA)/EPA study just completed. It was begun in May 1980, and tested effluents at five organic chemical plants. CMA technical director Geraldine Cox said that the tests used "exhaustive, comprehensive scientific procedures," and prove that the chemical industry "has done a superb job in cleaning up wastewater using conventional treatment procedures." CMA says the study found that biological treatment removes nearly all organic pollutants from waters to go to streams, and that before assessments can be made, exhaustive analysis is needed.

To build "Solar 100," the nation's first large-scale solar central receiver, Southern California Edison (SCE) is seeking proposals from private industry. Solar 100 is to produce 10 times more power than does the 10-MW federally supported "Solar One" at Barstow, Calif. Deadline for response is Sept. 17. Proposals from a variety of firms will be considered. The Solar One consists of a 300-ft central receiver and 1818 sun-tracking mirrors reflecting the sun's energy to the tower. For more information, contact "Solar 100," Research and Development, Southern California Edison Co., P.O. Box 800, Rosemead, Calif. 91770.

The national hazardous waste disposal system is starting to work, but still has serious problems, the National Solid Wastes Management Association (NSWMA, Washington, D.C.) says. It is advocating removing the "small generator" exemption (up to 1.1 t/mo); increasing EPA's level of enforcement; accelerating "interim status" review; and a research effort to ascertain what wastes should not be allowed to be deposited untreated in land facilities. Also, NSWMA wants EPA to require final permit applications as of effective dates of regulations, and predicts that far fewer operators would seek final permits than are now operating under interim status.

RIGHT NOW*...PCBX

Sunohio PCBX rigs arrive at the site of contamination "clean", no PCBs onboard. And the rigs leave "clean", no PCBs onboard. Contaminated oils are processed at the rate of 500 gallons per hour, and are perfectly reusable after processing. Over a half million gallons have been processed for customers.

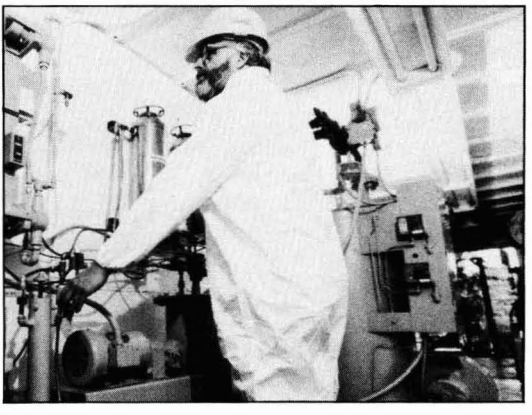

PCBX destroys PCBs. They are not buried, to become an ecological problem for future generations. They are not burned, a process that wastes valuable naphthenic base oils. They are not transported (over land . . . or sea) with the associated high risks of spills. They are not given off to the land, the air or the water.

Sunohio's PCBX process accomplishes the following while the transformer is ENERGIZED:

1. Destroys PCB s.
2. Restores oil for reuse.
3. Reclassifies the transformer to a non-PCB status. Should a fault occur in the future, the transformer can be repaired, eliminating the high cost of disposal and replacement.
4. Preserves valuable, and increasingly rare, naphthenic base oil.

Don't burn, don't bury, don't transport PCB-contaminated oil. Let Sunohio's PCBX process destroy the PCBs and return high quality, reusable oil to you.

TYPICAL LABORATORY ANALYSES OF INSULATING OILS TREATED BY THE SUNOHIO PCBX PROCESS

	CUSTOMER A		CUSTOMER B	
	BEFORE PCBX	6 MONTHS AFTER PCBX	BEFORE PCBX	6 MONTHS AFTER PCBX
PCB	91	◄2	66	◄2
Dielectric	40	55	41	55
H_2O	38 ppm	5 ppm	28 ppm	13 ppm
Color	2.0	1.0	2.0	1.0
Power Factor	Not Tested	.05	Not Tested	.04
Neut. No.	.06	.025	.06	.02
IFT	33.3	43.4	32.8	36.0
DBPC	.2%	Not Tested	.22%	Not Tested

*The only process approved in all U.S. EPA Regions

SUNOHIO

1700 GATEWAY BLVD., S.E., CANTON, OHIO 44707
PHONE (216) 767-3411 OR (216) 452-0837

CIRCLE 8 ON READER SERVICE CARD

ES&T
OUTLOOK

Trends in nuclear power

The industry supplies more of our electricity than ever before, but is beset by safety and economic problems

Over the past half decade the future of the U.S. nuclear power industry has become increasingly clouded by troubling developments. At present, 72 operating reactors supply about 13% of the nation's electricity. This year alone, construction was halted or deferred on two reactors in Oklahoma, three in the state of Washington, and 10 in North Carolina, Mississippi, and Tennessee. Three of the facilities in Mississippi and Tennessee were 30–40% complete and one in Washington State was 60% complete. These cancellations and deferments involved billions of dollars in losses for the power companies and their rate payers, but the utilities involved believed there would be even higher losses if construction were to be continued.

Of the 139 reactors ordered between 1971 and the present, 79 have been canceled. Since the accident at Three Mile Island near Harrisburg, Pa., no utility has placed an order for a new reactor. Sixty-four large plants are still under active construction; the Nuclear Regulatory Commission estimates that at least 10 of these will eventually be abandoned. A group of Harvard economists concluded recently that "commercial nuclear power in the U.S. has reached a dead end."

Why this recent spate of cancelations and deferments? The Reagan administration blames it on overregulation. Actually the reasons are multiple and far more complex than this. Overregulation seems to play a very small part. The primary reasons for the industry's problems seem to be:

- falling growth in the demand for electricity
- cost overruns
- a heightened awareness of the economic and safety risks involved
- a change in the relationship between the cost of coal and nuclear power
- uncertainties about how to dispose of nuclear waste.

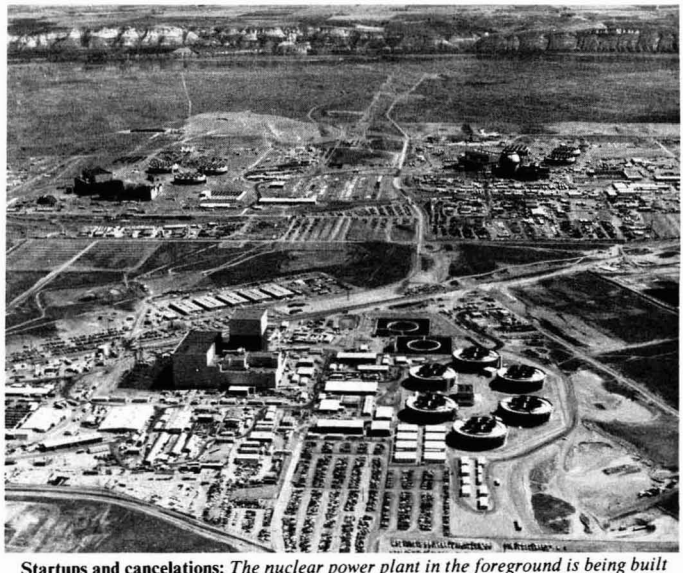

Startups and cancelations: *The nuclear power plant in the foreground is being built by Washington Public Power near Richland, Wash. The two nuclear plants in the background, which were being built for this utility, have now been canceled.*

Cost overruns resulting from high interest rates, technical problems, management failings, labor problems, and construction delays and mistakes have in some cases caused the reactors to cost 10 times the original estimate to construct. The initially favorable economics of nuclear power compared to coal-fired generation appears to have reversed in recent years. One factor that has made nuclear power relatively more expensive is that nuclear plants have developed many problems lately which have shut them down for safety or required repairs. On the average, the operating plants were out of commission for repairs, refueling, and maintenance 40% of the time in 1981, half of which was required for repairs alone. Uncertainties about how to dispose of nuclear waste have also been a factor in the cancelation or decision not to order some plants (see *ES&T*, Vol. 16, No. 5, 1982, p. 271A). Seven states—California, Connecticut, Maine, Maryland, Montana, Oregon, and Wisconsin—now have laws banning the construction of nuclear plants until the waste disposal problem is solved.

Overregulation?

Changing the regulatory setup for the licensing of nuclear plants will not create a nuclear renaissance. There are only two times when regulations play a part in the cost or delays of these utilities. In the beginning, when utilities seek construction permits for new plants, streamlining the regulations could accelerate the process. However, according to Victor Gilinsky, one of

0013-936X/82/0916-0373A$01.25/0

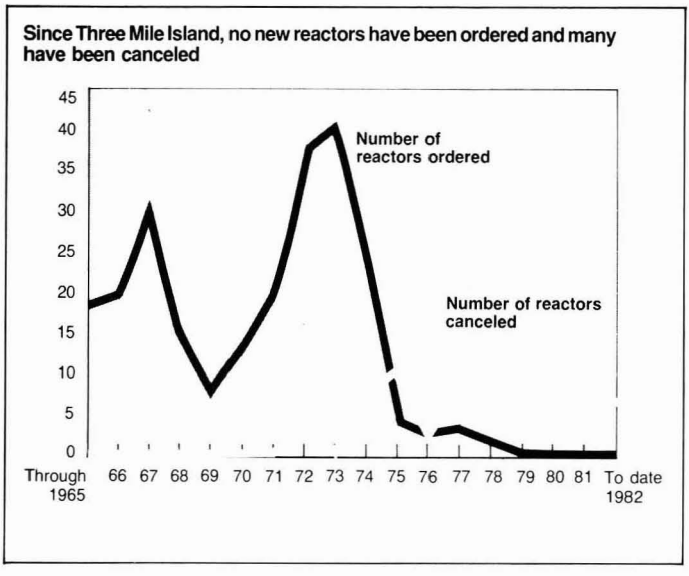

Outside the U.S., the number of reactors has nearly doubled and the total generating capacity has nearly tripled since 1976

	1976		1980		1981	
	Net MWe	Foreign reactors	Net MWe	Foreign reactors	Net MWe	Foreign reactors
Operable	35 773	116	79 735	179	97 206	199
Under construction	85 182	117	133 605	160	127 283	151
On order	53 787	58	21 285	27	23 544	29

Source: Atomic Industrial Forum.

five commissioners at the Nuclear Regulatory Commission (NRC), this would be no more than an academic exercise if the present situation remains, in which only one or two utilities seek to build a new plant.

After a plant is constructed, it must obtain an operating license. Delays occur not because of an inherently slow regulatory process or the tactics of antinuclear groups, but because the plant may not yet satisfy the equipment or safety requirements of the NRC. This part of the process could be accelerated by abandoning some of the safety requirements. After the accidents at Three Mile Island and at the Robert E. Ginna plant in Ontario, N.Y., few would want to relax the safety regulations.

Declining demand

Prior to the late 1970s, the utility industry predicted that the demand for electricity would continue to double every 10 years. Indeed, electrical consumption was generally increasing rapidly and steadily up to that time. But beginning in 1974, the rate of increase fell off sharply from an annual rate of approximately 7% to a current average rate of less than 2% (Table 1).

Taken together, the existing power plants (fossil fuel, nuclear, and others) can produce substantially more electricity than the country currently uses. Because the primary cost of nuclear power is the cost of the plant itself—the fuel is comparatively cheap—nuclear plants are run at the highest feasible operating rate consistent with maintenance or repair requirements.

Coal and oil fired plants have relatively high fuel costs and are now run at reduced capacity, coal at an average capacity of about 60%, and oil at approximately 42%. As a result, no new power plants, neither fossil fuel nor nuclear, are needed at this time except in isolated sections of the country. Streamlining regulations could not change the market situation.

There is no reliable way to predict when or if demand will rise. Many economists believe the high price of electricity relative to other energy sources will prevent any foreseeable resurgence in demand. A revival of the economy could produce a modest one-time increase in consumption; but recent studies suggest that a wider use of conservation, cogeneration, and small hydroelectric facilities could obviate the need for new large power plants, even while industrial production and the living standard rise.

Safety concerns

So far the safety record of the nuclear industry has been good. No one has been killed outright in a commercial nuclear accident, though some cancers in uranium miners and plant workers may be related to radiation exposure. In the worst accident at a nuclear power plant, Three Mile Island, the public was exposed to radiation that was only slightly above natural background at a distance of more than five miles from the plant.

Several safety concerns, however, have received a great deal of attention lately, and have caused many observers to question the advisability of expanding nuclear power. Some of these safety problems have made it necessary to shut down plants over extended periods of time.

There is much controversy about whether safety precautions taken at the plants since Three Mile Island have been sufficient. Federal and industry officials maintain that recent improvements have greatly reduced the risk of another serious accident. On its own, the industry has created an organization to monitor nuclear operations and improve safety. Carl Walske, president of the Atomic Industrial Forum, the nuclear industry trade association, said in February, "Above 90% of the really important (safety) stuff is done."

Other critics would disagree strongly with this statement and point out that many problems remain unresolved, some improvements ordered by NRC are behind schedule, and others will not be completed for years. In March, NRC commissioner Peter A. Bradford said, ". . . there seems to be an inverse relationship between the distance in time since the last serious accident and the attention paid to safety issues."

Prior to Three Mile Island, the NRC had focused most of its attention on the large, but highly unlikely, problems that might occur. Three Mile Island revealed that a series of small and far more probable slip-ups may be just as disastrous. One pressing safety question that does not seem to have been answered is how to handle backfitting, NRC commissioner Gilinsky said. In other words, to what extent should new requirements be applied to

TABLE 1

The yearly growth rate in electrical generation declined from an average of about 7% before 1974 to less than 2% at present

Year	Nuclear		Coal		Oil		Gas		Hydro		Other [a]		Total kWh	Percent increase over previous year
	Billion kWh	% of Total	Billion kWh	% of Total	Billion kWh	% of Total	Billion kWh	% of Total	Billion kWh	% of Total	Billion kWh	% of Total		
1957	[b]	[c]	346	54.7	40	6.3	114	18.0	130	20.6	0	0	632	5.2
1958	[b]	[c]	344	53.3	40	6.2	120	18.6	140	21.7	0	0	645	2.1
1959	[b]	[c]	378	53.2	47	6.6	147	20.7	138	19.4	0	0	710	10.1
1960	1	0.1	403	53.5	46	6.1	158	21.0	146	19.4	[b]	[c]	753	6.1
1961	2	0.3	422	53.3	47	5.9	169	21.3	152	19.2	[b]	[c]	792	5.2
1962	2	0.2	450	52.8	47	5.5	184	21.6	168	19.7	[b]	[c]	852	7.6
1963	3	0.3	494	53.9	52	5.7	202	22.0	166	18.1	[b]	[c]	917	7.6
1964	3	0.3	526	53.5	57	5.8	220	22.4	177	18.0	[b]	[c]	984	7.3
1965	4	0.4	571	54.1	65	6.2	222	21.0	194	18.4	[b]	[c]	1055	7.2
1966	6	0.5	613	53.7	79	6.9	251	21.9	195	17.0	1	0.1	1144	8.4
1967	8	0.7	630	52.0	89	7.3	265	21.8	222	18.3	1	0.1	1214	6.1
1968	13	1.0	685	51.5	104	7.8	304	22.9	222	16.8	1	0.1	1329	9.5
1969	14	1.0	706	49.0	138	9.6	333	23.1	250	17.3	1	0.1	1442	8.5
1970	22	1.5	704	47.2	184	12.0	373	24.6	248	16.6	1	0.1	1532	6.2
1971	38	2.4	713	44.2	220	13.6	374	23.2	266	16.5	1	0.1	1613	5.3
1972	54	3.1	771	44.1	274	15.6	376	21.5	273	15.6	2	0.1	1750	8.5
1973	83	4.5	848	45.6	314	16.9	341	18.3	272	14.6	2	0.1	1861	6.3
1974	114	6.1	828	44.4	301	16.1	320	17.1	301	16.1	3	0.1	1867	0.3
1975	173	9.0	853	44.5	289	15.1	300	15.6	300	15.6	3	0.2	1918	2.7
1976	191	9.4	944	46.3	320	15.7	295	14.5	284	13.9	4	0.2	2038	6.3
1977	251	11.8	985	46.4	358	16.9	306	14.4	220	10.4	4	0.2	2124	4.2
1978	276	12.5	976	44.2	365	16.5	305	13.8	280	12.7	3	0.2	2206	3.9
1979	255	11.4	1075	47.8	304	13.5	329	14.7	280	12.4	4	0.2	2247	1.9
1980	251	11.0	1162	50.8	246	10.8	346	15.1	276	12.1	6	0.2	2286	1.7

[a] Includes geothermal, wood, and waste.
[b] Less than 0.5 billion kWh.
[c] Less than 0.05%.
Note: Numbers may not add to totals because of independent rounding.
Source: *Annual Report to Congress 1980*, DOE/EIA-0173(80)/2, Volume 2 (of 3), Energy Information Administration, U.S. Department of Energy.

plants licensed for construction or operation?

The embrittlement problem

A safety issue that has aroused a great deal of concern is the possibility that under certain conditions of high pressure and rapid cooling, an older reactor pressure vessel, especially in a pressurized water reactor, could rupture and release radioactive material into the containment building and lead to a core meltdown. Emergency core cooling systems are not designed to prevent core melting caused by a complete failure of the vessel itself. (Any reactor vessel could rupture; but conditions in boiling water reactors are less severe because they operate at lower pressures and have walls that are thinner and exposed to less radiation, being at a great distance from the reactor core.)

While a reactor is being turned on or shut down and especially during an emergency shutdown, it can be subject to high pressure and low temperatures from the cold water used to cool it. For each reactor vessel and pressure, there is a critical transition temperature below which fractures can occur under low stress. As the reactor grows older and the steel vessel becomes more embrittled from radiation, the critical temperature rises. This problem has been recognized and studied for years, but has received more attention recently because of evidence that reactors are becoming embrittled faster than was originally anticipated and because of an unplanned shutdown in 1978 at the Rancho Seco reactor near Sacramento, Calif. According to an NRC study, the reactor walls at the Rancho Seco plant could have cracked and ruptured during this transient if the facility had been 10 instead of three years old at the time, and if an imperfection had been present at a critical location in the vessel.

Certain welds in thick-walled, steel pressure vessels seem to be causing the most severe embrittlement problem. These welds contain impurities that make them more sensitive to radiation than the plates or forgings they hold together. Originally, it was assumed that the plates, forgings, and welds would lose toughness at the same rate.

The NRC is addressing embrittlement now as one of the high-priority, unresolved safety issues. There is much disagreement, however, over whether the agency is attacking the problem vigorously enough or taking precautions that are timely enough.

Reactor vessel fracture from pressurized thermal shock (PTS) is probably much more likely to be caused by a series of failures and operator errors than by a single deficiency of the basic reactor design or by a single operator error. In March, the NRC Executive Director for Operations, William J.

Embrittlement can be a problem in pressurized water reactors

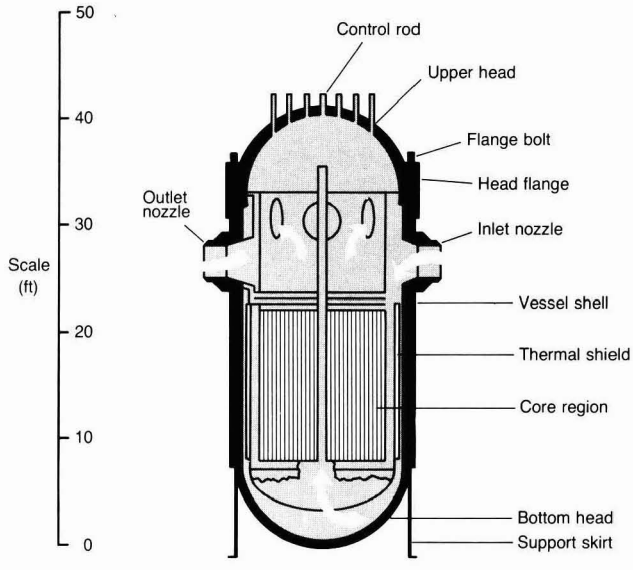

Pressurized water reactor vessel

Dircks, wrote, "We note that all of the pressurized thermal shock precursor events that have occurred have been multiple problem events. We believe that there are many scenarios . . . that can lead to PTS events. The large number of such scenarios creates the potential for a risk that is not negligible, even though each individual sequence may be calculated to have very low probability . . ."

Whether or not operators will behave correctly in a crisis seems to be the largest uncertainty. Using two techniques, Oak Ridge National Laboratory performed a study of pressurized thermal shock that came to the opposite conclusion depending upon whether or not correct operator action was assumed. Industry believes that the people in the control room will not make critical mistakes and points out that operator training and awareness in regard to thermal shock have improved.

This year the NRC staff concluded that under normal operation or anticipated transients, no reactor vessel in the U.S. is in any danger of cracking. But the NRC also stated in a recent report that "approximately 20 operating PWRs [pressurized water reactors] will have beltline materials with marginal toughness . . . after comparatively short periods of operation," and told the operators of 44 plants to have their reactor pressure vessels tested. According to Denwood F. Ross, Jr., Deputy Director of the Office of Nuclear Regulatory Research at NRC, the technical staff "expects to determine by this summer whether any immediate actions should be required." In 1983 the agency will decide what licensing actions will be taken.

So far U.S. manufacturers have made no major changes in reactor pressure vessel design to avoid fractures resulting from thermal shock. In contrast, West Germany has decided to eliminate welds in the beltline regions of reactor vessels. West Germany has also changed the way fuel is loaded in at least two reactors.

Deteriorating steam generators

Each steam generator in a pressurized water reactor consists of thousands of tubes about 0.05 in. thick. Degradation of these tubes is another problem that has aroused a great deal of concern recently. The problem first appeared in 1976 and now affects at least 40 operating reactors.

Three U.S. companies design steam generators. Those made by Westinghouse and Combustion Engineering have suffered degradation due to wastage and stress corrosion cracking. The Babcock & Wilcox steam generators have had cracks of unknown origin propagated in the circumferential direction by flow-induced vibration, and have also suffered a second form of degradation called erosion–cavitation. The problems in the Westinghouse and Combustion Engineering generators have been decreased by conversion from phosphate to an all-volatile secondary water treatment. This, however, has led to a second problem known as denting, which occurs when the supporting plates begin to rust and squeeze the tube until they buckle or crack. There is no panacea for the problems with the present generators. The cures are only partially effective, and some create a new set of problems.

Steam generator degradation is both an economic and a safety concern. Last year, approximately 23% of the nonrefueling outage time was related to problems with steam generators. Many have had to be repaired and some have been replaced entirely. New generators at the Surry Units I and II in Virginia were installed at a cost of approximately $200 million, including the cost of make-up power. The steam generators at Tuckey Point in Florida are being replaced at a cost of $460 million.

Most leaks in steam generators have been slow and are not considered accidents. But four plants have had significant ruptures involving steam generators. The last one at the Robert E. Ginna power plant in January was the most serious accident since Three Mile Island. During this incident, 11 000 gal of radioactive coolant spilled from a steam generator to the plant floor. Some of the radioactive water passed through the ruptured tubes and turned to steam, part of which was vented to the atmosphere.

According to Dircks, there is a possibility of a large accident with a steam generator. In February 1982 he wrote, ". . . the consequences of steam generator tube ruptures under normal operating conditions have been small; however, such events can present a significant challenge to plant operators and safety systems."

Another concern is that the people who repair, replace, or resleeve steam generators are exposed to a high level of radiation. The dose is so high that a person can do this repair work safely for only a few days each year. Consequently, thousands of temporary laborers called "jumpers" or "sponges" have been employed to repair the generators. After being given a very short training, they jump into the hot zones of the reactor to plug or put sleeves on leaking pipes. No medical follow-up is provided for these workers.

Manufacturers now claim that they have designed a better generator. The

reactors that the NRC plans to license for operation by the end of 1983, however, will have generators with older designs.

Pools for spent fuel

Thirteen other items are labeled high priority in the NRC's list of unresolved safety issues. But what may be the most serious safety problem is not even included. This problem, mentioned in the May issue of *ES&T*, concerns the pools that are used to store spent fuel. A large fraction of these pools hold many more spent fuel rods than they were originally designed to contain. In the event of a major earthquake that could crack a pool or cause a power failure, called station blackout, the cooling system in the pool could fail, allowing it to come to the boiling point much faster than it would if it held fewer rods. This could allow a reaction to occur between the zirconium cladding on the rods and steam, releasing a large amount of hydrogen. An explosion could occur promptly. If the pool is above ground, as many of them are, the explosion could damage or destroy the building over the pool, which is not designed to withstand a large explosion, and expose radioactive materials to the environment.

At a time when concern about safety issues is growing, federal expenditures to support NRC research and implementation in safety areas have dropped. Compared to 132 people in 1980, NRC now employs 309 in licensing. In safety-related projects the number of personnel has fallen from 401 to 326. However, there is a possibility that the 1983 budget may reverse this trend.

Warning system

After Three Mile Island, it was decided that nuclear power plants should have an emergency warning system. If a major accident occurs, the system would be used to notify those living within 10 miles of the plant in 30 minutes. Utilities are also required to have plans for alerting these people to take shelter or evacuate, depending on the circumstances. Plans have not been instituted at some plants, however. In February, NRC announced that seven utilities failed to meet the deadline for installing warning systems. Also, the operating licenses for seven plants could be delayed for up to 16 months while they devise and obtain approval of emergency contingency plans.

Cost of coal and nuclear power

The expense incurred in remedying safety problems has been one of the many factors that have helped to change the relative cost of coal and nuclear power. A survey published in February 1981 by the Atomic Industrial Forum (AIF) showed that for plants entering service after 1974, the electricity produced by coal plants was cheaper than that produced by nuclear plants. For example, coal utilities entering service in 1978 had a 1979 generating cost that was 20% less than the generating cost of reactors that came on line that same year. In contrast, the survey found that the average cost of nuclear power for all plants included in the survey was less by 17% than the cost of coal power.

However, according to Charles Komanoff, an independent energy consultant to Congress and to many state government agencies, the AIF survey was skewed in several important ways. By correcting the errors, Komanoff reversed the relationship so that the average cost of nuclear power for all plants became higher than coal power. One important error was a simple arithmetical mistake in computing a weighted average for a column of figures. Another was that several of the most expensive reactors—reactors with an average generating cost of 5.16¢/kWh—were omitted from the survey. There may be even more missing reactors; no plant-by-plant cost data were provided (for average costs see Table 2). Furthermore, allowances for the expenses of nuclear waste disposal and reactor decommissioning were made for only a few of the plants in the AIF survey. These costs are considerable, adding at least 0.20¢/kWh.

Finally, the survey failed to include idle plant capacity. If idle plant capacity had been taken into consideration, the calculated cost per kilowatt hour for coal plants would have been even less, because coal-fired plants can operate at 70–80% of capacity, but actually operated at 54.1% of capacity because of an insufficient demand for electricity. In contrast, nuclear plants are always run at maximum possible

TABLE 2

Electricity produced by coal plants was cheaper than that produced by nuclear plants for utilities entering service after 1974[a]

	Nuclear				Coal				Oil			
Year of commercial startup	Number of units	Generating capacity (MWe)	1979 Average generating cost (¢/kWh)	1979 Capacity factor (%)	Number of units	Generating capacity (MWe)	1979 Average generating cost (¢/kWh)	1979 Capacity factor (%)	Number of units	Generating capacity (MWe)	1979 Average generating cost (¢/kWh)	1979 Capacity factor (%)
1970	4	2419	1.4	71.7	3	2065	1.9	53.1	0	0	—	—
1971	4	2735	1.4	63.9	2	1450	2.4	43.9	1	410	5.6	19.5
1972	8	5532	1.6	62.7	2	1500	2.9	39.3	3	1492	4.1	39.4
1973	7	5132	1.6	58.3	4	3760	2.4	48.7	2	836	4.1	34.8
1974	12	9918	1.7	64.3	1	1140	2.0	53.5	4	2356	3.7	55.3
1975	7	6276	2.8	62.3	5	3693	2.5	56.7	2	1202	4.5	49.2
1976	4	3632	2.9	52.7	3	2347	2.5	58.7	1	764	4.6	35.8
1977	5	4474	2.6	50.1	3	2130	2.2	65.2	3	2133	4.8	39.9
1978	3	2905	2.5	52.2	2	1393	2.0	65.6	2	1173	5.7	19.0
Weighted averages—1979			1.9[b]	60.2			2.3	54.1			4.3	40.5

[a] Base-load units of 400 MWe of larger capacity, entering commercial operation from 1970 through 1978 and in service during all of 1979.
[b] This figure is incorrect. The weighted average of the nine figures is 2.01¢, not 1.9¢. The difference is too great to be a rounding error.
Source: Adapted from Atomic Industrial Forum report.

Fill a Staff Position on Capitol Hill

Two ACS Congressional Fellowships Available To Begin Fall 1983

The objectives of the fellowship program are:

- To provide an opportunity for scientists to gain firsthand knowledge of the operations of the legislative branch of the federal government,
- To make available to the government an increasing amount of scientific and technical expertise, and
- To broaden the perspective of both the scientific and governmental communities regarding the value of such scientific-governmental interaction.

Applications should be submitted by January 31, 1983 to:

Dr. Annette T. Rosenblum
Department of Public Affairs
American Chemical Society
1155—16th St., N.W.
Washington, D.C. 20036

Applications consist of a letter of intent, resume, and two letters of reference. The letter of intent should include a description of the applicant's experience in public-oriented projects in which scientific or technical knowledge was used as a basis for interaction and a statement that tells why they have applied for the Fellowship and what they hope to accomplish as an ACS Congressional Fellow. The resume should describe the candidate's education and professional experience and include other pertinent personal information. Letters of reference should be solicited from people who can discuss not only the candidate's competence but also the applicant's experience in public-oriented projects. Arrangements should be made to send the letters of reference directly to ACS.

For further information call (202) 872-4384.

If there were a major nuclear accident at one of the Indian Point nuclear reactors north of New York City, almost 300 000 people living within a 10-mile radius might have to be evacuated. Working out an evacuation plan for such a large number of people is almost impossible[a]

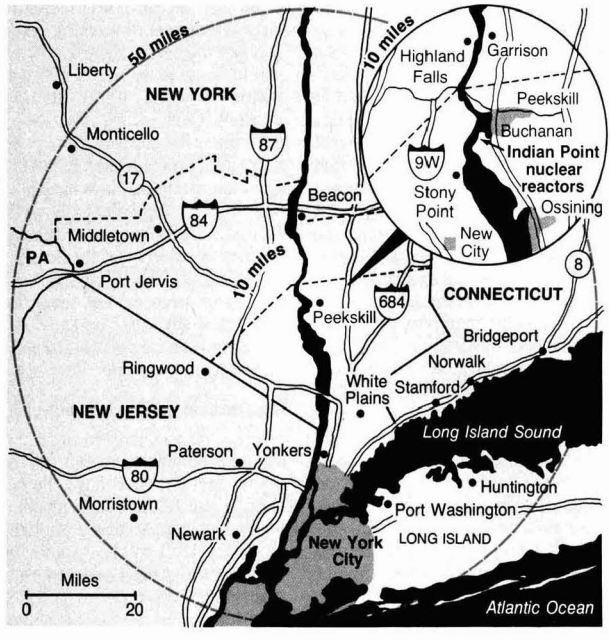

[a]Some nuclear critics say that evacuation plans should be devised for all people living within a 50-mile radius.
Source: Adapted from *New York Times*, March 13, 1982.

capacity when in good repair, because the fuel expense is relatively lower.

Alternatives

Many knowledgeable people say that they are aware of the risks associated with nuclear power; but they believe we will have to live with these risks because nuclear power is the only economical alternative to fossil fuels for the immediate future, and perhaps for the next few centuries. We cannot reduce our dependence on foreign oil, they say; besides, fossil fuels cannot last forever. Eventually we will need a long-term option. In addition, fossil fuel plants contribute to acid rain and perhaps to the greenhouse effect.

Fossil fuel and nuclear power may not be the only alternatives, however. Recent studies have shown that using a combination of conservation, cogeneration, small existing hydroelectric facilities, and other alternative methods of producing electricity is cheaper than building new coal-fired or nuclear plants. California has saved its rate payers money by requiring these alternative methods to be used before new coal or nuclear plants are built. In late May, New York State passed a law that requires large utilities to provide reserve or supplemental power to small producers of electricity and to buy electricity from them, if they wish to sell excess power. Other methods of producing electricity such as solar power or wind power may eventually become competitive with nuclear and fossil fuel generation. At a time when Germany, France, and Japan have greatly increased their expenditures for research into solar power, we have cut ours drastically. The Reagan administration fired the director and 300 staff members of the Solar Energy Research Institute and asked Congress to abolish the Solar and Conservation Bank, which would provide low-interest financing for builders and other individuals installing solar devices. It is obvious that there would be a severe shortage of electricity in some areas if all nuclear plants shut down tomorrow. But the federal government would be well advised to put its resources into a wider variety of options.

—Bette Hileman

Important Reading in Biological Chemistry

Biological Effects of Nonionizing Radiation

Four sections deal with the molecular dynamics in aqueous solution, the dielectric and spectroscopic properties of membrane systems and biological tissue, including the frequency response of membrane compounds in nerve axons, the dielectric and spectroscopic properties of nonequilibrium systems, and the microwave acoustic effect.
ACS Symposium Series 157, 342 pages, 1981
ISBN 0-8412-0634-1, Cloth **$28.50**

Biomimetic Chemistry

Areas of biomimetic chemistry relating to enzyme systems that function with and without coenzymes are represented. Special emphasis has been placed on the following topics: vitamin B_{12} and flavens; oxygen binding and activation; bioorganic mechanisms; and nitrogen and small molecule fixation.
Advances in Chemistry Series 191, 437 pages, 1980
ISBN 0-8412-0514-0, Cloth **$57.00**

Bioelectrochemistry: Ions, Surfaces, Membranes

Five chapters are grouped under "Surface Interactions" and include research on electrical properties of membrane systems, the adsorption of Ca^2 and Mg^2 to phosphatidylcholine bilayers, and the influence of VDW-London forces on cell interactions. The next section deals with "Macromolecules" and is concerned with enzymatic clotting processes, the electrochemical basis of heparin-induced RBC aggregation, and hemoglobin oxygenation. "Membrane Processes" is an eight-chapter segment that details ongoing research. The final group of chapters is collected under the heading "Cells and Tissues."
Advances in Chemistry Series 188, 527 pages, 1980
ISBN 0-8412-0473-X, Cloth **$58.00**

Immobilized Microbial Cells

This state-of-the-art review surveys several important aspects of immobilized cell technology: methods of cell attachment, biophysical and biochemical properties, carriers for immobilization, and reactor design. Several chapters detail the physical characteristics of fixed microbial cell systems. Biochemical processes mediated by bound cells are discussed. The remaining topics outline important industrial applications such as the conversion of dextrose to fructose.
ACS Symposium Series 106, 247 pages, 1979
ISBN 0-8412-0508-6, Cloth **$29.95**
ISBN 0-8412-0644-9, Paper **$19.95**

CALL TOLL FREE
800-424-6747

American Chemical Society, 1155 16th St., N.W. Washington, D.C. 20036

Please send me the following ACS biological books:

Quantity	Title	Price

☐ MasterCard/Interbank Code: _____ Expiration Date: _____
☐ VISA
Account Number: _____ (California residents add 6% sales tax) _____
Signature _____ Total Payment (Enclosed) _____
☐ Purchase Order Enclosed P.O. Number _____
Send books to:
Name _____
Address _____
City _____ State _____ Zip _____

46

Fixed-film biological processes

While these wastewater treatment systems still have problems, they could become viable energy-saving or even energy-producing alternatives that might also generate less sludge

During the last decade, interest in fixed-film biological (FFB) processes for wastewater treatment has increased markedly. One reason is that these systems have a potential for considerable energy savings, as compared to conventional suspended-growth or activated-sludge systems. Indeed, certain fixed-film processes may turn out to be energy producers. Another reason is that according to several researchers in the field, some FFB processes may be better able to withstand and recover from attacks by toxic substances. Such substances have been known to cause municipal wastewater treatment plants using the conventional activated-sludge process to perform poorly, or even shut down. Also, recent developments of improved filler media have made it possible to construct FFB systems that can be smaller in size, but otherwise technologically and economically competitive with activated-sludge systems.

In an activated-sludge system a large amount of energy is needed to force in the necessary air or oxygen, Leslie Grady, Jr., of Clemson University (S.C.) reminded *ES&T*. He explained that in a trickling filter, a fixed-film technique, aeration occurs through normal mass transfer, so nothing needs to be forced in; thus, energy savings are achievable right there. With the rotating biological contactor (RBC) type of fixed-film system, less energy is needed to force air or oxygen into the system's liquid phase than is necessary for the same function in an activated-sludge system. In the U.S. at present, 236 municipal wastewater treatment plants employ RBC technology; it is also being used at certain industrial installations, recreational areas, and remote sites.

This energy use comparison refers to aerobic systems. But because *anaerobic* fixed-film processes have the potential of actually *producing* energy, increased research and development efforts are being exerted in that direction. Here the term "anaerobic" covers methanogenic fermentation processes. An FFB system of this type, properly designed, built, and operated, could produce gas consisting of as much as 85% methane. Moreover, costs of supplying air or oxygen need not be considered. Finally, anaerobic systems produce much less sludge than activated-sludge or even aerobic fixed-film processes do; in some cases, reductions can reach 90%. At present, however, anaerobic systems are mostly at laboratory scale, or in early pilot stages.

To be sure, fixed-film systems have been in existence for a long time. For instance, a 31-acre trickling filter started up in Baltimore 75 years ago is still operating. But 31 acres is a large amount of land. If such large land areas were still necessary, FFB processes would not have remained a viable option. Had it not been for the development and improvement of shaped inert filter media of polyvinyl chloride (PVC), other plastics, stainless steel, or redwood, and of media suitable for RBCs, fixed-film technology would probably not have advanced beyond the use of stones and gravel spread over large tracts of land to perform the filtering function.

Shaped synthetic media allow this filtering function to be carried out in a much smaller space, with a more concentrated and active biofilm, and therefore far more efficiently and economically. Microorganisms capable of reducing BOD_5, COD, and certain other pollutants attach themselves to the media as they come into the system with the wastewater, and form the "fixed film." The biomass they create performs the pollution abatement function by metabolism or adsorption of polluting materials by the film and the organisms comprising it. Another configuration of this process involves rotating biological contactors. RBCs consist of a series of rotating discs, normally submerged; they are the media to which the biofilm affixes itself.

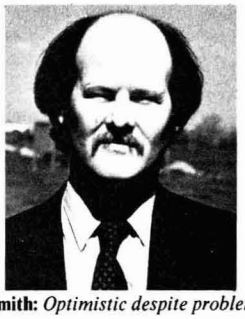

Smith: *Optimistic despite problems*

Overshadowed for a while

During the later 1960s and through most of the 1970s, the fixed-film concept was generally overshadowed by a strong trend toward activated-sludge systems. Efforts were also being made toward building physical-chemical plants that, it was believed and hoped, could turn out a highly "polished" effluent that could meet wastewater treatment standards existing and expected at the time. But it soon became evident that capital, operational, and energy costs of physical-chemical plants would render that concept essentially unworkable.

Though widely accepted and used now, in addition to constantly escalating costs, the activated-sludge treatment method also has problems. For instance, certain toxic organic chemicals, inorganics, and metal ions have seriously impaired, or even "knocked out" activated-sludge systems. Also, spent sludge must be disposed of somewhere; options for its management and disposal are becoming increasingly limited. Moreover, some engineers and scientists say that controlling activated-sludge systems may be very difficult at times. These

0013-936X/82/0916-0380A$01.25/0

problems also help to explain why FFB processes are being regarded with increasing favor.

Would fixed-film systems offer cost advantages? Grady said that it is still too early to predict differences in capital costs between fixed-film and activated-sludge systems; each installation would have to be evaluated on its own merits. He expressed more optimism about lower operating costs; but again, every system must be considered on a case-by-case basis at this time.

Devil's advocate

Growing interest in the FFB concept was pointed up by the more than 325 participants from 19 countries who attended the First International Conference on Fixed Film Biological Processes at Kings Island, Ohio, in April. Discussing the concept in general, and rotating biological contactors in particular, keynote speaker Ed Smith of the U.S. Army Construction Engineering Research Laboratory (CERL, Champaign, Ill.), said, "For municipal and industrial wastewater treatment, fixed-film, and especially RBCs, are gaining wide acceptance with the pollution abatement community."

But in his overview of the state of knowledge, Smith played Devil's advocate. He explained that media and shaft failures and media degradation "have left the RBC industry with egg on its face. However, the industry has learned from past problems, and has dedicated a lot of dollar, research, and engineering resources to develop a viable pollution abatement technology. Consequently, although efforts need to continue in order to increase the structural reliability of the technology, and to reduce the dependence of design guidance on proprietary know-how, I am very optimistic about the future of RBC technology."

Wu (*l*) *and* **Grady** (*r*)*: "big 'push' toward anaerobic processes"*

Research center plans

Smith's opinion was accentuated by conference chairman Yeun Wu of the University of Pittsburgh's School of Engineering, which sponsored the conference in cooperation with EPA, CERL, and the National Science Foundation. Wu sees promise in this technology—especially that stemming from army-supported research begun in earnest in 1979. "We hope to set up a fixed-film research center at Pitt in the near future," Wu told *ES&T*.

Both Wu and Grady predict a bright future in FFB, partly because of improved energy efficiency; Grady added that he believes the fluidized-bed version of this process to be "more controllable than, say, conventional activated-sludge processes." Wu and Grady foresee a big research and development push in anaerobic processes that produce energy in the form of methane generation. Sludge formation is reduced; when there is sludge, it is much more settleable and otherwise generally manageable in a clarifier, Wu said. By contrast, in the activated-sludge process, troubles can crop up during clarification, he added.

But there are also difficulties with fixed-film technology that must be corrected. For instance, once on line, a fixed-film system has difficulty in building up enough biomass at the beginning of its operation. FFB systems need a long time, sometimes as

Media development boosted FFB

It is possible that fixed-film biological (FFB) processes for wastewater treatment would still be limited to stone and gravel media, and perhaps not a viable technology had it not been for certain pioneering efforts at Dow Chemical Co. (Midland, Mich.) begun 28 years ago. Starting in June 1954, Dow evaluated its Dowpac HCS plastic medium (since renamed Surfpac) as an inert support for biofilms, and compared it with crushed blast furnace slag used at the company's full-scale treatment plant.

The initial experimental unit (10 ft in diameter and 10 ft deep), half slag and half honeycombed plastic, was inoculated by passing the unsettled effluent from Dow's conventional (slag) trickling filters, treating strong phenolic wastewater, over the media for one week. The unit was then switched to a synthetic wastewater containing pure phenol and ammonium phosphate dissolved in Midland's tap water.

During the period 1954–1960, Dow's research and development effort was led by Edward Bryan, now program director of Water Resources and Environmental Engineering at the National Science Foundation. It was expanded to include more than 30 applications in domestic and industrial wastewater treatment.

During the 1960s and onward, various plastic (or wood) media and designs were developed for wastewater treatment and water cooling by numerous firms, including The Munters Corp., B.F. Goodrich, and Neptune Microfloc, Inc.

Typical media can be corrugated PVC

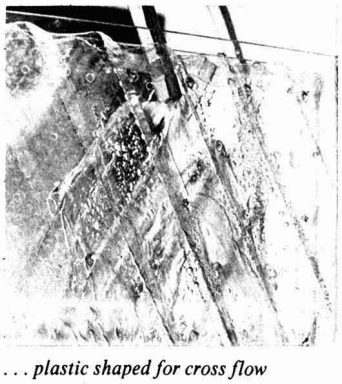

. . . plastic shaped for cross flow

. . . or redwood

long as three months, to achieve steady state. Also, an anaerobic system is sensitive to temperature changes because of the nature of the anaerobes in the biomass. Moreover, one cannot exceed a certain loading rate on the system, nor can one wash out biomass, Wu explained. On the other hand, aerobic systems normally cannot treat high waste concentrations because of limits imposed by the oxygen transfer process, he said. Wu has been able to run several anaerobic reactors in his laboratory for more than one year, with very low sludge production.

Present systems: mostly aerobic

Most of the FFB reactors now in use are aerobic, the original types being the well-known and often-used trickling filter. Wastewater is sprayed onto media such as stones or gravel on which a film of aerobic microorganisms grows as the attached fixed film. These "bugs" treat the wastewater's dissolved BOD and COD-causing materials by adsorption to metabolism, as the fluid filters through.

Performance of these aerobic processes is being enhanced by the use of shaped synthetic media, such as PVC, polyethylene, polystyrene, stainless steel, or even redwood. These media may be stationary, often with a corrugated shape, or in the case of the RBC, a series of rotating discs. What is common to all of these media is that they provide inert support and a large surface area to which microbes can attach themselves and grow.

Aerobic systems are often arranged so that flow is downward, with air or oxygen forced upward in a counterflow, though other configurations are possible. One type of plastic medium is so shaped as to cause a crossflow; this arrangement provides more surface area for biofilm. A major advantage of synthetic or wood media is that such an FFB system can be much smaller than the old stone system, engineer Sheldon Roe, Jr., of The Munters Corp. (Ft. Myers, Fla.) explained to *ES&T*.

Heterotrophic bacteria (requiring nourishment from outside sources) grow on the medium, particularly on upstream portions, and oxidize wastes. Downstream, ammonia and ammonia byproducts serve as energy sources for chemoautotrophic bacteria (capable of self-nourishment), such as *Nitrosomonas* and *Nitrobacter*, respectively. Certain protozoa, nematodes, rotifera, worms, and even small insect larvae may live at different portions of the filter system, and feed on (predate) the biofilm wherever the film produces the necessary nutrients for these predators. This predation, or "grazing," is one mechanism that is supposed to keep the biofilm's thickness under control. The hydraulic action of fluid flow is another.

If the bacterial film's thickness becomes too great, oxygen would not reach its inner layers and the medium surface. Then, anaerobes can grow; these live on end products of aerobes, and on nutrients released by lysis (dissolution) of dead aerobes. As aerobes starved of oxygen die and lyse, large portions of the biofilm can slough off the medium, impairing the film's efficiency for treating wastewater. One method suggested for preventing the film from becoming thick enough to harbor anaerobes consists of periodic hydraulic load increases. In addition, especially with the newer plastic-media trickling filters, it may be possible to arrange for an optimum distribution of numbers and types of organisms that prey upon bacteria comprising the biofilm.

Erik Särner of the University of Lund (Sweden) points out that in addition to micro- and macroorganism ecology, certain other factors can limit trickling filter reaction rates. For instance, oxygen transfer could limit the rates upstream, while substrate transfer could limit them downstream. Other such factors are various biochemical processes. Moreover, if organic loading is very high, or if phosphorus reduction is required, suspended solids and BOD in the effluent may still be above regulatory tolerance, and further "polishing," perhaps by post-precipitation, would be needed.

Särner notes that similar organisms exist in aerobic FFB systems and in activated-sludge systems. What sets fixed-film systems apart is the *succession* of ecological communities, as opposed to the generally uniform mix one finds in activated-sludge systems.

Anaerobic moves ahead

Advances in scientific knowledge, technological know-how, and control engineering techniques are contributing to progress in anaerobic FFB system research and development. To be sure, anaerobic methods have problems. They have not been as widely demonstrated as their aerobic counterparts have. Also, their optimum operation takes place within a fairly narrow temperature range, mainly 35–37 °C, although they have been operated successfully at higher and lower temperatures. Bruce Rittmann of the University of Illinois (Urbana) told *ES&T* that he has operated units at as low as 20 °C; however, at lower temperatures, loading rates may have to be decreased.

Richard Speece of Drexel University (presently on sabbatical at Stanford) pointed out that a slower accumulation of biomass, which extends the startup interval, may be a serious disadvantage of methanogenic anaerobic systems. However, this disadvantage could be neutralized by giving *careful* attention in the system's design to bacterial solids retention time during the period of biofilm buildup, or during recovery from or acclimatation to toxicants, Speece said. On the other hand, he listed several advantages:

- With a well-planned and well-designed system, sludge production could be on the order of 30% of that of an aerobic FBB system, and less than 10% of that of conventional systems.
- Gas generated may consist of as much as 70–85% methane, which could furnish the necessary energy for temperature control, with some left over for other uses or sale.
- No energy is needed for oxygen transfer, since there is none in the anaerobic process. More energy efficient than the aerobic process, anaerobic treatment can save as much as 2×10^7 Btu/t of COD.
- Nutrient requirements are substantially reduced.

Describing an anaerobic FFB system for possible industrial applications, Edward Chian of the Georgia Institute of Technology spoke of a technique for treating wastes with high phenol concentrations. With such wastes, aerobic processes are often unstable; "intense" mixing is needed for high oxygen transfer which is energy-consuming, and "makes much sludge."

Chian used a fluidized-bed column (183 cm long and 10 cm in diameter) with Raschig rings, and another with 160–175 cm of expanded granular activated carbon (GAC). Digester sludge was used to "seed" the rings with anaerobes, which in turn were used to "seed" the GAC. The temperature was maintained at 35 °C.

The anaerobes could become acclimated to phenol; that step may be further enhanced by adding glucose. About 10–12 weeks were needed for full acclimatation; after only three weeks, COD removal exceeded 90%. At an optimum 1600-mg/L phenol concentration, and loading of 4.7 kg/m^3·day of COD, about 94% of the phenol was removed. With system refinements, as much as 99.7% removal may be possible, Chian said. Sludge was sharply reduced, and the gas normally contained 75–85% methane.

Chian believes that his technique may be adaptable to treating coal gasification plant wastewater.

Working at Stanford University, André Bachmann and Perry McCarty noticed that in an anaerobic rotating biological contactor system, rotation of the discs has virtually no effect on the efficiency of the process. They went on to develop the anaerobic baffled reactor (ABR) system in which the liquid flows horizontally, and around several baffles that serve to maintain microorganism populations within the reactor. The biological solids retention time can be as great as 100 days; however, McCarty says that this is advantageous in that with such a retention time, more biomass builds up.

Influent COD concentration was 7–8.6 kg/m^3; hydraulic loading was 2 m^3 of waste fluid per cubic meter of reactor volume each day. Bachmann said that COD removal efficiencies reached 60–80% for organic loadings of 10–20 kg/m^3·day of BOD. When trace nutrients were added, COD reduction increased to 91% at an organic loading of about 10 kg/m^3·day of BOD. Varying with the organic loading, methane content of the gas generated ranged 55–75%. Bachmann expressed the belief that the ABR approach "has excellent promise" for treating industrial wastewaters.

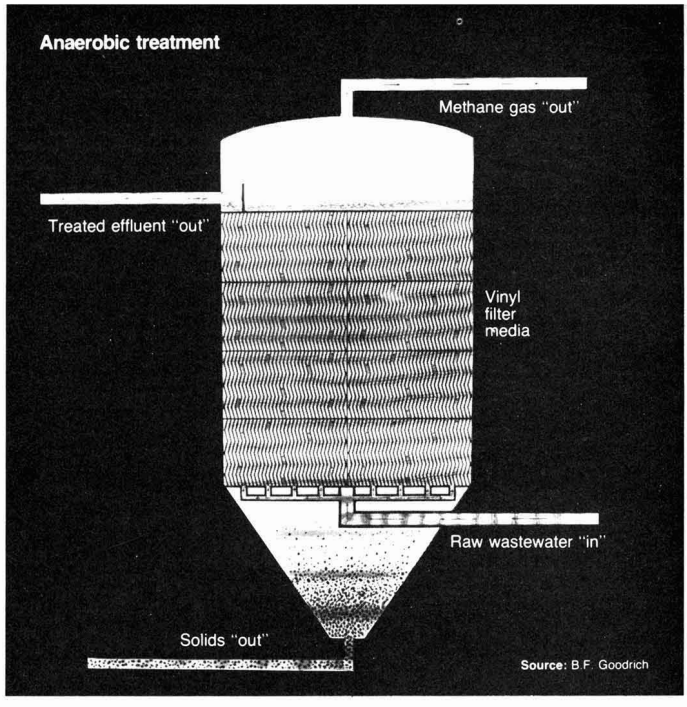

Toxic assaults

Various opinions were expressed as to what may happen if an aerobic or anaerobic FFB system suffers an "assault" by toxic organics, inorganics, or metals. Clemson University's Grady spoke of a paucity of "good, hard data" on the subject. He noted that in a conventional activated-sludge system, the pollutant will be distributed throughout; thus, dilution could be so great that the system would continue to operate, though with reduced efficiency. But a "slug" of toxic material might kill all the biota in such a system, requiring it to be "taken down," cleaned, and refurbished. On the other hand, in an aerobic FFB system, the toxic material could kill even a large portion of the biomass, which would then slough off the medium and leave a much thinner film, or even some bare spots. But after the end of the toxic attack, the biofilm could begin to regenerate.

With an FFB reactor of the fluidized-bed configuration, concentrations of toxic materials could be reduced through recycling, especially if the chemical is biodegradable. In any case, Grady explained, effects on a reactor will be mediated by the concentration gradient of toxicants within that reactor. It may also be possible to "seed" a fixed-film system with either naturally occurring or genetically "engineered" organisms that can be selected from a "menu" (*ES&T*, Vol. 16, No. 3, p. 173A), to break up target chemicals.

A chromium inhibition study

One scientist said that a potent toxicant, such as hexavalent chromium (Cr^{+6}), "can kill everything." Is Cr^{+6} a universal killer? If not, what does Cr^{+6} attack, and in what fashion? Working on that problem together with Jack Borchardt at the University of Michigan, Shin Joh Kang, now with the consulting firm of McNamee, Porter & Seeley (Ann Arbor, Mich.), deliberately fed Cr^{+6} into a rotating biological contactor system. The system consisted of discs 2 ft in diameter, in two separate chambers, with four discs to a chamber. The chambers were in series. The feed was a synthetic wastewater with 200 mg/L of BOD_5; 300 mg/L of COD; and 20 mg/L of total nitrogen. Carbon and nutrients were furnished from cornstarch, and nitrogen from urea and beef consommé (which also provided the needed phosphorus and trace materials). Cr^{+6}, in the form of potassium dichromate, was added.

The nitrification process was affected; in that process, *Nitrosomonas* converts ammonia to nitr*ite*, and *Nitrobacter* further oxidizes the nitrite to nitr*ate*. Kang found that while nitrate production was essentially impaired, recovery could occur in as short a time as one week, even with a 50-mg/L shock load of Cr^{+6}. Kang believes that the *Nitrosomonas* is very adversely affected, but that *Nitrobacter* "suffers" much less.

Other factors might lead to problems in evaluating Cr^{+6} effects on nitrification microorganisms. For example, these microbes are at a competitive disadvantage if they exist in the same living space with heterotrophic bacteria, and might be adversely affected by this ecological competition as well as by Cr^{+6} toxicity. That problem might be avoided by sequestering the nitrifying microorganisms in a given stage of a wastewater treatment system, Kang proposed. He added that more must be learned about the extent, if any, to which the biofilm adsorbs the chromium, and certain other factors involved in the fate and transport of the metal in fixed-film systems.

Methanogenic bacteria effects

There is an ongoing debate concerning how severe the effects of toxic substances may be on anaerobic fixed-film systems. Grady said that such systems are generally more sensitive to toxicants. He added that if the

Effect of time of exposure to CN^- on gas production

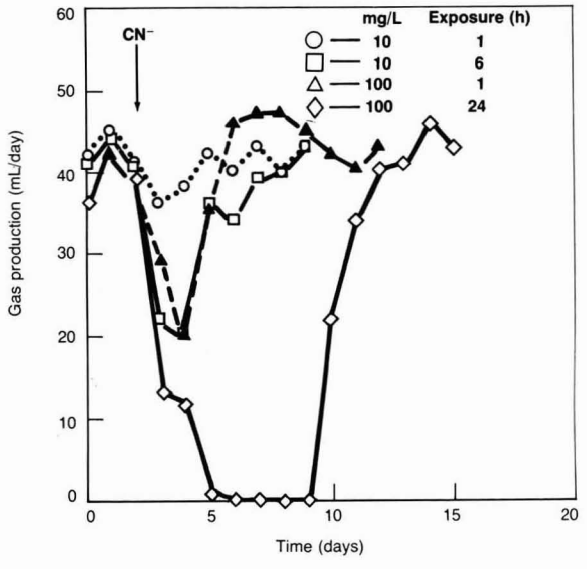

Source: Paper by Parkin and Speece, presented at Copenhagen, Denmark, seminar.

toxicants are inorganic, and especially metallic, no biomass will resist them; however, after an episode, it may be that a small amount of biomass may be left to regenerate, and may eventually restore the system to its former effectiveness. Not all agree with this assessment. Rittmann said that recent research indicates that toxicant effects on an anaerobic system may not be as adverse as originally estimated.

To test toxicant effects on both suspended-growth (activated-sludge) and attached-growth (fixed-film) anaerobic reactions, Speece exposed methanogenic bacteria in such reactions to a variety of poisons. The methanogen cultures were acetate-enriched, with acetate levels restored to 2000 mg/L each day. Toxicants selected were ammonium ion, chloroform, cyanide (CN^-), formaldehyde, nickel, and sulfide. If a toxicant has an adverse effect, methane production should decline, Speece said in a paper that he and Gene Parkin, also of Drexel, gave at last month's International Association for Water Pollution Research seminar at Copenhagen, Denmark.

It appears that while both suspended- and attached-growth systems are basically resilient, the FFB system comes back faster after an acute toxicant episode, particularly if effluent is not recycled. Speece found that prolonged periods of zero gas production "do not necessarily indicate actual or eventual process failure," and that "microorganism acclimatation to concentrations of toxicants as high as 10–25 times those which would inhibit unacclimated methanogens is sometimes possible." If toxicity is more chronic, fixed-film systems, if properly designed and built, can provide solids retention necessary to prevent biomass sloughing or washout prior to acclimation. In that event, effluent recycling may actually be beneficial because it allows a more gradual exposure to a toxicant, with better chances for successful microorganism acclimatation.

Possibly, genetic engineering will provide microbes tailor-made for various toxicants; system startup and recovery, as well as "bug" acclimation time could be materially reduced. With such microorganisms and faster startup time, many experts believe that a stable anaerobic system might have promise not only for municipal wastewater treatment, but for handling difficult industrial wastewaters.

—Julian Josephson

Additional reading

Särner, E. "Plastic-Packed Trickling Filters"; Ann Arbor Science Publishers, Inc.: P.O. Box 1425, Ann Arbor, Mich. 48106, 1980.

The Council on Environmental Quality: an enviable record in jeopardy

Michael R. Deland

In August 1970, President Nixon presented the first report of the Council on Environmental Quality (CEQ) to Congress. In it he stated, "It represents the first time in the history of nations that a people has paused, consciously and systematically, to take comprehensive stock of the quality of its surroundings."

The council was created on Jan. 1, 1970, when President Nixon signed into law the National Environmental Policy Act (NEPA) as his first official act of the decade. Throughout the Nixon, Ford, and Carter years, CEQ not only met its responsibilities in implementing NEPA and in reporting annually on the state of the environment, but it also helped to draft legislation and to bring policy leadership to a wide range of issues, including toxic substances control, acid rain, and global resource and pollution problems. It sponsored or cosponsored numerous farsighted reports ranging from "The Quiet Revolution in Land Use Control" (1971) to "The Global 2000 Report to the President" (1980). The council became the leading source of information and analysis on broad environmental policy matters, and was a crucial catalyst in ensuring that the 1970s were the "decade of the environment."

Reagan's redirection

The continuance of this enviable 11-year record appears to be in serious jeopardy, given the steps taken by the Reagan administration. The most damaging is the severe cut in the council's budget. The president has requested $926 000 for CEQ for fiscal 1983, nearly a two-thirds reduction from the $2.54 million allocated in the last fiscal year of the Carter administration.

The budget cuts have resulted in a drastic reduction in staff. Under Carter, the staff numbered approximately 50 persons, down from the high of 70 during the Nixon administration. Reagan's proposal would slash it to 15 positions, only 11 of which are currently filled. While no professional CEQ staff member had ever been terminated with any previous change in administration, Reagan chose to dismiss the entire professional staff, thereby eliminating experience and expertise that had been developing since the council's inception.

Equally telling of the priority now given the council is that the third council member slot has yet to be filled, and that for the first time in CEQ's history, its chairman is not invited to Cabinet meetings. Further, the Annual Report on the Environment, which routinely has appeared in January, is not scheduled to be published until this month.

Those familiar with CEQ's history question whether, given the budget cuts and loss in technical capability, it can continue to maintain the meaningful role it has played. Clearly, it cannot fulfill the directive first set forth by Nixon to coordinate the government's overall environmental research effort, "as well as to undertake its own environmental studies and research."

CEQ's reaction

The current council and staff members counter by asserting that in the past, CEQ exceeded its intended authority and became "a line, as opposed to a staff organization." Chairman Alan Hill recently set forth the priorities he envisions for the council. The first is to conduct a major review of NEPA by examining ways in which the environmental impact statement process might be streamlined. Toward this end, the council is scheduling public hearings during the course of the summer. Secondly, the council is assuming coordination of the president's acid precipitation task force; and thirdly, it is taking the lead role in an interagency working group studying global issues and policies. This latter group has been less than active to date, and appears to be starting from the premise that one of its main missions is to criticize the data and conclusions of the Global 2000 Report.

Finally, the council will continue to prepare the Annual Report on Environmental Quality. The first chapter of the soon-to-be-released 1981 report is an eloquent exposition of the Reagan philosophy that "perhaps the pendulum has swung too far in the direction of reliance on governmental regulation to solve environmental problems," and that the federal government in particular should reduce its role.

CEQ until recently was working toward achieving a status comparable to that of the Council of Economic Advisors. That clearly will not occur now. What remains to be seen is whether CEQ can meet the more limited responsibilities it has redefined for itself. The 1981 Annual Report and the upcoming NEPA hearings merit close scrutiny as indicators of whether CEQ still does have some viability, or whether it indeed now is an "empty shell," as many assert.

Deland writes this monthly column and is employed by ERT, Concord, Mass.

0013-936X/82/0916-0385A$01.25/0

ES&T FEATURES

A case history of the North Dakota PSD program

It has provided a flexible framework for state management of air quality

Myron F. Uman
National Research Council
Washington, D.C. 20418

One of the more controversial provisions of the Clean Air Act is Part C, Title 1, which establishes a program for the prevention of significant deterioration (PSD) of air quality in regions of the country that meet the national ambient air quality standards for protecting public health and welfare (*1*). Much of the controversy, at least since adjudication of the original suit in favor of the concept (*2*), has centered on the specific provisions of the PSD regulations promulgated by the U.S. Environmental Protection Agency (EPA) and on the process of implementation. Since 1974, the regulations have been challenged in court and subsequently revised a number of times; in the past few years reauthorization of the Clean Air Act has subjected the legislative provisions themselves to intense debate.

Major studies of the PSD program were conducted by the National Commission on Air Quality and the National Academy of Sciences (NAS), while position papers and recommendations for changes have been issued by the Business Roundtable, the National Environmental Development Association, and the National Clean Air Coalition, among others (*1*, *3–6*). The PSD program is intended to be carried out by the respective states through implementation plans each develops in accordance with its own needs. EPA then approves the state programs and provides technical assistance. To date, however, only six states have EPA-approved implementation plans for the PSD program, while 13 other states have been delegated authority to conduct full or partial review of applications for permits to construct new or modified facilities that produce major emissions in PSD areas (Table 1). EPA administers the PSD program in all other states. Even where EPA has delegated review authority, the regulations being enforced are, for the most part, the federal ones. Thus, chances are that views about how the PSD program has been implemented are influenced by EPA's enforcement of the federal regulations rather than by state implementation of programs designed to meet the needs and concerns of the respective states. The NAS report found that EPA was executing the PSD program in some ways that are contrary to congressional intent.

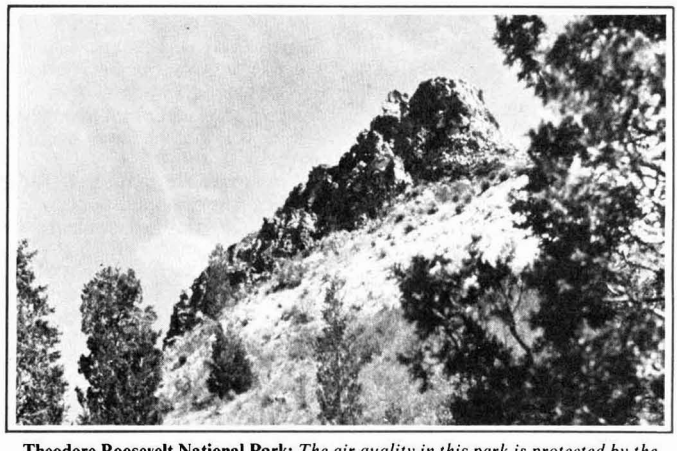

Theodore Roosevelt National Park: *The air quality in this park is protected by the PSD program in North Dakota.*

In this article, we summarize a case history of the PSD program in North Dakota. The purpose is to use this history to understand PSD, the problems encountered in its implementation, and the opportunities it provides for protecting air quality while accommodating industrial development.

We focus on the Class I increments at the Theodore Roosevelt National Park in the western part of the state. (An increment is the allowable increase in pollution levels that is not considered significant.) None of the serious proposals for changing the Clean Air Act includes elimination of Class I areas. Furthermore, this case involves most of the difficult problems likely to be encountered in a mature PSD program: Stringent limits on emissions have been required; new technology has been employed to meet these standards; the air quality has deteriorated enough to use up the Class I increment for the 24-h maximum concentration of SO_2; an offset has been used; the state encourages construction of a certain type of facility; and some major emitting facilities are relatively far from Class I areas, so long-range modeling must be employed. North Dakota is among the

0013-936X/82/0916-0386A$01.25/0

first states to be faced with carrying out those parts of the PSD program that come into play when increments are consumed.

North Dakota's PSD program

North Dakota's PSD regulations became effective in February 1976 and were first approved by EPA in May 1977 (*7*). They have subsequently been revised several times in response to changes in federal regulations. The state regulations are enforced by the State Department of Health (NDSDH) and parallel the federal program. Thus, lands are designated Class I, II, or III, with significant increments of degradation defined for each class of land; major sources are subject to emission limits defined according to what can be achieved with the best available control technology; and construction permits are issued on a first-come, first-served basis and are based on the results of modeling the effects of emissions on air quality. North Dakota has no Class III areas; it has two Class I areas—the Lostwood Wilderness area in the northern part of the state and the Theodore Roosevelt National Park, which comprises three separate parcels of land in the west.

There are, however, a few differences between the state and federal programs. For example, state regulations specify smaller increments of deterioration in Class II areas than the Clean Air Act allows (Table 2). Unlike the federal government, the state also considers sunflower oil processing plants to be major sources and has regulations under which lands may be reclassified by petition.

Theodore Roosevelt National Park was originally intended to commemorate the history of the region, but its natural resources are now widely believed to be its primary values. As a consequence, the park is managed to perpetuate an undisturbed prairie ecosystem rather than to preserve conditions that prevailed when Theodore Roosevelt ran the Elkhorn Ranch in the area. As many as one million people per year have visited the park; typically two-thirds of the visitors are from outside the state (*8*).

Extensive deposits of lignite, oil, and natural gas underlie central and western North Dakota (Figure 1). Reserves of lignite are currently estimated to be 16 billion tons; reserves of oil and gas, the equivalent of 700 million barrels. Strip mines, lignite-fired electric generating plants, plants to convert coal to synthetic gas and methanol, and plants to remove hydrogen sulfide from natural gas are examples of the types of industrial activities (operating, permitted, or planned) that exploit these resources and affect air quality in the park and over North Dakota.

The lignite in North Dakota has an average energy content of 6500 Btu/lb, with an average water content of 38% and a sulfur content ranging between 0.7 and 1.2% (9). The characteristics of the coal make long-distance transport uneconomical; hence, the preferred use is at the mouth of the mine. The availability of water is generally not a constraint in the

TABLE 1
Status of state PSD programs as of Nov. 1, 1980

EPA region	Approved PSD SIP	Full or partial delegation of PSD review to state	PSD administered completely by EPA
I	Maine, Vermont		Connecticut, Massachusetts, New Hampshire, Rhode Island
II			New York, New Jersey, Puerto Rico, Virgin Islands
III			Delaware, District of Columbia, Maryland, Pennsylvania, Virginia, West Virginia
IV	Georgia, Tennessee	Alabama, Florida, Kentucky, Mississippi, North Carolina, South Carolina	
V		Illinois, Indiana, Michigan, Minnesota, Ohio, Wisconsin	
VI			Arkansas, Louisiana, New Mexico, Oklahoma, Texas
VII		Nebraska	Iowa, Kansas, Missouri
VIII	North Dakota, Wyoming		Colorado, Montana, South Dakota, Utah
IX			Arizona, California, Guam, Hawaii, Nevada
X			Alaska, Idaho, Oregon, Washington

Source: Reference 1.

TABLE 2
PSD increments in North Dakota and in federal law

	Increment ($\mu g/m^3$)				
	Class I		Class II		Class III
Pollutant	Both federal and state	Variance	Federal	State	Both federal and state
Particulate matter					
Annual geometric mean	5	10	19	10[a]	37
24-h maximum	10	30	37	30[a]	75
Sulfur dioxide					
Annual geometric mean	2	15	20	15[a]	40
24-h maximum	5	191	91	91	182
3-h maximum	25	325	512	512	700

Source: Federal Clean Air Act as amended August 1977 (42 USC 1857 et seq.) and North Dakota State Department of Health Regulations, Chapter 33-15-15, 1978.

[a] The value contained in the original EPA regulations (of Dec. 3, 1974) was retained by the state after passage of the Clean Air Act amendments of 1977.

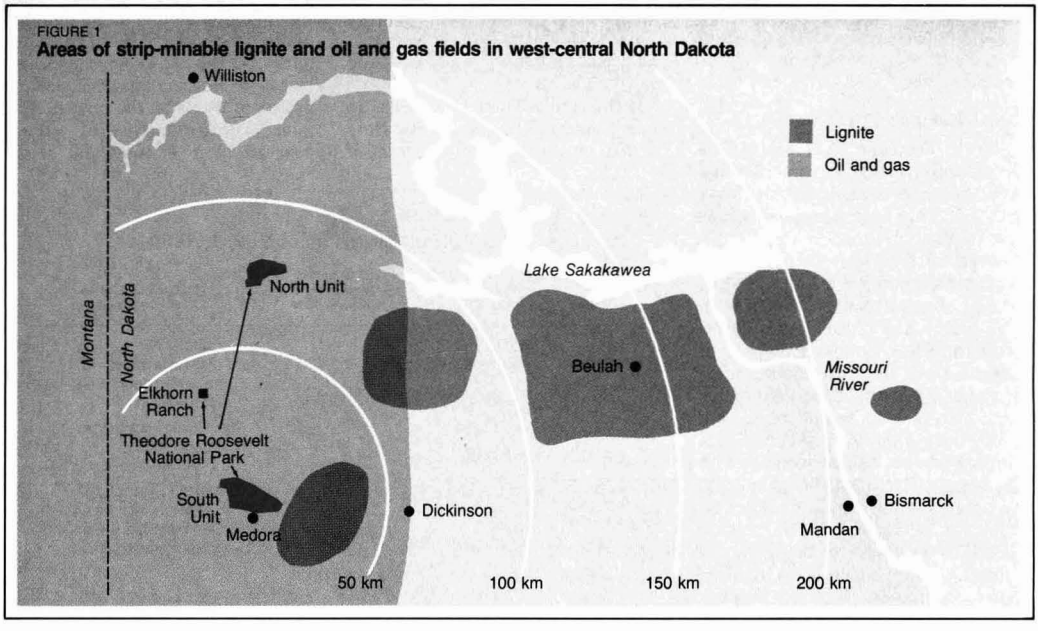

burning of lignite, which is currently mined at a rate of about 18 million tons per year.

In 1980 production of crude oil and natural gas in North Dakota exceeded 40 million barrels and 55 billion ft^3, respectively, and was valued at more than $800 million (*10*). The average well yields the equivalent of 41 barrels of oil per day. Some of the North Dakota gas is sour; that is, it contains quantities of hydrogen sulfide (H_2S) ranging up to nearly 23% by volume. To form pipeline quality gas the H_2S must be removed. The state has 11 natural gas processing plants. Gas that is not processed is flared, usually at ground level, so the H_2S is incinerated to sulfur oxides and water.

Status of the Class I increments

Air quality modeling by NDSDH indicates that the limiting factor in granting PSD construction permits in western North Dakota has been the 24-h Class I SO_2 increment (Table 2). In fact, calculations using EPA-approved models indicate that this increment has been used up in the south unit of the park by sources that now have PSD permits. A number of applications are pending until proposals to use state-of-the-art models that have not yet been incorporated into EPA modeling guidelines are either approved or disapproved. Figure 2 shows the locations of major sources with permits and with applications pending as of January 1982. The sources with permits are numbered in the order the permits were granted; those with applications pending are indicated by letters in the order that the completed applications were filed.

Determining emission limits

Early in the history of PSD in North Dakota, determinations of what comprised the best available control technology (BACT) for specific cases yielded emission limits equivalent to those provided by the applicable New Source Performance Standard (NSPS). Such was the case for the Coyote power plant (Figure 2). The NSPS was also applied to the Coal Creek station; the final application for a construction permit for this facility was granted after the state's PSD baseline date (Jan. 1, 1975), but before the PSD regulations were implemented. Hence, the Coal Creek application was not subjected to a PSD review; but the emissions from the Coal Creek station nevertheless were counted against the increments allowed under the PSD regulations.

No NSPS had been established for coal gasification plants, so emission limits for the Great Plains facility were set by using EPA guidelines and looking at in-plant processes such as liquid-fuel boilers, which are required to meet the NSPS.

BACT for Antelope Valley

When the application to construct Antelope Valley Units 1 and 2 was filed, modeling using EPA guideline models RAM and CRSTER indicated that emissions from the Coal Creek, Coyote, and Great Plains facilities increased the maximum 24-h concentration of SO_2 in the south unit of the park by 3.7 $\mu g/m^3$. The models also indicated that if Antelope Valley were subjected to the applicable NSPS, its SO_2 emissions would cause an increase of an additional 4 $\mu g/m^3$, thus causing the SO_2 increment, 5 $\mu g/m^3$, to be exceeded (Figure 3). To avoid this, modeling was used to determine that emissions from the Antelope Valley station should be restricted to a rate that is 67.5% below that of the applicable NSPS.

Basin Electric Power Cooperative, operator of Antelope Valley, had originally proposed to use wet scrubbers and electrostatic precipitators on the two units. The more stringent emission limit made it necessary to redesign the Antelope Valley pollution control program based on research Basin Electric had conducted at its Laramie River facility in Wyoming (*12*). As a result, BACT for Antelope Valley was determined to consist of spray-dry scrubbing and fabric filtration. A comparison of costs between the wet and dry scrubbing techniques for Antelope Valley showed a modest cost advantage for dry scrubbing (*12*). The actual cost advantage for the operating plant is of course uncertain.

An example of an offset

Emissions from the Stanton plant, built in 1966, were considered to be in the baseline for PSD purposes; that is,

FIGURE 2
Permitted and proposed major PSD sources in west-central North Dakota

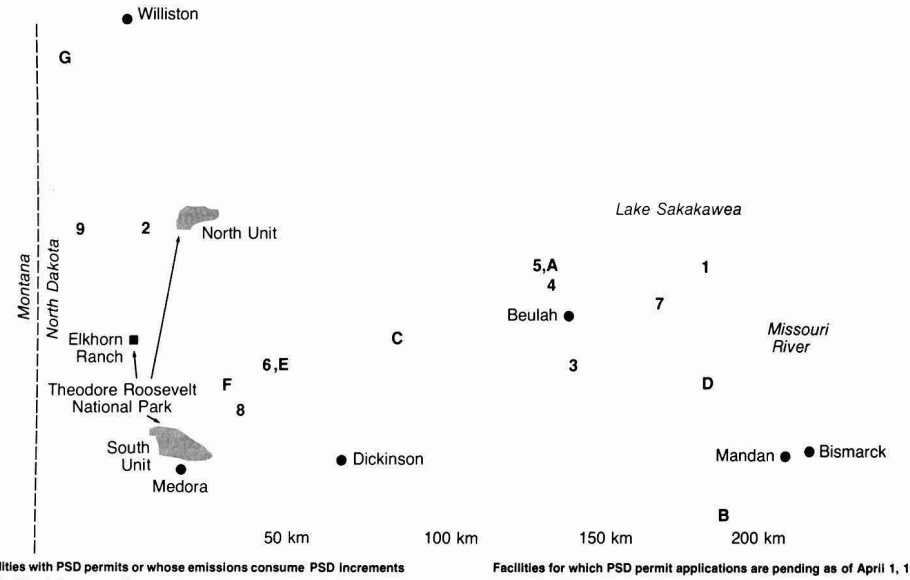

Facilities with PSD permits or whose emissions consume PSD increments

1. Coal Creek Generating Station, Units 1 and 2
2. Box Car Butte Natural Gas Processing Plant
3. Coyote Generating Station
4. Great Plains Gasification Plant
5. Antelope Valley Generating Station, Units 1 and 2
6. Little Knife Natural Gas Processing and Sulfur Recovery Plant
7. Stanton Generating Station, Supplemental Boiler
8. Teddy Roosevelt Natural Gas Processing and Sulfur Recovery Plant
9. McKenzie County Natural Gas Processing and Sulfur Recovery Plant

Facilities for which PSD permit applications are pending as of April 1, 1982

A. Antelope Valley Generating Station, Unit 3
B. Sunrise East Generating Station
C. Nokota Dunn County Methanol Plant
D. Minnesota Power and Light Generating Station
E. Little Knife Natural Gas Processing and Sulfur Recovery Plant Expansion
F. White Tail Natural Gas Processing and Sulfur Recovery Plant
G. Phillips Petroleum Natural Gas Processing and Sulfur Recovery Plant

these emissions contributed to the general air quality that existed when the PSD program began. Because of the high sodium content in the lignite burned by this plant, however, the boiler usually operated at less than rated capacity, which was 187 MW. To take advantage of the unused capacity of the turbine, United Power Association (UPA), operator of Stanton, proposed to add a supplemental boiler to obtain additional steam. The existing boiler had no controls for SO_2. Since emissions from Coal Creek, Coyote, Great Plains, and Antelope Valley were deemed to have used up the increment, emissions from a new 60 MW boiler would have exceeded the 24-h SO_2 increment at the south unit of the park by a significant amount.

To obtain its permit, UPA agreed to operate so that the total SO_2 emissions from the plant would be less than those from the fully rated, uncontrolled original boiler. That is, the existing boiler would not operate at more that 127 MW when the supplemental boiler operated at 60 MW. The supplemental boiler would use dry scrubbing and fabric filtration to achieve emission limits equivalent to NSPS. Thus, derating the original boiler would provide an "offset" for emissions from the supplemental boiler. It is not possible to tell if the combined emissions from the modified facility will in practice be less than those from the original plant, which could run only at something less than rated capacity. The state's decision, which was the result of negotiations and consultations with the operator, demonstrates flexibility in the implementation of PSD.

BACT for gas processing plants

Natural gas processing plants have the effect of reducing the total regional burden of SO_2, because the sulfur recovered from sour gas in such a plant (and marketed as a byproduct) would otherwise be emitted as SO_2 from ground-level flares. Flares may be minor sources; nonetheless, their contribution to consumption of increments should be counted. In practice, however, there are so many flared wells (about 200 in the vicinity of the park) that it is not practical to account for these sources. The gas processing plants may be considered controls on emissions from the wells that are connected to the plants and therefore environmental benefits. Thus, NDSDH has encouraged the development of such projects. For example, it has allowed construction to begin before a permit was granted in cases where increments were not likely to be threatened.

Three technologies are commonly available for controlling emissions from gas processing plants: the conventional Claus technology, a Claus unit with cold bed absorption (CBA), and a Claus unit with Scott tail gas cleanup (*13*). The technologies are listed in the order of increasing efficiency for sulfur removal, increasing cost, and increasing consumption of energy, some of which is usually supplied by diverting gas from the output of the plant. The Clean Air Act as amended in 1977 required BACT decisions to take account of energy, environmental, and economic impacts and other costs on a case-by-case basis. The dependability of the control equipment is also a consideration. NDSDH decisions on emission limits

for gas processing plants illustrate the inherent flexibility of BACT determinations.

The PSD review of the application for the Little Knife gas processing plant considered emissions from Coal Creek, Coyote, Great Plains, and Antelope Valley. Air quality models showed that emissions from Little Knife would not violate the PSD increments in the south unit of the park because of the geographical locations of the five facilities and the combination of meteorological conditions that comprise the worst case. Table 3 shows the results of analyzing the three technologies for Little Knife. Claus-CBA technology was determined to be the BACT in this case, because the Claus-Scott technology is only slightly more efficient and considerably more expensive to install and use. The Claus-CBA unit's greater efficiency in removing SO_2 seemed to justify its additional cost over the Claus technology.

The Box Car Butte gas processing plant first received a permit to operate in June 1976. The plant handles a small amount of gas per day, approximately 1.0 million ft^3, although it is permitted to process 6.0 million ft^3 per day. This facility was constructed after Jan. 1, 1975, but received a permit before the PSD regulations that now apply were implemented. Therefore, the Box Car Butte plant, like the Coal Creek Station, was not subjected to PSD review; but its emissions were counted against the PSD increments. It processes gas that contains relatively little H_2S (approximately 1% by volume). Given the low H_2S content and the small quantity of gas processed, the applicable ambient standards could be met without any sulfur recovery/control equipment other than a "flare" type stack.

The Teddy Roosevelt gas processing plant was proposed in March 1979. According to the original plan, this plant would handle gas from wells closer to the south unit of the park than were being flared at that time. Modeling showed that PSD increments would be exceeded in the south unit if the plant were built at the location originally proposed. With the help of the state, the plant's owner, Western Gas Processors, found a new location where emissions caused the 24-h SO_2 increment to be exceeded on only two days per year. One day of violation is permitted. On the second worst day, the total increase over baseline concentration due to all sources was calculated to be 5.04 $\mu g/m^3$, with 0.04 $\mu g/m^3$ attributed to the Teddy Roosevelt plant. The air quality effects analysis prepared by NDSDH states that contributions to consumption of an increment are not significant unless they equal or exceed one percent of the increment, which in the case of the 24-h Class I SO_2 increment is 0.05 $\mu g/m^3$. Because the plant would not cause a violation by a significant amount under this rule, the permit was granted for the corresponding level of emissions, which required only conventional Claus technology. NDSDH issued a variance to begin construction in May 1979 and a permit in July 1979. Table 4 gives the results of the NDSDH analysis of technologies for this facility.

The McKenzie County gas processing plant, proposed in mid-1980, was designed to process 60 million ft^3 of gas per day. As shown in Figure 2, the plant is on the west side of the north unit of the park. It gathers and processes gas from wells averaging approximately 4% H_2S by volume. It was determined through modeling that the Claus-CBA technology (98% SO_2 removal) was required to protect the Class I increments in the north unit, given emissions from the Box Car Butte facility and two gas processing plants in eastern Montana. Consequently, in October 1980 the McKenzie County plant received a construction permit with Claus-CBA technology as BACT.

Pending applications

A number of operators have submitted applications for construction permits that have yet to be approved. The approximate locations of the proposed facilities are indicated by letters in Figure 2. All the applications have been held in abeyance while NDSDH reviews the suitability of a number of state-of-the-art models for calculating the effects of emissions at large distances from the source.

Basin Electric has proposed both a third 500-MW unit for its Antelope Valley station and a new generating station, Sunrise East. The Sunrise East application, which consists of two 500-MW units, is currently inactive. The Nokota Company has proposed a 96 000-barrel-per-day synthetic methanol plant. Minnesota Power and Light Company has filed an application for an electric generating station that would consist of one 500-MW unit. The applicants have supported their applications with models that purport to show that the 24-h SO_2 increment in the south unit of the park would not be consumed. These results are contrary to the results obtained using the EPA guideline models.

Three additional applications for gas processing plants are pending: an expansion of the Little Knife facility, the White Tail plant proposed by

FIGURE 3
The PSD increment would be exceeded if the Antelope Valley Station used NSPS technology

Contributions to consumption of the 24-h SO_2 increment in the park from four facilities if the Antelope Valley Station uses NSPS technology.

Facility	(Location)	Contribution
Antelope Valley #1	(5)	2.0 $\mu g/m^3$
Antelope Valley #2	(5)	2.0 $\mu g/m^3$
Great Plains Gasification	(4)	1.6 $\mu g/m^3$
Coyote	(3)	0.7 $\mu g/m^3$
Coal Creek	(1)	1.4 $\mu g/m^3$

Contributions to consumption of the 24-h SO_2 increment in the park if BACT limits are imposed on the Antelope Valley Station.

Facility	(Location)	Contribution
Increment (5 $\mu g/m^3$)		
Antelope Valley #1 & 2	(5)	1.3 $\mu g/m^3$
Great Plains Gasification	(4)	1.6 $\mu g/m^3$
Coyote	(3)	0.7 $\mu g/m^3$
Coal Creek	(1)	1.4 $\mu g/m^3$

Amoco Production Company, and the Phillips petroleum plant in Williams County. The Phillips plant received a variance to begin construction during the fall of 1980.

Pre-1980 modeling procedures

Computer models that simulate atmospheric transport, dispersion, chemical transformation, and removal of air contaminants are used to analyze how emissions from proposed new sources will affect air quality. Before major new sources or new modifications to existing sources are built, modeling has been and remains the only tool available to determine their effect on air quality.

NDSDH requires applicants to perform air quality modeling studies and checks the applicants' work by performing its own modeling analyses. The state uses several research models, but historically has relied on EPA's Users Network for Applied Modeling of Air Pollution (UNAMAP) package for regulatory decision making. The most frequently used UNAMAP models are CDM, CRSTER, PTMTP, PTMAX, PTDIS, RAM, and VALLEY. CDM was designed to predict annual or seasonal concentrations in urban areas, but can be modified for rural areas. CRSTER is a model for estimating short-term (1-, 3-, and 24-h) maximum concentrations during a one-year period from a single rural plant. CRSTER also computes annual averages. PTMTP is a short-term model for multiple sources and receptors. RAM is a short-term model for point and area sources in rural settings. Even though it was not designed for this purpose, RAM is sometimes used to evaluate applications involving long-distance transport. PTMAX and PTDIS are short-term models for single sources in open country. VALLEY is a model for estimating maximum 24-h and annual concentrations from a single source in complex terrain. All of these models are intended for short-range (less than 50 km) applications (*11*).

Meteorological inputs to NDSDH models are based on hourly data taken during 1964, the last year for which hour-by-hour data are available. CRSTER and RAM use actual sequential hour-by-hour meteorological data for Bismarck or other stations. The data for Bismarck are used the most frequently because this city is the only one for which upper air data are available. Surface data are available for Dickinson, Minot, and Williston. Engineering data are supplied by the applicants.

The usual procedure has been to employ less complicated models as screening tools to determine the conditions for which the more complicated (and more costly) models are to be run. For example, in order to analyze the Antelope Valley application, CRSTER was employed to select the "worst case" meteorological conditions for the emissions from each of the previously permitted PSD sources and the proposed new source. Data for the "worst case" days were then used in the multiple-source RAM model to assess the combined effect of all the sources. Figure 3 summarizes the results of this combined analysis.

As indicated earlier, by 1978 computer modeling led NDSDH to conclude that allocations to the sources that had been granted PSD construction permits since 1975 (indicated by numbers in Figure 2) had consumed the 24-h Class I increment for SO_2 in the park on days with certain meteorological conditions (*14*). This conclusion implied that no additional sources could be given permits to construct and operate within the geographic corridor bounded by the units of the park and the sources located to the east of the park, unless provisions in the Clean Air Act for a waiver or variance were invoked (*1*).

Advances in computer modeling

Through 1979, NDSDH used steady-state models including RAM to project the effects of emissions on air quality in Class I areas. NDSDH recognized the limitations of these models, but applied them out of necessity in response to the requirement in federal and state PSD regulations to assess air quality deterioration (*14*). In addition, these models had been incorporated into EPA guidelines (*11*); alternatives were not available. More recently, newer models, suitable for medium range, mesoscale (50–250 km) applications have become available.

EPA guideline models are steady-state models designed for conditions leading to persistent directional transport of air contaminants from sources for distances less than 50 km (*11*). Wind speeds and directions, however, vary not only with time, but also from place to place. Furthermore, sources, especially those in North Dakota, are often distant (more than 50 km) from a PSD Class I area. The primary technical inadequacy of short-range steady-state models is recognized by EPA (*11*). For example, their guidelines suggest that the short-range models, such as CRSTER and RAM, should not be used to project ambient concentrations at distances greater than 50 km from sources. Clearly, where guideline models are not appropriate, it makes sense either to modify the best available guideline model or to substitute a more appropriate nonguideline model. North Dakota's PSD regulations provide this flexibility.

The state, however, has not had ac-

TABLE 3

Analysis of control technologies for the Little Knife gas plant processing 15 million ft^3/day

Technology	Sulfur recovery (%)	Installation cost (million dollars)	Annual energy costs (dollars)
Claus	97.5	1.5	44 000
Claus-CBA	99.25	2.0	51 000
Claus-Scott	99.99	4.0	212 000

Source: North Dakota State Department of Health (1978) Air Quality Effects Analysis of Warren Petroleum Natural Gas Processing Plant.

TABLE 4

Analysis of control technologies for the Teddy Roosevelt gas plant processing 15 million ft^3/day

Technology	Sulfur recovery (%)	Installation cost (million dollars)	Annual energy costs (dollars)
Claus	96.0	1.04	26 000
Claus-CBA	98.0	1.43	30 800
Claus-Scott	99.8	2.54	178 000

Source: North Dakota State Department of Health (1979) Air Quality Effects Analysis of Western Gas Processors, Ltd., Natural Gas Processing and Sulfur Recovery Plant.

cess to alternative models unless they are proposed in applications for air quality permits, and EPA has not yet attempted to assess the applicability of any mesoscale models. Since the time when the 24-h SO_2 Class I increment was determined to be consumed, three permit applications have been filed in which a nonguideline model was used in the required analysis. In addition, three other applications have been filed that applied guideline models to source-receptor distances greater than 50 km.

Of the applicants who submitted nonguideline mesoscale models, Basin Electric's application for a third unit at Antelope Valley employed the MESOHEFF model, as modified by Rockwell International (*15*). The Dames and Moore models DMSTRAM and RADM were submitted to support the application of the Nokota Dunn County methanol plant (*16*). In its application, Minnesota Power and Light used the MESOPUFF system of models developed by Environmental Research and Technology, Inc. (*17*).

NDSDH recognized that the state of the modeling art had advanced since the time when guideline models indicated the 24-h Class I SO_2 increment had been consumed. It also believed that a mesoscale model was conceptually more appropriate and that its use might show that part of the increment in the park was available. Therefore, at its discretion, NDSDH conducted an intensive evaluation of the mesoscale models in the three applications for the purpose of developing a mesoscale modeling procedure appropriate for use in reviewing air quality permit applications in North Dakota.

To conduct the evaluation, NDSDH acquired the three mesoscale model systems that were used in pending applications as well as the RTM model system developed by Systems Applications, Inc. (*18*). Test data furnished by the applicants were run by NDSDH to ensure that the models would reproduce the results obtained by the respective applicants. A technical comparison of the physical processes treated in the models was performed and all the models were tested for performance using a common set of hypothetical input data. Based on this analysis of the models submitted to the state and experience in applying them, NDSDH concluded that the MESOPUFF and RTM systems were better suited for PSD applications in North Dakota and that it was desirable to use MESOPUFF as a screening model and RTM in regulatory decision making (*19*).

These results were the subject of a public hearing in Bismarck on Sept. 1-3, 1981. All interested parties were invited to participate in the hearing and to comment on the results of the comparative evaluation. As a result of the hearing, the state agency reaffirmed its earlier conclusion regarding the appropriateness of MESOPUFF and RTM, but also concluded that modifications to these models would, if workable and reasonable, be desirable for typical applications in North Dakota. Among the desirable modifications are: incorporation of wet deposition; representation of transport winds at stack height, plume height, or the 850 millibar level; incorporation of methods to determine the depth of the mixing layer; use of a seasonally dependent, dry deposition rate; use of running averages; and use of different techniques for determining diffusion coefficients in near and far fields (*20*).

NDSDH is currently preparing to review the pending applications in light of its findings concerning an appropriate procedure for mesoscale modeling.

Conclusions

The PSD provisions of the Clean Air Act were intended to provide a framework for flexible state management of air quality consistent with two national goals—development of industrial capacity and energy resources and protection of highly valued clean air resources (*1*). The history of the implementation of PSD by the state of North Dakota, which ranks 45th among the states in population and 33rd in personal income, suggests thus far that PSD can be made to work as intended.

Before preparing an application, potential applicants are encouraged to consult NDSDH to clarify their needs, the status of the increment, and the technical details requiring attention in the application. These conferences are intended to facilitate the permitting process. In the case of gas processing plants, such conferences have led to variances that allow construction to begin while conditions of the permit are being determined. Construction variances have saved money for the operators, increased the supply of natural gas, and reduced the total burden of emissions to the atmosphere.

NDSDH has also demonstrated flexibility in determining BACT. Comparing the BACT requirements imposed on gas processing plants in North Dakota shows how balancing environmental, energy, and economic factors may yield different decisions in different cases. When economic costs and environmental effects held the potential for an unacceptable solution, the state was able to help the owner of the Teddy Roosevelt gas processing plant find an alternative site where environmental concerns would be satisfied within economic constraints. On the other hand, the technology-forcing characteristic of the BACT requirement led to the adoption of a new technology (dry gas scrubbing), which promises higher removal efficiencies and modestly lower costs than the traditional wet scrubbing (*1*).

The state agency has also demonstrated that it is possible to use offsets in administering PSD. Consumption of a Class I increment is likely to focus attention on the potential for obtaining offsets from baseline sources (sources in operation when the PSD program began). Such potential may exist in western North Dakota, but it remains to be seen whether firms holding that potential will be willing to trade or sell offsets to another operator or will retain the potential for their own future use.

Rather than emphasizing air quality-related values such as visibility or precipitation chemistry, the PSD process has so far focused on air quality modeling for Class I increments specified in the act. The EPA guideline models were accepted without question until increments appeared to be consumed. Then, all aspects of modeling—treatment of physical and chemical phenomena, input data, and interpretation of output—became subject to careful scrutiny. NDSDH was able to examine how well the nonguideline mesoscale models would apply to the North Dakota situation and, in the absence of guidance from EPA, adopt a more realistic modeling procedure.

Implementing PSD in North Dakota to protect air quality in a Class I area has involved both problems and opportunities typical of the program. The ability of a relatively small state to work flexibly with industry to find solutions that accommodate both industrial expansion and protection of air quality demonstrates that PSD can be an effective tool for achieving these two important national goals.

Acknowledgment

This work was begun with support from the U.S. EPA, contract No. 68-02-3354. The cooperation of personnel at NDSDH and of the operating companies is gratefully appreciated. In particular, Jay

Crawford, Martin Schock, and Dana Mount of NDSDH made significant contributions to this paper, providing technical information and advice. The opinions expressed, however, are my own.

Before publication, this article was read and commented on for appropriateness and suitability as an *ES&T* feature article by John H. Seinfeld, Associate Editor, *Environmental Science & Technology*, and Professor, Department of Chemical Engineering, California Institute of Technology, Pasadena, Calif. 91125; and Dr. James P. Lodge, consultant in atmospheric chemistry, Boulder, Colo. 80303.

References

(1) "On Prevention of Significant Deterioration of Air Quality"; National Academy Press: Washington, 1981.
(2) Sierra Club et al. vs. Ruckelshaus 344 F. Supp. 253 (D.D.C.) was affirmed on appeal Env. Rep. Cas. 1815 (D.C. Cir. 1972) and again affirmed by an equally divided Supreme Court 412 U.S. 541 (1973).
(3) "To Breathe Clean Air"; National Commission on Air Quality: Washington, 1981.
(4) "The Effects of Prevention of Significant Deterioration on Industrial Development", Vol. 2 of "The Business Roundtable Air Quality Project"; Arthur D. Little, Inc.: Cambridge, Mass., 1980.
(5) "Clean Air Act & Industrial Growth"; National Environmental Development Association: Washington, undated.
(6) "National Clean Air Coalition Positions on the Clean Air Act"; National Clean Air Coalition: Washington, 1981.
(7) North Dakota Century Code, Chapters 24-25 and Regulations of the North Dakota State Department of Health, Article 33-15.
(8) "Statement for Management of the Theodore Roosevelt National Park"; U.S. National Park Service, Rocky Mountain Region, December 1981.
(9) North Dakota Lignite Council, personal communication, March 1982.
(10) "1981 Facts and Figures—North Dakota Oil and Gas Industry"; North Dakota Petroleum Council: Bismarck, N.D., undated.
(11) "Guideline on Air Quality Models"; U.S. Environmental Protection Agency: Research Triangle Park, N.C., EPA-450/2-78-027, April 1978.
(12) Ericksen, R. L. "The Development of Dry Flue Gas Desulfurization at Basic Electric Power Cooperative," presented at *2nd Conf. Air Quality Manage. Electric Power Ind.*, Austin, Tex., 1980.
(13) "An Investigation of the Best Systems of Emissions Reduction for Sulfur Compounds from Crude Oil and Natural Gas Field Processing Plant"; U.S. Environmental Protection Agency, Research Triangle Park, N.C., revised April 1977.
(14) "Final West-Central North Dakota Regional Environmental Impact Study on Energy Development"; Bureau of Land Management, U.S. Department of the Interior, State of North Dakota, available from State Department of Health: Bismarck, 1978.
(15) Wang, I. T., Waldron, T. L.; Bushey, R. R. "A Mesoscale transport and dispersion model for industrial plumes," In *Proc. 2nd Joint Conf. Appl. Air Pollut. Meteorol.*, American Meteorological Society: Boston, 1980.
(16) Runchal, A. K. "A Random Walk Atmospheric Dispersion Model," In *Proc. 2nd Joint Conf. Appl. Air Pollut. Meteorol.*, American Meteorology Society: Boston, 1980.
(17) "User's Guide to MESOPAC"; U.S. Environmental Protection Agency, 1979, NTIS PB80-228042; "User's Guide to MESOPUFF"; U.S. Environmental Protection Agency, 1979, NTIS PB80-227796.
(18) "User's Guide to the Regional Transport Model"; Systems Applications, Inc.: San Raphael, Calif., 1980, SAI No. EF80-215.
(19) "Selection of a computer modeling procedure for the simulation of mesoscale ground level air quality concentrations"; North Dakota State Department of Health: Bismarck, N.D., 1981.
(20) "Background, findings of fact, and conclusions of law in the matter of the consideration of certain air quality models"; North Dakota State Department of Health: Bismarck, N.D., undated.

Myron F. Uman *is senior staff officer and associate executive secretary of the Environmental Studies Board of the National Academy of Sciences, National Academy of Engineering. He has been with NAS since 1973. He received his Ph.D. in electrical engineering from Princeton University in 1968.*

Sampling and analysis of mercury and its compounds in the atmosphere

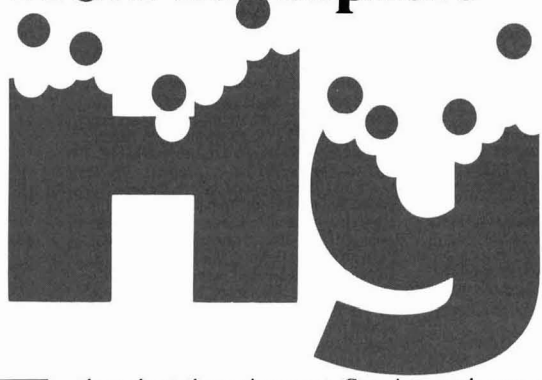

William H. Schroeder
Environment Canada
Downsview, Ontario, M3H 5T4

Since the late 1960s and early 1970s, growing recognition of the widespread occurrence and toxicological importance of mercury in the environment (Johnels et al., 1967; Friberg and Vostal, 1972; D'Itri, 1972) has generated a requirement for highly sensitive, selective, and reliable methods for determining this trace contaminant in a diverse array of environmental matrices. Instrumental methods of analysis have almost entirely replaced the cumbersome, classical wet chemical schemes. As a result of the foregoing as well as more recent investigations, both inorganic and organic chemical forms of mercury are now known to be extensively dispersed throughout the environment. Contributions to the atmospheric mercury burden come from both natural and anthropogenic emission sources (McCarthy et al., 1970; Eshleman et al., 1971; Van Horn, 1975).

The behavior and importance of Hg as an environmental contaminant are intimately related to the special physical, chemical, and toxicological features (Tables 1 and 2) of this "heavy metal" belonging to the Group IIB elements in the periodic table. Thus, for example, mercury is the only metal (and the only element besides bromine) that is liquid at ordinary room temperatures. As a consequence, the vapor pressure of mercury in its elemental state is substantial even at ambient temperatures.

In nature, mercury can be found in any one of three different oxidation states: elemental (0), mercurous (+1), and mercuric (+2). Except for their novelty, insofar as they involve a binuclear cation, the compounds of mercury (I) are typical metallic compounds. All are ionized in aqueous solution; however, most—with the no-

TABLE 1
Features of the toxicology of mercury and its compounds

Mercury is the only metal (and, besides bromine, the only element in the periodic table) that is a liquid at room temperature.
Mercury, in its elemental state and in several of its organometallic forms, is a highly volatile environmental contaminant.
Mercury and its compounds (both inorganic and organic types) are widely dispersed in the environment.
Organomercurials, particularly monomethyl mercury, are highly toxic.
Inorganic forms of mercury can be converted to highly toxic organic forms by microbial action in the biosphere.
Mercury and its compounds have a pronounced tendency to bioaccumulate in the food chain and ultimately in humans.

TABLE 2
Physical and chemical properties of Hg^0 influence its behavior and importance as an environmental contaminant [a]

Melting point	−38.9 °C
Boiling point	356.6 °C
Density	13.53 g/cm^3 at 25 °C
Vapor pressure	0.246 Pa at 25 °C (1.85×10^{-3} Torr)
Solubility	6.4×10^{-5} g/L H_2O at 25 °C
Ionization potentials	
1st	10.4 eV
2nd	18.7 eV
3rd	34.3 eV
Electrode potentials	
$Hg_2^{2+} + 2e^- \rightarrow 2Hg$	0.789 V
$Hg^{2+} + 2e^- \rightarrow Hg$	0.854 V
$2Hg^{2+} + 2e^- \rightarrow Hg_2^{2+}$	0.920 V
$Hg_2^{2+} \rightarrow Hg(\ell) + Hg^{2+}$	−0.115 V

[a] Falchuk et al., 1977; Krenkel, 1974; Levason and McAuliffe, 1977.

0013-936X/82/0916-0394A$01.25/0

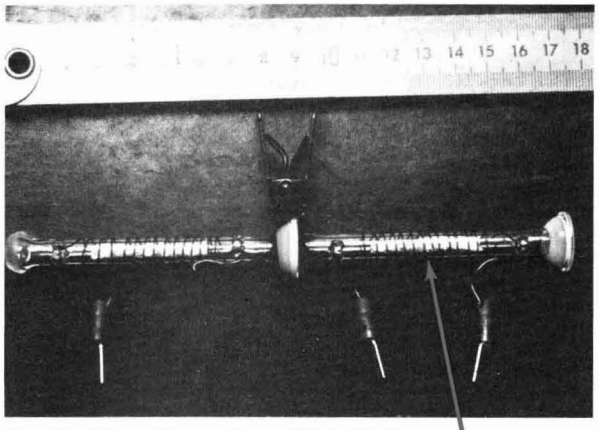

Sampling. *These collector tubes are filled with silver wool and are used for field sampling of atmospheric mercury.*

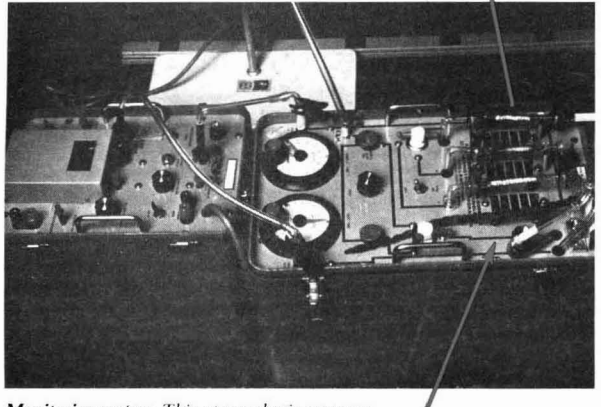

Monitoring system. *This atmospheric mercury monitoring system comprises a sampling module with two silver wool collector tubes in tandem and a detector module with a dual beam/cell UV spectrophotometer.*

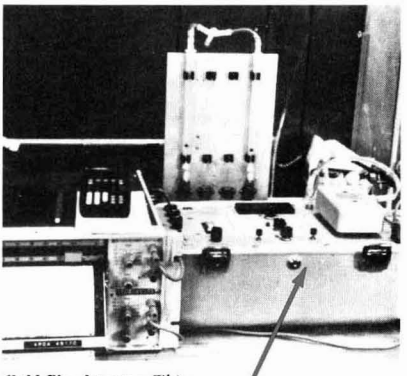

Gold film detector. *This portable mercury monitor utilizes a thin gold film detection technique; the detector output is displayed on a strip chart recorder.*

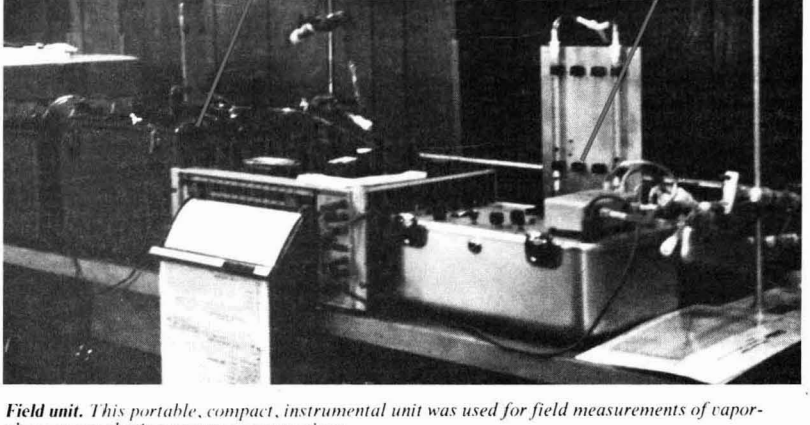

Field unit. *This portable, compact, instrumental unit was used for field measurements of vapor-phase atmospheric mercury concentrations.*

table exception of the nitrate and the perchlorate—are only sparingly soluble in water at ordinary temperatures. Another common feature of all mercury (I) salts is their tendency to disproportionate. Since mercury (I) does not form covalent bonds with other elements, organometallic derivates containing mercury in a +1 oxidation state are unknown. Probably the most characteristic property of mercury in its highest oxidation state is its tendency toward the formation of covalent rather than ionic bonds. Exceptions to this rule are the sulfate, the nitrate, and the perchlorate derivatives that are salts, being completely dissociated in aqueous solution and, by inference, in rain droplets or cloud water.

Despite the obvious importance of knowing the identity of the individual chemical species of mercury present in the atmosphere, only a few attempts have so far been made to separate and/or identify qualitatively the predominant compounds in ambient air (Campbell et al., 1973; Braman and Johnson, 1974; Soldano et al., 1975; Henriques and Isberg, 1975; Rawlings and Cooper, 1975). Based on the limited amount of information available to date, the principal mercury species found to be present in samples of ambient air are described in Table 3.

Vapor-phase mercury

Whereas conventional gaseous pollutants such as sulfur dioxide, carbon monoxide, and nitrogen oxides, for example, are usually present in ambient air at concentrations in the part-per-million (ppm) or part-per-billion (ppb) range, vapor-phase mercury concentrations encountered in the atmosphere are normally in the part-per-trillion (ppt) (v/v) or nanogram per cubic meter (w/v) range. Vapor-phase and/or particulate-phase mercury concentrations indicative of three "types of environments" (remote and rural areas, urban areas, and industrial sites) are summarized in Table 4.

Because of the low concentrations (trace to ultra-trace levels) of vapor-phase mercury found in remote, rural, and even urban settings, continuous real-time monitoring of vapor-phase mercury (or particulate-phase mercury, for that matter) is generally not practicable even with the most sensitive types of detectors currently available. Thus, for most ambient air measurements, in order to collect a sufficient amount of mercury for quantitative analysis, it is necessary to sample over a period of time generally ranging from a fraction of an hour up to 24 hours or more. The actual sampling period required is contingent upon the mercury concentrations encountered and the sensitivity of the analytical method employed. This cumulative (or integrated) sampling technique allows selective preconcentration of the mercury in the air stream being sampled. However, the resulting data quite often lack sufficient time resolution for investigations of temporal and/or spatial trends involving airborne mercury.

Sampling—vapor-phase mercury

Ambient air sampling for elemental mercury vapor and/or volatile mercury compounds has primarily involved threee techniques for collection and preconcentration:

- absorption into a liquid (e.g., aqueous $KMnO_4$)
- collection by a solid sorbent (e.g., charcoal)
- amalgamation on a metal surface (e.g., silver wool).

Selected information on these techniques is provided in Table 5.

For acceptable collection efficiencies at ambient temperature, with either absorption or adsorption techniques, sampling flow rates must be kept relatively low, typically in the range from several hundred mL/min to a few liters per minute ("low-vol" sampling regime). Using a suitable analytical methodology subsequent to the sampling step, the mercury collected is then determined:

- directly in the absorbing solution with the aid of a colorimetric reagent
- after stripping the mercury (in its elemental form) from the absorbing solution with a stream of inert carrier gas
- after solvent extraction or thermal desorption from a solid sorbent or noble metal surface.

The collection efficiencies of the various noble metals, solid sorbents, and absorbing solutions described in Table 5 have only been tested with respect to a selected few mercury species (Hg^0, $HgCl_2$, RHgCl, and RHgR with R being a methyl, ethyl, or phenyl moiety). None of the trapping media appear to have a collection efficiency of 100% even for the few species tested; nevertheless, most, if not all, are highly efficient in trapping at least elemental mercury.

In those instances where this parameter is desired, "total vapor-phase mercury" is most easily determined by subjecting the air sample to a pyrolysis step (with or without the use of a catalyst) followed by noble metal amalgamation of the elemental mercury

TABLE 3

Principal mercury species reported to be occurring in the atmosphere

Elemental mercury vapor	Hg^0
Mercury (II) chloride vapor (and possibly other volatile inorganic compounds)	$HgCl_2$
Organomercury compounds	
Methylmercuric chloride	CH_3HgCl
Dimethyl mercury	$(CH_3)_2Hg$
Particulate mercury—unknown inorganic and/or organic mercury species associated with airborne particulate matter/atmospheric aerosols	

TABLE 4

Summary of recent data on atmospheric mercury levels for various types of locations

Type of location	Concentration range (ng/m^3)	Mean value
REMOTE & RURAL AREAS		
Oceanic Particulate	<0.005–0.06	<0.15
Vapor	0.6–0.7	0.7
Terrestrial		
Nonmineralized		
Particulate	<0.005–2	0.15
Vapor	1–10	4.0
Mineralized		
Particulate + vapor	7–20 000	—
URBAN AREAS		
Particulate	<0.01–220	2.4
Vapor	0.5–50	7.0
INDUSTRIAL[a]	7–5 000 000	—

[a] These measurements include chlor-alkali plants, thermometer factories, smelters, and mercury mines.

Source: National Academy of Sciences, 1977.

TABLE 5

Overview of sampling methodology for vapor-phase mercury absorption into a liquid

Absorption into a liquid

Absorbing medium	References
Acidic permanganate solution	Henriques et al., 1973
$KMnO_4$—H_2SO_4	Makris et al., 1977
$KMnO_4$—HNO_3	Aruin, 1960
Iodine monochloride solution	Linch et al., 1968 *Federal Register*, 1971
Iodine/potassium iodide solutions	ACGIH, 1957 AIHA, 1969
Bromine, hypobromite, or chlorine solutions	Asperger & Murati, 1954
Carbonate–phosphate solution	Kimura & Miller, 1960
Ethyl alcohol	Burke et al., 1948 ACGIH, 1957
99% isopropyl alcohol	Quino, 1962
Sodium borohydride solution	Miller et al., 1975

Collection by a solid sorbent

Sorbing medium	References
Activated carbon/charcoal	Matsumura, 1974 Van der Sloot & Das, 1974 Trujillo & Campbell, 1975 Makris et al., 1977
Activated carbon/charcoal treated with acid or base	Braman & Johnson, 1974 Soldano et al., 1975
Activated charcoal/mineral wool impregnated with	Sargeant et al., 1957 Moffitt & Kupel, 1970
Iodine	Belozovskii et al., 1972
Ferric chloride	James & Webb, 1964
Palladium chloride	Windham, 1972
Cadmium sulfide	Corte & Dubois, 1973 Nguyen, 1979 Christie et al., 1967
Silica gel or alumina; coated with gold chloride	Campbell et al., 1973 Grosskopf, 1938
Hopcalite	Rathje & Marcero, 1976 McCullen & Michaud, 1978

Collection by a solid sorbent

Sorbing medium	References
Indicating papers impregnated with solutions of	Hemeon & Haines, 1961
Potassium iodide	Demidov & Mokhov, 1962
Copper iodide	Stitt & Tomimatsu, 1951
Selenium	Nordlander, 1927
Selenium sulfide	Beckman et al., 1948

Amalgamation on a metal surface

Metal	References
Silver (gauze, wool, wire, thin film/coating on a substrate having a large surface area)	Vaughan & McCarthy, 1964 Campbell et al., 1973 Corte et al., 1973 Long et al., 1973 Spittler, 1973 Braman & Johnson, 1974 Wroblewski et al., 1974 Corte et al., 1975 Gallay et al., 1975 Henriques & Isberg, 1975 APHA, 1977 Eberling et al., 1977 Mercer, 1979
Gold (foil, wire, chips, thin film/coating on a substrate having a large surface area)	Vaughan & McCarthy, 1964 Williston, 1968 Leong & Ong, 1970 Hoggins & Brooks, 1973 Baldeck et al., 1974 Braman & Johnson, 1974 Henriques & Isberg, 1975 Rawlings & Cooper, 1975 Scullman & Widmark, 1975 Eberling et al., 1977 Fitzgerald & Gill, 1979 Mercer, 1979 Slemr et al., 1979
Platinum	Thilliez, 1968 Henriques & Isberg, 1975
Palladium	Henriques & Isberg, 1975
Copper, zinc, cadmium, tin, lead, bismuth	Henriques & Isberg, 1975

liberated in the pyrolyzer. Thermal desorption is used ultimately to quantitatively release the mercury from the noble metal surface for the purpose of analysis.

All of the sampling techniques described so far are dynamic in nature. The application of passive sampling devices (i.e., dosimeter-type samplers) has not yet been reported for collection of elemental mercury or mercury compounds in outdoor atmospheres. Such sampling devices have a number of desirable features (including low cost, compact size, ruggedness, and portability) and deserve to be investigated for their suitability to atmospheric mercury monitoring. Unfortunately, with none of the foregoing procedures is it possible to obtain any information on the chemical form(s) in which mercury existed in the ambient air parcel that was sampled and subsequently analyzed. This is so because:

- Absorbing solutions are generally strongly acidic and highly oxidizing media that convert all of the trapped mercury into its highest (+2) state of oxidation.
- Temperatures required for thermal desorption of mercury compounds previously adsorbed onto a noble metal surface, such as gold, are sufficiently elevated to result in their complete dissociation (and liberation of the mercury entirely in its elemental state).
- The analytical methods most commonly employed require that all of the mercury present in the sample, irrespective of its actual chemical form or valence state, be quantitatively determined (after conversion if necessary) either as elemental mercury or as mercuric ion.

Sampling—particulate-phase mercury

We have previously seen that "background concentrations" for total vapor-phase mercury in the atmosphere are generally in the range of 1–10 ng/m^3, while in urban or industrialized localities it is not uncommon to encounter vapor-phase concentrations approaching 50 ng/m^3 of air. It is currently believed that, in remote areas, particulate-phase mercury accounts for no more than about 1–10% of the total atmospheric mercury burden, but may constitute a significantly larger fraction of the airborne mercury in urban and/or industrialized environments (Department of the Environment, U.K., 1976; National Academy of Sciences, 1977).

Thus, for example, an average concentration of 0.03 ng/m^3 particulate-phase mercury was found at an elevation of 3752 m at a remote site in the Swiss Alps, whereas concentrations in the range of about 0.2–30 ng/m^3 have been reported by various investigators for urban centers.

Reliable analytical determinations of mercury in suspended particulate matter at these concentrations require collection of large volumes of air. This is usually accomplished either by sampling at a high rate of filtration (typically 0.5–1.5 m^3 of air/min) for periods of a few hours to a few days, or alternatively by using a lower rate of throughput (anywhere from 5 L to 50 L of air/min) over a longer period of time (say, several days to several weeks). Sample collection techniques for suspended particulate matter in air that are based on these two approaches are commonly known as high-volume (or Hi-Vol) and low-volume sampling methods, respectively. For multi-element atmospheric trace metal determinations, Hi-Vol sampling techniques using various types of commercially available, off-the-shelf systems have traditionally been the method of choice.

Mercury (in its elemental state and/or as unknown inorganic or organic compounds) can become associated with atmospheric aerosols in a variety of ways, including:

- adsorption (physical or chemical) onto the surface of host particles
- incorporation into or intimate blending with host particles
- constituting the bulk of the individual particles
- dissolution in liquid droplets suspended in air.

The remainder of this discussion will focus exclusively on mercury associated with solid particles present in air (i.e., particulate-phase mercury); but analogous arguments and similar reasoning also apply to mercury that may be dissolved in droplets of liquid dispersed in air.

During the collection process with a Hi-Vol sampler, the particulate matter impacted and retained on the surface of the filter medium is continually subjected to the streaming effect of large volumes of air (with constantly changing physical and chemical characteristics) at a very high linear velocity. The conditions existing at the collecting face of the filter in a Hi-Vol sampler are undoubtedly drastically different from the environmental conditions previously surrounding the individual particles, and can be expected to be extremely conducive to desorption or volatilization of substances with even moderate vapor pressures associated with airborne particulate matter in one of the three modes previously described. In view of the well-known volatility of elemental mercury and a number of its environmentally significant compounds (e.g., organomercury compounds, mercuric chloride), the suitability of Hi-Vol sampling methods in the quantitative or qualitative determination of particulate-phase mercury (or for that matter other trace elements known to occur as volatile species in the environment, e.g., arsenic, selenium, lead, etc.) is open to serious doubt.

Methods of analysis for mercury

A truly astounding array of analytical methods and techniques has been proposed and used in the determination of mercury in a wide variety of "environmental" samples such as soils, sediment, sludge, water, ice, snow, fish, vegetables and other foodstuffs, as well as human hair, tissue, and blood. A number of excellent, comprehensive reviews of instrumental methods for mercury analysis have been published within the last 10 years (Friberg & Vostal, 1972; Reimers et al., 1973; Uthe & Armstrong, 1974; Chilov, 1975; National Academy of Sciences, 1977; Environment Canada, 1977; Jaworski, 1979). Although the number of instrumental methods and techniques successfully applied to the analysis of mercury and its compounds in ambient air samples is not quite as extensive, it is still rather impressive (Table 6). Whereas detailed descriptions, intercomparisons, or even examination of the pros and cons of all these techniques/methods is clearly beyond the scope of this paper, a few general comments and observations are warranted.

TABLE 6
Instrumental analytical methods that have been used to determine mercury in ambient air

Vapor-phase mercury
UV absorption spectrophotometry
Atomic absorption spectrophotometry (AAS)
Cold-vapor techniques
Zeeman method
Flame methods
Flameless methods (e.g., graphite furnace)
Atomic fluorescence spectrometry (AFS)
Atomic emission spectrometry (AES)
DC discharge
Microwave plasma
Gas chromatography (GC)
Mass spectrometry (MS)
Thin gold film resistance
Piezoelectric detection
Colorimetric methods
Electrochemical methods
Radiochemical techniques
Particulate-phase mercury
Instrumental neutron activation analysis (NAA)/gamma-ray spectrometry
X-ray fluorescence spectrometry
Pyrolysis/amalgamation/AAS or AFS
Plasma emission spectrometry DCP/ICP/MIP
Spark-source mass spectrometry (SSMS)
Proton induced X-ray emission spectrometry (PIXE)

For a number of reasons, including their sensitivity, selectivity, availability, reliability, and cost, ultraviolet (UV) and atomic absorption (AA) spectrophotometric methods have been the most popular instrumental techniques by far for the analysis of elemental mercury or gaseous mercury compounds present in the atmosphere (Barringer, 1966; Jepsen, 1973; Hadeishi et al., 1975; Oikawa, 1977; Siemer, 1978). These methods are based on the fact that elemental mercury vapor has a very strong (resonance) absorption line at 253.65 nm in the UV region of the electromagnetic spectrum. Consequently, instruments using this principle of detection respond only to that portion of total atmospheric mercury that exists in the elemental state. To be detected, combined forms of mercury must first be converted to elemental mercury vapor (e.g., by pyrolysis).

Several AA spectrophotometric techniques have been developed over the years and have found application in atmospheric trace metal analysis. They include cold-vapor techniques, flame as well as nonflame or flameless methods, and the so-called Zeeman AA method, which involves the application of a suitable magnetic field to split the energy levels of the mercury vapor in the low-pressure discharge lamp serving as the radiation source in the spectrophotometer. The Zeeman effect thus generates a reference signal used in correcting for broad-band absorption due to certain interfering substances. Without the application of special techniques such as the Zeeman effect, the pressure-broadening principle described by Barringer (1966), or the use of double-beam UV spectrophotometers with a mercury-scrubbing agent in the reference beam, a large number of substances can exert an in-

terfering effect in the spectrophotometric methods. Some substances potentially capable of attenuating the intensity of UV light having a wavelength of 254 nm, either by scattering or absorption of electromagnetic radiation, are listed in Table 7.

TABLE 7
Substances potentially capable of attenuating UV light at a wavelength of 254 nm [a]

Smoke	Benzene
Soot	Toluene
Fine particulates	*p*-Xylene
Water vapor	Acetone
Sulfur dioxide	Ethanol
Hydrogen sulfide	Chloroform
Ozone	Dioxane
Nitrogen dioxide	Pyridine
	Ethyl acetate

[a] Mayz et al., 1971; U.S. Dept. of H.E.&W., 1969; Long et al., 1973; Corte and Dubois, 1973.

Atomic fluorescence spectrometry (AFS) involves excitation of analyte mercury atoms in the vapor phase by resonance radiation from a mercury lamp followed by detection of the resulting resonance emission (fluorescence) at a wavelength of 253.7 nm. AFS is reported to be more sensitive than AAS by at least one order of magnitude (Subber et al., 1974). Part of this increased sensitivity is derived from the fact that the AA signal is determined as a very small difference between two relatively large signals, whereas with AFS the emitted radiation that represents the analytical signal is determined directly against a much lower background spectrum.

As mercury and its compounds are generally present in the atmosphere only as trace constituents, the detection limit of an analytical technique represents an important parameter in establishing its suitability and usefulness for most investigations into the atmospheric pathways of this heavy metal. Detection limits of various instrumental methods applied to mercury analysis as reported by Reimers et al. (1973) and Chilov (1975) have been summarized in Table 8.

TABLE 8
Detection limits of various instrumental methods applied to mercury analysis

Analytical method	Detection limit (ng) as quoted by Reimers et al., 1973	Detection limit (ng) as quoted by Chilov, 1975
Cold-vapor AA	1	1
Flame atomic absorption	20	20
Atomic fluorescence	—	3 [a]
Atomic emission	1	2
GC with EC detector	—	0.1 [b]
Mass spectrometry (SSMS)	1	—
Thin gold film resistance	—	0.05 [c]
Colorimetry	200	50
Polarography	1000	50
Neutron activation	0.1	0.5
X-ray fluorescence [d]	1	1

[a] Flame method. [b] For alkyl mercury compounds. [c] Elemental mercury vapor. [d] With preconcentration.

Summary

In this article the author has presented and discussed various procedures, principles, and techniques used in sampling and analysis of mercury and its compounds in the atmosphere. For the majority of ambient air measurements, collection of an integrated sample or sampling with preconcentration is a necessary prerequisite for chemical analysis of airborne mercury either in the particulate phase or in the vapor phase. Whereas some information now exists about the principal volatile mercury species likely to be encountered in the atmosphere, very little is known about the chemical identity of mercury associated with airborne particulate matter or atmospheric aerosols. Knowledge regarding the mercury species found on the surface of suspended particulate matter is important, for example, in selecting suitable sampling conditions and in determining the extent of the health hazard posed by mercury-bearing particles present in ambient air. This knowledge could also provide important clues about the origin of such particles.

In view of the plethora of sampling and analytical methods or techniques described in papers, patents, journal articles, books, or government reports and used over the years by their proponents as well as other investigators to generate data pertaining to mercury in air, the desirability of standardizing measurement procedures in this area should be obvious. Standardization of methods and techniques relating to sampling, sample treatment, calibration, analysis, and interpretation/reporting of data is an extremely significant step in promoting and ensuring comparability and compatibility of laboratory and field data for mercury.

Hybrid methods such as gas chromatography/mass spectrometry or gas chromatography coupled with highly sensitive and selective detection techniques such as cold-vapor AAS or AFS, or plasma emission spectrometry hold tremendous potential for obtaining much-needed, reliable analytical data on the chemical species of mercury (and other volatile trace metals) of significance in the atmosphere. Eventually, laser-based spectroscopic techniques can be expected to achieve real-time, in situ detection, identification, and quantitation of individual mercury species through their characteristic absorption and/or emission spectra, which can serve as "chemical fingerprints" for these substances when present in ambient air.

After graduating with a B.Sc. in chemistry from the University of Calgary, **William H. Schroeder** *attended the University of Colorado where he obtained his Ph.D. in 1971. His thesis research, directed by Professor Paul Urone, involved investigations of reaction kinetics, mechanisms and products formed during thermal and photochemical reactions of sulphur dioxide, nitrogen dioxide, and ethylene in air. Prior to joining Environment Canada in 1973, he spent a year at the Fresenius Institute in Wiesbaden, West Germany, as a postdoctoral fellow. Within Environment Canada, Schroeder has worked in both the Air and the Water Pollution Control directorates and has been with the Atmospheric Environment Service in Downsview since November 1977. His current research*

activities are directed towards toxic trace metals in air, particularly mercury.

References

ACGIH. *Am. Conf. Govt. Ind. Hyg.* "Manual of Analytical Methods.—Recommended for Sampling and Analysis of Atmospheric Contaminants", **1957.**

AIHA. *Am. Ind. Hyg. Assoc. J.* **1969,** *30,* 327.

APHA Intersociety Committee. In "Methods of Air Sampling and Analysis," 2nd ed.; Katz, M., Ed.; American Public Health Association: Washington, 1977; pp. 488–492.

Aruin, A. S. In "Survey of U.S.S.R. Literature on Air Pollution and Related Occupational Diseases"; Levine, B. S., Ed.; Inst. for Applied Tech., National Bureau of Standards: Washington, 1960; Vol. 3, pp. 18–20.

Asperger, S.; Murati, I. *Anal. Chem.* **1954,** *26*(3), 543–545.

Baldeck, C. M.; Kalb, G. W.; Crist, H. L. *Anal. Chem.* **1974,** *46*(11), 1500–1505.

Barringer, A. R. *Inst. Mining Metall. Trans., Sect. B* **1966,** *75*(714), 120–124.

Beckman, A. O.; McCullough, J. D.; Crane, R. A. *Anal. Chem.* **1948,** *20*(7), 674–677.

Belozovskii, A. B.; Fedorov, A. A.; Ketov, A. N. *Khim. Khim. Tekhnol.* **1972,** *15*(3), 368–370; *Chem. Abstr.* **1972,** *77*, 9944h.

Braman, R. S.; Johnson, D. L. *Environ. Sci. Technol.* **1974,** *8*, 996–1003.

Burke, W. J.; Moskowitz, S.; Dolin, B. H. *Ind. Air Anal.* **1948,** *3*(M), 22.

Campbell, E. E.; Trujillo, P. E.; Wood, G. O. "Development of a Multi-Stage Tandem Air Sampler for Mercury"; Los Alamos Scientific Laboratory: New Mexico, 1973; Report No. LA-5467-PR.

Campbell, E. E.; Wood, G. O.; Trujillo, P. E.; Stein, P. "Evaluation of Methods for Determining Mercury"; Los Alamos Scientific Laboratory: New Mexico, 1973; Project R-060, Report No. LA-5188-PR.

Chilov, S. *Talanta* **1975,** *22*, 205–232.

Christie, A. A.; Dunsdon, A. J.; Marshall, B. S. *Analyst* **1967,** *92*(1092), 185–191.

Corte, G. L.; Dubois, L. "Application of Selective Absorbers in the Analysis of Mercury in Air," presented at the *68th Ann. APCA Meeting*, Chicago, Ill., 1973.

Corte, G.; Dubois, L.; Monkman, J. L. *Sci. Total Environ.* **1973,** *2*(1), 89–96.

Corte, G. L.; Thomas, R. S.; Lao, R. C.; Dubois, L. *Mikrochim. Acta* **1975,** 533–538.

Demidov, A. V.; Mokhov, L. A. In "Survey of U.S.S.R. Literature on Pollution and Related Occupational Diseases"; Levine, B. S., Ed.; Inst. for Appl. Tech., Natl. Bureau of Stds.: Washington, D.C., 1962; Vol. 10, p. 114.

Department of the Environment (U.K.). "Environmental Mercury and Man," Report of an Inter-Departmental Working Group on Heavy Metals; Pollution Paper No. 10; Her Majesty's Stationery Office: London.

D'Itri, F. M. "The Environmental Mercury Problem"; Chemical Rubber Company: Cleveland, Ohio, 1972.

Eberling, C.; Geins, W.; Slemr, F.; Seiler, W. "A Method for Measurements of Mercury in the Atmosphere and Some Results of the Global Hg-Distribution." In "Air Pollution Measurement Techniques—Special Environmental Report No. 10."; WMO Publication No. 460, 1977.

Environment Canada. "Mercury: Methods for Sampling, Preservation and Analysis," report of the Mercury Sampling and Analysis Review Committee to the Environmental Contaminants Program Steering Committee of Fisheries and Environment Canada, 1977.

Eshleman, A.; Siegel, B. Z.; Siegel, S. M. *Nature* **1971,** *233*, 471–472.

Falchuk, K. H.; Goldwater, L. J.; Vallee, B. L. In "The Chemistry of Mercury"; McAuliffe, C. A., Ed.; MacMillan of Canada/MacLean-Hunter Press: Toronto, 1977; Part 4, p. 262.

Fed. Regist. **1971,** *36*(234), 23, 246.

Fitzgerald, W. F.; Gill, G. A. *Anal. Chem.* **1979,** *51*(11), 1714–1720.

Friberg, L.; Vostal, J., Eds. "Mercury in the Environment—An Epidemiological and Toxicological Appraisal"; CRC Press; Cleveland, Ohio, 1972.

Gallay, W.; Egan, H.; Monkman, J. L.; Truhaut, R.; West, P. W.; Widmark, G. "Determination of Mercury in Air," In "Environmental Pollutants—(SCOPE 6)"; Ann Arbor Science Publishers, Inc.: Ann Arbor, Mich., 1975; pp. 165–171.

Grosskopf, K. J. *J. Ind. Hyg. Toxicol.* **1938,** *20*, 21A.

Hadeishi, T.; Church, D. A.; McLaughlin, R. D.; Zak, B. D.; Nakamura, M.; Chang, B. *Science* **1975,** *187*(4174), 348–349.

Hemeon, W. C. L.; Haines, G. F., Jr. *Am. Ind. Hyg. Assoc. J.* **1961,** *22*, 75–79.

Henriques, A.; Isberg, J. *Chemica Scripta* **1975,** *8*(4), 173–176.

Henriques, A.; Isberg, J.; Kjellgren, D. *Chemica Scripta* **1973,** *4*(3), 139–112.

Hoggins, F. E.; Brooks, R. R. *J. Assoc. Off. Anal. Chem.* **1973,** *56*(6), 1306–1312.

James, C. H.; Webb, J. S., *Bull. Inst. Mining Metall. (G.B.)* **1964,** *73*, 633, 691.

Jaworski, J. F., "The Determination of Mercury and Its Compounds," In "Effects of Mercury in the Canadian Environment"; NRC Publication No. 16739, 1979; pp. 188–200.

Jepsen, A. J. "Measurements of Mercury Vapor in the Atmosphere," In "Trace Elements in the Environment"; Advances in Chemistry Series 123, Am. Chem. Soc.: Washington, 1973; Chap. 5, pp. 81–95.

Johnels, A. G.; Westermark, T.; Berg. W.; Persson, P. I.; Sjostrand, B. *Oikos* **1967,** *18*, 323–333.

Kimura, Y.; Miller, V. L. *Anal. Chem.* **1960,** *32*(3), 4240–4244.

Krenkel, P. A. *CRC Crit. Revs. Environ. Control* **1974,** *4*(3), 251–339.

Leong, P. C.; Ong, H. P. *Anal. Chem.* **1970,** *43*, 940–941.

Levason, W.; McAuliffe, C. A. In "The Chemistry of Mercury"; McAuliffe, C. A., Ed.; MacMillan of Canada/MacLean-Hunter Press: Toronto, 1977; Part 2, p. 50.

Linch, A. L.; Stalzer, R. F.; Lefferts, D. T. *Am. Ind. Hyg. Assoc. J.* **1968,** *29*(1), 79–86.

Long, S.J.; Scott, D. R.; Thompson, R. J., *Anal. Chem.* **1973,** *45*(13), 2227–2233.

Makris, W. E.; Crawford, C. J.; Miller, R. O.; Bell, Z. G., Jr. "The Comparison of Five Published Methods for the Determination of Mercury-in-Air," presented at *4th Joint Conf. Sensing Environ. Poll., New Orleans*, November 1977.

Matsumura, Y. *Atmos. Environ.* **1974,** *8*(12), 1321–1327.

McCarthy, J. H.; Meuschke, J. R.; Ficklin, W. H.; Learned, R. E. "Mercury in the Environment," U.S. Department of the Interior, Geological Survey Professional Paper 713, 1970; p. 37.

McCullen, R. E.; Michaud, M. T. *Am. Ind. Hyg. Assoc. J.* **1978,** *39*(8), 684–687.

Mercer, T. T. *Anal. Chem.* **1979,** *51*(7), 1026–1030.

Miller, J. A.; Schmidt, F. J.; Natusch, D. F. S.; Thorpe, T. M. "Total and Inorganic Mercury Analysis by Sequential Borohydride Reduction and Flameless Atomic Absorption Spectrometry," presented at *26th Pittsburgh Conf. Anal. Chem. Appl. Spectrosc., Cleveland*, March 1975.

Moffitt, A. E., Jr.; Kupel, R. E. *Atmos. Absorption Newsletter*, **1970,** *9*(6), 113–118.

National Academy of Sciences. "An Assessment of Mercury in the Environment," Report prepared by the Panel on Mercury of the Coordinating Committee for Scientific and Technical Assessments of Environmental Pollutants; National Research Council: Washington, 1977.

Nguyen, X. T. *J. Air Pollut. Control Assoc.* **1979,** *29*(3), 235–237.

Nordlander, B. W. *Ind. Eng. Chem.* **1927,** *19*, 518.

Oikawa, K. "Trace Analysis of Atmospheric Samples"; John Wiley & Sons: New York, 1977; pp. 113–119.

Quino, E.-A. *Am. Ind. Hyg. Assoc. J.* **1962,** *23*(3), 231–234.

Rathje, A. O.; Marcero, D. H. *Am. Ind. Hyg. Assoc. J.* **1976,** *37*(5), 311–314.

Rawlings, G. D.; Cooper, H. B. H., Jr. "Organic, Elemental, and Particulate Mercury in Urban Atmospheres," presented at *Specialty Conf. Ambient Air Quality Measurements, Austin, Tex.*, March 10–12, 1975.

Reimers, R. S.; Burrows, W. D.; Krenkel, P. A. *J. Water Pollut. Control Fed.* **1973,** *45*, 814–828.

Sargeant, G. A.; Dixon, B. E.; Lidzey, R. G. *Analyst* **1957,** *82*, 27–33.

Scullman, J.; Widmark, G. In "Analytical Aspects of Mercury and Other Heavy Metals in the Environment"; Frei, R. W.; Hutzinger, O., Eds.; Gordon and Breach Science Publishers: New York, 1975; pp. 69–76.

Siemer, D. D. *Environ. Sci. Technol.* **1978,** *12*(5), 539–543.

Slemr, F.; Seiler, W.; Eberling, C.; Roggendorf, P. *Analyt. Chim. Acta*, **1979,** *110*, 35–47.

Soldano, B. A.; Bien, P.; Kwan, P. *Atmos. Environ.* **1975,** *9*, 941–944.

Spittler, T. M. "A System for Collection and Measurement of Elemental and Total Mercury in Ambient Air over a Concentration Range of .004 to 25 $\mu g/m^3$," presented at *165th Natl. Mtg., Am. Chem. Soc., Dallas*, 1973.

Stitt, F.; Tomimatsu, Y. *Anal. Chem.* **1951,** *23*, 1098.

Subber, S. W.; Fihn, S. D.; West, C. D. *Am. Lab.* **1974,** *6*(11), 38–40.

Thilliez, G. *Chim. Anal. (Paris)* **1968,** *50*(5), 226–232.

Trujillo, P. E.; Campbell, E. E. *Anal. Chem.* **1975,** *47*(9), 1629–1634.

Uthe, J. F.; Armstrong, F. A. J. *Toxicol. & Environ. Chem. Revs.* **1974,** *2*, 45–77.

Van der Sloot, H. A.; Das, H. A. *Analyt. Chim. Acta* **1974,** *70*, 439–442.

Van Horn, W. "Materials Balance and Technology Assessment of Mercury and its Compounds on National and Regional Bases," Prepared for U.S. Environmental Protection Agency, Report No. EPA 560/3-75-007, 1975.

Vaughan, W. W.; McCarthy, J. H., Jr., "An Instrumental Technique for the Determination of Submicrogram Concentrations of Mercury in Soils, Rocks, and Gas," U.S. Geol. Survey, Prof. Papers 501-D, D 123-7, 1964.

Williston, S. H. *J. Geophys. Res.* **1968,** *73*(22), 7051–7055.

Windham, R. L. *Anal. Chem.* **1972,** *44*(7), 1334–1336.

Wroblewski, S. C.; Spittler, T. M.; Harrison, P. R. *J. Air Pollut. Control Assoc.* **1974,** *24*(8), 778–781.

ES&T
CRITICAL REVIEW

Statistical distributions of air pollutant concentrations

The authors present methodologies and limitations in describing air quality through statistical distributions of pollutant concentrations, and explain the use of extreme statistics in the evaluation of different forms of air quality standards, as well as the interpretation of rollback calculations with regard to such standards

Panos G. Georgopoulos
John H. Seinfeld
Department of Chemical Engineering
California Institute of Technology
Pasadena, Calif. 91125

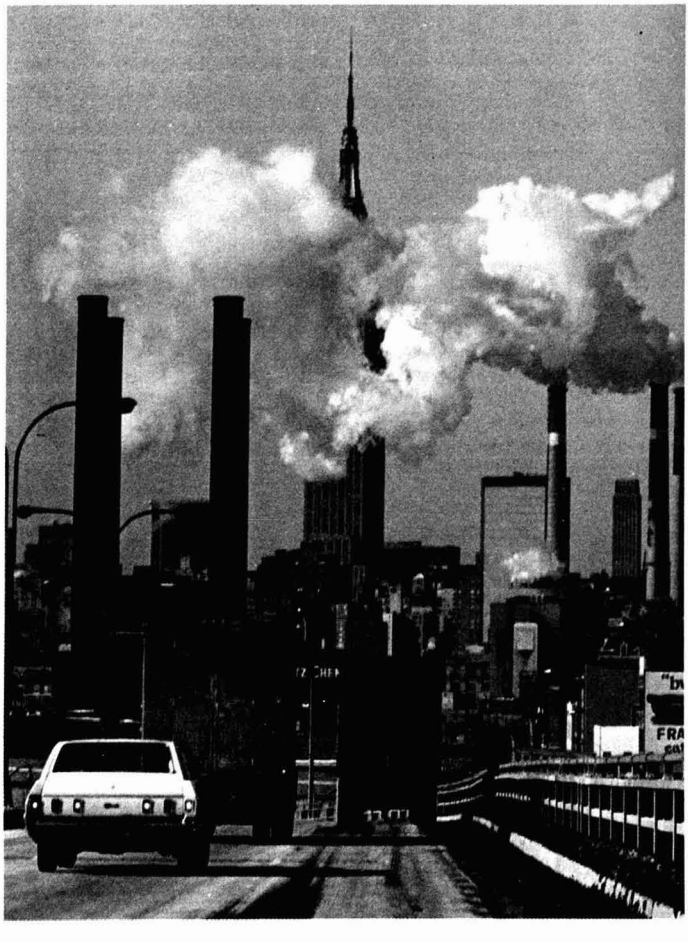

Air pollutant concentrations are inherently random variables because of their dependence on the fluctuations of a variety of meteorological and emission variables. When sets of air quality data are available, various statistical characteristics can be determined and assigned to the pollutant concentrations.

If certain assumptions are made, this statistical information can be incorporated into distribution functions and thus be used in an organized and efficient manner thereafter; specific types of distributions, like the log-normal and the Weibull, have been proved particularly useful in such treatments.

With respect to air quality standards, extreme events are usually of the most interest. The proper description of these events requires taking into account characteristic random variables such as maximum concentrations, frequencies of exceedances of critical levels, etc. The tools appropriate for a relevant analysis are provided by the order (or extreme) statistics theory. Using elementary results of this analysis, one can evaluate alternative forms of air quality standards and examine how statistical distribution theory complies with simple roll-

0013-936X/82/0916-0401A$01.25/0

back calculations in determining levels of emission control.

Air quality data

Air quality data are usually available as sets of successive observations of concentrations measured sequentially in time at some specific location, and (usually) averaged over successive equal nonoverlapping time periods. These data constitute statistical (nondeterministic) *time series* of the discrete form

$$x_\tau(t_1), x_\tau(t_2), \ldots, x_\tau(t_n); \quad t_1 < t_2 < \ldots < t_n$$

where $\tau = t_2 - t_1 = t_3 - t_2 = \ldots = t_n - t_{n-1}$ is the averaging time, and t_i is the index for the time period over which the averaging is done, arbitarily set equal to the beginning of the period. The above time series can be viewed as a *sample realization* from an infinite population of random concentrations generated by a stochastic process

$$c_\tau(t_1), c_\tau(t_2), \ldots, c_\tau(t_n); \quad t_1 < t_2 < \ldots < t_n$$

(Note: Random variables are ordinarily denoted by capital letters and the values they assume by lower case letters. This convention will not be followed here; rather, lower case c will be used to denote the random concentration.)

The length of the averaging time τ affects the degree of correlation of successive data points, $x_\tau(t_i)$. (Concentrations averaged over long periods of time tend to be less correlated than concentrations averaged over shorter successive intervals.) The information in the data $\{x_\tau(t_i)\}$ can be organized by various methods of statistical analysis in forms useful to the study of questions related to forecasting, evaluation of air quality standards, validation of numerical dispersion models, and so forth (*1–3*).

The objective of the present work is to study the cases where the statistical information relevant to aerometric data, available in the form discussed above, can be embodied in a probability density function (pdf), or, in general, in a set of pdfs. In order that a time invariant probability density, common for all the members of the process $\{c_\tau(t_i); i = 1, \ldots, n\}$, exists, $\{c_\tau(t_i)\}$ must be a strictly *stationary process* (that is, with constant statistical properties). Further, since only one sample realization of the process (the time series $\{x_\tau(t_i)\}$) will be available, one has to assume further that the process is also *ergodic*, in order that the parameters of the pdf can be estimated from this sample. The ergodicity property implies that the ensemble mean (or expected value) of $c_\tau(t_i)$, independent of i, will be the time average (mean value) of the observations $x_\tau(t_i)$ as their number tends to infinity. In fact, what one has to examine and confirm is the sufficiently approximate stationary character of the data; such confirmation is a matter of engineering judgment. Then ergodicity is always implicitly assumed.

The most convenient case would be that of a set of independent, identically distributed random variables, $c_\tau(t_i)$ (i.i.d. variates), which of course constitute a strictly stationary process. In this case the data $x_\tau(t_i)$ form what is called in statistics a "random sample" from which statistical inference is especially convenient. Indeed, this case is amenable to extensive theoretical treatment; one can extend this treatment, in special cases, to autocorrelated and even nonidentically distributed data. Nevertheless, it is fortunate that application of theoretical results concerning i.i.d. concentrations to real situations often leads to satisfactory agreement with observations. Thus, although the assumption of independence for air pollutant data is not strictly a valid one, it can often be applied in simplified statistical analysis.

A fact that also has to be pointed out is that it is possible that different distributions (or, usually, the "same" distribution with different parameters) fit different ranges of the concentrations of given pollutants better; in such a case, one may wish to have an optimal fit for a particular range of concentrations (for example, for high concentrations that are of the most interest in air pollution) and thus decide to disregard the rest of the data (or fit another distribution to them). In this work the focus will be mainly on the case in which the statistical properties of the available data are described adequately by a single distribution; however, the entire analysis that follows applies directly to cases in which a distribution is intended to describe a particular range of concentrations.

With the assumed distribution one will be able to make statistical inferences about, for example, the expected number of occurrences of certain concentration levels. However, one will

FIGURE 1
Hypothetical distributions of air pollutant concentrations

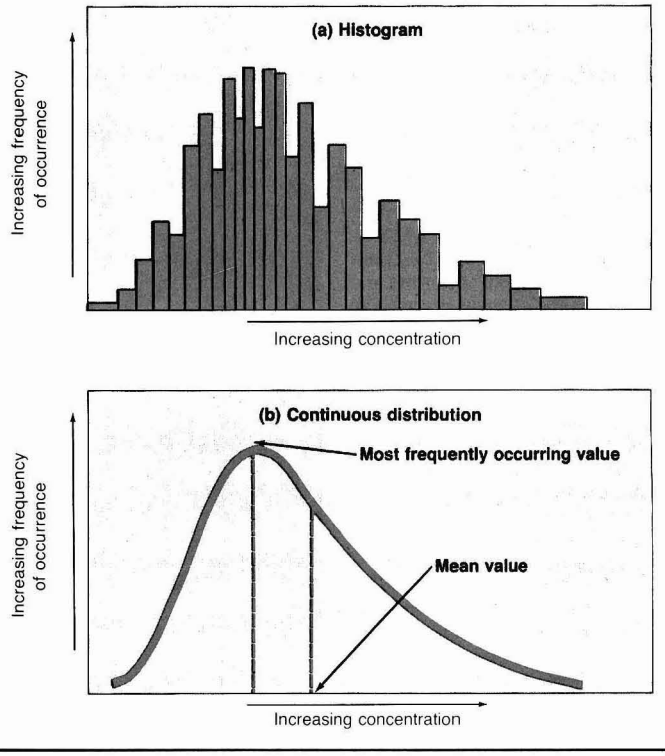

not be able to predict when these occurrences will take place; all information concerning the time evolution of the process is disregarded.

Before the specific forms of pdfs that fit actual aerometric data are examined, it is interesting to visualize the genesis of such a distribution from the data. Figure 1(a) presents a hypothetical histogram in which the frequency of occurrence of time-averaged concentrations is plotted as a function of the time-averaged concentration. Such a histogram generally exhibits irregular behavior for small numbers of observations (in general for finite samples). For infinite sample size, the histogram should tend to a smooth curve, such as that in Figure 1(b). The distribution, under the conditions of stationarity and ergodicity, is valid for all the observations, although it will be different for different averaging times. Note that very low and very high concentrations occur only rarely, and that the concentration that occurs most frequently (the mode) need not be the average or mean concentration.

Sometimes only appropriate characteristic subsequences of $\{x_\tau(t_i)\}$ are considered in statistical analysis. For example, the daily maxima of hourly average concentrations of a pollutant are often considered instead of the whole set of data, when the behavior of high concentrations is under question. However, the results from the reduced set of data are not always equivalent to the ones from the complete set. This problem will be discussed later, in the section entitled "Evaluating alternative forms of air quality standards."

Statistical distributions

While there is no a priori reason to expect that air pollutant concentrations would adhere to a specific statistical distribution, a number of pdfs have been proved useful in representing air quality data. All of these pdfs have the general features of the curve shown in Figure 1(b); they represent the distribution of a nonnegative random variable c that has probabilities of occurrence approaching zero as $c \to 0$, and as $c \to \infty$. (For convenience the subscript τ is omitted; however, it should be kept in mind that all data and parameters are related to a fixed averaging time.) Table 1 summarizes the functional form of several of these pdfs. Naturally, the larger the number of parameters in the functional form of the distribution, the greater is its flexibility of fitting sets of observed data.

The two-parameter distributions in Table 1 (log-normal, Weibull, and gamma) assume that the random variable admits all nonnegative values. The three-parameter log-normal, Weibull, and gamma distributions assume that the random variable is restricted to values greater than γ, where γ is a parameter of the distribution. The beta distribution is extremely flexible. In general, the beta distribution is symmetrical when $\alpha = \beta$, skewed to the right if $\alpha < \beta$ and skewed to the left if $\beta < \alpha$. The beta distribution also assumes an upper bound on the random variable and may or may not include a lower bound γ. The beta and gamma distributions in fact are members of the general Pearson system of probability density curves that includes 12 types of distributions (*5*).

There exists a substantial literature in which various distributions have been fit to air quality data (*1*, *6*, *7*). In addition, Holland and Fitz-Simons (*8*) have developed a computer program for fitting statistical distributions to air pollutant data.

The answer to the question of which distribution should fit best air quality data has been shown to depend in general on the pollutant, the time period of interest, the averaging time τ of the data, the location, and other factors. Thus, because there appears to exist no "universal" distribution, that most appropriate for the particular data set must be selected by employing standard statistical methods for analysis. We also note that, as pointed out by many investigators (*9*, *10*), there are differences between the frequency distribution of urban air pollution, resulting from the combined effects of many sources, and that of concentrations from a single isolated source.

Among the distributions of Table 1 the two-parameter log-normal has been the most popular in representing urban air pollutant concentration data. The conformity of this representation with field measurements, as well as various other aspects concerning log-normally distributed aerometric data, have been discussed extensively elsewhere (*1*, *11*, *12*).

For the purpose of this work, and as far as applications are concerned, we will focus on the two most popular of

TABLE 1
Probability density functions useful in representing atmospheric concentrations

Distribution	Probability density function $p(x)$
Log-normal	$\frac{1}{x\sigma(2\pi)^{1/2}} \exp\left[-\frac{(\ln x - \mu)^2}{2\sigma^2}\right]$ $x > 0; \quad \sigma > 0, -\infty < \mu < \infty$
Weibull	$\frac{\lambda}{\sigma}\left(\frac{x}{\sigma}\right)^{\lambda-1} \exp\left[-\left(\frac{x}{\sigma}\right)^{\lambda}\right]$ $x \geq 0; \quad \sigma, \lambda > 0$
Gamma	$\frac{1}{\sigma\Gamma(\lambda)}\left(\frac{x}{\sigma}\right)^{\lambda-1} \exp\left(-\frac{x}{\sigma}\right)$ $x \geq 0; \quad \sigma, \lambda > 0$
Three-parameter log-normal	$\frac{1}{(x-\gamma)\sigma(2\pi)^{1/2}} \exp\left[-\frac{[\ln(x-\gamma)-\mu]^2}{2\sigma^2}\right]$ $x > \gamma; \quad \sigma > 0; \quad -\infty < \mu < \infty$
Three-parameter gamma	$\frac{1}{\sigma\Gamma(\lambda)}\left(\frac{x-\gamma}{\sigma}\right)^{\lambda-1} \exp\left(-\frac{x-\gamma}{\sigma}\right)$ $x > \gamma; \quad \sigma, \lambda > 0$
Three-parameter Weibull	$\frac{\lambda}{\sigma}\left(\frac{x-\gamma}{\sigma}\right)^{\gamma-1} \exp\left[-\left(\frac{x-\gamma}{\sigma}\right)^{\lambda}\right]$ $x > \gamma; \quad \sigma, \lambda > 0$
Three-parameter beta	$\frac{\Gamma(\alpha+\beta)}{\Gamma(\alpha)\Gamma(\beta)} \theta^{1-\alpha-\beta} x^{\alpha-1} (\theta - x)^{\beta-1}$ $0 \leq x \leq \theta$
Four-parameter beta	$\frac{\Gamma(\alpha+\beta)}{\Gamma(\alpha)\Gamma(\beta)} (\theta-\gamma)^{1-\alpha-\beta} (x-\gamma)^{\alpha-1} (\theta - x)^{\beta-1}$ $\gamma < x < \theta; \quad \alpha, \beta > 0$

the distributions of Table 1; that is, the two-parameter (or ordinary) log-normal and the two-parameter Weibull. However, virtually all of what is presented here can be extended to the other distributions of this table.

A brief discussion of some properties of these two distributions follows. For further details and for relevant material concerning other distributions, one may consult standard references on statistical distributions, as for example the extensive treatises of Johnson and Katz (*13*), and Elderton and Johnson (*14*).

The two-parameter log-normal distribution. If a concentration c is log-normally distributed, its pdf is

$$p_L(c) = \frac{1}{c\sigma(2\pi)^{1/2}} \times \exp\left[-\frac{(\ln c - \mu)^2}{2\sigma^2}\right] \quad (1)$$

where μ and σ are parameters that depend on the particular situation. The logarithm of the concentration when described by Equation 1 has expected value and variance, $E\{\ln c\} = \mu$, and $\text{Var}\{\ln c\} = \sigma^2$. The corresponding mean and variance of c are

$$E\{c\} = \exp\left(\mu + \frac{\sigma^2}{2}\right)$$

$$\text{Var}\{c\} = \{\exp(2\mu + \sigma^2)\}[e^{\sigma^2} - 1] \quad (2)$$

The log-normal distribution (Equation 1) is also commonly expressed in the form

$$p_L(c) = \frac{1}{c\ln\sigma_g(2\pi)^{1/2}} \times \exp\left[-\frac{(\ln c - \ln\mu_g)^2}{2(\ln\sigma_g)^2}\right] \quad (3)$$

where $\mu_g = e^{\mu}$ and $\sigma_g = e^{\sigma}$. μ_g and σ_g are termed the *geometric mean* and the *standard geometric deviation*, respectively. We note that

$$\ln E\{c\} = \ln\mu_g + \tfrac{1}{2}(\ln\sigma_g)^2 \quad (4)$$

The probability that a log-normally distributed variable c exceeds the value x is given by the complementary distribution function

$$\bar{F}_L(x) = \Pr\{c > x\} = 1 - \Phi\left[\frac{\ln x - \mu}{\sigma}\right] \quad (5)$$

where

$$\Phi(\eta) = \frac{1}{(2\pi)^{1/2}}\int_{-\infty}^{\eta} e^{-t^2/2}\,dt \quad (6)$$

is the cumulative distribution function for the unit normal distribution with mean zero and unit standard deviation. (The cumulative distribution function $F(x) = \Pr\{c \le x\}$, whereas the complementary distribution function $\bar{F}(x) = 1 - F(x)$.) Tables of $\Phi(\eta)$ are readily available, so that the probability of c exceeding a given value x can be easily calculated from Equation 5. Note that if $\ln x = \mu$, or $x = \mu_g$, the argument of Φ equals zero, so that $\Pr\{c > e^{\mu}\} = \Pr\{\ln c > \mu\} = 0.5$. Thus, $\mu_g = e^{\mu}$ is the median value of a log-normally distributed variable.

The log-normal distribution has the useful property that when the complementary distribution function $\bar{F}_L(x)$ is plotted against the logarithm of the concentration on special graph paper ("normal curve graph paper"), a straight line results. The point at which $\bar{F}_L(x) = 0.5$ occurs where $\ln x = \ln\mu_g$. The point at which $\bar{F}_L(x) = 0.16$ occurs for $\ln x = \ln\mu_g + \ln\sigma_g$, or $x = \sigma_g\mu_g$. Figure 2 shows sample points of the distribution of one-hour average SO_2 concentrations equal to or in excess of the stated values for Washington, D.C., for the seven-year period from Dec. 1, 1961, to Dec. 1, 1968 (*11*). A log-normal distribution has been fitted to the high-concentration region of these data.

The log-normal distribution is completely characterized by two parameters, the geometric mean μ_g and the standard geometric deviation σ_g. The geometric mean or median is the concentration at which the straight line plot crosses the 50th percentile. The slope of the line is related to the standard geometric deviation, which can be calculated from the plot by dividing the 16th percentile concentration (which is one standard deviation from the mean) by the 50th percentile concentration (the geometric mean). (This is the 16th percentile of the *complementary* distribution function $\bar{F}(x)$; equivalently it is the 84th percentile of $F(x)$.) For the distribution of Figure 2, $\mu_g = 0.042$ ppm and $\sigma_g = 1.96$. Plots such as Figure 2 are widely used in air quality analysis because it is important to know how often concentrations equal or exceed certain values.

The two-parameter Weibull distri-

FIGURE 2
Frequency of 1-hour average SO_2 concentrations equal to, or in excess of stated values[a]

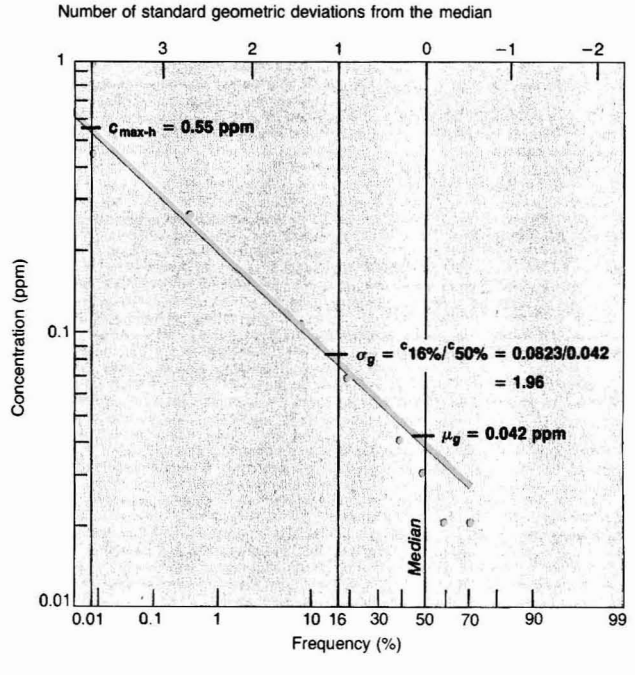

[a] At Washington, D.C., Dec. 1, 1961–Dec. 1, 1968 (after Larsen, 1971).

Note: Quantile values of c refer to the complementary distribution function.

bution. The Weibull pdf is given in Table 1. If a set of data conforms to a Weibull distribution, then the data, when plotted on extreme-value probability paper, should lie on a straight line. (Extreme-value probability paper has coordinates log x and log [ln (1/$\bar{F}(x)$)].) The complementary distribution function for the Weibull distribution is

$$\bar{F}_W(x) = \exp\left[-\left(\frac{x}{\sigma}\right)^{\lambda}\right] \quad (7)$$

Taking logarithms and changing sign

$$\ln\left(\frac{1}{\bar{F}_W(x)}\right) = \left(\frac{x}{\sigma}\right)^{\lambda} \quad (8)$$

Now we can take the logarithm (base 10) of both sides of Equation 8:

$$\log\left[\ln\left(\frac{1}{\bar{F}_W(x)}\right)\right] = \lambda\left[\log x - \log \sigma\right] \quad (9)$$

Therefore we can plot log[ln (1/$\bar{F}_W(x)$)] vs. log x and expect a straight line if the data fit a Weibull distribution. The values log[ln (1/$\bar{F}_W(x)$)] are the values on the ordinate scale of Figure 3. The scale is drawn so that a computation of log[ln (1/$\bar{F}_W(x)$)] of each value of $\bar{F}_W(x)$ would yield a linear scale (actually a negative linear scale).

We can find σ by letting the left-hand side of Equation 9 equal zero. This corresponds to $\bar{F}_W(x) = e^{-1} = 0.368$. At this $\bar{F}_W(x)$, the corresponding value of x will equal σ. The parameter, λ, which is the slope of the straight line, can be found by using any other point on the line and solving Equation 9 for λ:

$$\lambda = \frac{\log\left[\ln\left(\frac{1}{\bar{F}_W(x)}\right)\right]}{\log x - \log \sigma} \quad (10)$$

Suppose we use, for a second point, that point on the line which crosses $\bar{F}_W(x) = 0.01$. Then,

$$\lambda = \frac{0.663}{\log x_{0.01} - \log \sigma}$$

FIGURE 3
Weibull distribution fits of the 1971 hourly-average, and daily maximum hourly-average oxidant concentration[a]

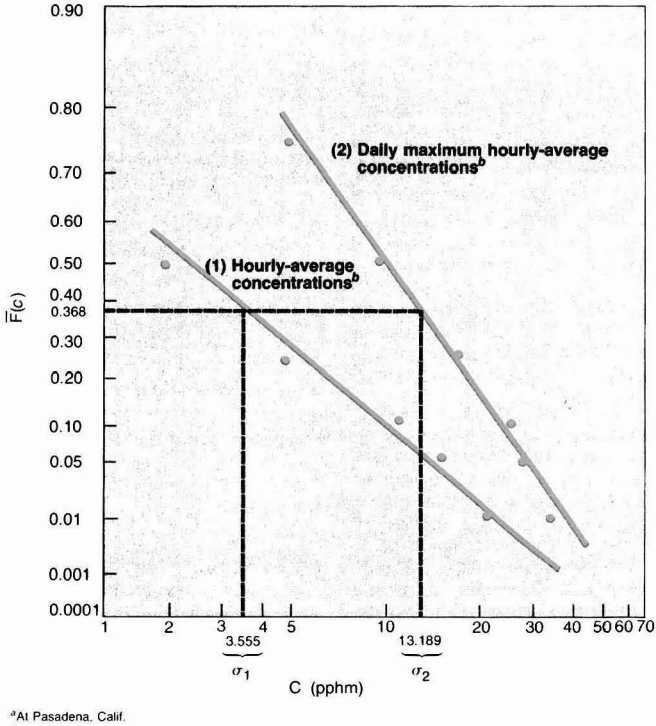

[a]At Pasadena, Calif.
[b]Points represent the values listed in Table 2.

Estimation of parameters. Each of the two distributions is characterized by two parameters. The fitting of a set of data to any distribution involves determining the values of the parameters of the distribution so that the distribution fits the data in an optimal manner. Ideally, this fitting is best carried out using a systematic optimization routine that estimates the parameters for several distributions from the given set of data and then compares how these estimated distributions fit the data using various criteria of "goodness of fit" (*8*).

Three methods of estimation are presented. The first is the method of moments, which requires the computation of the first (as many as the parameters of the distribution) sample moments of the "raw data." Next is the method of maximum likelihood, which gives estimates that are optimal in a certain statistical sense, but may require more complicated calculations than the method of moments. Finally, the method of quantiles, which is very versatile as it can usually be formulated in a manner especially appropriate for a specific problem, is discussed.

The procedure suggested for the estimation, if computer subroutines are not available, and if sample distributions such as the log-normal or the Weibull are to be tried, should start with the construction of a plot of the available data on the appropriate graph paper (that gives a straight line for the theoretical distribution), in order to get a preliminary notion of the goodness of fit. Then one would apply one of the following methods to evaluate the parameters of the "best" distribution.

The method of moments. To estimate the parameters of a distribution by the method of moments, the moments of the distribution are expressed in terms of the parameters. Estimates for the values of the moments are obtained from the data, and the equations for the moments are solved for the parameters. For a two-parameter distribution, values for the first two moments are needed; in general these would comprise estimators of the first n moments of an n-parameter distribution.

The r-th noncentral moment of a random variable X with pdf $p(x)$ is defined by:

$$\mu_r' = \int_o^{\infty} x^r p(x)\, dx$$

and the r-th central moment is:

$$\mu_r = \int_o^{\infty} (x - \mu_1')^r p(x)\, dx$$

The mean value of the random variable is μ_1', and the variance is μ_2.

Consider first the estimation of μ and σ for the log-normal distribution by the method of moments. The first and second noncentral moments of the log-normal distribution are

$$\mu_1' = \exp\left[\mu + \frac{\sigma^2}{2}\right] \quad (11)$$

$$\mu_2' = \exp(2\mu + 2\sigma^2) \quad (12)$$

After solving equations 11 and 12 for μ and σ^2, we have

$$\mu = 2 \ln \mu_1' - \tfrac{1}{2} \ln \mu_2' \quad (13)$$

$$\sigma^2 = \ln \mu_2' - 2 \ln \mu_1' \quad (14)$$

μ_1', μ_2' and μ_2 are related through $\mu_2 = \mu_2' - \mu_1'^2$ and are estimated from the data by

$$M_1' = \frac{1}{n} \sum_{i=1}^{n} x_i \quad (15)$$

and

$$M_2' = \frac{1}{n} \sum_{i=1}^{n} x_i^2,$$

$$M_2 = \frac{1}{n-1} \sum_{i=1}^{n} (x_i - M_1')^2 \quad (16)$$

where n is the number of data points. Thus, the moment estimates of the parameters of the log-normal distribution are given by

$$\hat{\mu} = 2 \ln M_1' - \tfrac{1}{2} \ln M_2' \quad (17)$$

and

$$\hat{\sigma}^2 = \ln M_2' - 2 \ln M_1' \quad (18)$$

For the Weibull distribution, the mean and variance are given by

$$\mu_1' = \sigma \Gamma\left(1 + \frac{1}{\lambda}\right) \quad (19)$$

and

$$\mu_2 = \sigma^2 \left[\Gamma\left(1 + \frac{2}{\lambda}\right) - \Gamma^2\left(1 + \frac{1}{\lambda}\right)\right] \quad (20)$$

In solving these equations for σ and λ, we can conveniently use the coefficient of variation given by $(\mu_2)^{1/2}/\mu_1'$. Then the moment estimators of the sample correspond to $\hat{\lambda}$ so that

$$\left[\frac{\Gamma\left(1 + \frac{2}{\hat{\lambda}}\right)}{\Gamma^2\left(1 + \frac{1}{\hat{\lambda}}\right)} - 1\right]^{1/2} = \frac{(M_2)^{1/2}}{M_1'} \quad (21)$$

$$\hat{\sigma} = \frac{M_1'}{\Gamma\left(1 + \frac{1}{\hat{\lambda}}\right)} \quad (22)$$

The method of maximum likelihood. Optimal estimates of parameters for a distribution (of given functional form) can be obtained by employing the method of maximum likelihood, which usually involves more complicated computations than the method of moments. The method consists in evaluating the parameters $\theta_1, \theta_2, \ldots, \theta_k$ of a k-parameter distribution so as to maximize the likelihood function, defined as the joint pdf of the observations in a random sample of size n

$$L(\theta_1, \ldots, \theta_k) = \prod_{i=1}^{n} p(x_i; \theta_1, \ldots, \theta_k)$$

The maximum likelihood is obtained by taking the partial derivatives of L with respect to each parameter, setting them equal to zero and solving the resulting k equations simultaneously. It is convenient to take the derivative of the logarithm of L; thus the maximum likelihood equations are

$$\frac{\partial}{\partial \theta_k} \ln L(x_1, x_2, \ldots, x_n; \theta_1, \ldots, \theta_k) = 0$$

For the two-parameter log-normal distribution one finds that the maximum likelihood estimates $\hat{\mu}$ and $\hat{\sigma}$ of the parameters μ, σ are given by

$$\hat{\mu} = \frac{1}{n} \sum_{i=1}^{n} \ln x_i \quad (23)$$

and

$$\hat{\sigma}^2 = \frac{1}{n} \sum_{i=1}^{n} (\ln x_i - \hat{\mu})^2 \quad (24)$$

For the Weibull distribution it can be shown that the maximum likelihood estimates $\hat{\lambda}$ and $\hat{\sigma}$ of λ and σ satisfy the set of equations

$$\hat{\lambda} = \left[\left(\sum_{i=1}^{n} x_i^{\hat{\lambda}} \ln x_i\right)\left(\sum_{i=1}^{n} x_i^{\hat{\lambda}}\right)^{-1} - \frac{1}{n} \sum_{i=1}^{n} \ln x_i\right]^{-1} \quad (25)$$

$$\hat{\sigma} = \left[\frac{1}{n} \sum_{i=1}^{n} x_i^{\hat{\lambda}}\right]^{1/\hat{\lambda}} \quad (26)$$

(For details see (*13*), Vol. 1.) Note: The maximum likelihood method can also be used as a criterion for evaluating goodness of fit of different distributions; among various distributions that fit a given set of data, the one with maximum L is considered optimal.

The method of quantiles. The parameters of a distribution can be estimated so that the theoretical distribution fits optimally (for example in the least square sense) a set of points $(\hat{x}_{q_i}, q_i)$ where the $\hat{x}_{q_i}$s are quantiles of the sample, or empirical distribution function. For a given probability distribution, the quantile x_q is defined by the equation

$$\int_o^{x_q} p(x)\, dx = F(x_q) = q \quad (0 < q < 1) \quad (27)$$

For a sample of size n the empirical cumulative distribution function is

$$\hat{F}(x_q) = \frac{1}{n} \text{ (number of } x_i \text{ less than or equal to } \hat{x}_q)$$

and the quantile $\hat{x}_q$ is chosen so as to satisfy $\hat{F}(\hat{x}_q) = q$. For the two-parameter log-normal and Weibull distributions one can employ the transformations of coordinates used in the graphs of the Figures 2 and 3, respectively, so that a straight line should fit the data. In the case that inspection of a plot of the data in such coordinates shows that a very good linear fit exists (at least for a region of concentrations that is of interest), and a very quick (and approximate) estimation of the parameters is wanted, it is sufficient to use only two quantiles of the empirical distribution to obtain two relations that can be solved simultaneously to determine the parameters of the theoretical distribution. Usually quantiles corresponding to high values of q will be used since the region of high concentrations is of the most interest.

For the log-normal distribution, for example, we have already illustrated how μ_g and σ_g are estimated from the concentrations at the 50% and 84% quantiles; that is

$$\ln \hat{x}_{0.50} - \ln \hat{\mu}_g = 0$$

$$\ln \hat{x}_{0.84} - \ln \hat{\mu}_g = \ln \hat{\sigma}_g$$

Choosing as a further illustration the 95% and 99% quantiles, we obtain

$$\ln \hat{x}_{0.95} - \ln \hat{\mu}_g = 1.645 \ln \hat{\sigma}_g$$

$$\ln \hat{x}_{0.99} - \ln \hat{\mu}_g = 2.326 \ln \hat{\sigma}_g$$

For the Weibull distribution, the quantile concentration is given by

$$x_{q_i} = \sigma \left[\ln\left(\frac{1}{1 - q_i}\right)\right]^{1/\lambda}$$

Using the 0.80 and 0.98 quantiles, for example, we obtain the estimates for the parameters λ and σ as

$$\hat{\lambda} = \frac{0.88817}{\ln \hat{x}_{0.98} - \ln \hat{x}_{0.80}}$$

$$\hat{\sigma} = \exp(1.53580 \ln \hat{x}_{0.80} - 0.53580 \ln \hat{x}_{0.98})$$

As an example, we consider the fitting of a Weibull distribution to 1971 hourly average oxidant data from Pasadena, Calif. (*15*). The data consist of 8303 hourly values (there are 8760 hours in a year). The maximum hourly value reported was 53 parts per hundred million. The arithmetic mean and standard deviation of the data are M_1'

= 4.0 pphm and $M_2^{1/2}$ = 5.0 pphm, and the geometric mean and standard geometric deviation are 2.4 and 2.6 pphm, respectively.

If one assumes that the hourly average oxidant concentrations fit a Weibull distribution, the parameters of the distribution can be estimated from Equations 21 and 22 to give $\hat{\lambda}$ = 0.808 and $\hat{\sigma}$ = 3.555 pphm. To aid in the determination of λ in fitting a set of data to the Weibull distribution, one can use Figure 4, in which the left hand side of Equation 21 is shown as a function of λ for $0 < \lambda < 9$.

It is interesting also to fit only the daily maximum hourly average oxidant values to a Weibull distribution. For these data there exist 365 data points, the maximum value of which is, as already noted, 53 pphm. The arithmetic mean and standard deviation of the data are M_1' = 12.0 pphm and $M_2^{1/2}$ = 8.6 pphm; the geometric mean and standard geometric deviation are 9.1 and 2.2 pphm, respectively. Table 2 gives a comparison of the data and the Weibull distribution concentration frequencies in the two cases. Both fits are very good, the fit to the daily maximum values being slightly better.

FIGURE 4
Calculation of parameter λ[a]

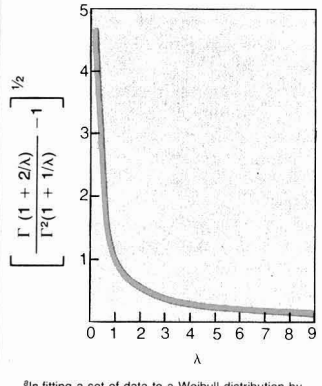

[a]In fitting a set of data to a Weibull distribution by the method of moments.

Figure 3 shows the two distributions plotted on extreme-value probability paper.

Distribution theory of order statistics

One of the major uses of statistical distributions of pollutant concentrations is to assess the degree of compliance of a region with ambient air quality standards. These standards define acceptable upper limits of pollutant concentrations and acceptable frequencies with which such concentrations can be exceeded. The probability that a particular concentration level, x, will be exceeded in a single observation is given by the complementary distribution function

$$\bar{F}(x) = \text{Prob}\{c > x\} = 1 - F(x)$$

where

$$F(x) = \text{Prob}\{c \leq x\}$$

The larger the concentration level x, the smaller is $\bar{F}(x)$.

When treating sets of air quality data, available as successive observations that form time series, we may be interested in certain random variables, as, for example:

- the highest (or, in general, the r-th highest) concentration in a finite sample of size m
- the number of exceedances of a given concentration level in a number of measurements or in a given time period
- the number of observations (waiting time or "return period") between exceedances of a given concentration level.

The distributions and pdfs, as well as certain statistical properties of these random variables, can be determined by applying the methods and results of *order statistics* (or statistics of extremes). The classic reference on order statistics is Gumbel (*16*). Relevant useful material can also be found in Sarhan and Greenberg (*17*), whereas the most recent comprehensive treatment of the subject is David (*18*), which includes extensive bibliographic information. (See also References *19–23* for applications in the field of air pollution data processing.)

Basic notions and terminology. Consider the m random unordered variates, $c_\tau(t_1)$, $c_\tau(t_2)$ . . . , $c_\tau(t_m)$, that are members of the stochastic process $\{c_\tau(t_i)\}$ that generates the time series, $x_\tau(t_1), \ldots, x_\tau(t_m)$ of available air quality data. If we arrange the time series $\{x(t_i)\}$ by order of magnitude, $x_{1;m} \geq x_{2;m} \geq \ldots \geq x_{m;m}$, then a "new" random sequence of ordered variates $c_{1;m} \geq c_{2;m} \geq \ldots \geq c_{m;m}$ is formed corresponding to the sequence $\{x_{i;m}\}$, $i = 1, 2, \ldots m$. We call $c_{i;m}$ the i-th *highest order statistic* or i-th *extreme statistic* (or $(m - i + 1)^{\text{th}}$ order statistic) of this random sequence of size m.

In the exposition that follows we assume in general that:

- The concentration levels $x_\tau(t_i)$ measured in successive nonoverlapping periods—and hence the unordered random variates $c_\tau(t_i)$—are independent of one another.
- The random variables $c_\tau(t_i)$ are identically distributed.

The case of extreme values. Assume that the distribution function $F(x)$, as well as the pdf $p(x)$, corresponding to the total number of available measurements, are known. They are called the *parent* (or initial) distribution and pdf respectively.

The probability density function $p_{r;m}(x)$ and the distribution function $F_{r,m}(x)$ of the r-th highest concentration out of samples of size m are evaluated directly from the parent pdf $p(x)$ and the parent distribution function $F(x)$ as follows:

The probability that $c_{r;m} = x$ equals the probability of $m - r$ trials producing concentration levels lower than x, times the probability of $r - 1$ trials producing concentrations above x, times the probability density of attaining a concentration equal to x, multiplied by the total number of combinations of arranging these events (assuming complete independence of the data). In other words, the pdf of the r-th highest concentration has the trinomial form

TABLE 2
1971 hourly-average Pasadena, Calif., oxidant data fitted to a Weibull distribution

	Concentration (pphm) equalled or exceeded by the stated percent of observations								
	1%	2%	3%	4%	5%	10%	25%	50%	75%
Data (hourly-average)	24	20	18	16	15	11	5	2	1
Weibull distribution	23.5	19.2	16.8	15.1	13.8	10	5.3	2.3	0.76
Data (daily max.)	34	33	32	30	28	25	17	10	5
Weibull distribution	38.8	34.6	32	30.1	28.6	24.8	16.6	10.2	5.5

$$p_{r;m}(x) = \frac{m!}{(r-1)!(m-r)!} \times [F(x)]^{m-r}[1 - F(x)]^{r-1}p(x)$$

$$= \frac{1}{B(r, m-r+1)} [F(x)]^{m-r} \times [1 - F(x)]^{r-1}p(x) \quad (28)$$

where B is the beta function. In particular, for the highest and second highest concentration values ($r = 1, 2$) we have

$$p_{1;m}(x) = m[F(x)]^{m-1}\, p(x) \quad (29)$$

and

$$p_{2;m}(x) = m(m-1) \times [F(x)]^{m-2}[1 - F(x)]p(x) \quad (30)$$

The probability $F_{r;m}(x)$ that $c_{r;m} \leq x$ is identical to the probability that no more than $r - 1$ measurements out of m result in $c_{r;m} > x$. Every observation is considered as a Bernoulli trial with probabilities of "success" and "failure" $F(x)$ and $1 - F(x)$, respectively. Thus,

$$F_{r;m}(x) = \sum_{k=0}^{r-1} \binom{m}{k} \times [1 - F(x)]^k [F(x)]^{m-k} \quad (31)$$

It can further be shown (*24*) that

$$F_{r;m}(x) = r\binom{m}{r} \int_o^{F(x)} \times t^{m-r}[1-t]^{r-1}\, dt \quad (32)$$

The integral in this expression is the incomplete beta function, and is tabulated for various values of m, r and F (*25*). For the particular cases of the highest and the second highest values ($r = 1, 2$), Equation 31 becomes

$$F_{1;m}(x) = [F(x)]^m \quad (33)$$

$$F_{2;m}(x) = m[F(x)]^{m-1} - (m-1)[F(x)]^m \quad (34)$$

Equations 28–34 are not practically useful from a computational point of view, especially for very large values of m. In this case the *asymptotic theory of extremes* can be used (see below). It is worthwhile to note the dependence of the probability of the largest value on the sample size. From Equation 33 we obtain

$$F_{1;n}(x) = [F_{1;m}(x)]^{n/m} \quad (35)$$

Thus, if the distribution of the extreme value is known for one sample size, it is known for all sample sizes.

Now once the pdf of the r-th highest concentration is known, all statistical properties of this random variable are determined in principle. For example, the k-th noncentral moment of the r-th highest concentration out of a sample of m measurements is

$$E\{c^k_{r;m}\} = \int_o^\infty x^k\, p_{r;m}(x)\, dx \quad (36)$$

Thus, the expected value of $c_{r;m}$ is

$$\mu_{r;m} \equiv E\{c_{r;m}\} = m\binom{m-1}{m-r} \times \int_{-\infty}^{\infty} x[F(x)]^{m-r} \times [1 - F(x)]^{r-1}\, dF(x) \quad (37)$$

and the variance of $c_{r;m}$ is

$$\sigma^2_{r;m} = \int_o^\infty (x - \mu_{r;m})^2\, p_{r;m}(x)\, dx \quad (38)$$

It is also interesting to note that $\sum_{r=1}^{m} \mu_{r;m} = m\mu$ where μ is the mean of the parent distribution.

The results presented above show how the parameters of the distributions of order statistics are evaluated from the parent distribution. However, the integrals involved in the expressions for the expectation and higher order moments are not always easily evaluated, and thus there arises the need for techniques of approximation. The most important result concerns the evaluation of the expected value of $c_{r;m}$. In fact, for sufficiently large m, an approximation for $E\{c_{r;m}\}$ is provided by the value of x satisfying Equation 39 (*18*):

$$F(x) = \frac{m-r+1}{m+1}. \quad (39)$$

In terms of the inverse function of $F(x)$, $F^{-1}(x)$ (that is $F^{-1}[F(x)] = x$), we have the asymptotic relation

$$E\{c_{r;m}\} \cong F^{-1}\left(\frac{m-r+1}{m+1}\right), \quad \text{as } m \to \infty \quad (40)$$

The above results do not hold for non-i.i.d. random variables. What order statistics theory can provide in this case are certain inequalities estimating bounds for individual expected values of order statistics. See Reference *18* for relevant material.

Asymptotic theory of extremes. For large sample sizes ($m \to \infty$) the theory of extreme value statistics provides us with asymptotic estimates for the distributions of the highest order statistics of the stochastic process that generates these samples (*16*, *18*, *26*). Let us consider i.i.d. variates $c_T(t_i)$, $i = 1, 2, \ldots, m$. For the distributions of interest in the description of aerometric data (the log-normal, the normal, the Weibull, and the gamma distributions), we have the following result for the distribution of their highest order statistic:

$$F_{1;m}(x) = \text{Prob}\{c_{1;m} \leq x\} = \exp\{-\exp[-(x - b_m)/a_m]\}, \quad \text{as } m \to \infty \quad (41)$$

(where $F(x)$ is log-normal, normal, Weibull, or gamma) or, equivalently

$$\Lambda(x) = \lim_{m\to\infty} \text{Prob}\{c_{1;m} \leq a_m x + b_m\} = F_{1;m}(c^*_{1;m}) = \lim_{m\to\infty} \text{Prob}\{c^*_{1;m} \leq x\} = \exp(-e^{-x}) \quad (42)$$

where

$$c^*_{1;m} = \frac{c_{1;m} - b_m}{a_m}$$

Similarly, for the analogous standardized form of the r-th extreme $c_{r;m}$, we have the following limiting distribution as $m \to \infty$:

$$\Lambda_r = \frac{1}{(m-r)!} \int_{-\lambda(x)}^{\infty} e^{-t}\, t^{m-r}\, dt = \Lambda(x) \sum_{j=0}^{m-r} \frac{\lambda^j(x)}{j} \quad (43)$$

where $\lambda(x) = -\ln \Lambda(x) = e^{-x}$. In Gumbel's (*16*) terminology, the double exponential distribution $\Lambda(x)$ is the "first asymptotic distribution of largest values"; it is one of the three possible forms that $\lim_{m\to\infty} F_{1;m}(x)$ may have (if it exists), and corresponds to the so-called exponential type of parent distributions.

The normalizing constants a_m, b_m in Equation 42 depend on the sample size m and on the form of the parent distribution; they are estimated from quantiles of the parent distribution as follows:

$$b_m = F^{-1}\left(1 - \frac{1}{m}\right) \quad (44)$$

and

$$a_m = F^{-1}\left(1 - \frac{1}{me}\right) - F^{-1}\left(1 - \frac{1}{m}\right) \quad (45)$$

Gumbel (*16*) thoroughly discusses various techniques of analysis utilizing the asymptotic form $\Lambda(x)$. Roberts (*21*, *22*) presents a brief discussion, as well as applications, of the asymptotic theory in processing air quality data; Part b of his work is devoted to the determination of the asymptotic distribution from the appropriate treatment of the data. Analytic expressions for the coefficients a_m and b_m corresponding to the normal, log-normal and gamma distributions are given, respectively, by Gumbel (*16*), Singpurwalla (*19*), and Gurland (*27*).

Once the parameters a_m, b_m are determined, the expected value of the extreme statistic is given directly by

$$E\{c_{1;m}\} = \gamma a_m + b_m \quad (46)$$

where $\gamma = 0.577\ldots$ is Euler's number. For log-normally distributed initial samples a_m, b_m are estimated analytically (*19*) from

$$a_m = \frac{b_m}{\lambda_m},$$

$$b_m = \exp(\mu + \alpha_m \sigma) \quad (47)$$

where μ, σ are the parameters of the parent log-normal distribution $F(x)$, and

$$\lambda_m = \frac{\sqrt{2 \ln m}}{\sigma} \quad (48)$$

$$\alpha_m = \sqrt{2 \ln m} - \frac{\ln(\ln m) + \ln 4\pi}{2\sqrt{2 \ln m}} \quad (49)$$

Horowitz and Barakat (*23*) extended this analysis and presented generalizations of Equations 47–49 for nonstationary autocorrelated data that satisfies certain mild conditions.

Exceedances of critical levels. The number of exceedances (episodes), $N_x(m)$ of a given, time-averaged, concentration level x_τ in a set of m successive observations (time averages) $x_\tau(t_i)$, is itself a random function. Similarly, the number of averaging periods (or observations) between exceedances of the concentration level x_τ is another random function, called *waiting time*, *passage time*, or *return period*, of crucial interest in the study of pollution episodes.

Distribution of exceedances. In the case of i.i.d. variates, each one of the observations is a Bernoulli trial; therefore, the probability density function of $N_x(m)$ is, in terms of the parent distribution $F(x)$:

$$\phi(N_x; m, x) = \binom{m}{N_x} [1 - F(x)]^{N_x} \times [F(x)]^{m - N_x} \quad (50)$$

From this relation, we conclude that the expected number of exceedances $E\{N_x(m)\}$ of the level x in a sample of m measurements is the following function of m:

$$\overline{N}_x(m) = E\{N_x(m)\} = m[1 - F(x)] = m\,\overline{F}(x) \quad (51)$$

(We omit the subscript τ for convenience; however, we reiterate that all concentrations are based on a fixed averaging time.) Alternatively, the expected percentage of exceedances of a given concentration level x, observed in any set of the data under consideration is:

$$\Pi(x) = 100\,\overline{F}(x) \quad (52)$$

The theory of order statistics provides us with another quite general and distribution-free result concerning the distributions of exceedances. As was first shown by Thomas (*28*), the probability that n observations of a random variable X will result in N_r^* values of X that exceed the r-th highest value of m initial observations (*regardless* of the magnitude of the r-th highest value and the form of the distribution of X) is:

$$\phi(N_r^*; r, m, n) = \frac{\binom{m}{r}\binom{n}{N_r^*}}{(n+m)\binom{n+m-1}{N_r^*+r-1}} \quad (53)$$

where

$$\sum_{N_r^*=0}^{n} \phi(N_r^*; r, m, n) = 1 \quad (54)$$

Thus, for example, the probability of at least one exceedance of $c_{r;m}$ is

$$\text{Prob}\{N_r^* \geq 1\} = 1 - \phi(0; r, m, n) = 1 - \frac{m!(n+m-r)}{(m-r)!(n+m)!} \quad (55)$$

For $r = 1$ we obtain

$$\text{Prob}\{N_r^* \geq 1\} = \frac{n}{m+n} \quad (56)$$

Hence if $n = m$ we have $\text{Prob}\{N_1^* \geq 1\} = 0.5$. From Equation 56 we see that the larger the difference between m and n, the smaller the probability of exceedance of the maximum value. Various other conclusions can be obtained from Equation 56 when appropriate values of N_r^*; r, m, n are introduced. For large m, n, Equation 53 is approximated by

$$\phi(N_1^*; 1, m, n) = \binom{m}{m+n}\binom{n}{m+n}^{N_1^*} \quad (57)$$

for $r = 1$.

The expected value and the variance of the number of exceedances over the r-th highest value of the m initial observations are calculated from Equation 53. Thus,

$$E\{N_r^*\} = \frac{rn}{m+1}, \quad \text{Var}(N_r^*) = \frac{rn(n+m+1)(m-r+1)}{(m+2)(m+1)^2} \quad (58)$$

A final interesting result is that for large equal m and n, the average and variance of the number of concentrations that exceed the r-th highest values of m initial observations in a set of n subsequent ones are approximately

$$E\{N_r^*\} = r, \quad \text{Var}\{N_r^*\} = 2r$$

independent of the sample size.

Expected return period or waiting time. The expected return period is defined as the average number of averaging periods (or observations) between exceedances of a given level x. The level x must of course be an average over the fixed average time τ. The probability that the concentration will exceed x for the first time at observation n is:

$$f_n = \Pr\{c \leq x\}^{n-1} \Pr\{c > x\} = [F(x)]^{n-1}[1 - F(x)] \quad (59)$$

By definition

$$E\{n\} = \sum_{n=1}^{\infty} n f_n \quad (60)$$

Using Equations 59 and 60 we obtain

$$E\{n\} = \sum_{n=1}^{\infty} n[F(x)]^{n-1}[1 - F(x)] = [1 - F(x)] \sum_{n=1}^{\infty} n[F(x)]^{n-1} \quad (61)$$

Since $F(x) < 1$, we can write

$$\sum_{n=1}^{\infty} n[F(x)]^{n-1} = 1 + 2F + 3F^2 + \ldots = \frac{1}{[1 - F(x)]^2} \quad (62)$$

Combining Equations 61 and 62, we obtain

$$E\{n\} = \frac{1}{1 - F(x)} = [\overline{F}(x)]^{-1} \quad (63)$$

The variance of the number of observations between exceedances of a given level x is

$$\text{Var}\{n\} = \sum_{n=1}^{\infty} (n - E\{n\})^2 f_n = \sum_{n=1}^{\infty} \left[n - \frac{1}{1-F}\right]^2 F^{n-1}(1 - F) = (1 - F)\sum_{n=1}^{\infty} n^2 F^{n-1} - 2\sum_{n=1}^{\infty} n F^{n-1} + \frac{1}{1-F}\sum_{n=1}^{\infty} F^{n-1} \quad (64)$$

Using the relations

$$\sum_{n=0}^{\infty} F^n = \frac{1}{1-F},$$

$$\sum_{n=1}^{\infty} n F^{n-1} = \frac{1}{(1-F)^2}$$

$$\sum_{n=1}^{\infty} n(n-1) F^{n-2} = \frac{2}{(1-F)^3}$$

we obtain from Equation 64

$$\text{Var}\{n\} = \frac{F}{(1-F)^2} \qquad (65)$$

Alternative forms of air standards

Four possible forms of an oxidant air quality standard are listed in Table 3. In the application of these standards, aerometric data are to be used to estimate expected concentrations and their frequency of occurrence. If one assumes that the data conform to a specific probability distribution, then the distribution is fit to actual data, and the parameters of the distribution are estimated. As we have already pointed out, the distribution determined from the set of available data is time-invariant. It is assumed that this condition holds for future data also, since the distribution will be used to predict expected future concentration frequencies. That is, one will be able to make statistical inferences about the expected number of occurrences (or frequency) of certain concentration levels. One will not, of course, be able to predict *when* the events will occur but only how often.

The choice of one form of the standard over another, from a regulator's point of view, can be based on the impact (health effects, for example) that each form implies for the concentration distribution as a whole (*29*, *30*). For example, one form could be stated in such a way that it requires a lower maximum concentration to be attained

Evaluating an air quality standard

The first step in the evaluation of an air quality standard is to select the statistical distribution that supposedly best fits the data. We will assume that the frequency distribution that best fits hourly-averaged oxidant concentration data is the Weibull distribution (*31*). Since the standards are expressed in terms of expected events during a one-year period of one-hour average concentrations, we will always use the number of trials m equal to the number of hours in a year, 8760. We would use $m < 8760$ only to evaluate the distribution (determine how well the data fit the assumed distribution), since some of the 8760 hours are usually missing from the data set.

Expected number of exceedances of 0.12 ppm hourly average less than or equal to one per year. The expected number of exceedances $\bar{N}_x(m)$ of a given concentration level in m measurements is given by Equation 51, which in the case of the Weibull distribution becomes

$$\bar{N}_x = m \exp\left[-\left(\frac{x}{\sigma}\right)^{\lambda}\right] \qquad (66)$$

If we desire the expected exceedance to be once out of m hours, that is, $\bar{N}_{x_1} = 1$, the concentration corresponding to that choice is

$$x_1 = \sigma(\ln m)^{1/\lambda}. \qquad (67)$$

For $m = 8760$, Equation 67 becomes

$$x_1 = \sigma(9.08)^{1/\lambda}.$$

The 0.12 ppm hourly average not to be exceeded on the average by more than 0.01% of the hours in one year. The expected percentage of exceedance of a given concentration, x, is given by Equation 52, which for the Weibull distribution is

$$\Pi(x) = 100 \exp\left[-\left(\frac{x}{\sigma}\right)^{\lambda}\right] \qquad (68)$$

Equation 68 can be rearranged to determine the concentration level that is expected to be exceeded $\Pi(x)$ percent of the time,

$$x = \sigma\left[\ln\left(\frac{100}{\Pi(x)}\right)\right]^{1/\lambda} \qquad (69)$$

Therefore, we can calculate the concentration that is expected to be exceeded 0.01 percent of the hours in one year,

$$x_{0.01} = \sigma(9.21)^{1/\lambda} \qquad (70)$$

The 0.12 ppm annual expected maximum hourly average and 0.12 ppm annual expected second highest hourly average. The "exact" expected value of the r-th highest concentration is given by Equation 37. For the Weibull distribution, Equation 37 becomes

$$\text{E}\{c_{r;m}\} = \frac{m!}{(r-1)!(m-r)!}\int_o^{\infty}\left(\frac{x}{\sigma}\right)^{\lambda} \times\left\{1-\exp\left[-\left(\frac{x}{\sigma}\right)^{\lambda}\right]\right\}^{m-r} \times\left\{\exp\left[-\left(\frac{x}{\sigma}\right)^{\lambda}\right]\right\}^{r} dx \qquad (71)$$

We wish to evaluate this equation for $r = 1$ and $r = 2$ corresponding to standards 3 and 4, respectively, in Table 2. The results, $\text{E}\{c_{1;m}\}$ and $\text{E}\{c_{2;m}\}$, are the expected highest and second highest hourly concentrations, respectively, in the year, when $m = 8760$. Unfortunately, the integral in Equation 71 cannot be evaluated easily. Even numerical techniques fail to give consistent results, because of the singularity at $x = 0$. Thus, the asymptotic relation for large m (Equation 40) must be used in this case. For the Weibull distribution we have

$$1-\exp\left[-\left(\frac{\text{E}\{c_{r;m}\}}{\sigma}\right)^{\lambda}\right] = \frac{m-r+1}{m+1} \qquad (72)$$

For $m = 8760$ and $r = 1, 2$ we must solve, respectively, the equations

$$1-\exp\left[-\left(\frac{\text{E}\{c_{1;m}\}}{\sigma}\right)^{\lambda}\right] = \frac{8760}{8761}$$

and

$$1-\exp\left[-\left(\frac{\text{E}\{c_{2;m}\}}{\sigma}\right)^{\lambda}\right] = \frac{8759}{8761}$$

to obtain

$$\text{E}\{c_{1;m}\} = \sigma(9.08)^{1/\lambda} \qquad (73)$$

and

$$\text{E}\{c_{2;m}\} = \sigma(8.38)^{1/\lambda} \qquad (74)$$

As an alternative we can also use an empirical result from Larsen (1971), who approximated the probability of occurrence of a concentration greater or equal to the r-th highest concentration as

$$\bar{F}(c_{r;m}) = \frac{r-0.4}{m} \qquad (75)$$

Therefore, the probabilities of a concentration exceeding the maximum and second highest concentrations ($c_{1;m}$ and $c_{2;m}$) are:

$$\bar{F}(c_{1;m}) = \frac{0.6}{m} \quad \text{and} \quad \bar{F}(c_{2;m}) = \frac{1.6}{m}$$

We can now determine the expected concentrations by the use of the estimated distribution parameters, λ and σ, and Equation 8:

$$\text{E}\{c_{1;m}\} = \sigma\left[\ln\left(\frac{8760}{0.6}\right)\right]^{1/\lambda} = \sigma(9.59)^{1/\lambda}$$

$$\text{E}\{c_{2;m}\} = \sigma\left[\ln\left(\frac{8760}{1.6}\right)\right]^{1/\lambda} = \sigma(8.61)^{1/\lambda}$$

for $m = 8760$. Notice that this approach is independent of the assumption for Weibull distributed data.

Evaluation of alternative forms of

TABLE 3

Alternative statistical forms of the photochemical oxidant standard [a]

No.	Form
1	0.12 ppm hourly average with expected number of exceedences per year less than or equal to one
2	0.12 ppm hourly average not to be exceeded on the average by more than 0.01% of the hours in one year
3	0.12 ppm annual expected maximum hourly average
4	0.12 ppm annual expected second highest hourly average

[a] For most practical purposes forms 1 and 3 can be considered equivalent.

the oxidant air quality standard with 1971 Pasadena, Calif., data. Earlier, 1971 hourly-average and maximum daily hourly-average oxidant concentrations at Pasadena, Calif., were fit to Weibull distributions. We now wish to evaluate the forms of the oxidant air quality standard that have been discussed. For convenience all concentration values will be given as pphm rather than ppm.

Expected number of exceedances of 12 pphm hourly-average concentration less than or equal to one per year. The expected number of exceedances of 12 pphm, based on the Weibull fit of the 1971 Pasadena, Calif., hourly-average data, is from Equation 66:

$$N_{12} = 8760 \exp\left[-\left(\frac{12}{3.555}\right)^{0.808}\right]$$

$$= 605.2$$

The hourly-average that is exceeded at most once per year is from Equation 67:

$$x_1 = 3.555(ln\ 8.760)^{1/0.808}$$

$$= 54.51 \text{ pphm}$$

which agrees well with the actual measured value of 53 pphm.

If, instead of the complete hourly-average Weibull distribution, we use the distribution of daily maximum hourly-average values, the expected number of exceedances of a daily maximum of 12 pphm is

$$\bar{N}_{12} = 365 \exp\left[-\left(\frac{12}{13.189}\right)^{1.416}\right]$$

$$= 152.2$$

and the daily maximum 1-h concentration that is exceeded once per year, at most, is

$$x_1 = 13.189(ln\ 365)^{1/1.416}$$

$$= 46.2 \text{ pphm}$$

It is interesting to note that this value is underpredicted if we use the distribution of daily maxima instead of the distribution based on the complete set of data.

The 12-pphm hourly average not to be exceeded on the average by more than 0.01% of the hours in one year. The expected percentage of exceedances of 12 pphm is, from Equation 68:

$$\Pi(12) = 100 \exp\left[-\left(\frac{12}{3.555}\right)^{0.808}\right]$$

$$= 6.91\%$$

The concentration that is expected to be exceeded 0.01% of the hours in the year is, from Equation 69:

$$x_{0.01} = 3.555\left(ln\frac{100}{0.01}\right)^{1/0.808}$$

$$= 55.5 \text{ pphm}$$

This form of the standard cannot be evaluated from the distribution of daily maxima.

The 12-pphm annual expected maximum hourly average and 12-pphm annual expected second highest average. The annual expected maximum hourly average is obtained from Equation 73 for $E\{c_{1:m}\}$, and for $\sigma = 3.555$, $\lambda = 0.808$. We have

$$E\{c_1\} = 54.51 \text{ pphm}$$

(whereas the observed (sample) maximum hourly average value was 53 pphm). Similarly, for the annual expected second highest hourly average concentration we have from Equation 74:

$$E\{c_2\} = 49.40 \text{ pphm}$$

The comparable calculations from the distribution of daily maxima are

$$1 - \exp\left[-\left(\frac{x}{13.189}\right)^{1.416}\right]_{x=E\{c_1\}} = \frac{365}{366}$$

giving

$$E\{c_1\} = 46.21 \text{ pphm}$$

and

$$1 - \exp\left[-\left(\frac{x}{13.189}\right)^{1.416}\right]_{x=E\{c_2\}} = \frac{364}{366}$$

giving

$$E\{c_2\} = 42.31 \text{ pphm}$$

(The agreement with the measured concentrations is not very good now, but this is to be expected since we use an asymptotic relation for infinite m which now is $m = 365$.)

Using the empirical relation (Equation 75), we obtain

$$E\{c_1\} = 3.555\left[ln\left(\frac{8760}{0.6}\right)\right]^{1/0.808}$$

$$= 58.3 \text{ pphm}$$

Note that this value differs by 10% from the observed value of 53 pphm. However, the estimation is based on the empirical formula of Equation 75, the accuracy of which cannot be assessed in this case. Similarly, for the annual expected second highest hourly average concentration we obtain:

$$E\{c_2\} = 3.555\left[ln\left(\frac{8.760}{1.6}\right)\right]^{1/0.808}$$

$$= 51.04 \text{ pphm}$$

The comparable values calculated from the distribution of daily maxima are

$$E\{c_1\} = 13.189\left[ln\left(\frac{365}{0.6}\right)\right]^{1/1.416}$$

$$= 49 \text{ pphm}$$

and

$$E\{c_2\} = 13.189\left[ln\left(\frac{365}{1.6}\right)\right]^{1/1.416}$$

$$= 43.6 \text{ pphm}$$

Again, these two quantities are both underpredicted when based on the distribution of daily maxima relative to the distribution of hourly average values.

than that defined by a second standard; however, the *average* concentration under the first standard may be higher than that under the second standard. Standards may also be expressed in terms of different averaging times.

It has been pointed out that a more logical structure for air quality standards would be in terms of a largest concentration with an acceptable return period (*21*, *22*). That is, the standard would be specified in terms of accepted return periods within which, for example, the highest and the second highest concentrations would exceed given values. The evaluation of this kind of air quality standard, as well as of the previous ones, is done by using elementary results of the methods presented in the previous sections.

Rollback calculations

The reduction in emission source strength, R, required to meet an air quality goal c_s is often calculated by the so-called simple rollback equation (*32*):

$$R = \frac{\kappa c - c_s}{\kappa c - c_b} \qquad (76)$$

where κ is a growth factor for future emission sources (the ratio of future source strength to present source strength in the absence of controls), c_b is a value for the background concentration, and c_s is the air quality standard. Some of the assumptions implicit in the statement of Equation 76 (such as unchanged spatial distribution of emission sources, common growth factor for all sources, unchanged average meteorological conditions, etc.) are discussed in (*32*). Many modifications of the formula have appeared in the literature representing efforts to relax some of the above assumptions (*33*–*37*). Here the focus will be on the proper interpretation of the values of c in Equation 76, as related to the distributional characteristics of the concentration.

In the usual manner in which Equation 76 seems to have been applied, c_s is the air quality standard and c is the present concentration corresponding to c_s. For example, if c_s is a value of the hourly-average concentration not to be exceeded more than once per year, then c would be the highest hourly-average concentration observed in the present year. Used in the manner just described, Equation 76 implies that the yearly maximum concentration is linearly proportional to source emissions. That is, it is presumed that a 50% reduction in source strength leads to a 50% reduction in the maximum concentration observed (neglecting effects of background concentration).

Can this assumption be true? What we would expect, upon some thought, for yearly data that conform to a common distribution with mean $E\{c\}$, is that the expected concentration $E\{c\}$ would be proportional to source strength (at least for inert pollutants). In fact, if c in Equation 76 is interpreted as the yearly maximum observed concentration, then that equation contains a mixture of deterministic (κ, c_s, c_b) and stochastic ($c = c_{max}$) variables. (Actually c_b also has a distribution and may even change with time (*33*, *35*); thus it should be considered as a stochastic variable like c. However, for the purpose of this work we will assume that the value of c_b and its variation is very small; therefore, an approximate choice of the correct order of magnitude for c_b would be sufficient). To apply Equation 76 to the expected concentration $E\{c\}$ satisfies the basic notion of conservation of mass of nonreactive species; that is, long-term mean concentrations are proportional to the total emissions of the species.

It appears, therefore, that the correct statement of the rollback formula should be of the form

$$R = \frac{\kappa E\{c\} - E\{c\}_s}{\kappa E\{c\} - c_b} \qquad (77)$$

where $E\{c\}_s$ denotes a yearly mean (expected) concentration of a distribution the extreme statistic of which that corresponds to c_s is equal to c_s. However, there are many indeterminate factors involved in the estimation of $E\{c\}_s$ from such a distribution; further, from an air quality regulation point of view we are really interested in how the extreme statistics of the future distribution and c_s compare. In order to state this formally we must first replace the observed maximum value of c with the extreme statistic of the distribution of c that corresponds to c_s. For the analysis that follows we replace c_{max} with $\hat{c}$, which is defined as the concentration level that has probability of exceedance equal to that stated in the definition of the air quality standard c_s, under present conditions. Thus, if future emissions were to double, we want to know whether $\hat{c}$ would also double or increase by more or less than that amount. In other words we want to know if the quantiles (and in particular those corresponding to extreme values) of the concentration distribution scale linearly with emissions as does the expected value $E\{c\}$. In general such a linear relation does *not* exist. However, in the particular case of log-normally distributed concentrations, empirical results (*33*) can be used to show the approximate validity of a linear relation.

Assume that a concentration in question can be represented by a log-normal distribution (under present as well as future conditions). If a current emission rate changes by a factor κ ($\kappa > 0$) while the source distribution remains the same (if meteorological conditions are unchanged, and if background concentrations are negligible), the expected total quantity of inert pollutants having an impact on a given site over the same time period should also change by the factor κ. The expected concentration level for the future period is therefore given, for a log-normally distributed variable, by

$$E\{c'\} = e^{\mu' + \sigma'^2/2} = \kappa e^{\mu + \sigma^2/2} \qquad (78)$$

where the primed quantities c', μ', σ'^2 apply to the future period, and the unprimed quantities apply to the present. It has been argued by Larsen (*33*) and others that if meteorological conditions remain unchanged, the standard geometric deviation of the log-normal pollutant distribution remains unchanged; that is, $e^{\sigma'} = e^{\sigma}$. Thus, $e^{\mu'} = \kappa e^{\mu}$, or

$$\mu' = \mu + \ln \kappa \qquad (79)$$

The probability that future concentration level c' will exceed a level x is

$$\begin{aligned} \bar{F}_{c'}(x) &= 1 - \Phi\left(\frac{\ln x - \mu'}{\sigma'}\right) \\ &= 1 - \Phi\left(\frac{\ln x - \mu - \ln \kappa}{\sigma}\right) \\ &= 1 - \Phi\left(\frac{\ln \frac{x}{\kappa} - \mu}{\sigma}\right) \\ &= \bar{F}_c(x/\kappa) \end{aligned} \qquad (80)$$

Similarly,

$$\begin{aligned} \bar{F}_{c'}(\kappa x) &= \Pr\{c' > \kappa x\} \\ &= 1 - \Phi\left(\frac{\ln \kappa x - \mu'}{\sigma'}\right) \\ &= 1 - \Phi\left(\frac{\ln x - \mu}{\sigma}\right) \\ &= \bar{F}_c(x) \end{aligned} \qquad (81)$$

Thus, the probability that the future level κx will be exceeded just equals the probability that with current emission sources the level x will be exceeded.

Therefore, with equal σ, all frequency points of the distribution shift according to the factor κ. This results in a parallel translation of the graph of $F(x)$ or $\bar{F}(x)$, when plotted against $\ln$

x. Figure 5 shows two log-normal distributions with the same standard geometric deviation but with different geometric mean values. The geometric mean concentrations of the two distributions are 0.05 ppm and 0.10 ppm, and the standard geometric deviations are both 1.4. The mean concentrations can be calculated with the aid of Equation 4 and the material presented above. We find that $E_1\{c\} = 0.053$ ppm, and $E_2\{c\} = 0.106$ ppm for the two distributions, respectively. The variances can likewise be calculated with the aid of Equation 2 to obtain $Var_1\{c\} = 0.00034$ ppm^2 and $Var_2\{c\} = 0.00134$ ppm^2.

Suppose that distribution No. 1 represents current conditions, and therefore, that the current probability of exceeding a concentration of about 0.13 ppm is about 0.0027—which corresponds to about one day per year if the distribution is of 24-hour averges. If the emission rate were doubled, the new distribution function would be given by distribution No. 2. The new distribution has a median value twice that of the old one, since total loadings attributable to emissions have doubled. In the new case, a concentration of 0.13 ppm will be exceeded 22% of the time, or about 80 days a year, and the concentration that is exceeded only one day per year rises to 0.26 ppm.

The expected return period and its variance can be calculated from Equations 63 and 65 for any given concentration level. For $c = 0.2$ ppm, for example,

$$E_1\{n\} \to \infty \quad Var_1\{n\} \to \infty$$

$$E_2\{n\} = 47.3 \quad Var_2\{n\} = 2190$$

In summary, we have shown that the conventional manner in which the rollback equation, Equation 76, has been used (in which the concentrations are extreme values) is incorrect. Whereas annual mean concentrations can be expected to scale linearly with emission levels, the extreme values, in general, do not. However, in particular, a log-normally distributed concentration will scale linearly with emission level changes, when it is assumed that the geometric mean scales with the emission level changes, and the standard geometric deviation remains constant. In such a case one can use Equation 76 modified as

$$R = \frac{\kappa\hat{c} - c_s}{\kappa\hat{c} - c_b} \qquad (82)$$

where $\hat{c}$, as defined earlier, is calculated from a log-normal distribution that has been fitted to the whole set of present-year concentration data (averaged over the time period that is stated in the definition of c_s).

Conclusions

Prediction of the degree of compliance with air quality standards resulting from control strategy implementation generally requires knowledge of the statistical behavior of air pollutant concentrations. This knowledge can usually be incorporated in sets of statistical distributions of concentrations and used appropriately thereafter. In this perspective, a variety of similar distributions have been proposed to fit aerometric data. Moreover, the properties of certain random variables crucial in characterizing aerometric data, such as extreme concentrations, exceedances of critical levels, and waiting times between exceedances, have been studied and formulated in terms of these distributions by applying order statistics and level crossing theory. Using this analysis, one can show, for example, how different forms of air quality standards can be evaluated and how rollback calculations can be properly carried out when extreme values are involved.

FIGURE 5
Two log-normal distributions with the same standard geometric deviation

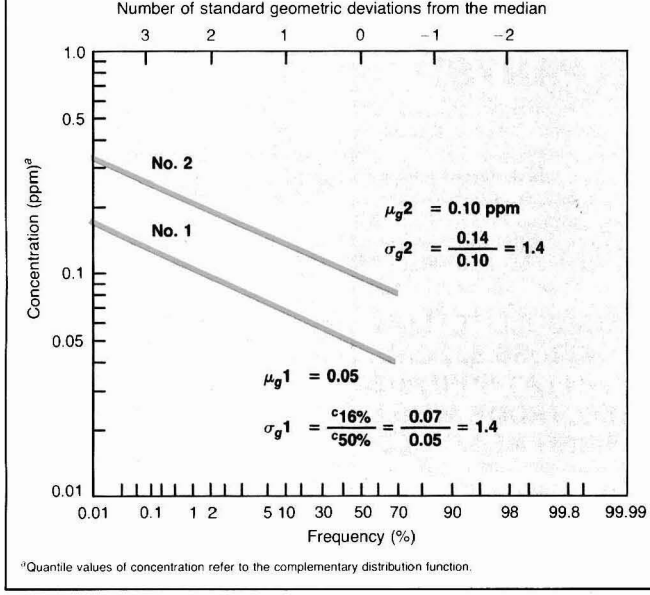

[a]Quantile values of concentration refer to the complementary distribution function.

References

(1) Environmental Protection Agency. *Proc. Symp. Statistical Aspects Air Quality Data*, Report EPA-650/4-74-038; Research Triangle Park, N.C., 1974.
(2) Merz, P. H.; Painter, L. J.; Ryason, P. R. *Atmos. Environ.* **1972,** *6*, 319.
(3) Myrabo, L. N.; Wilson, K. R.; Trijonis, J. C. *Adv. Environ. Sci. Technol.* **1975,** *7*, 391.
(4) Seinfeld, J. H.; Lapidus, L. "Mathematical Methods in Chemical Engineering, Vol. 3: Process Modeling, Estimation, and Identification"; Prentice Hall: Englewood Cliffs, N.J., 1973.
(5) Lynn, D. A. "Fitting Curves to Urban Suspended Particulate Data." *Proc. Symp. Statistical Aspects Air Quality Data* E.P.A.: Research Triangle Park, N.C., 1974.
(6) Hillyer, M. J. Report No. EF 78-SO, Systems Applications, Inc.: San Rafael, Calif., 1978.
(7) Tsukatami, T.; Shigemitsu, K. *Atmos. Environ.* **1980,** *14*, 245.
(8) Holland, D. M.; Fitz-Simons, T. *Atmos. Environ.* **1982,** *16*, 1071.
(9) Gifford, F. A. "The Form of the Frequency Distribution of Air Pollution Concentrations," *Proc. Symp. Statistical Aspects Air Quality Data*, E.P.A.: Research Triangle Park, N.C., 1974.
(10) Barry, P.J. "Use of Argon-41 to Study the Dispersion of Stack Effluents," *Proc. Symp. Nuclear Techniques Environ. Pollut.* Int. Atomic Energy Agency, 1971.
(11) Larsen, R. I. EPA Publication No. AP-89, Research Triangle Park, N.C., 1971.
(12) Bencala, K. E.; Seinfeld, J. H. *Atmos. Environ.* **1976,** *10*, 941.
(13) Johnson, N. L.; Kotz, S. "Continuous Univariate Distributions"; Houghton-Mifflin: Boston, 1970; Vols. 1 and 2.
(14) Elderton, W. P.; Johnson, N. L. "Systems of Frequency Curves"; Cambridge University Press: Cambridge, Mass., 1969.
(15) State of California Air Resources Board. "Ten-Year Summary of California Air Quality Data 1963-1972"; 1974.
(16) Gumbel, E. J. "Statistics of Extremes"; Columbia Univ. Press.: New York, 1958.
(17) Sarhan, A. E.; Greenberg, B. G., Eds. "Contributions to Order Statistics"; John Wiley & Sons: New York, 1962.
(18) David, H. A. "Order Statistics," 2nd ed.; John Wiley & Sons: New York, 1981.

(19) Singpurwalla, N. D. *Technometrics* **1972,** *14*, 703.
(20) Barlow, R. E.; Singpurwalla, N. D. "Averaging Time and Maxima for Dependent Observations," *Proc. Symp. Statistical Aspects of Air Quality Data* EPA: Research Triangle Park, N.C., 1974.
(21) Roberts, E. M. *J. Air Pollut. Control Assoc.* **1979,** *29*, 632.
(22) Roberts, E. M. *J. Air Pollut. Control Assoc.* **1979,** *29*, 731.
(23) Horowitz, J.; Barakat, S. *Atmos. Environ.* **1979,** *13*, 811.
(24) Feller, W. "An Introduction to Probability Theory and its Applications," 3rd ed.; John Wiley & Sons: New York, 1968; Vol. 1.
(25) Pearson, K. "Tables of the Incomplete Beta Function"; Biometrika Office: London, 1934.
(26) Galambos, J. "The Asymptotic Theory of Extreme Order Statistics"; John Wiley: New York, 1978.
(27) Gurland, J. *Ann. Math. Statist.* **1975,** *26*, 294.
(28) Thomas, H. A., Jr. "Frequency of Minor Floods," *J. Boston Soc. Civ. Eng.* **1948,** *35*, 425; *Grad. School of Eng. Pub. No. 466* Harvard Univ.: Cambridge, Mass., 1948.
(29) Mage, D. T. *J. Air Pollut. Control Assoc.* **1980,** *30*, 796.
(30) Curran, T. C.; Hunt, W. F., Jr. *J. Air Pollut. Control Assoc.* **1975,** *25*, 711.
(31) Environmental Protection Agency. "Alternative Forms of the Ambient Air Quality Standard for Photochemical Oxidants," Staff paper, Research Triangle Park, N.C., 1978.
(32) de Nevers, N.; Neligan, R. E.; Slater, H. H. In "Air Pollution," 3rd. ed.; Stern, A. C., Ed.; Academic Press: New York, 1977; Vol. 5.
(33) Larsen, R. I. *J. Air Pollut. Control Assoc.* **1969,** *19*, 24.
(34) de Nevers, N.; Morris, J. R. *J. Air Pollut. Control Assoc.* **1975,** *25*, 943.
(35) Horie, Y.; Overton, J. "The Effect on Rollback Models Due to Distribution of Pollutant Concentrations," *Proc. Symp. Statistical Aspects of Air Quality Data* EPA: Research Triangle Park, N.C., 1974.
(36) Chang, T. Y.; Weinstock, B. *J. Air Pollut. Control Assoc.* **1975,** *25*, 1033.
(37) Peterson, T. W.; Moyers, J. L. *Atmos. Environ.* **1980,** *14*, 1439.

Panos G. Georgopoulos (*l.*) *received the Dipl. Ing. degree from the National Technical University of Athens, Greece, in 1980. He is currently a Ph.D. candidate in the Department of Chemical Engineering at the California Institute of Technology, and is studying the mathematical modeling of air pollution.*

John H. Seinfeld (*r.*) *is Louis E. Nohl Professor and Executive Officer for Chemical Engineering at the California Institute of Technology. Seinfeld has been a faculty member at the California Institute of Technology for 15 years; his primary research interests are the chemistry and physics of urban air pollution. He serves as an associate editor of* Environmental Science & Technology.

Spill detector
An elastic membrane held in tension by a magnetic reed switch detects spills of crude oil, distillates, solvents, and chemicals in water. A warning signal is sent by radio or cable with a reaction time that varies from 5 s to 10 min. Matlin Company **101**

Minicomputer
Thirty-two bit computer suited to laboratory applications supports up to four megabytes of directly addressable main memory for up to 32 users. This model is an ideal processor for Perkin-Elmer's laboratory information management system. The device is contained within a 30 × 24-in. chassis and is software-compatible with all other Perkin-Elmer 3200 series processors. Perkin-Elmer **102**

Data reporting system
Transmits and processes data from an air quality monitoring network of almost any size. A standard dial phone network or radio link is used to relay data from remote sites to a central site, where it is stored on a Winchester disk that provides up to 9.6 megabytes of data storage. Monitor Labs **103**

Flue gas analyzer
Microprocessor-controlled system measures opacity, SO_2, NO_x, O_2, CO, and CO_2, and gives automatic daily and quarterly reports of overemissions, average emissions, and calibration data. The system can be configured for any combination of opacity and gases. Datatest **104**

Need more information about any items? If so, just circle the appropriate numbers on one of the reader service cards bound into this issue and mail in the card. No stamp is necessary.

Electronic recorder
Provides automatic conversion with analog signals ranging from one millivolt to 10 volts full scale. This two-channel system amplifies with 0.05–0.1% precision. It includes a digital plotter for stripchart graphical display and automatically stores recorded data on 8-in. floppy disks. Bascom-Turner Instruments **105**

Automated chromatography system
This combines a chromatograph and an advanced computer with high-resolution graphics. The chromatograph has a pulse-free pump, ternary gradient capability, and a variety of detectors. The computer system includes application software and a keypad for control of the chromatograph. IBM Instruments **106**

Chemical product
When mixed with water and fly ash, this chemical forms light-weight building materials that are stronger than those made from cement or clay. No calcining, sintering, or firing are required. Oh-Kay Chemical **107**

Sample preparation kit
Contains five columns each of octadecyl, phenyl, cyanopropyl, aminopropyl, benzene sulfonic acid, quaternary amine diol, and unbonded silica. These can be used to solve sample preparation problems. Analytichem International **108**

NO_x analyzer
Portable unit is a chemiluminescent gas phase analyzer with four selectable ranges that vary from 0.5–50 ppm full scale, and have automatic zeroing circuitry. The device has five automatic LED displays and an adjustable audible alarm. Internal batteries allow five hours of continuous operation. Columbia Scientific Industries **109**

Analytical balances
With these balances, the display can be continuously updated during fast filling or pouring. This feature is available on all Arbor 0.1-mg balances, which have capacities ranging from 60–500 g. Arbor Laboratories **110**

Autoclavable reagent dispensers
Made entirely of borosilicate glass with ground glass joints, these dispensers can be used with any reagent except HF, and may be autoclaved at 250 °F. for 15 min. Sizes are available from 0.5–100 mL. Each dispenser is adjustable over the full length of its 100 division scale. Labindustries **111**

Portable incubator
Holds 108 petri dishes with an outside diameter of 57 mm and a height of 12.7 mm, and has a digital LED display. The incubator can be powered with 12 V DC or 120 V AC. It has variable temperature settings from slightly above ambient to 60 °C and a temperature uniformity of ±0.25 °C. Lab-Line Instruments **112**

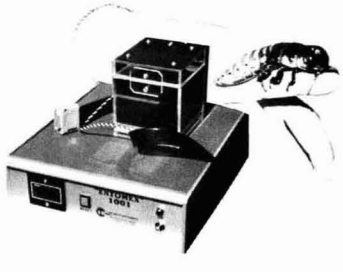

Insect activity meter
With an array of photooptical sensors, this measures the activity of crawling insects and gives numerical values for the efficiency of different pesticides. Many insects can be tested at the same time in the same cage without mutual signal interference. Columbus Instruments **113**

***Companies interested in a listing** in this department should send their releases directly to Environmental Science & Technology, Attn: Products, 1155 16th St., N.W., Washington, D.C. 20036*

Counter current chromatograph
Performs liquid–liquid separations of polar to semipolar compounds such as natural products, peptides, lipids, and glycosides. The instrument requires little laboratory space and consumes small amounts of solvent. It has six racks with 48 columns each and space for four additional racks. Brinkmann Instruments **114**

Flue gas analyzers
Model CV-I is an oxygen analyzer for continuous monitoring of excess oxygen in flue gases of oil, coal, or gas-fired industrial package boilers. Model CV-IC monitors both oxygen and excess combustibles in flue gases. These analyzers operate on 115 or 230 V AC power and do not require reference gas or compressed air connections. AMETEK **115**

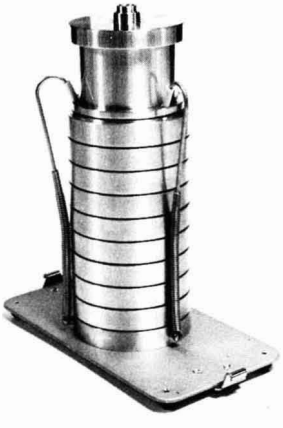

Ambient sampler
Eight-stage cascade impactor collects and aerodynamically sizes all airborne particulates and divides them into nine size ranges from 11 μm down to less than 0.4 μm. It is normally employed for in-plant sampling and may be used with special collection substrates. Andersen Samplers **116**

Solar integrators
Receives data from one or two pyranometers and integrates it over selected time intervals. The instrument prints out real time and integrated radiation for the total period and the day. Kipp & Zonen **117**

Dissolved oxygen analyzer
Portable instrument detects concentrations down to zero oxygen levels and records the results continuously. It may be used to determine oxygen leakage in feedwater pumps and condensers. Drew Chemical **118**

Data system
Data system adapts Nelson Analytical's chromatography software to the HP 9826 computer and allows up to 10 chromatographs to be connected simultaneously to the computer. Interfaces store raw run data and are offered in two models: one with 16 000 bytes, and another with 64 000 bytes. Nelson Analytical **119**

Freeze-dry containers
Stainless steel containers are available in 1-, 2-, 4-, and 8-L volumes and are fitted with a clear top for visibility of the product during drying. FTS Systems **120**

Dual-channel thermometer
Two channels monitor temperature from two points simultaneously. Each channel has its own user-selectable alarm modes and high and low alarm set points. The temperature range is from 0–50 °C. An optional recorder adapter records temperature data from both channels. Yellow Springs Instrument **121**

Spectrophotometer
Double-beam, dual-wavelength spectrophotometer contains built-in data processing to provide automatic baseline and spectra correction, spectra storage, memory display on any oscilloscope, and plotting of acquired data on the recorder. The instrument can be operated in several different modes: double-beam, dual-wavelength, dual-wavelength scanning, rapid kinetics, and optical derivative. SLM Instruments **122**

Ozone calibrator
Using a variable shutter, this instrument produces ozone concentrations from 0.001–0.5 ppm and is suitable for the calibration of ozone meters. An ultraviolet source whose temperature is controlled irradiates air that passes through a quartz tube to generate a precise ozone standard. The generator is calibrated using the EPA-approved UV extinction technique. Analytical Instrument Development **130**

pH controller/monitor
Controls the total alkalinity in cooling towers and air washers. When the pH reaches the setpoint limit, the monitor switches on the acid pump, which causes acid to be injected into the system to lower pH. Morr Control **131**

Water level recorder
Detects water levels in narrow bores or wells with a 0.7-in. diameter probe and a portable, self-powered water level recorder. This device may be used to monitor level fluctuations, unattended, on a monthly basis, and has a range of interface cards to change the data into standard form for data acquisition systems. R. W. Munro, Ltd. **132**

Radiation detector
This system is sensitive to photosynthetically active radiation and is designed for use with a family of radiometers in plant biology and biochemical studies. It exhibits a flat quantum response over a 400–700 nm band pass and permits any IL700 or IL1500 radiometer to measure radiation over a range from 1×10^{-9} to 1×10^{-1} microeinsteins/s/cm^2. International Light **133**

Photometric analyzer
Measures suspended or dissolved solids with a resolution up to 0.05%. Spans range from 0.1–80% by weight or volume full scale depending on the optical properties of the material being measured. Concentration units are switch selectable for full scale ranges of 0.1, 0.2, 0.5, 1, 2, and 5. Monitek **134**

Microbalance
Portable unit has ranges of 1.0 μg–200 mg and 10 μg–1000 mg. Tare and range push-buttons simplify operation. Access to the lighted weighing chamber is through a front door. Cahn Instruments **135**

ES&T LITERATURE

Sewer cleaning. Catalog on sewer cleaning details six machines, among which are water jets, continuous rodders, sectional rodders, and cable machines. O'Brien **151**

Biomass determination. News release announces improved line of reagents, and a system using bioluminescence to detect and determine bacteria, as required in procedures for biocide control, polluted waters, industrial waters, and sewage plant effluents. Diagnostic Sciences **152**

Digital pH meters. Brochure BR453 describes two digital pH meters, one of which can read 0.000–14.000 pH, and 0–±1999.9 mV. The other reads 0.00–14.00 pH, and 0–±1999 mV. Sybron/Brinkmann **153**

Laboratory safety. Comprehensive laboratory safety equipment handbook is now available that lists and describes 1168 products for safety enhancement. Arthur H. Thomas **154**

Water clarification. Data Sheet 32-1 describes a liquid cationic polyelectrolyte as a primary water clarification coagulant to replace inorganics, such as ferric salts or alum. Uses are in industry. Calgon **155**

GC phases. Booklet lists applications for high-temperature gas chromatographic (GC) phases, with special applications to alcohols, drugs, biomedical, hydrocarbons, steroids. Over 380 references cited. Dexsil Chemical **156**

HPLC switching. Technical Note No. 4 tells how to switch HPLC columns in and out of a chromatograph with selection valves, and lists situations in which such procedures are advantageous. Rheodyne **157**

Safety supplies. March 1982 catalog lists workplace and laboratory safety supplies, and features eye and ear protection, respirators, clothing, first aid, safety receptacles, and storage cabinets. Interex **158**

Groundwater safeguards. Brochure lists capabilities and services in hydrogeology and related sciences. Title is, "Protecting Groundwater Resources." Ecology and Environment **159**

Oil burner nozzles. Catalog 1709C describes full line of oil burner nozzles and accessories for residential and industrial applications. They aim at minimizing problems associated with low oil flow. Delavan **160**

Hydraulic filters. Brochure details models DF, LF, and MDF hydraulic pressure filters (1500, 3000, 6000 psi), associated items, and technical specifications. Hycon **161**

Constant temperature. Brochure BR 448 illustrates 24 refrigerating and heating models of Lauda constant temperature baths, and a variety of accessories. Sybron/Brinkmann **162**

Pressure transducers. Catalog highlights specifications of full line of pressure transducers, load cells, and related items. Data Instruments **163**

Spectrophotometer. Brochure describes DMS 90/Plus computerized ultraviolet-visible spectrophotometer system with Apple II Plus computer. Varian Instruments **164**

Solids pump. Technical Bulletin 4-2-31/1A discusses pump that can feed high-consistency slurries to reactors, dryers, and other unit operations at up to 150 psi. Other liquid-solid mixtures can be pumped at 300–2500 gpm. Ingersoll-Rand **165**

HPLC components. Catalog is devoted to fittings, filters, valves, other needs for high performance liquid chromatography (HPLC). Soft Seal LC Column System is featured. Scientific Systems **166**

Image processing. Catalog No. OP382 shows image processing and industrial inspection and enhancement systems. LogE/Spatial Data Systems **167**

Stack sampler. Brochure presents the "Universal" stack sampler weighing 20 lb, with digital temperature readout, modular pitot tip standard, other features. Andersen Samplers **168**

Monochromatic illumination. Brochure describes line of monochromatic illumination systems (MIS), 150–2000 W, for analytical instruments requiring monochromatic light. Selective 180–3000 nm. Kratos **169**

Respirators. New edition of Respirator Guide reflects latest recommendations of American Conference of Governmental Industrial Hygienists. Provides specifications for more than 500 common airborne contaminants in workplaces. HSC **170**

Primary coagulant. Data Sheet 32-3 tells why and how IPL-312, a liquid cationic polyelectrolyte now accepted by EPA, can be used instead of ferric salts or alum to treat drinking water supplies at concentrations not exceeding 5 ppm. Calgon **171**

Formaldehyde barrier. Brochure describes HYDE-CHEK, a clear latex vapor barrier coating to use on wood products containing urea-formaldehyde glues. Chemical scavengers absorb escaping formaldehyde fumes. Mortell **172**

Wetland management. Company brochure outlines services in wetland management, including marine and freshwater wetland creation. Management and restoration accomplishments are included. Mangrove Systems **173**

Analytical chemicals. 1982 chemicals catalog lists entire line of analytical and fine chemicals, along with available quantities and prices. GFS Chemicals **174**

Need more information about any items? If so, just circle the appropriate numbers on one of the reader service cards bound into this issue and mail in the card. No stamp is necessary.

***Companies interested in a listing** in this department should send their releases directly to Environmental Science & Technology, Attn: Literature, 1155 16th St., N.W., Washington, D.C. 20036*

ES&T BOOKS

The Love Canal: My Story. Lois M. Gibbs. xvii + 174 pages. State University of New York Press, State University Plaza, Albany, N.Y. 12246. 1982. $11.95, hard cover.

This is the story of the person who became the spokesperson and political strategist for the association of many families adversely affected by the Love Canal contamination at Niagara Falls, N.Y. About 1000 families were represented. Events at Love Canal were later to have a strong impact on national policy. Problems and frustrations in dealing with government bodies are narrated, and the author shows how, when necessary, "even the average citizen with limited education and no funds can 'fight City Hall.' "

Life on a Warmer Earth. H. Flohn. xi + 66 pages. Office of Communications, IIASA, A-2361, Laxenburg, Austria. 1981. Free of charge, paper.

What happens if, because of carbon dioxide "greenhouse effect," or some other reason, the climate of the earth warms up markedly? This report explores the interaction between energy and climate, and impacts on fossil, nuclear, and solar fuels. Expected global warming effects caused by CO_2 released by burning fossil fuels and other trace gases are described.

Marine Geology. James F. Kennett. xv + 813 pages. Prentice-Hall, Inc., Englewood Cliffs, N.J. 07632. 1982. $34.95, hard cover.

This work covers the field of marine geology, or if one wishes, geological oceanography. It discusses structure, tectonics, ocean margins, sediments, fossils, paleooceanography, and many other pertinent topics.

Biomass Conversion Processes for Energy and Fuels. Samir S. Sofer, Oskar R. Zaborsky, Eds. xvi + 420 pages. Plenum Publishing Corp., 223 Spring St., New York, N.Y. 10013. 1981. $49.50, hard cover.

Biomass may be looked to as a renewable source of fuel as petroleum supplies dwindle and increase in price. Articles in this book cover biomass sources, thermodynamic and thermochemical processes, biochemical processes, and technical and economic considerations.

Survey of Contemporary Toxicology. Vol. 2. Anthony T. Tu, Ed. xi + 248 pages. John Wiley & Sons, Inc., 605 Third Ave., New York, N.Y. 10016. 1982. $50, hard cover.

This volume examines biocides and their prudent, efficient use in agriculture. It also discusses mechanisms of the interaction of radiation with human tissue, and consequent risks of radiation exposure. Venoms and their composition, and modern techniques and applications in forensic toxicology are also covered.

Environmental Regulation and the U.S. Economy. Henry M. Peskin et al., Eds. ix + 163 pages. Johns Hopkins University Press, Baltimore, Md. 21218. 1981. $15, hard cover.

Environmental regulations in particular have been singled out as a major cause of declines in the U.S. economy's rate of growth, productivity, and value of the dollar. Is this accusation valid or not? This volume seeks to separate truth from rhetoric; to achieve this goal, it examines many facets of the environmental regulation/economy relationship. One major finding is that many factors other than environmental (and other social) regulations influence the economy far more significantly than do these regulations.

Occupational Exposure Guide. 800+ pages. J. J. Keller & Associates, Inc., 145 West Wisconsin Ave., Neenah, Wis. 54956-0368. 1982. $176, three-ring binder (add $95 for updating service).

This guide and its updating service has the objective of keeping users fully knowledgeable about changing OSHA regulations. For instance, what rules were eased; which were made more stringent. Record-keeping regulations, employee notification, hazardous substances and their control, and many other pertinent matters are dealt with.

Foundations for the Solar Future. Richard L. Koral, Ed. Association of Energy Engineers, 4025 Pleasantdale Rd., Atlanta, Ga. 30340. 1982. $36, hard cover.

This work presents an overview of a large array of solar energy products, and discusses their applications and performance. It examines the state of the art, evolution of the solar building, specific equipment items, systems, hydrogen fuel, heat pumps, and many other topics, including what is going on in other countries.

Atmospheric Aerosol: Source/Air Relationships. Edward S. Macias, Ed. 359 pages. B & J Business Operations, American Chemical Society, 1155 16th St., N.W., Washington, D.C. 20036. 1981. $39.75, hard cover.

Papers contained in this book analyze recent research on pollutant source resolution methods that bridge the gap between measurements of chemical and physical properties of aerosol and aerosol precursor pollutant emissions (source characterization), and measurements of ambient aerosol (air quality characterization).

Solar Cells. T. J. Coutts, et al., Eds. Periodical, 8 issues/year. Elsevier Sequoia S.A., B.P. 851, CH-1001 Lausanne 1, Switzerland. Annual subscription, S.Fr.380, or $190.

Among subjects discussed in this journal are the physics and chemistry of solar cells, specific applications, economic aspects, social implications, environmental implications, and specific analysis of individual cells. Inquire for the policy for submitting manuscripts for publication.

Blueprint for Clean Water. Deborah A. Sheiman. 24 pages. League of Women Voters Education Fund, 1730 M St., N.W., Washington, D.C. 20036. 1982. 75¢, paper (add 50¢ for shipping).

This booklet explains water pollutant types and effects; the history and aims of the Clean Water Act, pollution control economics, and successes and failures in a manner that makes these topics understandable to the layperson.

Air and Water Pollution Control Law: 1982. Phillip D. Reed, Gregory S. Connecticut Ave., N.W., Washington, D.C. 20036. 1981. $67.50.

This manual provides in-depth coverage of enforcement, administrative procedure, environmental auditing, and federal common law of nuisance. It is designed to be a complete legal research and reference tool.

professional consulting services directory

A.F. Meyer and Associates, Inc.

Environmental, System Safety, and Occupational Health Consultants

Free Brochure Upon Request

1317 Vincent Place • McLean, VA 22101
703/734-9093

Complete Analytical Services

SINCE 1919

- Screening of Industrial Waste for EPA Priority Pollutants using Finnigan OWA-30 GC/MS.
- NPDES & SPDES Organic & Inorganic Testing.
- Drinking Water Analysis to EPA Standards.
- Bioassay, Bioaccumulation & Toxicity Studies of Industrial Waste, Municipal Sludge & Dredge Spoils.
- Leachate Potential Studies & Analysis.
- Total Instrumental Analysis: A.A., GC/MS, G.C., I.R., TOC & TOD.
- RCRA Hazardous Waste Testing.

NEW YORK TESTING LABORATORIES
81 Urban Avenue, Westbury, N.Y. 11590
(516) 334-7770

Enviro-Med Laboratories, Inc.

Environmental, Bio-Medical, and Chemical Specialists

Sampling, Testing, and Consulting Services

Priority Pollutants - GC/MS, GC, AA
Hazardous Waste Characterization
PCB/Pesticide Analyses
Industrial Hygiene Services
Permit Preparation
Drinking Water Analyses
Animal Toxicity
Resource Recovery
Research and Development
Customized Seminars and Workshops

THE PROBLEM SOLVERS

Corporate Headquarters

414 W. CALIFORNIA
RUSTON, LA 71270 (318)255-0060

Other Offices:

BATON ROUGE, LA 70806 (504)928-0232

HOUSTON, TX 77040 (713)462-1631

Laboratory and Process Development
Industrial Waste Water Control
Liquid and Solid Incineration
Air Pollution Control
In-Plant Control and Process Modifications
Environment Impact and Permits

CATALYTIC, INC.

Consultants • Engineers • Constructors
Environmental Systems Division
Centre Square West
1500 Market St.,
Philadelphia, PA 19102 • 215-864-8000
Charlotte, NC 704-542-4220
Baton Rouge, LA 504-293-6200

Scott Environmental Technology, Inc.

The Air Pollution Specialists

• Research and Consulting •
• Source Emissions Testing •
• Control Device Efficiency •
• Continuous Source Monitoring •
• Ambient Monitoring •
• Fuel Additive & Automotive Testing •

Route 611, Plumsteadville, PA 18949
215 – 766-8861
2600 Cajon Blvd., San Bernardino, CA 92411
714 – 887-2571
1290 Combermere St., Troy, MI 48084
313 – 589-2950

envirodyne engineers

a consulting engineering and sciences firm

- environmental engineering
  analytical chemistry
  priority pollutant analyses
  environmental monitoring and assessment
  hazardous waste monitoring
  hazardous waste management
- transportation engineering
- energy engineering
- construction management

12161 Lackland Road
St. Louis, Missouri 63141
(314) 434-6960

Baltimore / Chicago / Knoxville / New York

Dames & Moore

Engineering and Environmental Consultants

- Environmental Impact Assessment
- Geotechnical and Environmental Engineering
- Meteorology and Air Quality Monitoring
- Water Pollution Control Engineering
- Modelling and Numerical Analyses
- Permitting and Licensing Consultation
- Solid and Hazardous Waste Management

San Francisco • Denver
Chicago • New York • Atlanta
Offices in Principal Cities Throughout the World

TRC Environmental Consultants, Inc.

Environmental Planning and Problem Solving for Industry and Government

•AIR •WATER •SOLIDS •NOISE •ODOR

•MEASUREMENT •IMPACT ASSESSMENT
•CONTROL •INFORMATION SYSTEMS
•MODELING •PERMIT PLANNING

800 Connecticut Blvd., E. Hartford, CT 06108
(203) 289-8631
•EAST HARTFORD •DENVER •SAN DIEGO

SIRRINE

ENGINEERS · ARCHITECTS · PLANNERS

-Permit Assistance
-Air & Water Quality Modeling
-Site Selection Studies
-Laboratory Analyses
-Environmental Impact Assessments
-Hazardous Solid Waste Management
-Complete Design Services
-Construction Management

Greenville, SC 29606
Research Triangle Park, NC 27709
Houston, TX 77042

WESTON

DESIGNERS CONSULTANTS

HEADQUARTERS West Chester, PA 19380 • 215-692-3030
OFFICES Atlanta, GA • Boston, MA • Camden, NJ
Chicago, IL • Cleveland, OH • Concord, NH
Houston, TX • Nashville, TN • New Orleans, LA
New York, NY • Richmond, VA • St. Paul, MN
Washington, DC • Amman, Jordan • Cairo, Egypt

ENVIRONMENTAL CONSULTANTS INC

ANALYTICAL TESTING AND SAMPLING SERVICES:

- EPA—Drinking water
- Certified bacteriological testing
- N.P.D.E.S. Permit
- Priority pollutant analysis
- Workplace environments
- EPA Hazardous wastes evaluation
- Particle identification and sizing
- Process Quality Control
- Research and Development

USING:

Gas chromatography/Mass spectrometry; Atomic Absorption Spectroscopy; Infrared spectroscopy; Microscopy; TOC; E.P.A. and OSHA certified methods.

CONSULTATION—PLANNING

391 NEWMAN AVE
CLARKSVILLE, INDIANA 47130
812-282-8481

BC Laboratories

EPA Drinking Water Stds. & Priority Pollutants
Haloforms, PCB's—Gases, TOC, Solid Waste
Extractions, Heavy Metals

4100 Pierce Road (805) 327-4911
Bakersfield, California 93308

Ground Water Associates, Inc.

Water Supply Geologists and Engineers

- **Quantitative and qualitative ground water evaluations**
- **Iron removal by VYREDOX process**

P.O. Box 280
Westerville, Ohio 43081
614/882-3136

Cranford, New Jersey
Arlington, Massachusettes

DAVID KEITH TODD

CONSULTING ENGINEERS, INC.

Groundwater Planning, Development, Management, and Protection

2914 Domingo Avenue
Berkeley, California 94705 415/841-2091

SpectroChem LABORATORIES INC.

545 Commerce St., Franklin Lakes, New Jersey 07417
(201) 337-4774 (201) 891-8787

- Atomic Absorption
- Gas Chromatography
- Chemical
- Optical Emission
- X-ray Spectrometry
- ICP

TRACE ANALYSIS Est.
Complete Analytical Services 1948

professional consulting services directory

ES&T

MEETINGS

July 21–23 Denver, Colo.
Practical Groundwater Monitoring Considerations for the Mining Industry. The National Water Well Association

Fee: $350. *Write:* Monitoring Mining Conferences, National Water Well Association, 500 W. Wilson Bridge Rd., Worthington, Ohio 43085

July 29–30 Columbus, Ohio
Practical Groundwater Monitoring Considerations for the Mining Industry. The National Water Well Association

Fee: $250. *Write:* Monitoring Mining Conferences, National Water Well Association, 500 W. Wilson Bridge Rd., Worthington, Ohio 43085

August 2–3 San Francisco, Calif.
Water Reclamation and Reuse—California Experiences. Resource Seminars

Fee: $250. *Write:* Jannie Dresser, Seminar Coordinator, Resource Seminars in Water Resources, 2914 Domingo Ave., Berkeley, Calif. 94705; (415) 841-2091

August 3–5 Pittsburgh, Pa.
Ninth Annual International Conference on Coal Gasification, Liquefaction, and Conversion to Electricity (COGLAC '82). School of Engineering at University of Pittsburgh

Write: Dr. Alan J. Brainard, Department of Chemical & Petroleum Engineering, 1234 Benedum Hall, University of Pittsburgh, Pittsburgh, Pa. 15261

August 8–11 New Orleans, La.
37th Annual Meeting of the Soil Conservation Society of America—The Politics of Conservation. Soil Conservation Society of America (SCSA)

Write: Max Schnepf, SCSA, 7515 N. E. Ankeny Rd., Ankeny, Iowa 50021; (515) 289-2331

COURSES

July 13–16 Boston, Mass.
Dispersion Modeling. Northrop Services, Inc.—Environmental Training

Fee: $500. *Write:* Manager, Northrop Environmental Training, P.O. Box 12313, Research Triangle Park, N.C. 27709; (919) 549-0652

July 19–22 Boston, Mass.
Air Pollution Meteorology. Northrop Services, Inc.—Environmental Training

(continued on page 424A)

CLASSIFIED SECTION ■ POSITIONS OPEN

POSITION ANNOUNCEMENT
(Condensed form for advertisement)

The Department of Land, Air and Water Resources, UNIVERSITY OF CALIFORNIA, DAVIS announces a position in the area of RESOURCE SCIENCE. Tenured track (11 mos) position will be divided 25% teaching and 75% research. The appointment will be at the Assistant or Associate Professor level, depending on qualifications.

QUALIFICATIONS: A Ph.D. in a physical science (Physics or closely allied field) with an expertise in solar and other alternate energy sources and the impacts of energy development on the environment. Applicants should have strong training in radiation physics, solar radiation as a resource, methods of data analysis in natural resources, and monitoring programs.

The appointee would be expected to teach undergraduate and graduate courses in solar energy resources and applications, an undergraduate course in air pollution, and additional teaching duties including graduate and undergraduate advising. The appointee will be expected to develop a research program in energy resources analysis with emphasis on solar energy and other natural energy resources. This research program is also expected to evaluate the impacts of energy development, in general, on the environment.

APPLICANTS: Applicants should submit curriculum vitae, transcripts, statement of research and teaching interests and background in each, copies of publications and manuscripts and the names and addresses of at least three references to: L. O. Myrup, Chair, Search Committee, Department of Land, Air and Water Resources, 165 Hoagland Hall, University of California, Davis, California 95616, prior to August 1, 1982.

THE UNIVERSITY OF CALIFORNIA IS AN EQUAL OPPORTUNITY AFFIRMATIVE ACTION EMPLOYER AND INVITES APPLICATIONS FROM ALL QUALIFIED INDIVIDUALS.

FACULTY POSITION: Assistant Professor in Civil Engineering (Sanitary/Environmental Engineering), University of California, Division of Sanitary, Environmental, Coastal and Hydraulic Engineering. The applicant must have a doctorate degree or equivalent in Sanitary/Environmental Engineering. Person will be expected to teach undergraduate and graduate courses in the field. The position is to be filled as soon as possible. Send complete resume to Search Committee, Sanitary/Environmental Engineering, Department of Civil Engineering, 635 Davis Hall, University of California, Berkeley, Berkeley, California 94720. The closing date is August 31, 1982. The University of California is an equal opportunity, affirmative action employer.

CLASSIFIED ADVERTISING RATES

Rate based on number of insertions used within 12 months from date of first insertion and not on the number of inches used. Space in classified advertising cannot be combined for frequency with ROP advertising. Classified advertising accepted in inch multiples only.

Unit	1-T	3-T	6-T	12-T	24-T
1 inch	$90	$85	$82	$79	$77

(Check Classified Advertising Department for rates if advertisement is larger than 10″.) SHIPPING INSTRUCTIONS: Send all material to

Environmental
Science & Technology
Classified Advertising Department
25 Sylvan Road South
P.O. Box 231
Westport, CT. 06881
(203) 226-7131

HAZARDOUS WASTE/ CHEMICAL SPILL INVESTIGATIONS

The nation's leading consultant in the investigation and assessment of today's most critical environmental concerns is staffing to meet growing needs. Exciting career challenges are available for technically qualified individuals wishing to join the vanguard of the industry.

Positions require minimum BS degree with pertinent experience in the following areas:

Chemical Engineering
Hydrogeology
Sanitary/Waste Water Engineering
Environmental/Civil Engineering
Public Health/Industrial Hygiene
Environmental Science

Opportunities are available in several E & E regional offices. Send current resume, salary requirements and locational preference to Terri Slimko at:

ecology and environment, inc.
International Specialists in the Environmental Sciences
P.O. BOX D,
BUFFALO, NEW YORK 14225
An Equal Opportunity Employer

ENVIRONMENTAL ENGINEER

The New Mexico Institute of Mining & Technology is seeking to fill a tenure track position in the College of Engineering commencing with the 1982–83 academic year. The position is at the Assistant Professor rank and the individual filling the position would be in charge of revitalizing and developing a strong undergraduate Environmental Engineering Program focusing primarily on air and water pollution and solid waste disposal. An earned doctorate in an appropriate engineering field is required for appointment to a professional rank. The successful candidate will be expected to teach in his or her field of specialization at the undergraduate level and to work closely with a group of internationally known atmospheric scientists in the development of new technology air pollution control devices. The individual may on occasion be asked to teach basic engineering science courses as well. Salary is competitive. Please send a current resume and three letters of recommendation to: Geoffrey Purcell, Chairman, Department of Metallurgical and Materials Engineering, New Mexico Institute of Mining and Technology, Socorro, New Mexico 87801.

New Mexico Institute of Mining and Technology is an Equal Opportunity/Affirmative Action Employer and Institution.

MEETINGS *(continued)*

Fee: $500. *Write:* Manager, Northrop Environmental Training, P.O. Box 12313, Research Triangle Park, N.C. 27709; (919) 549-0652

July 19–22 Research Triangle Park, N.C.
Source Sampling for Particulate Pollutants. Northrop Services, Inc.—Environmental Training

Fee: $500. *Write:* Manager, Northrop Environmental Training, P.O. Box 12313, Research Triangle Park, N.C. 27709; (919) 549-0652

July 26–30 Bloomington, Ind.
Environmental Applications of Gas Chromatographic Mass Spectrometry. The School of Public and Environmental Affairs, Indiana University

Fee: $700. *Write:* Executive Education Program, Poplars 323, 400 East Seventh St., Bloomington, Ind. 47405; (812) 335-3601

July 28–30 Madison, Wisc.
Creative Action in Engineering and Science. University of Wisconsin—Extension

Fee: $545. *Write:* C. W. Little, Jr., Engineering Registration, The Wisconsin Center, 702 Langdon St., Madison, Wisc. 53706; (608) 263-3646

August 9–11 East Brunswick, N.J.
Hazardous Spill Cleanup. The Center for Professional Advancement

Fee: $650. *Write:* The Center for Professional Advancement, Dept. NR, P.O. Box H, East Brunswick, N.J. 08816; (201) 249-1400

August 17–19 Denver, Colo.
Ambient Air Quality Monitoring Systems. Northrop Services, Inc.—Environmental Training

Fee: $375. *Write:* Manager, Northrop Environmental Training, P.O. Box 12313, Research Triangle Park, N.C. 27709; (919) 549-0652

INTERNATIONAL

September 1–3 Wembley, London
Third International Environment and Safety Conference and Exhibition. Internal Environment and Safety, Labmate Ltd.

Write: International Environment & Safety, Labmate Ltd., Newgate, Sandpit Lane, St. Albans, Herts AL4 OBS, U.K.; Tel.: St. Albans (0727) 51993

September 20–23 Odense, Denmark
1st International Symposium on Operating European Centralized Hazardous (Chemical) Waste Management Facilities. Kommunekemi a/s The Danish Environmental Protection Agency and others

Fee: $750. *Write:* K. Kathrina Sorensen, Chemcontrol A/S, Dagmarhus, DK-1553 Copenhagen V, Denmark

CALL FOR PAPERS

July 30 deadline
Arab Water Technology Conference. Middle East Water and Sewage Journal.

Conference to be held March 7-8, 1983, in Dubai. *Write:* Miss Y. Ketley, Arab Water Technology Conference, Room 204, Queensway House, 2 Queensway, Redhill, Surrey RH1 1QS England; Tel.: 0737 68611, Ext. 269.

August 10 deadline
ET'83—10th Annual Energy Technology Conference and Exposition. American Gas Association, and others

Conference to be held Feb. 28-Mar. 2, at the Sheraton Washington Hotel, Washington, D.C. Write: ET'83 Program Chairman, c/o Government Institutes, Inc., 966 Hungerford Dr., #24, Rockville, Md. 20850

INDEX TO THE ADVERTISERS IN THIS ISSUE

Advertising Management for the American Chemical Society Publications

CENTCOM, LTD.

Thomas N. J. Koerwer, President; James A. Byrne, Vice President; Alfred L. Gregory, Vice President; Clay S. Holden, Vice President; Benjamin W. Jones, Vice President; Robert L. Voepel, Vice President; 25 Sylvan Road South, P.O. Box 231, Westport, Connecticut 06881 (Area Code 203) 226-7131

ADVERTISING SALES MANAGER

James A. Byrne

SALES REPRESENTATIVES

Atlanta, Ga. . . . Donald B. Davis, CENTCOM, LTD., Phone (Area Code 203) 226-7131

Boston, Ma. . . . Thomas Carey, CENTCOM, LTD., (Area Code 212) 972-9660

Chicago, Ill. . . . Bruce Poorman, CENTCOM, LTD., 540 Frontage Rd., Northfield, Ill 60093 (Area Code 312) 441-6383

Cleveland, Oh. . . . Bruce Poorman, CENTCOM, LTD., 17 Church St., Berea, OH 44017 (Area Code 216) 234-1333

Denver, Co. . . . Clay S. Holden, CENTCOM, LTD., (Area Code 213) 325-1903

Houston, Tx. . . . Robert E. LaPointe, CENTCOM, LTD., (Area Code 415) 781-3430

Los Angeles, Ca. . . . Clay S. Holden, Robert E. LaPointe, CENTCOM, 3142 Pacific Coast Highway, Suite 200, Torrance, CA 90505, (Area Code 213) 325-1903

New York, N.Y. . . . Thomas Carey, CENTCOM, LTD., 60 E. 42nd Street, New York 10165 (Area Code 212) 972-9660

Philadelphia, Pa. . . . Thomas Carey, CENTCOM, LTD., GSB Building, Suite 425, 1 Belmont Ave., Bala Cynwyd, Pa 19004 (Area Code 215) 667-9666

San Francisco, Ca. . . . Paul M. Butts, CENTCOM, Ltd., Suite 112, 1499 Bayshore Highway, Burlingame, CA 94010. Telephone 415-692-1218

Westport, Ct. . . . Thomas Carey, CENTCOM, LTD., 25 Sylvan Road South, P.O. Box 231, Westport, Ct. 06881, (Area Code 203) 226-7131

United Kingdom:
Lancashire, England—Technomedia, Ltd. . . . c/o Meconomics Ltd., Meconomics House, 31 Old Street, Ashton Under Lyne, Lancashire, England 061-308-3025
Reading, England—Technomedia, Ltd. . . . Wood Cottage, Shurlock Row, Reading RG10 OQE, Berkshire, England 0734-343302

Continental Europe . . . Andre Jamar, Rue Mallar 1, 4800 Verviers, Belgium. Telephone: (087) 22-53-85. Telex No. 49263

Tokyo, Japan . . . Shigeo Aoki, International Media Representatives Ltd., 2-29, Toranomon 1-Chrome, Minatoku, Tokyo 105 Japan. Telephone: 502-0656

PRODUCTION DEPARTMENT

PRODUCTION DIRECTOR

Joseph P. Stenza

PRODUCTION MANAGER

Sarah H. Faus

ES&T RESEARCH

Kinetics of Ozone Decomposition: A Dynamic Approach

Mirat D. Gurol*

Department of Civil Engineering, Drexel University, Philadelphia, Pennsylvania 19104

Philip C. Singer

Department of Environmental Sciences and Engineering, University of North Carolina, Chapel Hill, North Carolina 27514

■ Decomposition kinetics of ozone in aqueous solution were studied at 20 °C and in the pH range 2–10, under both quiescent and dynamic conditions. The data obtained in a batch reactor under quiescent conditions were analyzed by integral, initial-rate, and differential methods. The results indicated that ozone decomposes by a second-order reaction with respect to ozone concentration. The second-order decomposition kinetics determined in the batch reactor was confirmed by using a mathematical model developed for ozone decomposition in an ozone contact column and the experimental observations under such dynamic conditions. The rate of decomposition was found to be relatively insensitive to pH below 4 and relatively slow under such acidic conditions (k_d = 0.27 L/(mol s)). Above pH 4, the rate is pH dependent with $k_d = k_0[OH^-]^{0.55}$, where k_0 is specific to the chemical composition of the aqueous system.

Introduction

Ozone is considered to be an attractive alternative to chlorine for water and wastewater disinfection and for the oxidation of various organic and inorganic contaminants. The rate of disinfection of microorganisms by ozone is proportional to the concentration of ozone in solution. Since ozone is unstable in aqueous solution, its effectiveness as a disinfectant depends upon the rate at which it decomposes. With respect to its behavior as an oxidant, ozone can react via a direct reaction pathway involving molecular ozone or by an indirect pathway involving various highly reactive radicals that arise from the decomposition. Therefore, to be able to design an efficient ozonation system, it is important to determine the kinetics of decomposition of ozone and the variables affecting the rate of decomposition.

The decomposition of ozone in aqueous solution has been studied for several decades. In a review of the literature on the kinetics of ozone decomposition, the most common observation is the reported disagreement among different researchers as to both the order of the decomposition reaction and the magnitude of the reaction rate constant. The range of conditions investigated by various researchers and their conclusions concerning the reaction order relative to ozone were summarized by Peleg (*1*). This information is updated in Table I. Furthermore, although it is generally agreed that the reaction is catalyzed by the hydroxide ion, there are also substantial differences regarding the pH dependence of the reaction, as shown in Table II.

Table I. Summary of the Kinetics of Ozone Decomposition Decomposition in Water

ref	pH	temp, °C	reaction order
2	2-4	0	2
3	5.3-8	0	2
4	acidic		3/2
	basic		1
5	1-2.8	0-27	1
6	7.6-10.4	1.2-19.8	1
7	0-6.8	25	3/2
7	8-10	25	2
8	5.4-8.5	5-25	3/2
9	10-13	25	1
10	9.6-11.9	25	1
11	6	10-50	3/2-2
11	8	10-20	1
11	2-4	30-60	2
12	0.22-1.9	5-40	1 or 2
13	9	20	1
14	8.5-13.5	18-27	1
15	0.5-10.0	3.5-60	1
16	2.1-10.2	25	3/2
17	acidic	25	1-2
	basic	25	1

Table II. Rate Equations for Decomposition of Ozone

ref	rate eq, $r = -d[O_3]/dt$
3	$k_0[OH^-]^{0.36}[O_3]^2$
4[a]	$k_1[OH^-][O_3] + k_2[OH]^{0.5}[O_3]^{1.5}$
5	$k_0[OH^-]^{0.5}[O_3]$
6	$k_0[OH^-]^{0.75}[O_3]$
14[b]	$k_0[OH^-]^{1.0}[O_3]$
15	$k_0[OH^-]^{0.12}[O_3]$
16	$k_0[OH^-]^x[O_3]^{3/2}$, x is pH dependent
17	$k_0[OH^-]^{0.88}[O_3]$

[a] Formulated from a mechanistic model. [b] Packed column.

These major differences among the findings of the various researchers are believed to be due to (a) the use of different, sometimes questionable, analytical techniques to measure the concentration of dissolved ozone, (b) uncertainties in the data analysis and data interpretation,

0013-936X/82/0916-0377$01.25/0

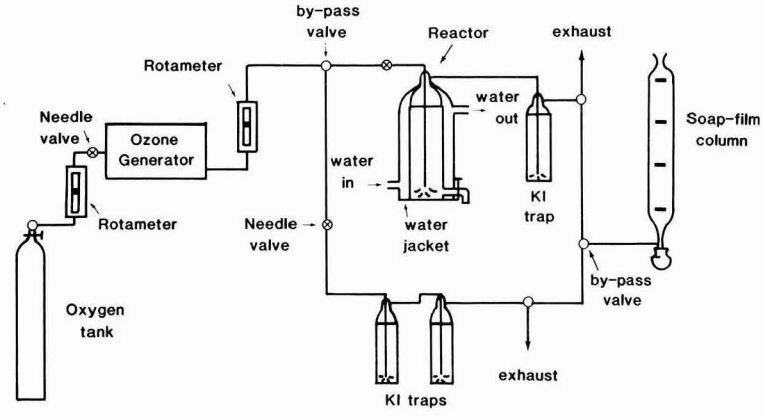

Figure 1. Experimental apparatus.

(c) the effect of solution composition, e.g., the ionic medium, on decomposition, and (d) the possible presence of impurities in the reagents used. Additionally, most of the researchers studied the decomposition reaction in batch reactors and analyzed their data only by the integral method.

Method of Approach

In this investigation, the kinetics of ozone decomposition were studied under both static and dynamic conditions. As a first step, the reaction was carried out in a batch reactor under quiescent conditions. Measurement of the ozone concentration with time allowed the determination of the order (n) and the reaction rate constant (k_d) in accordance with

$$r_{O_3} = -d[O_3]/dt = k_d[O_3]^n \quad (1)$$

The decomposition kinetics were also studied in an ozone contact column at constant temperature and under dynamic conditions whereby ozone was bubbled continuously through buffered solutions of known ionic composition to provide complete mixing. Under such conditions, the rate of change of ozone with time can be expressed as

$$d[O_3]/dt = k_La([O_3]^* - [O_3]) - r_{O_3} \quad (2)$$

where k_La is the mass transfer coefficient governing the absorption of ozone by the solution, $[O_3]^*$ is the saturation concentration of ozone in accordance with Henry's Law and the applied partial pressure of ozone in the gas stream contacting the solution, and r_{O_3} is the rate of decomposition of ozone. Here, it was assumed that the mass transfer of ozone is controlled by the liquid film since ozone is slightly soluble in water. At steady state, the rate of ozone absorption is equal to the rate of ozone decomposition, or

$$k_La([O_3]^* - [O_3]_{ss}) = (r_{O_3})_{ss} \quad (3)$$

where $[O_3]_{ss}$ is the concentration of ozone at steady-state.

The saturation concentration of ozone and the mass-transfer coefficient of the system were measured independently in a solution of pH where the rate of ozone decomposition is negligible. Equation 2 for this system would be modified to

$$d[O_3]/dt = k_La([O_3]^* - [O_3]) \quad (4)$$

Concentration of ozone was followed with time until the equilibrium concentration of ozone was reached. This concentration was taken as $[O_3]^*$. k_La was determined from the slope of the straight line obtained according to the integrated form of eq 4

$$\ln \frac{[O_3]^* - [O_3]}{[O_3]^* - [O_3]_0} = (k_La)t \quad (5)$$

where $[O_3]_0$ is the concentration of dissolved ozone at $t = 0$.

This mass transfer information from eq 5 and the decomposition kinetics as determined under quiescent conditions (eq 1) were used in eq 3 to predict the steady-state concentration of ozone at various pH values in the ozone contact column. $[O_3]_{ss}$ values were also measured experimentally and compared to the predicted values to confirm the kinetic expression of the decomposition reaction as determined from the batch experiments.

Experimental Setup

The experimental setup used in this study is shown in Figure 1. Oxygen gas was supplied in standard cylindrical tanks and fed to an ozone generator. The percentage of ozone produced in the oxygen gas was controlled by changing the power input to the generator. The rotameters before and after the ozone generator were frequently calibrated by a soap-film technique during the experimental runs. The soap-film column was connected to the system downstream of the reactor and the KI traps. A bypass valve located after the second rotameter was used to divert the flow to either the reactor or the traps. The needle valves were used to balance the gas flow and maintain it constant into the traps and the reactor.

The reactor consisted of a gas washing bottle fitted with a ground-glass joint. A coarse sintered-glass dispersion tube delivered ozone gas to the bottom of the reaction vessel. The height to diameter ratio of the vessel was about 4:1 to maintain good mixing of the solution by the bubbling gas. Since optimization of gas transfer was not the objective of this investigation, no attempt was made during the study to modify the reactor system to improve gas transfer. To keep the temperature of the contents of the reactor constant at 20 °C, water was continuously circulated by a water pump from a 20 °C water bath through a water jacket around the reactor. A liquid sampling port was located about 1 cm from the bottom of the bottle. Excess ozone gas passed out through the top of the reactor into a gas washing bottle containing 2% KI solution. Two gas absorption bottles in series were connected to the system in parallel to the reactor to determine the quantity

of ozone generated and applied to the column per unit time and the partial pressure of ozone in the feed stream.

Experimental Procedure

Ozone-demand-free water was prepared by ozonating distilled and deionized water for about 15 min. Residual ozone was then stripped out of solution by nitrogen gas; the resulting water was used to prepare the test solutions. At pH values less than 4, pH was controlled with dilute sulfuric acid. Sodium sulfate, which has been observed to have no effect on ozone decomposition in water (Hoigné and Bader (*18*)), was used to adjust the ionic strength, μ, of these solutions of low pH. A KH_2PO_4/K_2HPO_4 buffer system was used over the pH range 6–9 and a H_3BO_3/NaOH buffer system was used over the range 7–10 for pH control. Some overlap of the two buffer systems was examined to test the reproducibility of the kinetic results with respect to the two buffer systems. The ionic strength of the borate solution was adjusted with Na_2SO_4. The KH_2PO_4 and K_2HPO_4 salts were mixed in precalculated amounts to adjust both the ionic strength as well as the pH of the buffer solutions. In order to observe any possible ionic-strength effects, the decomposition reaction was studied in solutions of ionic strength 0.1 and 1.0.

For the first phase of the investigation in the batch reactor, the buffered solutions were brought to 20 °C and then ozonated with an oxygen stream containing about 5% (by weight) of ozone at a flow rate of approximately 0.4 L/min for approximately 15 min. Depending on the pH of the test solution, dissolved ozone concentrations of 5–40 mg/L were reached. The gas flow was then turned off, and the residual dissolved ozone concentration was followed iodimetrically in accordance with "Standard Methods" (*19*) (procedure 143 B). Potassium iodide solution was buffered at pH 7 by phosphate buffer. The concentration of residual dissolved ozone was also followed by the indigo procedure (Hoigné and Bader (*20*)). This procedure is more sensitive to low ozone concentrations and is believed to be subject to less interference from other oxidizing species that might arise as products of ozone decomposition. The water-soluble trisulfonated potassium salt of indigo ($C_{16}H_7K_3N_2O_{11}S_3$, MW = 616.7) was prepared by treating the water-insoluble indigo ($C_{16}H_{10}N_2O_2$) with concentrated sulfuric acid according to the procedure of Dorta-Schaeppi and Treadwell (*21*). The procedure was calibrated by using ozone solutions standardized by the KI procedure. So that any interference in the KI procedure arising from decomposition products of ozone would be minimized, the calibrations were made at pH 3. The change in absorbance of the indigo solution was also calibrated against UV absorption measurements of ozone at 260 nm to assure no interference of decomposition products.

In the ozone contact column, k_La and $[O_3]^*$ were measured in a solution with pH 3, a constant ionic strength, and a temperature of 20 °C. The solution was ozonated at a constant gas flow rate, and the ozone concentration was followed by taking frequent samples of solution at small time intervals and analyzing them iodimetrically.

For measurement of the concentration of ozone in the gas stream, the ozone–oxygen mixture was diverted around the reactor into the traps containing neutral buffered 2% KI solution for a constant period of time (30–75 s) at the termination of the experimental run. The ozone generated per unit time was assumed to be constant throughout the experimental run. The contents of the traps were titrated with standardized $Na_2S_2O_3$, and the ozone concentration in the gas stream was calculated by knowing the flow rate through the traps.

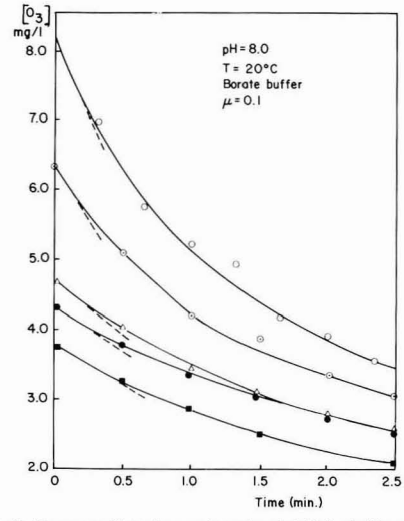

Figure 2. Decomposition of ozone in water at pH 8.0, at different initial ozone concentrations.

The experimental procedure was repeated for pH values in the range 2–10 to observe the effect of pH on the steady-state concentration of ozone in water at 20 °C. For each experimental run, the gas flow rate, partial pressure of ozone in the gas mixture, and ionic strength of the solution were kept constant. The pH was buffered as described above.

Results and Discussion

Kinetics of Ozone Decomposition in Batch Systems. The data collected from the batch experiments over the pH range 2–10 were analyzed by the integral, initial-rate, and differential methods. When the integral method was applied, the correlation coefficients for least-square fit to second-order kinetics were always higher than those calculated for first- and $^3/_2$-order kinetics. For pH values below pH 7, the second-order fit was significantly better than a first- or $^3/_2$-order fit in a 95% confidence interval. However, statistical analyses of the experimental results at pH values above 7 were unable to distinguish between first-, $^3/_2$-, and second-order kinetics, even in the 90% confidence interval. Consequently, to test the decomposition kinetics further in the basic pH range, the initial-rate method was applied to the experimental data.

It was assumed that the initial rate of decomposition $(r_{O_3})_0$ is

$$(r_{O_3})_0 = k_d[O_3]_0^n \tag{6}$$

where $[O_3]_0$ is the initial ozone concentration. Then

$$\log (r_{O_3})_0 = \log k_d + n \log [O_3]_0 \tag{7}$$

The initial rates were determined by fitting a polynomial to the experimental data and differentiating at $t = 0$. The resulting initial rates are shown in Figure 2. In Figure 3, $\log (r_{O_3})_0$ is plotted against $\log [O_3]_0$ for the experiments at pH 8, 9, and 9.5. The slopes of the three lines, determined by least-squares analysis, indicate reaction orders of 1.8, 1.8, 2.0, respectively. Thus, for practical purposes, second-order kinetics represents the data much better than does first-order or $^3/_2$-order kinetics.

For a check on whether the application of eq 7 to the rest of the data for $t > 0$ will also fit second-order kinetics,

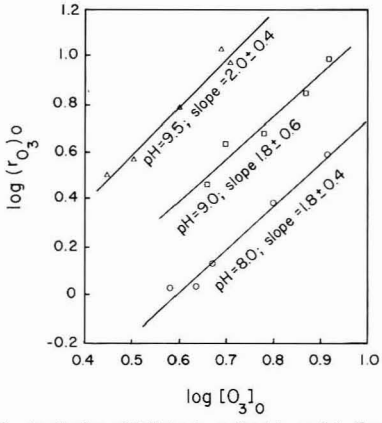

Figure 3. Application of initial rate method (μ = 0.1, T = 20 °C).

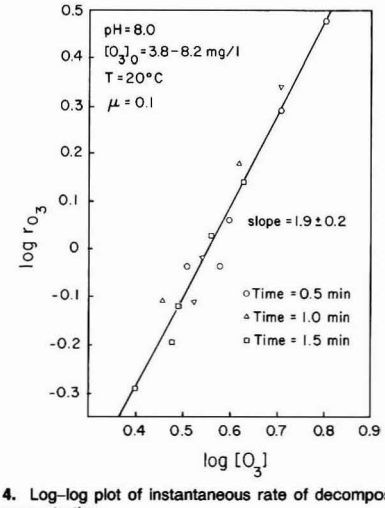

Figure 4. Log–log plot of instantaneous rate of decomposition vs. ozone concentration.

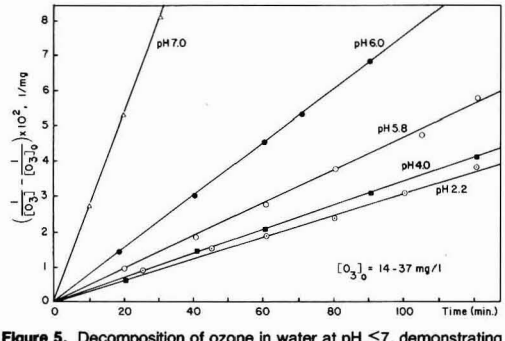

Figure 5. Decomposition of ozone in water at pH ≤7, demonstrating second-order kinetics (T = 20 °C, μ = 1.0).

log r_{O_3} values were plotted against log $[O_3]$ at t = 0.5, 1.0, and 1.5 min for five different experimental runs at pH 8 (see Figure 4). The data consistently indicated second-order kinetics for the decomposition of ozone, cofirming the results of the initial-rate analyses. This observation suggests further that the mechanism of the decomposition

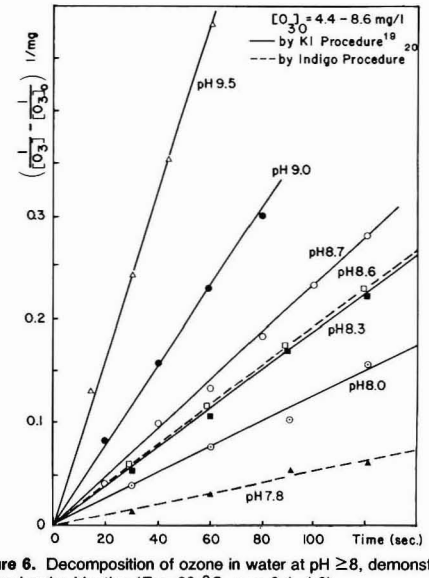

Figure 6. Decomposition of ozone in water at pH ≥8, demonstrating second-order kinetics (T = 20 °C, μ = 0.1, 1.0).

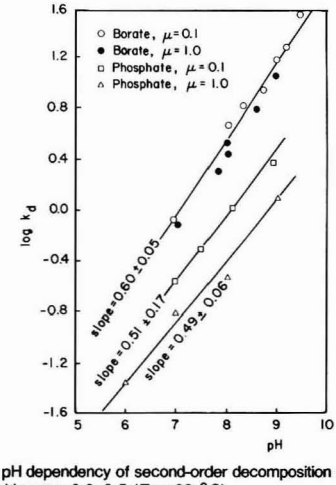

Figure 7. pH dependency of second-order decomposition rate constant over the pH range 6.0–9.5 (T = 20 °C).

reaction does not change during the course of the reaction.

So that the second-order reaction rate constants could be determined more precisely, the data were plotted according to the integral method as shown in Figures 5 and 6. Figure 5 indicates that the rate of decomposition of ozone is essentially independent of pH between pH 2 and 4 (k_d = 0.24 and 0.27 L/(mol s) at pH 2 and 4, respectively). Above pH 4, the rate increases markedly with increasing pH.

The second-order reaction rate constants are plotted in Figure 7 as a function of pH for the phosphate and borate buffers and for ionic strengths of 0.1 and 1.0. The kinetics of ozone decomposition can be expressed by the relationship

$$r_{O_3} = k_0[O_3]^2[OH^-]^{0.55} \quad (8)$$

k_0 is specific to the chemical composition of the aqueous solution. The order with respect to hydroxide ion is not

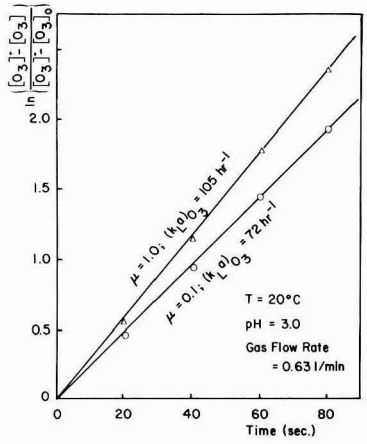

Figure 8. Effect of ionic strength on the mass-transfer coefficient of the system.

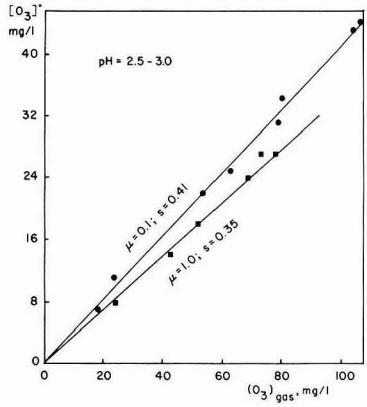

Figure 9. Solubility of ozone in water at 20 °C.

significantly different (within the 95% confidence interval) for the phosphate and borate buffers.

Figure 7 shows that phosphate has a significant retardation effect on the rate of ozone decomposition. Phosphate acts as an hydroxyl radical (OH·) scavenger (*22*); as a result, the decomposition rate in solutions of higher phosphate concentration (μ = 1.0) is much slower than the rate in the more dilute (μ = 0.1) phosphate solutions. Although the decomposition rate appears to be faster in borate solutions of lower ionic strength, the difference is not significant within the 95% confidence interval.

Expressions 9–11 were obtained for the second-order decomposition rate constant by applying the method of least squares to the data in Figure 7 for borate, phosphate with μ = 0.1, and phosphate with μ = 1.0, respectively, over the pH range 6.0–9.5, at 20 °C.

$$k_d = (2.2 \pm 0.2) \times 10^5[OH^-]^{0.60\pm0.05} \quad (9)$$

$$k_d = (1.4 \pm 0.4) \times 10^4[OH^-]^{0.51\pm0.17} \quad (10)$$

$$k_d = (4.8 \pm 1.6) \times 10^2[OH^-]^{0.49\pm0.06} \quad (11)$$

Due to questions associated with the KI procedure (e.g., interferences due to decomposition products of ozone, stoichiometric ratio of iodine liberated/mol of ozone reacting with iodine), the indigo method was also used to measure the residual ozone concentration with time. The application of the integral method to data gathered at pH 7.8 and 8.6 using the indigo procedure is included in Figure 6. The second-order rate constants determined by using the indigo procedure fall within the 95% confidence interval of the observations made with potassium iodide.

The conclusion that the decomposition of ozone over the pH range 2–9.5, under batch conditions, conforms to second-order kinetics adds to the confusion reported in the literature regarding the order of the ozone decomposition reaction (see Table I). In order to verify the results of the batch studies, the dynamic approach was adopted to provide an independent measure of the kinetics of the ozone decomposition reaction.

Decomposition of Ozone in Dynamic Systems. Absorption and Solubility of Ozone. The mass-transfer coefficient and saturation concentration of ozone were determined for the ozone contact column in a pH 3 solution of Na_2SO_4, where the rate of ozone decomposition is extremely slow. Figure 8 illustrates the application of eq 5 to determine the mass-transfer coefficient of the system.

Table III. Comparison of Literature Values for Ozone Solubility with Solubility Coefficients Determined in this Study

ref	solubility coeff
Mailfert,[a] 1894[b]	0.41 (19 °C)
Luther,[a] 1905[b]	0.25 (20 °C)
Kawamura,[a] 1932[b]	0.31 (20 °C)
Briner & Perottet,[a] 1939[b]	0.34 (19.8 °C)
Seidell, 1940[c]	0.35 (20 °C)
Stumm (*23*)	0.34 (20 °C)
Nyberg, 1962[d]	0.23 (20 °C)
Kirk-Othmer[a] (*24*)	0.30 (20 °C)
this work	0.35 (20 °C), μ = 1.0
	0.41 (20 °C), μ = 0.1

[a] Solubility coefficient calculated from absorption coefficient. [b] Data given by Hoather (*25*). [c] Data given by Taylor (*26*). [d] Data given by O'Donovan (*27*).

It was observed that the ionic strength of the solution has a pronounced effect on the mass-transfer coefficient. This might be due to changes in the interfacial area, "*a*", caused by changes in the sizes of the gas bubbles, which is a function of the surface tension of the solution and is influenced by ionic strength.

The saturation concentration of ozone, $[O_3]^*$, was measured for various ozone concentrations in the gas phase, $[O_3]_{gas}$. The solubility coefficient, *s* (the ratio of $[O_3]^*$ to $[O_3]_{gas}$), was also observed to be dependent on the ionic strength of the solution. Figure 9 shows that at 20 °C and atmospheric pressure, *s*, in units of (mg of ozone/L of water)/(mg of ozone/L of gas), is 0.35 for μ = 1.0 and 0.41 for μ = 0.1 Na_2SO_4. Table III compares the solubility coefficients determined in this study with the values reported in the literature. The results reported herein are essentially in agreement with the literature values, considering that most of the previous researchers have not reported the pH, chemical composition, and ionic strength of their solutions.

In Figure 10, the observed steady-state ozone concentrations obtained in the dynamic systems are shown at various pH values when $k_L a$ = 60 h^{-1}, $[O_3]_{gas}$ = 83 mg/L, T = 20 °C, and μ = 0.1. The data are represented by the discrete points shown in the figure. At pH values less than 6, decomposition is relatively slow, and under the experimental conditions, $[O_3]_{ss}$ is equal to $[O_3]^*$. Above pH 6, the rate of decomposition becomes significant, and $[O_3]_{ss}$ is determined by both the rate of ozone decomposition and the rate of ozone absorption. The rate of decomposition is not sufficiently fast, however, to make the decomposition

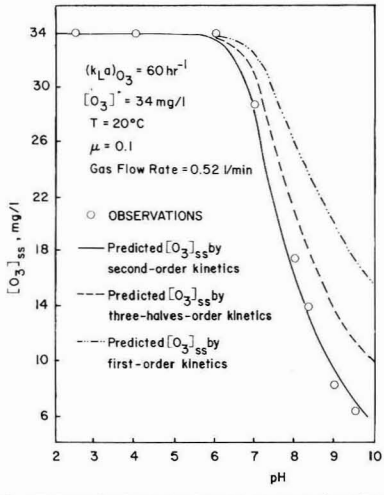

Figure 10. pH dependency of steady-state concentration of ozone and comparison of measured and predicted steady-state ozone concentration at various pH values.

reaction mass-transfer limited, even at pH 9.5.

Comparison of Measured and Predicted $[O_3]_{ss}$. After establishment of the decomposition kinetics as second order with respect to ozone concentration in the batch reactor, the second-order expression was applied to the dynamic system to calculate the steady-state ozone concentration in accordance with eq 3 as follows:

$$k_La([O_3]^* - [O_3]_{ss}) = k_d([O_3]_{ss})^2 \quad (12)$$

After substitution of the measured k_La, $[O_3]^*$, and appropriate k_d values from eq 9–11, eq 12 was solved for $[O_3]_{ss}$ at various pH values.

In Figure 10, the predicted steady-state concentrations of ozone from eq 12 are compared to the measured $[O_3]_{ss}$ values when k_La = 60 h^{-1}, $[O_3]^*$ = 34 mg/L, T = 20 °C, and μ = 0.1. The close match between the predicted and measured concentrations in the dynamic system confirms the second-order kinetic expression for ozone decomposition established in the batch system.

Calculations were also made for the steady-state ozone concentration by assuming first- and $^3/_2$-order kinetic expressions in eq 3. The appropriate rate constants for first- and $^3/_2$-order kinetics were obtained from the batch kinetic data for the various pH values investigated by using the lines of best fit from the integrated kinetic expressions and are listed in Table IV. The steady-state ozone concentrations predicted from first- and $^3/_2$-order kinetics are also shown in Figure 10 to emphasize the better fit of the dynamic data to second-order kinetics.

The second-order kinetic model was tested further by using the same dynamic procedure under different sets of experimental conditions. Details are presented elsewhere (*28*). In each case, the second-order kinetic model provided the best fit to the experimental data.

Some concerns have been expressed in the literature (*29*, *30*) regarding the catalysis of ozone decomposition in the gas phase by sintered-glass diffusers. Considering the possibility that this type of diffuser might also cause catalytic ozone decomposition in the solution phase, the above procedure was repeated with a glass impinger for gas transfer instead of the sintered-glass diffuser employed in the previous dynamic experiments. Figure 11 shows the observations for the impinger study, where k_La = 11 h^{-1},

Table IV. Calculated Decomposition Rate Constants[a] Assuming First-, Three-halves-, and Second-Order Kinetics (μ = 0.1, T = 20 °C)

	n = 1		n = $^3/_2$		n = 2	
pH	10^3k_d, s^{-1}	r^2	k_d, L$^{1/2}$/(mol$^{1/2}$ s)	r^2	k_d, L/(mol s)	r^2
7.0 (phosphate)	0.47	0.959	0.04	0.988	3.5	0.991
8.0 (borate)	6.0	0.975	0.60	0.990	56.0	0.992
9.0 (borate)	10.0	0.979	1.34	0.992	176.0	0.999
9.5 (borate)	16.0	0.984	2.74	0.995	480.0	0.996

[a] Constants were calculated from a least-squares analysis using the integrated kinetic expressions applied to the batch experimental data shown in Figures 5 and 6.

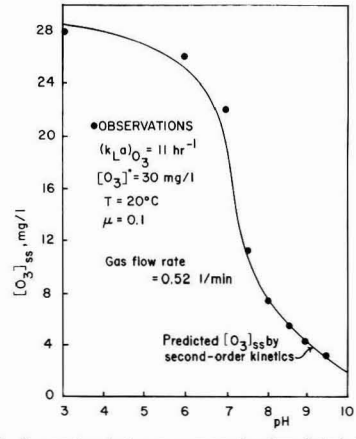

Figure 11. Comparison between measured and predicted steady-state concentration of ozone at various pH values with an impinger for Gas Transfer.

$[O_3]^*$ = 30 mg/L, T = 20 °C, and μ = 0.1 (note: k_La was measured for the impinger at an equivalent gas flow rate and was found to be significantly lower than for the sintered-glass diffuser, as expected). Again a very good match was obtained between the observed steady-state ozone concentration and the predictions of the expression based on second-order kinetics. It should be noted that, in view of the slower rate of mass transfer of ozone under these experimental conditions, the influence of ozone decomposition on the steady-state ozone concentration is evident at lower pH values than in the previous cases.

Comparison with Preceding Results. Most of the previous researchers who investigated the decomposition of ozone used batch reactors and applied only the integral method for kinetic analysis of their data. When the reaction was slow, at lower pH values, they were able to follow the reaction long enough to collect sufficient data to perform a reliable kinetic analysis. Several researchers (*2*, *3*, *11*, *12*, *17*) agreed that second-order kinetics govern the reaction for low pH values. At higher pH, it was not always possible to collect enough data to clearly distinguish between reaction orders. For example, Hewes and Davison (*11*) concluded that the kinetics might change from second to first order in the pH range 6–8. Sullivan and Roth (*15*), on the other hand, reported the adequacy of any order between $^1/_2$ and $^3/_2$ to describe their data but decided on

first-order for convenience. Our observation that for basic pH values the integral method could not provide a statistical distinction between first-, $^3/_2$-, and second-order kinetics supports these arguments and underscores the major shortcoming associated with the previous studies.

In this study, application of the initial-rate and differential methods as well as the integral method demonstrated the better fit of a second-order kinetic model to the data. This model was confirmed independently under dynamic conditions.

There are a limited amount of data in literature to provide a meaningful comparison with the second-order decomposition rate constants determined in this study at 20 °C. If the data of the other researchers could be molded to a second-order kinetic model, the resulting rate constants might compare favorably to those determined in this study.

Summary

The kinetics of ozone decomposition were studied in a batch reactor under quiescent conditions. Analysis of the data by initial-rate, differential, and integral methods demonstrated that decomposition of ozone can be approximated by a second-order reaction in the pH range 2–9.5. The second-order kinetic expression was confirmed independently under dynamic conditions, in an ozone contact column. Despite the apparent confusion in the literature, it appears that the rate of ozone decomposition can be expressed as

$$r_{O_3} = -d[O_3]/dt = k_0[OH^-]^{0.55}[O_3]^2$$

The dynamic approach represents a valid, useful, and independent method of testing kinetic data obtained from batch reactor studies.

Acknowledgments

This paper was presented at the 53rd Annual Conference of the Water Pollution Control Federation, Las Vegas, Nevada, September 28–October 3, 1980.

Literature Cited

(1) Peleg, M. *Water Res.* **1976**, *10*, 361–365.
(2) Rothmund, V.; Burgstaller, A. *Monatsh. Chem.* **1913**, *34*, 665–692.
(3) Sennewald, K. *Z. Phys. Chem.* **1933**, *A164*, 305–317.
(4) Weiss, J. *Trans. Far. Soc.* **1935**, *31*, 668–681.
(5) Alder, M. G.; Hill, G. R. *J. Am. Chem. Soc.* **1950**, *72*, 1884–1886.
(6) Stumm, W. *Helv. Chem. Acta* **1954**, *37*, 773–778.
(7) Kilpatrick, M. L.; Herrick, C. C.; Kilpatrick, M. *J. Am. Chem. Soc.* **1956**, *78*, 1784–1790.
(8) Rankas, M. M.; Siirode, E. K.; Kyulm, S. R. *Chem. Abstr.* **1964**, *60*, 2633e.
(9) Czapski, G.; Samuni, A.; Yellin, R. *Isr. J. Chem.* **1968**, *6*, 969–971.
(10) Rogozhkin, G. I, *Chem. Abstr.* **1970**, *73*, 81108y.
(11) Hewes, C. G.; Davison, R. R. *AIChE J.* **1971**, *17*, 1, 141–147.
(12) Merkulova, V. P.; Louchikov, V. S.; Ivanovskii, M. D. *Izv. Vyssh. Ucheb. Zaved. Khim. Technol.* **1971**, *14*, 5.
(13) Shambaugh, R. L.; Melnyk, P. B. Presented at IOI's Forum on Ozone Disinfection, Chicago, IL, 1976.
(14) Rizzuti, L.; Augugliaro, V.; Marrucci, G. *Chem. Eng. J.* **1977**, *13*, 219–224.
(15) Sullivan, D. E.; Roth, J. A. Presented at AIChE Symposium, Houston, TX, 1979.
(16) Li, K. Y. Ph.D. Dissertation, Mississippi State University, Starkville, MS, 1977.
(17) Teramoto, M.; Imamura, S. "Kinetic Analysis of Oxidation by Ozone"; Dept. of Indust. Chem. Kyoto Inst. of Tech., Makugasaki Kyoto, Japan, 1979.
(18) Hoigné, J.; Bader, H. *Water Res.* **1976**, *10*, 377–386.
(19) "Standard Methods for the Examination of Water and Wastewater", 13th ed.; APHA: Washington, D.C., 1971.
(20) Hoigné, J.; Bader, H. *Water Res.* **1981**, *15*, 449.
(21) Dorta-Schaeppi, Y.; Treadwell, W. D. *Helv. Chem. Acta* **1949**, *32*, 1, 356–364.
(22) Hoigné, J.; Stachelin, J., personal communication, 1979.
(23) Stumm, W. J. *Boston Soc. Civil Eng.* **1958**, *45*, 69–79.
(24) Kirk, R. E.; Othmer, D. F. "Encyclopedia of Chemical Technology", 2nd ed.; Wiley: New York, 1967; Vol. 14, p 412.
(25) Hoather, R. C. *J. Inst. Water Eng.* **1948**, *2*, 358–368.
(26) Taylor, J. J. *J. Inst. Water Eng.* **1947**, *1*, 187–201.
(27) O'Donovan, D. C. *Jour. AWWA* **1965**, *57*, 1167–1192.
(28) Gurol, M. D. Ph.D. Dissertation, University of North Carolina, Chapel Hill, NC, 1980.
(29) "Methods of Air Sampling and Analysis"; Intersociety Committee; APHA, 1972.
(30) Perrich, J.; McCammon J.; Cronholm, L.; Fleishman, M.; Pavoni, J.; Riesser, V. *AIChE Symp. Ser.* **1976**, *73*, 166, 225–229.

Received for review May 21, 1981. Revised manuscript received December 3, 1981. Accepted March 10, 1982. This study was partially supported by the World Health Organization and the School of Publich Health of the University of North Carolina at Chapel Hill.

Environ. Sci. Technol. 1982, 16, 384–387

Limits in Charged-Particle Collection by Charged Drops†

Keng H. Leong,*‡ James J. Stukel,§ and Philip K. Hopke§

Department of Civil Engineering, Institute of Environmental Studies, and Department of Mechanical Engineering, University of Illinois at Urbana–Champaign, Urbana, Illinois 61801

■ The effectiveness of particulate collection of single drops with different levels of charge in a subsaturated environment is modeled with reference to charged-droplet scrubbers. Results show that a monotonic increase in particulate collection cannot be achieved by continuously increasing the charge on the drops due to Rayleigh instability. Droplets formed from breakup may act as sources of particles by evaporating completely to solid particles. Effectiveness of particulate collection is optimized by the use of highly charged drops in a countercurrent aerosol flow with the condition that the drops reach the bottom of the scrubber chamber without breaking up. The present model also predicts that the comparison of theoretical penetration with experimental values will be difficult because of the high sensitivity of the penetration to the drop size.

Introduction

Theoretical and experimental investigations have established that charged-drop collection is an important method for controlling fine particles (*1–4*). Increases in collection efficiencies of about 15% for 1-μm-diameter particles to over 45% for 0.3-μm-diameter particles were obtained (*2*) by charging the drops in a scrubber. The work of Kraemer and Johnstone showed that collision efficiencies for fine particles of over 10 000% can be achieved by adequate charging of the collector metal sphere used and particles of opposite polarity. In particulate control, water drops are usually used. Unlike metal or solid spheres, the maximum charge that can be placed on liquid drops is not limited by corona breakdown but by the Rayleigh criterion that establishes the maximum charge a liquid drop can possess without becoming hydrodynamically unstable. Abbas and Latham (*5*) showed that highly charged evaporating drops become unstable when the charge exceeded the Rayleigh limit and subsequently eject charged droplets. Hence, the charge on an evaporating drop decreased, and the total number of drops present increased with time. These effects on the particulate collection characteristics are examined in this work.

Effects of Rayleigh Instability

The Rayleigh criterion (*6–8*) for hydrodynamic stability of a charge drop is given by

$$Q^2 < 64\pi^2\epsilon R^3\sigma \tag{1}$$

where Q is the drop charge, ϵ is the permitivity of air, R is the drop radius, and σ is the surface tension. Hence, the maximum charge on a drop increases with drop size and surface tension. For highly charged drops and small particles (<2 μm), Coulombic force is the dominant collection mechanism (*1*). The collision efficiency is given by

$$E = -4K_C = -Qq/(6\pi^2\epsilon\eta aR^2U) \tag{2}$$

where K_C is the electrostatic parameter, q is the particle charge, η is the dynamic viscosity, a is the particle radius, and U is the speed of the drop. In terms of the fraction f of the Rayleigh charge, the efficiency is

$$E = 4fq(\sigma/R)^{1/2}/(3\rho\eta\epsilon^{1/2}Ua) \tag{3}$$

where q is positive and the drop has a negative charge Q. For a positively charged drop, the maximum efficiency is usually lower due to breakdown of the surrounding air before the Rayleigh limit is reached (*9*). Equation (*3*) shows that the collision efficiency is optimized by maximizing the surface tension of the drop.

McCully et al. (*10*) and Goldshmid and Calvert (*11*) have shown that nonwettable particles are collected less efficiently by drops than wettable particles. The decreased collection efficiency was attributed to the nonwettable particles forming a layer on the drop surface and subsequent particles bouncing off this layer, whereas wettable particles were quickly incorporated into the drop (*12–14*). The addition of surfactants will enhance the wettability and, hence, the sticking efficiency of the nonwettable particles. An increased collection efficiency will then be obtained. However, surfactants decrease the surface tension, and this causes a decrease in the maximum charge attainable by the drop. Hence, the optimization of the collection efficiency for nonwettable particles depends on the increase of the sticking efficiency by addition of surfactants and the consequential counteracting effect of maximum charge decrease.

Effects of Evaporation on Highly Charged Drops

Air entering particulate control devices are usually not at 100% relative humidity, and charged drops injected into the aerosol will evaporate. When the drop decreases in size to that specified by the Rayleigh criterion, the drop becomes unstable and breaks up into a residual drop and several droplets with a charge to mass ratio much higher than the residual drop. Abbas and Latham's (*5*) data showed that the ratio of the residual drop radius to the original drop was approximately constant for radii 50–100 μm. This ratio depends on the rate of evaporation (*15*). The residual drops had approximately 98–99% of the maximum charge. The droplets ejected were estimated to be less than 15 μm in radius by Doyle et al. (*16*). Further evaporation may cause a cascading process leading to the formation of numerous droplets. The charge loss or the total charge on the ejected droplets is given by

$$Q_e = 8\pi(\epsilon\sigma)^{0.5}R^{1.5}(1 - f_r k^{1.5}) \tag{4}$$

where f_r and kR are the fraction of the maximum charge and the radius of the residual drop, respectively. With the assumption that the number N of droplets ejected have the same size and charge, the droplet charge is

$$Q_d = Q_e/N \tag{5}$$

The number of droplets may be estimated by using the restriction that the droplet radius is less than 15 μm and that the mass conservation equation for the liquid is

$$N = (1 - k^3)(R/r)^3 \tag{6}$$

† This work was presented at the 74th Annual Meeting of the Air Pollution Control Association, June 21–26, 1981, Philadelphia.

‡ Department of Civil Engineering and Institute of Environmental Studies.

§ Department of Civil Engineering and Department of Mechanical Engineering.

0013-936X/82/0916-0384$01.25/0

Hence, for $R = 100\ \mu m$ and $k = 0.9$

$$N > 81 \tag{7}$$

The fraction f_d of the maximum charge on the droplet is

$$f_d = Q_d/(8\pi(\epsilon\sigma)^{0.5}r^{1.5}) < (r/R)^{1.5}(1 - f_r k^{1.5})/(1 - k^3) \tag{8}$$

with the values given for R and k, and $f_r = 0.98$

$$f_d < 0.04 \tag{9}$$

This value of f_d implies that a 15-μm radius droplet will have to evaporate to 1.75-μm radius before reaching the Rayleigh limit. Hence, droplets ejected may break up into smaller droplets.

For the residual drop, the Rayleigh limit will be reached when the radius decreases to $f_r^{2/3}$ times its initial value. The rate of decrease is

$$dR/dt = -N_S D_v \Delta\rho_v/(2R\rho_d) \tag{10}$$

where N_S is the Sherwood number, D_v is the diffusion coefficient of the vapor, $\Delta\rho_v$ is the effective difference in the vapor densities for evaporation, and ρ_d is the density of the drop. Then the time interval before the residual drop becomes unstable is

$$\Delta t = f_d k^2 R^2 (1 - f_r^{4/3})/(N_S D_v \Delta\rho_v) \tag{11}$$

For a relative humidity of 90% at 50 °C

$$\Delta t = 0.4\ s \tag{12}$$

With the assumption that the drop falls at terminal velocity, the distance traveled in that time interval is less than 0.3 m. Hence, depending on the residence time of the drop in the chamber and the relative humidity, several breakups may occur with the production of numerous droplets and loss of charge. These small droplets may decrease the number of particles collected by the large drop by collecting particles themselves. However, due to their small size, they may evaporate to solid particles. Consequently these small droplets may act as sources of particles.

Effectiveness of Particulate Collection in Charged-Droplet Scrubbers

In scrubbers, for a given set of operating parameters, the particle penetration is minimized by maximizing the single-drop collection efficiency. For estimating the penetration, each drop is usually assumed to have a constant collection efficiency. If the drop size decreases from evaporation or breakup, the single-drop collection efficiency will change. An effective collection efficiency computed for a given set of conditions can be used to account for the change in drop size. However, the penetration depends on the total particle collection by each drop. This is a function of the effective volume V of particulate-laden air swept out by each drop, where V is given by

$$V = \int_0^L \pi R^2 E\ dx \tag{13}$$

Hence, the variation in penetration can be treated by examining the variation in this effective volume. If E is a constant over the distance L and only collection due to electrostatic charges is considered

$$V = QqL/(6\pi\epsilon\eta a\bar{U}) \tag{14}$$

where $\bar{U}$ is an appropriate mean value. If all drops reach the bottom of the chamber, the total volumn, V_t, swept out by all drops in the same time interval is

$$V_t = QqL_0/(6\pi\epsilon\eta a U_0) + \sum_i \int_{L_0}^{L} Q_i q/(6\pi\epsilon\eta a U_i)\ dx \tag{15}$$

where $\bar{U}_0$ is an appropriate mean value over the distance L_0, the distance travelled before drop breakup. Since $\sum_i Q_i = Q$ and U_i is smaller for smaller drops

$$V_t > QqL/(6\pi\epsilon\eta a\bar{U}) \tag{16}$$

Therefore, if all drops reach the bottom of the chamber, drop breakup will increase the effective volume that is swept out. Alternatively, V or V_t can be expressed in terms of the residence time τ of a drop in the chamber, where

$$V = \int_0^\tau \pi R^2 EU\ dt = Qq\tau/(6\pi\epsilon\eta a) \tag{17}$$

A longer residence time will be realized by a lower speed or fall through the chamber from either a smaller drop or a higher counter-current aerosol flow. However, in a charged droplet scrubber, the air-flow velocity may be higher than the terminal velocity of the small droplets formed by drop breakup. Consequently, the small droplets may be carried away by the air flow and not fall down the chamber.

For examination of the placement of charge in relation to drop size, consider a constant liquid-feed rate. The rate of monodisperse drop production will be larger for a smaller drop size. Taking this into account, the effectiveness of particulate collection for a drop is expressed as the effective volume swept out normalized by the drop volume

$$V_* = V/(4\pi R^3/3) \tag{18}$$

From eq 3 and 17

$$V_* = fq\tau\sigma^{1/2}/(\pi\eta\epsilon^{1/2}aR^{3/2}) \tag{19}$$

Hence, for a constant liquid-feed rate, a higher total effective volume swept out can be achieved with smaller drops, but it is limited by the residence time.

The effect of different levels of charge and different values of the aerosol flow velocity on the effectiveness of particulate collection of a drop is shown in Figure 1. The effective volume swept out by a drop of initial size of 100-μm radius is plotted as a function of the initial drop charge expressed as the fraction of the Rayleigh limit charge for different aerosol flow velocities in a chamber of 2 m height. Negative values of the velocity indicate that the aerosol flow is counter-current. The drops are assumed to be at their terminal velocities. The humidity in the chamber is assumed to linearly decrease from 100% at the top to 90% at the bottom. Temperature is assumed to be uniform at 50 °C. Particles collected by the drop are assumed to dissolve but not affect the surface tension (65 dyn/cm) significantly. Since the effect of charge–drop instability is the problem of interest, this assumption simplifies the model by ignoring the complex problem of the change in collection efficiency caused by insoluble particles on the drop surface. A decrease in surface tension caused by collection of soluble particles will increase the probability of drop instability but will not alter the prediction of possible drop instability effects by the model. The rate of decrease of drop size is obtained by using eq 10. When the drop reaches the Rayleigh limit specified by eq 1, the drop is assumed to break up into a residual drop $^9/_{10}$ ($k = 0.9$) the size of the original with a charge $^{98}/_{100}$ ($f_r = 0.98$) of the Rayleigh limit. Since droplets formed from Rayleigh instability may act as both collectors and source of particles, their effects are assumed to cancel additively, i.e., the droplets do not contribute to the total effective volume swept out. The maximum depths that the drops at different levels of charge fall are also shown in Figure 1. For values less than 2.0, the drops do not reach

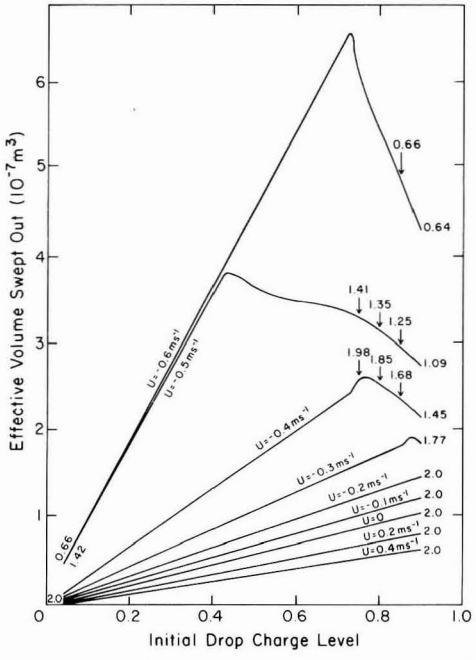

Figure 1. Effective volume swept out by a drop of initial radius of 100 μm at different levels of charge given in fractions of the initial Rayleigh charge limit. The chamber height is 2 m, and different aerosol flow velocities are used. Maximum depths in meters reached by a drop are shown on the curves.

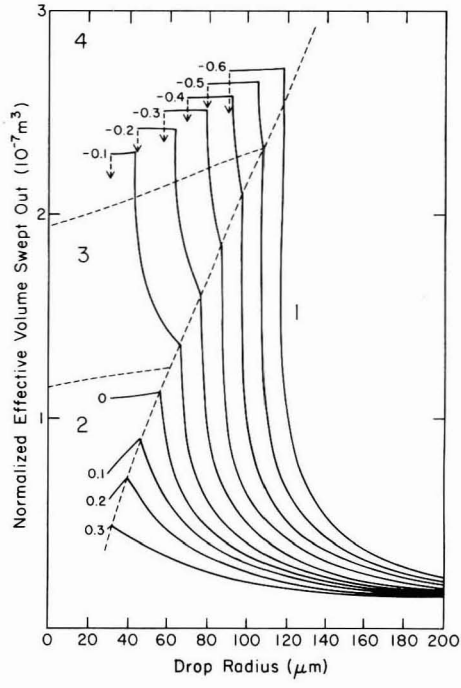

Figure 2. Normalized effective volume swept out by drops of different radii in chamber of 2 m height. The values of the aerosol flow velocity used are shown on the left-hand side of the curves. The charge to mass ratio of the drops is 1.37×10^{-3} C/kg. Region 1: no Rayleigh instability occurs and drops reach bottom of chamber. Region 2: Rayleigh instability occurs, and drops reach bottom of chamber. Region 3: Rayleigh instability occurs, and drops evaporate completely inside chamber. Region 4: Rayleigh instability occurs, and drops are carried out of chamber.

the bottom of the chamber. Decrease in size from evaporation and breakup causes the terminal velocity of a drop to become less than the counter-current flow speed. The drop is then carried upwards out of the chamber or may even evaporate completely in the chamber. Figure 1 shows that the effective volume swept out increases with lower cocurrent aerosol flow or higher counter-current flow. For aerosol flow velocities greater than –0.1 m/s, the effective volume swept out is a linear function of the drop charge since the residence time is too short for Rayleigh instability to occur. For longer residence times, Rayleigh stability occurs for drops with high charge and generally leads to decrease in effective volume swept out for higher initial charges.

Generally, residence times are longer for higher counter-current flow and drop breakups for lower initial charge. However, this trend is reversed for the case where the flow is –0.6 m s^{-1}. This change in the trend is an artifact of the assumption of the relative humidity variation in the chamber. The drops in the –0.6 m s^{-1} aerosol flow traverses only the top 0.62 m of the chamber compared to the 1.42 m for the –0.5 m s^{-1} case and have a smaller rate of evaporation. Consequently, a drop will have a longer residence time before breakup and, hence, a larger effective volume. A better assumption would be that the humidity variation is within the depth of the cloud (0.62 m) instead of the chamber (2.0 m). However, the artifact does show that a large increase in the effective volume can be realized when there is less drop breakup in a more humid environment.

Figure 2 shows the variation in the normalized effective volume swept out (V_n) for different drop sizes and different aerosol flow velocities. All drops have the same charge to mass ratio of 1.37×10^{-3} C/kg, which is equivalent to a 100-μm radius drop at $^3/_{10}$ of the Rayleigh limit charge or a 200-μm radius drop at $^9/_{10}$ of the Rayleigh limit charge. The effective volumes swept out are normalized to the mass of water in each drop with reference to the 100-μm radius drop case. As indicated in Figure 2, four regions can be distinguished: (1) no Rayleigh instability occurs and drops reach the bottom of the chamber; (2) Rayleigh instability occurs and drops reach bottom of the chamber; (3) Rayleigh instability occurs and drops evaporate completely inside chamber; (4) Rayleigh instability occurs and drops are carried out of the chamber. The characteristic (normalized effective volume (V_n) swept out as a function of the drop radius) curve is a consequence of the residence time in the chamber and the occurrence of Rayleigh instability. For example, in the case of the aerosol flow velocity of –0.3 m/s, V_n increases rapidly as the drop size decreases due to increase in residence time. As the residence time increases (drop size decreases) to when Rayleigh instability occurs, the rate of increase of V_n with drop size is decreased for smaller drop sizes. The combination of Rayleigh instability and changing residence times leads to no significant change in V_n. V_n becomes zero for drops too small (terminal velocity too low) to fall down the chamber.

For effective particulate removal the particles have to be captured by the drops and the drops collected and removed. In region 3, the drops evaporate completely, and no particles are removed from the chamber although smaller particles may be converted to larger ones through

the capture, drop breakup, and evaporation process. A possible solution in this region may be obtained by shortening the height of the chamber. In region 2, drop breakup causes a decrease in V_n. For region 4, drops fall down the chamber, evaporate, and decrease in size. When the drops are small enough their trajectories are reversed and they are carried ot through the top of the chamber. Hence, they have a relatively long residence time and high V_n in a short length of the chamber, but the drops have to be removed after exit.

Figure 2 can be used to optimize particulate collection for a given set of operating constraints for the same humidity variation in the chamber and charge to mass ratio used. For example, if the aerosol flow speed is constrained to be 0.3 m s^{-1}, Figure 2 shows that the flow should be counter-current. For particulate removal, i.e., operating in region 1 or 4, the initial drop radii should be larger than 87 μm or less than 80 μm. In region 1, V_n increases by 80% when the drop radius decreases from 89 to 87 μm (<3% change). Hence, a small change in the drop size may result in a large change in the effectiveness of particulate removal.

Summary and Conclusions

The utilization of charge in the collection of particles by drops has been shown to be an efficient method for increasing the collection of submicron particles. However, a monotonic increase in particulate collection cannot be achieved by continuously increasing the charge on the drops because of Rayleigh instability. In addition, the use of highly charged drops that evaporate to a smaller size in the collection chamber and break up into smaller drops may even decrease the particle collection. Droplets formed from drop breakup may act as sources of particles by breaking up into smaller droplets and evaporating completely to solid particles. Such small droplets or particles exiting particulate control chambers are difficult to remove by conventional means.

The operating conditions for the optimization of particle collection vary with the set of constraints of a specified aerosol flow velocity and values of the relative humidity and charge to mass ratio of the drops. Higher single-drop collection effectiveness can usually be achieved with countercurrent aerosol flow. Collection efficiencies are optimized by the use of highly charged drops with the condition that the chamber height is short enough or the relative humidity is high enough for the drops to reach the bottom without breakup occurring. In the region of operation where no breakup occurs and the drops reach the bottom of the chamber, verification of theoretical penetration values may be difficult since a large change in value may result from a small change in the drop size used.

Literature Cited

(1) Kraemer, H. F.; Johnstone, H. F. *Ind. Eng. Chem.* **1955**, *47*, 2426–2434.
(2) Pilat, M. J. *J. Air Pollut. Control Assoc.* **1975**, *25*, 176–178.
(3) Hoenig, S. A. Final Report EPA, 60/7-77-131, NTIS PB276645.
(4) Prem, A.; Pilat, M. J. *Atmos. Environ.* **1978**, *12*, 1981–1990.
(5) Abbas, M. A.; Latham, J. *J. Fluid Mech.* **1967**, *30*, 663–670.
(6) Rayleigh, Lord. *Philos. Mag.* **1882**, *14*, 184–186.
(7) Hendricks, C. D.; Schneider, J. M. *Am. J. Phys.* **1963**, *31*, 450–453.
(8) Carroll, C. E. *J. Phys. A: Math. Nucl. Gen.* **1978**, *11*, 225–229.
(9) Robertson, J. A. Ph.D. Thesis, University of Illinois, Urbana–Champaign, IL, 1969.
(10) McCully, C. R.; Fisher, M.; Langer, G.; Rosinski, J.; Glaess, H.; Werle, W. *Ind. Eng. Chem.* **1956**, *48*, 1512–1516.
(11) Goldshmid, Y.; Calvert, S. *Am. Inst. Chem. Eng. J.* **1963**, *9*, 352–358.
(12) Weber, E. *Staub-Reinhalt, Luft* **1968**, *28*, 37–43.
(13) Weber, E. *Staub-Reinhalt, Luft* **1969**, *29*, 12–18.
(14) Stulov, L. D.; Murashkevich, F. I.; Fuchs, N. *J. Aerosol Sol.* **1978**, *9*, 1–6.
(15) Dawson, G. A. *J. Geophys. Res.* **1973**, *78*, 6364–6369.
(16) Doyle, A.; Moffett, D. R.; Vonnegut, B. *J. Colloid Sci.* **1964**, *19*, 136–143.

Received for review July 10, 1981. Revised manuscript received February 1, 1982. Accepted March 2, 1982. This project has been financed entirely with Federal funds as part of the program of the Advanced Environmental Control Technology Research Center, University of Illinois at Urbana—Champaign, which is supported under Cooperative Agreement CR 806819 with the Environmental Protection Agency. The contents do not necessarily reflect the views and policies of the Environmental Protection Agency, nor does the mention of trade names or commercial products constitute endorsement or recommendation for use.

Characterization of Organic Contaminants in Environmental Samples Associated with Mount St. Helens 1980 Volcanic Eruption

Wilfred E. Pereira,* Colleen E. Rostad, Howard E. Taylor, and John M. Klein

U.S. Geological Survey, Denver Federal Center, Denver, Colorado 80225

■ Volcanic ash, surface-water, and bottom-material samples obtained in the vicinity of Mount St. Helens after the May 18, 1980, eruption were analyzed for organic contaminants by using capillary gas chromatography–mass spectrometry–computer techniques. Classes of compounds identified include *n*-alkanes, fatty acids, dicarboxylic acids, aromatic acids and aldehydes, phenols, resin acids, terpenes, and insect juvenile hormones. The most probable source of these compounds is from pyrolysis of plant and soil organic matter during and after the eruption. The toxicity of selected compounds and their environmental significance are discussed.

Introduction

After 100 years of dormancy, Mount St. Helens, in southwestern Washington, erupted on March 27, 1980. Following a month of minor ash and gas eruptions and seismic activity, a swelling was observed on the north flank of the mountain. This swelling increased outward at approximately 1–1.5 m/day.

On May 18 at 8:32 a.m., the swollen north flank slumped in response to a magnitude 5 earthquake, resulting in a massive debris avalanche and mudflow. The volcano then violently erupted. A hot, lateral blast completely devastated the area north of the volcano for 20 km. A vertical ash plume rose to 25 km and was transported to the east, turning the sky dark over much of eastern Washington. Major ash deposition occurred in eastern Washington, Idaho, and Montana. Massive mudflows and flooding, resulting from the melted glacial ice and snow, devastated

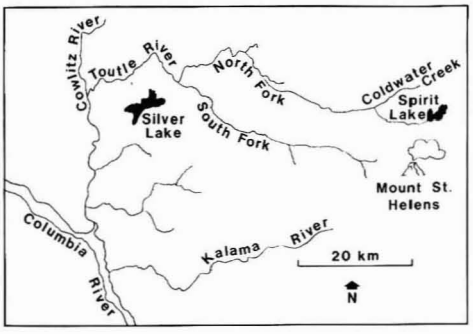

Figure 1. Sampling locations showing Spirit Lake, Coldwater Creek, and the Cowlitz River.

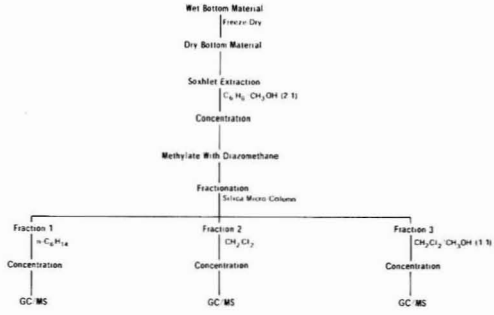

Figure 2. Sample preparation and fractionation scheme for bottom-material samples.

the Toutle and lower Cowlitz River valleys.

The forests, vegetation and soils in the immediate vicinity north of the volcano (Figure 1) were completely pyrolyzed. In sheltered areas such as North Coldwater Creek Canyon, fallen trees were burned and charred from the intense heat and then buried in the hot mud and ash. It is presumed that the high temperatures, in conjunction with the physical breakup of the trees and other vegetation, created conditions that fostered pyrolysis and retorting of the organic compounds associated with the vegetation.

Organic compounds mobilized by this hypothesized mechanism have been observed to be flowing into streams and ponds in the North Coldwater Creek drainage. North Coldwater Creek now is significantly contaminated by resinous and tarlike organic material. These "pockets" of burned vegetation that are buried in the high-temperature muds and ash are "in situ" steam distilling from the wood, seeping to the surface, and mixing with surface water. Contamination in nearby lakes such as Spirit Lake is severe. Spirit Lake is a black, odoriferous mixture of water, gases, organic compounds, and floating trees.

In addition, vast quantities of organic material, pyrolyzed and vaporized during the May 18 eruption, condensed on the particulates in the ash cloud (*1*). As the ash fell back to earth, this organic material was available for introduction into the environment. This is considered a possible secondary source for organic contamination in nearby surface waters. Because of the ecological significance of some of the organic compounds associated with the ash, a study was initiated to characterize and monitor organic contaminants in hydrologic samples in the vicinity of Mount St. Helens.

It has been previously recognized that nonspecific, gross-pollution parameters such as biochemical and chemical oxygen demand and total organic carbon measurements are of little value for samples that may contain trace amounts of toxic or hazardous contaminants (*2*). Because of the complexity and unknown chemical nature of ash, water, and sediment samples associated with the volcanic eruption of Mount St. Helens, it was decided that a broad spectrum approach to the problem (*3*) by using capillary gas chromatography–mass spectrometry–computer (GC–MS–COM) techniques would be most appropriate. Definitive chemical characterization of these samples would provide meaningful initial information with which to design additional studies concerned with the origin, transport, fate, and health effects of these organic contaminants in the hydrologic environment.

Experimental Section

Sample Collection and Preparation. A volcanic-ash sample was acquired from ash that fell near Richland, WA, on May 18. The sample was provided by Todd Hinkley, U.S. Geological Survey; it was collected by sweeping the ash from exposed metal surfaces such as picnic tables etc., where the probability of organic contamination was minimal.

Bottom-material samples were collected by the U.S. Geological Survey. Samples were collected from the channel of the Cowlitz River, at 0.32 and 20.6 km from its confluence with the Columbia River (Figure 1). Samples were collected by conventional grab-sampling techniques at a shallow depth (5–10 cm) on May 28 and June 4, respectively.

Surface-water samples were collected on August 7 at the south shore of Spirit Lake and from Coldwater Creek, 500 m from the confluence with the north fork of the Toutle River. Both samples were collected by grab sampling into a clean 1-L glass bottle, chilled to 4 °C, and transported to the laboratory within 48 h.

Volcanic Ash. A 20-g sample of ash was extracted with benzene/methanol (2:1) in a Soxhlet apparatus for 20 h. The extract was concentrated in a Kuderna–Danish apparatus to a volume of 4 mL. One milliliter of the concentrated extract was further concentrated to a volume of 0.5 mL and fractionated in a column containing 3 g of activated silica gel, to obtain an alkane fraction that eluted from the column in the first 10 mL of hexane. No further fractionation was done with use of silica gel. The hexane fraction was concentrated by evaporation in a stream of dry nitrogen to a volume of approximately 100 μL. After addition of a solution of biphenyl-d_{10} as internal standard, the hexane fraction was analyzed by gas chromatography–mass spectrometry (GC–MS). The remaining 3 mL of the concentrated extract was evaporated to dryness in a stream of dry nitrogen. The residue was then methylated with an ether solution of diazomethane (*4*) and evaporated in a stream of dry nitrogen to a volume of approximately 100 μL. Following addition of a solution of biphenyl-d_{10} as internal standard, the methylated extract was analyzed by GC–MS.

Bottom Material. Bottom-material samples were prepared for analysis as shown in Figure 2. The sample was mixed and a 100-g portion used for analysis. Water was removed by overnight lyophilization. Twenty grams of the dried material was extracted with benzene/methanol (2:1) in a Soxhlet apparatus for 24 h. The extract was concentrated to a volume of approximately 10 mL in a Kuderna–Danish apparatus. The solvent was further evaporated in a stream of dry nitrogen to a volume of approximately 100 μL and the residue methylated with diazomethane. The methylated extract was concentrated and fractionated in a microcolumn containing 3 g of ac-

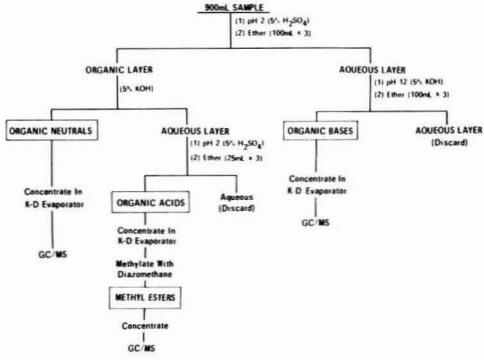

Figure 3. Sample preparation and fractionation scheme for surface-water samples.

tivated silica gel. Three elution fractions were collected with the following eluants: (1) 10 mL of hexane; (2) 10 mL of methylene chloride; (3) 10 mL of methylene chloride/methanol (1:1). Each fraction was concentrated to a volume of approximately 100 μL. Following the addition of biphenyl-d_{10} solution as internal standard, each fraction was analyzed by GC–MS.

Surface Waters. Water samples were fractionated as shown in Figure 3. Nine hundred milliliters of the sample was mixed and adjusted to pH 2 with 5% H_2SO_4 solution. The sample was extracted with ether (3 × 100 mL). The combined ether extracts were washed with 25 mL of 5% KOH solution to separate carboxylic acids and phenols from neutral compounds. The ether solution containing neutral organic compounds was dried over anhydrous Na_2SO_4 and concentrated to a volume of approximately 10 mL in a Kuderna–Danish apparatus. This solution was further concentrated to a volume of approximately 100 μL in a stream of dry nitrogen. Following addition of a solution of biphenyl-d_{10} as internal standard, the neutral fraction was analyzed by GC–MS. The KOH solution containing the acids and phenols was acidified to pH 2 with 5% H_2SO_4 and extracted with ether (3 × 25 mL). The combined ether solution was dried over anhydrous Na_2SO_4 and concentrated to a volume of approximately 1 mL in a Kuderna–Danish apparatus. The extract was methylated with diazomethane. The methylated extract was concentrated to a volume of approximately 100 μL. Following addition of a solution of biphenyl-d_{10} as internal standard, the methylated extract was analyzed by GC–MS. The aqueous acid solution obtained after removal of neutral and acidic compounds was adjusted to pH 12 with 5% KOH solution. This solution was extracted with ether (3 × 100 mL) to remove basic compounds. The combined ether solution was dried over anhydrous Na_2SO_4 and concentrated to a volume of approximately 1 mL in a Kuderna–Danish apparatus. The extract was further concentrated in a stream of dry nitrogen to a volume of approximately 100 μL. After addition of a solution of biphenyl-d_{10} as internal standard, the basic extract was analyzed by GC–MS.

Instrumentation. Instrumental analyses were performed on a Finnigan OWA 20 computerized gas chromatography–quadrupole mass spectrometry system (GC–MS–COM) (use of trade names is for identification purposes only and does not imply endorsement by the U.S. Geological Survey).

The GC was equipped with a wall-coated open tubular (WCOT) fused-silica capillary column 30 m × 0.26 mm i.d., coated with SE-54. The linear velocity of helium through the column was 26 cm/s, and injections were made by using the splitless-injection technique (*5*). The GC oven was held at 50 °C for 4 min, and programmed at 6 °C/min to 300 °C. The split-sweep valve and filament-multiplier status were under computer control for better system reproducibility. One microliter of each sample extract was injected at 50 °C. The vent valve was automatically opened at 45 s, and the filament and multiplier were automatically turned on at 240 s. Data acquisition was commenced simultaneously with the injection of the sample. The mass spectrometer was operated in the electron-impact mode using an ionizing voltage of 70 eV and ionization current of 250 μA. The mass spectrometer was repetitively scanned from 40 to 450 amu in 0.9 s. High-resolution mass spectra were recorded on a Kratos MS-30 capillary GC–MS system, interfaced with a DS-505 data system.

Compound Identification. All results reported are qualitative in nature. Because of the compositional complexity of the samples, no attempts were made to quantitate individual components. Compound identifications were based upon computerized matching of mass spectra in the sample with that of spectra contained in the National Bureau of Standards (NBS) library of approximately 32 000 compounds, comparisons with published spectra, and from a knowledge of mass spectral fragmentation patterns. Electron-impact mass spectra and relative retention times (RRT) of components, for which authentic standards were available, were matched against sample components, with biphenyl-d_{10} as internal standard (biphenyl-d_{10} had a retention index of 1385.87). Elemental compositions of characteristic ions in certain compounds were established by high-resolution mass spectrometry (HRMS). Special precautions were taken throughout the analysis to avoid introduction of artifacts or other contaminants. These included the baking of glassware, the use of high-purity distilled-in-glass solvents, and heat-treated chromatographic grade adsorbents and drying agents. Procedural blanks were analyzed with each set of samples. If an artifact appeared in the blank and sample, it was not reported.

After a data file had been acquired, the Biemann–Biller max-mass compound detection algorithm (*6*) was used to generate a scan list of detected components. The mass spectrum of each compound in the scan list was subjected to the Finnigan Library Search Program (*7*).

Results and Discussion

Volcanic Ash. A reconstructed ion chromatogram (RIC) of a methylated extract of volcanic ash obtained from Richland, WA, is shown in Figure 4. The chromatogram shows the complexity of this extract and the effectiveness of the WCOT fused-silica capillary column in resolving components in this mixture. Organic compounds tentatively identified in this ash sample are listed by general class-type in Table I, along with the relative retention times (RRT), with biphenyl-d_{10} as internal standard. Alkanes (n-C_{15} to n-C_{29}) with a pronounced odd/even predominance between C_{19} to C_{29} indicate that these compounds were derived from higher plants (*8*). A reconstructed mass chromatogram (m/z 57) characteristic of alkanes is shown in Figure 5a. The chromatogram is unimodal, maximizing at n-C_{25}, indicating a single source for these compounds.

Several polycyclic aromatic hydrocarbons were observed in the methylated extract of the ash, notably alkylated phenanthrene derivatives. The most probable source of these compounds is from pyrolysis of plant materials (*9*). The presence of fatty acids, dicarboxylic acids, phenolic

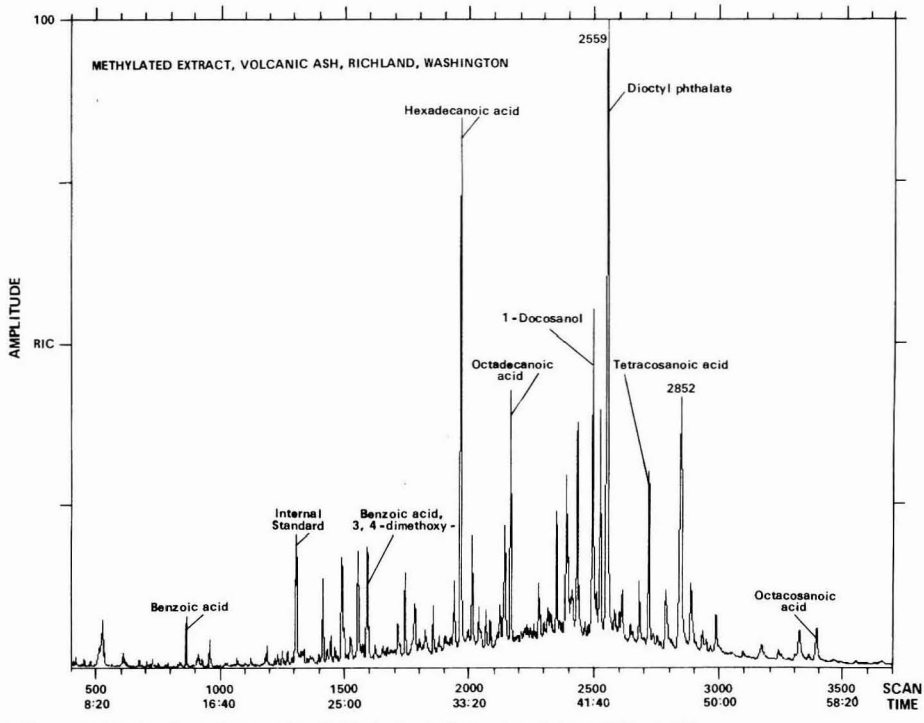

Figure 4. Reconstructed ion chromatogram of methylated extract of volcanic ash from Richland, WA.

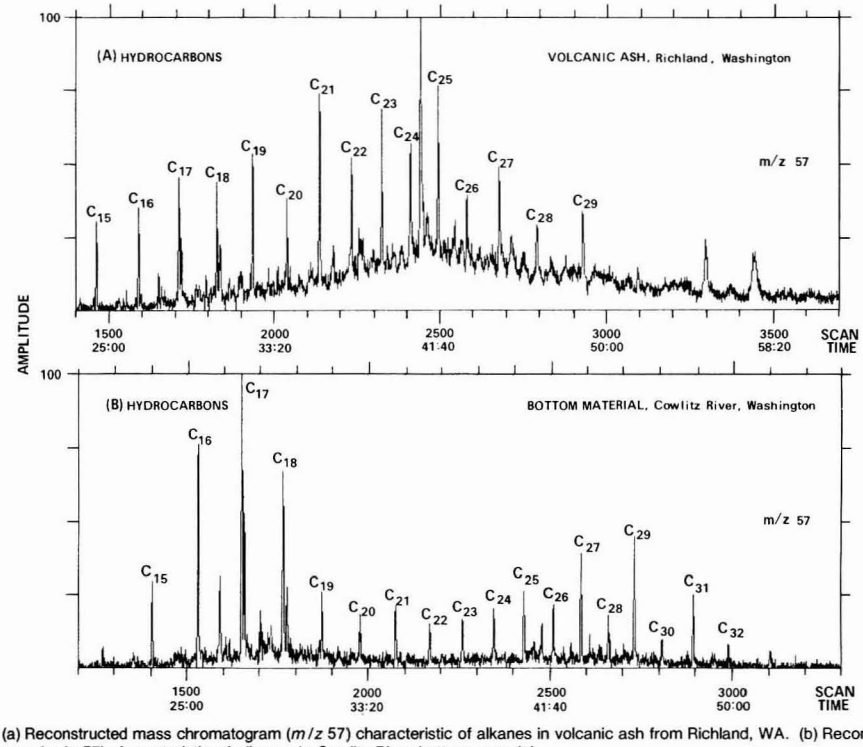

Figure 5. (a) Reconstructed mass chromatogram (m/z 57) characteristic of alkanes in volcanic ash from Richland, WA. (b) Reconstructed mass chromatogram (m/z 57) characteristic of alkanes in Cowlitz River bottom material.

Table I. Organic Compounds Identified in Volcanic Ash from Richland, WA

compound	RRT
I. Alkanes	
1. pentadecane[a]	1.12
2. hexadecane[a]	1.22
3. heptadecane[a]	1.31
4. octadecane[a]	1.40
5. nonadecane[a]	1.48
6. eicosane[a]	1.56
7. heneicosane	1.63
8. docosane[a]	1.71
9. tricosane	1.78
10. tetracosane[a]	1.84
11. pentacosane	1.91
12. hexacosane	1.97
13. heptacosane	2.05
14. octacosane[a]	2.13
15. nonacosane	2.24
II. Aromatic and Polycyclic Aromatic Hydrocarbons	
1. benzene, 1-ethenyl-3,5-dimethyl-	1.15
2. naphthalene, 1,6-dimethyl-4-(1-methylethyl)-	1.30
3. phenanthrene, methyl isomer	1.52
4. naphthalene, 1-phenyl-	1.56
5. phenanthrene, dimethyl isomer	1.62
6. phenanthrene, trimethyl isomer	1.70
7. phenanthrene, tetramethyl isomer	1.74
III. Alcohols	
1. 2-propanol, 1,3-dimethoxy-	0.37
2. 1,2-propanediol, 3-methoxy-	0.41
3. 3-piperidinol, 1-ethyl-6-methyl-	0.73
4. 1-phenanthrenemethanol, 1,2,3,4,4a,9,10,-10a-octahydro-1,4a-dimethyl-7-(1-methylethyl)-	1.85
5. 1-docosanol	1.91
IV. Fatty Acids	
1. pentanoic acid, 4-oxo-, methyl ester	0.52
2. octanoic acid, methyl ester[a]	0.70
3. nonanoic acid, methyl ester	0.82
4. decanoic acid, methyl ester[a]	0.93
5. undecanoic acid, methyl ester	1.04
6. dodecanoic acid, methyl ester[a]	1.14
7. tridecanoic acid, methyl ester[a]	1.24
8. tetradecanoic acid, methyl ester[a]	1.33
9. pentadecanoic acid, methyl ester[a]	1.42
10. hexadecanoic acid, methyl ester[a]	1.51
11. heptadecanoic acid, methyl ester[a]	1.58
12. 9-octadecenoic acid, methyl ester	1.64
13. octadecanoic acid, methyl ester[a]	1.66
14. nonadecanoic acid, methyl ester[a]	1.73
15. eicosanoic acid, methyl ester[a]	1.80
16. heneicosanoic acid, methyl ester[a]	1.87
17. docosanoic acid, methyl ester[a]	1.93
18. tricosanoic acid, methyl ester[a]	2.00
19. tetracosanoic acid, methyl ester	2.08
20. hexacosanoic acid, methyl ester	2.28
21. octacosanoic acid, methyl ester	2.59
V. Dicarboxylic Acids	
1. butanedioic acid, dimethyl ester[a]	0.58
2. hexanedioic acid, dimethyl ester[a]	0.84
3. octanedioic acid, dimethyl ester[a]	1.07
4. nonanedioic acid, dimethyl ester[a]	1.17
VI. Ketones	
1. 1*H*-inden-1-one, 2,3-dihydro	0.89
2. 1-propanone, 1-phenyl	0.97
3. ethanone, 1-(4-methoxyphenyl)-	0.97
4. 2,5-cyclohexadiene-1,4-dione, 2,6-bis(1,1-dimethylethyl)-	1.10
5. 1*H*-inden-1-one, 2,3-dihydro, 3,4,7-trimethyl	1.18
6. ethanone, 1-(3,4-dimethoxyphenyl)-	1.19
7. 1-propanone, 1-(2,4-dimethoxyphenyl)-	1.28
8. 9*H*-fluoren-9-one	1.36
9. 2-heptadecanone[a]	1.48
VII. Aromatic Acids	
1. benzoic acid, methyl ester[a]	0.66
2. benzeneacetic acid, methyl ester[a]	0.77
3. benzoic acid, 2-hydroxy-, methyl ester	0.79
4. benzoic acid, 3-methyl-, methyl ester[a]	0.80
5. benzoic acid, 4-methyl-, methyl ester[a]	0.81
6. benzoic acid, methoxy-, methyl ester isomer	0.96
7. benzoic acid, methoxy-, methyl ester isomer	1.00
8. benzoic acid, 3,4-dimethoxy-, methyl ester	1.22
9. 2-naphthalenecarboxylic acid, methyl ester[a]	1.27
10. 2-propenoic acid, 3-(3,4-dimethoxyphenyl)-, methyl ester	1.47
11. 1-phenanthrenecarboxylic acid, 1,2,3,4,4a,-5,6,7,8,9,10,10a-dodecahydro-1,4a-dimethyl-7-(1-methylethyl)-, methyl ester	1.81
12. 1-phenanthrenecarboxylic acid, 1,2,3,4,4a,-9,10,10a-octahydro-1,4a-dimethyl-7-(1-methylethyl)-, methyl ester	1.83
VIII. Aldehydes and Phenols	
1. benzaldehyde, 4-methoxy-	0.86
2. benzene, (trimethoxymethyl)-	0.99
3. benzaldehyde, 4-hydroxy-3-methoxy-	1.14
4. benzaldehyde, 3,4-dimethoxy-	1.19
5. 1-phenanthrenecarboxaldehyde, 1,2,3,4,4a,-9,10,10a-octahydro-1,4a-dimethyl-7-(1-methylethyl)-	1.78
IX. Chlorinated Aromatics	
1. benzoic acid, chloro-, methyl ester isomer	0.86
2. benzoic acid, chloro-, methyl ester isomer	0.88
3. benzoic acid, 3,4-dichloro-, methyl ester	1.03
4. pentachlorobiphenyl isomer	1.67
5. pentachlorobiphenyl isomer	1.73
6. pentachlorobiphenyl isomer	1.76

[a] Identity confirmed by comparison of EI spectra and RRT with authentic standard.

acids, and aromatic aldehydes indicates that these compounds were derived from plant and soil organic matter (*10, 11*). It is interesting to note that several compounds such as 3,4-dimethoxyacetophenone (compound VI, 6), vanillin (compound VIII, 3), methyl dehydroabietate (compound VII, 12), and 4-methoxybenzaldehyde (compound VIII, 1) have been identified previously in Kraft paper and pulp mill effluents (*12–14*). Of special significance is the presence of the tricyclic diterpenoid resin acid methyl dehydroabietate (compound VII, 12) and the corresponding aldehyde, dehydroabietal (compound VIII, 5), and the alcohol, dehydroabietol (compound III, 4). Dehydroabietic acid has been found in the parenchyma cells of coniferous wood species (*15*), conifer rosin, and other higher plant resins and supportive tissue; it has been advocated as a potential terrigenous marker compound (*16*). Dehydroabietic acid and dehydroabietal are reported to be toxic to fish (*17, 18*). The presence of the diterpene resin compounds associated with the ash indicates a terrigenous source. Several coniferous species, including Douglas Fir, were completely pyrolyzed in the eruption zone of the volcano.

Examination of the data in Table I reveals the presence of several chlorinated compounds, such as chlorinated derivatives of benzoic acid and three pentachlorobiphenyl isomers (PCB). It is suggested that aromatic compounds produced as a result of pyrolysis of plant and soil organic matter, in the presence of vaporized inorganic chloride salts, were chlorinated in the high-temperature eruption zone. Commercial PCB formulations are known to contain

Table II. Organic Compounds Identified in Bottom Material, Cowlitz River, WA

fraction 1	fraction 2	fraction 3
1. pentadecane[a]	1. 3-hexanone, 2,2-dimethyl-	1. benzene, (1-methylethenyl)-
2. hexadecane[a]	2. benzene, (1-methylethenyl)-	2. phenol[a]
3. heptadecane[a]	3. ethanone, 1-phenyl-[a]	3. ethanone, 1-phenyl-[a]
4. pentadecane, 2,6,10,14-tetramethyl-	4. benzenemethanol, α,α-dimethyl-	4. benzenemethanol, α,α-dimethyl-
5. octadecane[a]	5. 1*H*-indene, 2,3-dihydro-1,1,3-trimethyl-3-phenyl	5. ethanol, 2-phenoxy-
6. nonadecane[a]	6. hexadecanoic acid, methyl ester[a]	6. benzaldehyde, 3,4-dimethoxy-
7. eicosane[a]	7. octadecanoic acid, methyl ester[a]	7. ethanone, 1-(3,4-dimethoxyphenyl)
8. heneicosane	8. 1-phenanthrenecarboxylic acid, 1,2,3,4,4a,9,10,10a-octahydro-1,4a-dimethyl-7-(1-methylethyl), methyl ester	8. benzoic acid, 3,4-dimethoxy-, methyl ester
9. docosane[a]		9. 2-heptadecanone[a]
10. tricosane		10. hexadecanoic acid, methyl ester[a]
11. tetracosane[a]		11. octadecanoic acid, methyl ester[a]
12. pentacosane		12. 1-phenanthrenecarboxylic acid, 1,2,3,4,4a,9,10,10a-octahydro-1,4a-dimethyl-7-(1-methylethyl)-, methyl ester
13. hexacosane		13. heneicosanoic acid, methyl ester[a]
14. heptacosane		14. docosanoic acid, methyl ester[a]
15. octacosane[a]		15. tetracosanoic acid, methyl ester
16. nonacosane		
17. triacontane		
18. hentriacontane		
19. dotriacontane		

[a] Identity confirmed by comparison of EI spectra and RRT with authentic standard.

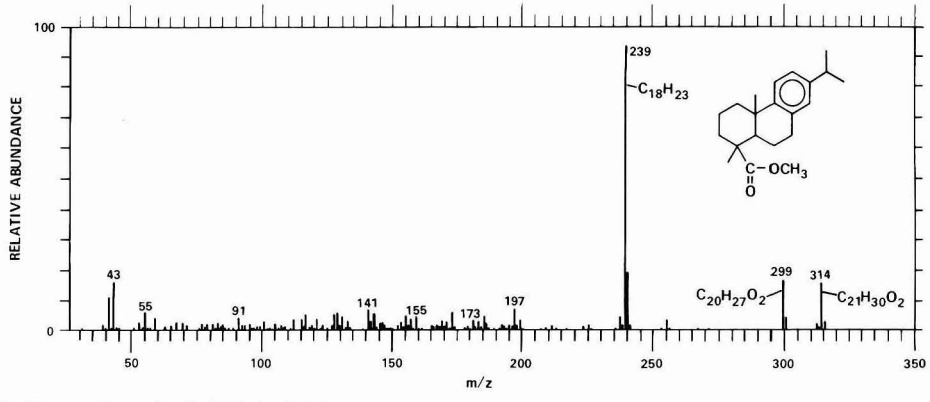

Figure 6. Mass spectrum of methyl dehydroabietate.

complex mixtures of isomers of chlorinated biphenyl. The presence of only three isomers of pentachlorobiphenyl indicates that these chlorinated compounds could have been preferentially synthesized by a combustion process. However, the possibility of contamination of the ash sample by PCB cannot be ruled out. The de novo formation of organochlorine compounds, produced as a result of pyrolysis of organic material in the presence of inorganic chlorides, has been previously reported (*19*). Volcanic pumice and ash samples obtained during the eruption of Mount St. Helens were also found to contain trace levels of adsorbed or absorbed methyl halides and chloroform (*20*).

Bottom-Material Samples. Organic compounds associated with bottom material samples, from the Cowlitz River, WA, are shown in Table II; *n*-alkanes (C_{15} to C_{32}) were identified. A reconstructed mass chromatogram (*m/z* 57) of the *n*-alkane fraction is shown in Figure 5b. The chromatogram shows a bimodal distribution of *n*-alkanes, maximizing at C_{17} in the first mode and C_{29} in the second mode, indicating two different sources for these compounds. The first mode (C_{15} to C_{19}) is indicative of an algal hydrocarbon contribution and the second mode (C_{25} to C_{32}) has its genesis from surface waxes of higher plants (*21*).

Examination of the data in Table II reveals the presence of 3,4-dimethoxybenzaldehyde (fraction 3, no. 6); 3,4-dimethoxyacetophenone (fraction 3, no. 7), methyl 3,4-dimethoxybenzoate (fraction 3, no. 8), and methyl dehydroabietate (fraction 3, no. 12). These compounds also were found associated with the volcanic ash, indicating that the Cowlitz River bottom material was contaminated by volcanic ash following the eruption of Mount St. Helens.

Surface-Water Samples. Samples from Spirit Lake and Coldwater Creek were analyzed for organic compounds. The sample from Spirit Lake was dark brown in color, while the sample from Coldwater Creek was black, indicating that the color might be due to partially degraded lignin molecules (*22*) and other pyrolyzed organic material. The basic fractions did not contain any compounds with basic functional groups. The only compounds found in these fractions were acidic and neutral compounds that carried over during the extraction. A list of compounds identified in the acid fraction of Spirit Lake is shown in Table III. In addition to fatty acids, dicarboxylic acids, phenolic acids, and benzoic and benzeneacetic acid derivatives, various phenols and cresols were identified. Phenols have been found in Kraft Paper Mill wastewaters (*14*). Phenolic compounds in Kraft Mill wastewaters have been found to impair the flavor of fish, shrimp, and other edible aquatic life (*14*, *23*).

Table III. Organic Compounds Identified in Acid Fraction, Spirit Lake, WA

compound	RRT
1. butanoic acid, 3-methyl-, methyl ester	0.21
2. hexanoic acid, 4-methyl-, methyl ester	0.35
3. benzene, methoxy-	0.39
4. benzene, ethoxy-	0.49
5. phenol[a]	0.51
6. benzene, 1-methoxy-4-methyl-	0.54
7. butanedioic acid, dimethyl ester[a]	0.58
8. cyclohexanecarboxylic acid, methyl ester	0.61
9. phenol, methyl isomer	0.65
10. benzoic acid, methyl ester[a]	0.67
11. butanedioic acid, methyl-, dimethyl ester	0.70
12. phenol, methyl isomers	0.75
13. pentanedioic acid, 2-methyl-, dimethyl ester	0.75
14. benzoic acid, 2-hydroxy-, methyl ester	0.78
15. octanoic acid, 2-methyl-, methyl ester	0.81
16. benzenepropanoic acid, methyl ester[a]	0.88
17. 3-nonenoic acid, 2-methyl-, methyl ester	0.91
18. benzeneacetic acid, 2,2-dimethyl-, methyl ester	0.93
19. benzoic acid, (1-methylethyl)-, methyl ester isomer	0.94
20. benzoic acid, 3-methoxy-, methyl ester	0.95
21. benzeneacetic acid, 2-methoxy-, methyl ester	0.96
22. benzoic acid, (1-methylethyl)-, methyl ester isomer	0.97
23. benzoic acid, (1-methylethyl)-, methyl ester isomer	0.99
24. biphenyl-d_{10} (internal standard)	1.00
25. benzoic acid, 4-methoxy-, methyl ester	1.00
26. benzeneacetic acid, 3-methoxy-, methyl ester	1.04
27. benzeneacetic acid, 4-methoxy-, methyl ester	1.06
28. octanedioic acid, dimethyl ester[a]	1.07
29. benzeneacetic acid, α-methoxy-, methyl ester	1.07
30. benzenepentanoic acid, methyl ester	1.12
31. benzeneacetic acid, 4-hydroxy-, methyl ester	1.13
32. nonanedioic acid, dimethyl ester[a]	1.18
33. benzoic acid, 3,5-dimethoxy-, methyl ester	1.23
34. decanedioic acid, dimethyl ester[a]	1.28
35. benzenepropanoic acid, methoxy-, methyl ester isomer	1.30
36. benzenepropanoic acid, methoxy-, methyl ester isomer	1.36
37. cyclohexanecarboxylic acid, 4-(1,5-dimethyl-3-oxohexyl)-, methyl ester isomer	1.51
38. hexadecanoic acid, methyl ester[a]	1.52
39. cyclohexanecarboxylic acid, 4-(1,5-dimethyl-3-oxohexyl)-, methyl ester isomer	1.55
40. 1-cyclohexene-1-carboxylic acid, 4-(1,5-dimethyl-3-oxohexyl)-, methyl ester	1.61
41. octadecanoic acid, methyl ester[a]	1.68
42. 1-phenanthrenecarboxylic acid, 1,2,3,4,4a,-4b,5,6,8a,9,10,10a-dodecahydro-1,4a-dimethyl-7-(1-methylethyl)-, methyl ester	1.83
43. 1-phenanthrenecarboxylic acid, 1,2,3,4,4a,-9,10,10a-octahydro-1,4a-dimethyl-7-(1-methylethyl)-, methyl ester	1.87

[a] Identity confirmed by comparison of EI spectra and RRT with authentic standard.

Two tricyclic diterpenoid resin acids also were identified in the acid fraction of Spirit Lake, methyl 13-abieten-18-oate (compound 42) and methyl dehydroabietate (compound 43). These two compounds were also found associated with the volcanic ash. These two resin acids have been identified previously in Kraft Mill wastes (*24*). The mass spectrum of methyl dehydroabietate is shown in

Table IV. Organic Compounds Identified in Neutral Fraction, Spirit Lake, WA

compound	RRT
1. sulfide, dimethyl	0.21
2. hexane, 2,2,5-trimethyl-	0.23
3. benzene, ethyl-[a]	0.32
4. cyclohexanone[a]	0.36
5. disulfide, 1,1-dimethylethyl methyl	0.41
6. bicyclo[2.2.1]heptane, 2,2-dimethyl-3-methylene- (camphene)	0.43
7. thiophene, tetrahydro-2-butyl-	0.44
8. trisulfide, dimethyl	0.46
9. phenol[a]	0.48
10. 1,3-cyclohexadiene, 2-methyl-5-(1-methylethyl)- (α-phellandrene)	0.51
11. 1,3-cyclohexadiene, 1-methyl-4-(1-methylethyl)-	0.53
12. benzene, 1-methyl-4-(1-methylethyl)- (*p*-cymene)	0.54
13. 1,4-cyclohexadiene, 1-methyl-4-(1-methylethyl)-	0.55
14. ethanone, 1-phenyl-[a]	0.60
15. phenol, methyl isomer	0.62
16. bicyclo[2.2.1]heptane-2-one, 1,3,3-trimethyl- (fenchone)	0.64
17. 3-octyne	0.66
18. bicyclo[2.2.1]heptane-2-one, 1,7,7-trimethyl- (camphor)	0.72
19. phenol, 3-ethyl-[a]	0.74
20. 3-cyclohexen-1-ol, 4-methyl-1-(1-methylethyl)- (terpinen-4-ol)	0.76
21. 3-cyclohexene-1-methanol, α,α,4-trimethyl- (α-terpineol)	0.78
22. bicyclo[3.1.0]hex-3-en-2-one, 4-methyl-1-(1-methylethyl)-	0.80
23. tetrasulfide, dimethyl	0.81
24. bicyclo[3.2.0]heptan-2-one, 1,4,4-trimethyl-	0.85
25. ethanone, 1-(4-methoxyphenyl)-	0.91
26. biphenyl-d_{10} (internal standard)[a]	1.00
27. benzene, (1,2-dimethylpropyl)-	1.08
28. cyclohexanecarboxylic acid, 4-(1,5-dimethyl-3-oxohexyl)-, methyl ester isomer (dihydrojuvabione)	1.51
29. cyclohexanecarboxylic acid, 4-(1,5-dimethyl-3-oxohexyl)-, methyl ester isomer (dihydrojuvabione)	1.55
30. 1-phenanthrenecarboxylic acid, 1,2,3,4,4a,-9,10,10a-octahydro-1,4a-dimethyl-7-(1-methylethyl)-, methyl ester (methyldehydroabietate)	1.87

[a] Identity confirmed by comparison of EI spectra and RRT with authentic standard.

Figure 6. Elemental compositions of m/z 314, 299, and 239 were established by HRMS. Resin acids have been reported to be toxic to fish at concentrations of 1–5 ppm (*25*, *26*). Resin acid salts, which are soaps, have been reported to be toxic to minnows at the 1-ppm level (*27*) and to the water flea, *Daphnia pulex*, at the 2-ppm level (*28*).

Of considerable interest is the presence of three insect juvenile hormones in the acid fraction of Spirit Lake. The compounds identified are two isomers of dihydrojuvabione (compounds 37 and 39) and the monocyclic sesquiterpenoid ester juvabione (compound 40). The mass spectrum of dihydrojuvabione is shown in Figure 7. Elemental compositions of the major ions were established by HRMS. The mass spectral fragmentation pattern of this compound has been reported (*29*). Juvabione, a monocyclic sesquiterpenoid ester with high juvenile hormone activity for *Pyrrhocoris apterus* (L.) has been isolated from balsam fir, *Abies balsamea* (L.) Miller (*30*). (+)-Todamatuic acid and *cis*-dihydrotodamatuic acid have been isolated from a variety of Douglas fir trees (*29*). The methyl

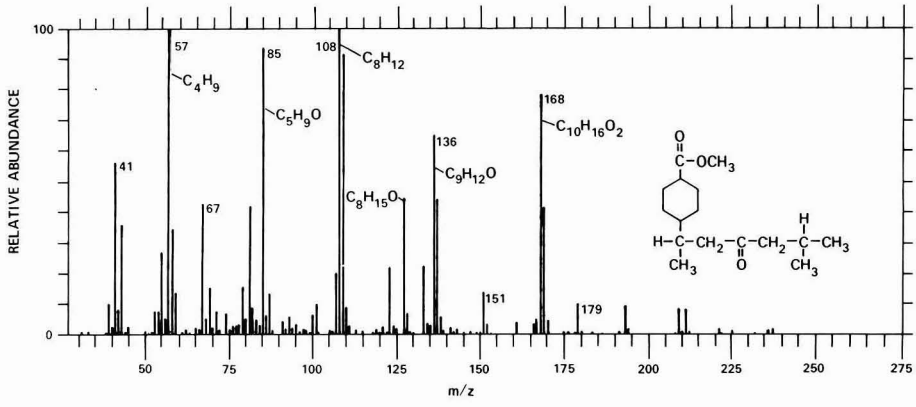

Figure 7. Mass spectrum of dihydrojuvabione.

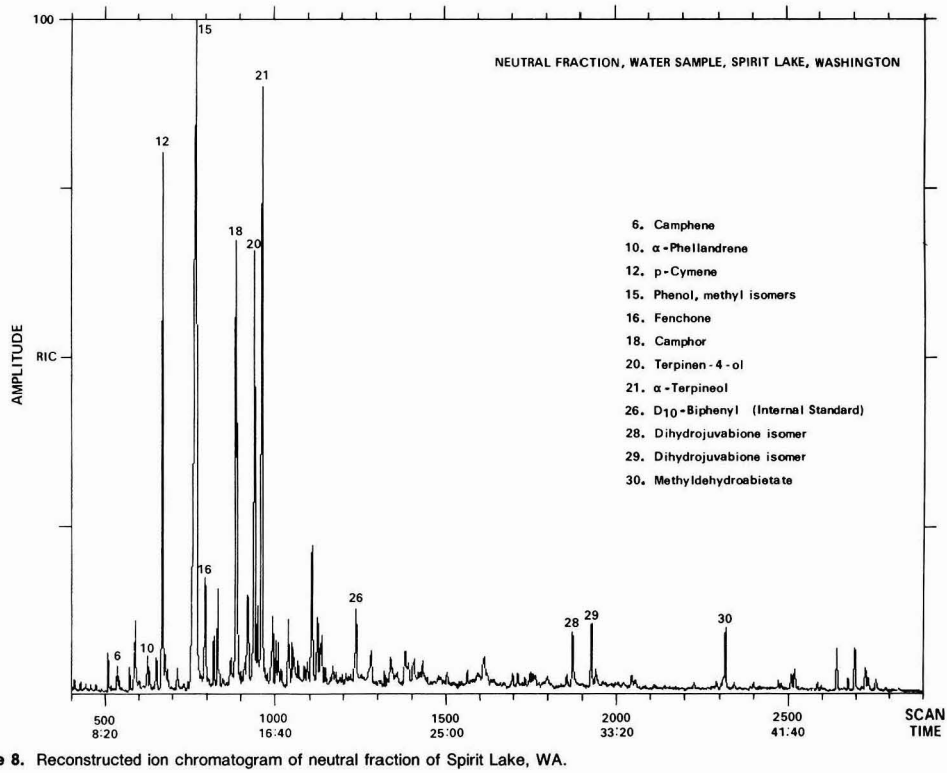

Figure 8. Reconstructed ion chromatogram of neutral fraction of Spirit Lake, WA.

esters of these compounds, juvabione and dihydrojuvabione, possess insect juvenile hormone activity. Biological assays on certain insects indicate that these compounds are effective ovicides and juvenilizing hormones (*29*). In addition, juvabione has been reported to be acutely toxic to fish (*31*).

A reconstructed ion chromatogram of the neutral fraction of Spirit Lake is shown in Figure 8. A list of compounds identified in the neutral fraction is shown in Table IV. In addition to methyl dehydroabietate (compound 30) and two isomers of dihydrojuvabione (compounds 28 and 29), various terpenes were identified. Monoterpene hydrocarbons included camphene (compound 6), α-phellandrene (compound 10), and α- and γ-terpinene (compounds 11 and 13). Oxygenated monoterpenes included α-terpineol (compound 21) and terpinen-4-ol (compound 20). Two ketones, camphor (compound 18) and fenchone (compound 16), were also identified. Several of these compounds have been reported to be present in Kraft Paper Mill wastewaters (*22*) and in the needle oil of *Pinus* species (32).

A sample of water from Coldwater Creek was similarly analyzed and characterized by GC–MS. A total of 47 organic compounds in the acid fraction and 24 organic compounds in the neutral fraction was identified. A list of organic compounds common to both Spirit Lake and Coldwater Creek are shown in Table V. The similarity of organic contaminants at both sites indicates a common

Table V. Organic Compounds Identified in Spirit Lake and Coldwater Creek, WA

compound	Spirit Lake, RRT	Cold-water Creek, RRT
Acid Fraction		
1. butanoic acid, 3-methyl-, methyl ester	0.21	0.22
2. benzene, methoxy-	0.39	0.38
3. benzene, 1-methoxy-4-methyl-	0.54	0.53
4. cyclohexanecarboxylic acid, methyl ester	0.61	0.59
5. benzoic acid, methyl ester[a]	0.67	0.65
6. butanedioic acid, methyl-, dimethyl ester	0.70	0.69
7. pentanedioic acid, 2-methyl-, dimethyl ester	0.75	0.74
8. benzoic acid, 2-hydroxy-, methyl ester	0.78	0.77
9. benzenepropanoic acid, methyl ester[a]	0.88	0.89
10. benzoic acid, (1-methylethyl)-, methyl ester isomer	0.94	0.94
11. benzoic acid, 3-methoxy-, methyl ester	0.95	0.96
12. benzoic acid, (1-methylethyl)-, methyl ester isomer	0.97	0.97
13. benzoic acid, (1-methylethyl)-, methyl ester isomer	0.99	0.99
14. biphenyl-d_{10} (internal standard)[a]	1.00	1.00
15. benzoic acid, 4-methoxy-, methyl ester	1.00	1.00
16. benzeneacetic acid, 3-methoxy-, methyl ester	1.04	1.05
17. octanedioic acid, dimethyl ester[a]	1.07	1.08
18. benzeneacetic acid, 4-hydroxy-, methyl ester	1.13	1.14
19. nonanedioic acid, dimethyl ester[a]	1.18	1.19
20. benzoic acid, 3,5-dimethoxy-, methyl ester	1.23	1.24
21. decanedioic acid, dimethyl ester[a]	1.28	1.29
22. cyclohexanecarboxylic acid, 4-(1,5-dimethyl-3-oxohexyl)-, methyl ester isomer	1.51	1.52
23. cyclohexanecarboxylic acid, 4-(1,5-dimethyl-3-oxohexyl)-, methyl ester isomer	1.55	1.56
24. 1-cyclohexene-1-carboxylic acid, 4-(1,5-dimethyl 3-oxohexyl)-, methyl ester	1.61	1.62
Neutral Fraction		
1. benzene, 1-methyl-4-(1-methylethyl)-	0.54	0.54
2. bicyclo[2.2.1]heptan-2-one, 1,3,3-trimethyl-	0.64	0.64
3. bicyclo[2.2.1]heptan-2-one, 1,7,7-trimethyl-	0.72	0.72
4. phenol, ethyl isomer	0.74	0.78
5. 3-cyclohexene-1-methanol, α,α,4-trimethyl-	0.78	0.79

[a] Identity confirmed by comparison of EI spectra and RRT with authentic standard.

source for these compounds, namely, pyrolysis of plant and soil organic matter.

Conclusion

The results presented in this report clearly demonstrate that the volcanic eruption of Mount St. Helens pyrolyzed plant and soil organic matter, generating a large number of organic compounds that contaminated ash, surface-water, and bottom-material samples. Many of these contaminants, including fatty acids, phenols, resin acids, insect juvenile hormones, and terpenes are similar to those found in effluents from the paper and pulp industry. The environmental effects of pollutants in wastewaters from paper and pulp mills such as oxygen depletion, toxicity to aquatic life, and taste and odor problems are well known. Because of the hydrophilic nature of these organic contaminants, the potential exists for a ground-water contamination problem. Preliminary analytical data on ground-water samples obtained from wells drilled in the area between the Cowlitz River and the Columbia River show no evidence to date of ground-water contamination resulting from organic pollutants associated with the eruption of Mount St. Helens.

Acknowledgments

We wish to express our thanks to Frank Rinella of the Oregon District, U.S. Geological Survey, for collecting bottom-material samples from the Cowlitz River, and to Donald Anders and David King of the U.S. Geological Survey, for the HRMS.

Literature Cited

(1) Pereira, W. E.; Rostad, C. E.; Taylor, H. E. *Geophys. Res. Lett.* **1980**, *7*, 953–954.
(2) Jungclaus, G. A.; Games, L. M.; Hites, R. A. *Anal. Chem.* **1976**, *48*, 1894–1896.
(3) Budde, W. L.; Eichelberger, J. W. *Anal. Chem.* **1979**, *51*, 1–4.
(4) Fales, H. M.; Jaouni, T. M.; Babashak, J. F. *Anal. Chem.* **1973**, *45*, 2302–2303.
(5) Grob, K.; Grob, G. *J. Chromatogr. Sci.* **1969**, *7*, 584–590.
(6) Biller, J. E.; Biemann, K. *Anal. Lett.* **1974**, *7*, 515–528.
(7) Sokolow, S.; Karnofsky, J.; Gustafson, P., The Finnigan Library Search Program, in Finnigan Application Report *2*, 1978, 1–45.
(8) Giger, W.; Schaffner, C. "Advances in Organic Geochemistry", 7th International Meeting on Organic Geochemistry, Spain, September 1975; pp 375–439.
(9) Youngblood, W. W.; Blumer, M. *Geochim. Cosmochim. Acta* **1975**, *39*, 1303–1314.
(10) Schnitzer, M. In "Soil Organic Matter"; Schnitzer, M., Kahn, S. U., Eds.; Elsevier: New York, 1978; pp 1–64.
(11) Kononova, M. M. In "Soil Organic Matter, Its Nature, Its Role in Soil Formation and Soil Fertility", 2nd ed.; Nowakowski, T. Z.; Newman, A. C. D., Eds.; Pergamon Press: New York, 1966; pp 47–155.
(12) Fox, M. E. In "Identification and Analysis of Organic Pollutants in Water"; Keith, L. H., Ed.; Ann Arbor Science: Ann Arbor, MI, 1976; pp 641–659.
(13) Brownlee, B.; Strachan, W. M. J. In "Identification and Analysis of Organic Pollutants in Water"; Keith, L. H., Ed.; Ann Arbor Science: Ann Arbor, MI, 1976; pp 661–670.
(14) Keith, L. H. In "Identification and Analysis of Organic Pollutants in Water", Keith, L. H., Ed.; Ann Arbor Science: Ann Arbor, MI, 1976; pp 671–707.
(15) Mahood, H. W.; Rogers, I. H. *J. Chromatogr.* **1975**, *109*, 281–286.
(16) Simoneit, B. R. T. *Geochim. Cosmochim. Acta* **1977**, *41*, 463–476.
(17) Rogers, I. H. *Pulp Paper Mag. Can.* **1973**, *74*, 303–308.
(18) Leach, J. M.; Thakore, A. N. *Progr. Water Technol.* **1978**, *9*, 787–798.
(19) Olie, K. E.; Vermeulen, P. L.; Hutzinger, O. *Chemosphere* **1977**, *6*, 455–459.
(20) Howard, B.; Mesereau, A.; Mariani, P. *Am. Lab.* **1980**, 117–119.
(21) Meyers, P. A.; Takeuchi, N. *Org. Geoch.* **1979**, *1*, 127–138.
(22) Keith, L. H. *Environ. Sci. Technol.* **1976**, *10*, 555–564.
(23) Shumway, D. C.; Chadwick, G. G. *Water Res.* **1971**, *5*, 997–1003.
(24) Rogers, I. H. *Pulp Paper Mag. Can.* **1973**, *74*, 111–116.
(25) Hagman, N. *Finn. Paper Timber J.* **1938**, *18*, 32–34, 40–41.
(26) Ebeling, G. *Vom Wasser* **1931**, *5*, 192–200; *Chem. Abstr.* *36*, 2262.
(27) Van Horn, W. M.; Anderson, J. B.; Katz, M. *TAPPI* **1950**, *33*, 209–212.

(28) Maenpaa, R.; Hynninen, P.; Tikka, J. *Pap. ja pun.* **1968**, *50*, 143–150.
(29) Rogers, I. H.; Manville, J. F.; Sahota, T. *Can. J. Chem.* **1974**, *52*, 1192–1199.
(30) Bowers, W. S.; Fales, H. M.; Thompson, M. J.; Uebel, E. C. *Science (Washington, D.C.)* **1966**, *154*, 1020–1021.
(31) Leach, J. M.; Thakore, A. N.; Manville, J. F. *J. Fish. Res. Board Can.* **1975**, *32*, 2556–2559.
(32) Ekundayo, O. *J. Chromatogr. Sci.* **1980**, *18*, 368–369.

Received for review February 23, 1981. Revised manuscript received November 16, 1981. Accepted March 22, 1982.

Oxidation of Phenol and Hydroquinone by Chlorine Dioxide

Johannes Edmund Wajon,† David H. Rosenblatt,* and Elizabeth P. Burrows

US Army Medical Bioengineering Research and Development Laboratory, Fort Detrick, Frederick, Maryland 21701

■ Rates of reaction of chlorine dioxide with phenol and with hydroquinone were determined with a stopped-flow spectrophotometer in the pH range 4–8. Second-order rate constants increase with increasing pH, consistent with a mechanism in which both the free phenol and the more reactive phenoxide anion react with ClO_2. Removal of an electron from the substrate by ClO_2 to form a phenoxyl radical and ClO_2^- ion is the rate-determining step. Subsequently, in the case of hydroquinone, ClO_2 removes another electron from the radical, forming *p*-benzoquinone and another ClO_2^- ion. In the case of phenol, ClO_2 adds to the phenoxyl radical para to the oxygen, and *p*-benzoquinone is formed with concomitant release of HOCl. The mechanism for phenol reaction accounts for (i) the immediate formation of *p*-benzoquinone without apparent intermediacy of hydroquinone, (ii) the chlorination observed in solutions containing excess phenol, and (iii) the production of only 0.5 mol of ClO_2^-/mol of ClO_2 consumed.

When aqueous chlorine is used as a disinfectant in phenol-bearing waters, malodorous chlorophenols are formed which persist for long periods unless large excesses of chlorine are applied (*1*). However, tastes and odors are completely avoided when chlorine dioxide in much smaller doses is used (*2*, *3*), and it is generally believed that chlorinated products will not form when chlorine dioxide is used as a disinfectant. At significantly higher concentrations of both reactants (millimolar or greater) at nearly neutral pH, increasing ratios of ClO_2 to monohydric phenols give larger amounts of oxidized products (e.g., *p*-benzoquinones and oxalic acid) relative to chlorinated products (e.g., chlorophenols and chloro-*p*-benzoquinones) (*4*, *5*). Chloro-*p*-benzoquinones, but not chlorophenols, have been found even when ClO_2 was in excess (*4*). With dihydric phenols such as hydroquinone only oxidation occurs when ClO_2 is in great excess (*6*), but chlorination may occur when ClO_2 is not in excess (*5*). It was supposed that in these concentrated solutions chlorination occurred before any oxidation, because *p*-benzoquinone and chlorinated *p*-benzoquinones do not react with chlorine (*4*).

In contrast, it was proposed, from studies in more dilute solutions at pH 2, that phenol is oxidized in the rate-determining step, and any excess phenol is then chlorinated (*7*). It was also postulated that HOCl, formed slowly from the disproportionation of $HClO_2$, reacts rapidly with more $HClO_2$ to form Cl_2O_2, which then chlorinates the phenol. However, this mechanism did not satisfactorily explain the yield of chlorite or chlorate from the reaction. Alternatively, HOCl may form directly from reaction of ClO_2 with a variety of phenols, especially guaiacols (*8*). Chlorination would then be a result of direct reaction of the phenol with HOCl or Cl_2 rather than with Cl_2O_2, which also forms from HOCl and ClO_2^- but quickly decomposes to ClO_2, ClO_3^-, and Cl^-.

Rates of reaction between ClO_2 and phenol have been measured between pH 0 and 2 (*7*) and between pH 2.5 and 4.5 (*8*). The rate increases with increase in pH, and from the dependence of the second-order rate constant on pH, it has been proposed that both the free phenol and the phenoxide anion react with ClO_2, though the phenoxide anion is more reactive by several orders of magnitude (*7*). Extrapolation of the rate constant suggested that the reaction should have a half-life of several milliseconds at millimolar concentrations and pH 7.

It was the aim of the present investigation to clarify the stoichiometry and mechanism of the oxidation of phenol by ClO_2 and especially to establish the extent of formation of chlorinated products at neutral pH under conditions approximating those of water treatment. Rates of reaction between $5–250 \times 10^{-5}$ M phenol and $2–65 \times 10^{-5}$ M ClO_2 (13–440 mg/L of ClO_2) were determined with a stopped-flow spectrophotometer in order to confirm the extrapolation of Grimley's data to pH 7 and to provide support for the mechanism proposed here. The reaction between $13–100 \times 10^{-5}$ M hydroquinone and $2–35 \times 10^{-5}$ M ClO_2 was also investigated.

Experimental Methods

Preparation of Solutions. All solutions were made with glass-distilled, deionized water which was irradiated with a mercury vapor lamp, then boiled, and regassed with N_2 before use. Solutions of ClO_2 (0.017 M) were prepared from reagent grade potassium persulfate and sodium chlorite (*9*) and stored in a low actinic glass bottle at 2 °C for no longer than 6 months. Phenol (MC/B reagent) was purified by distillation under nitrogen and stored at 2 °C. *p*-Benzoquinone (Baker reagent) and 2-chlorohydroquinone (Pfaltz and Bauer) were purified by steam distillation. The following chemicals were purified by recrystallization: $NaClO_2$ (MC/B), 4-chlorophenol (Chemical Service Co.), 2,6-dichlorophenol (Aldrich), hydroquinone (Aldrich), 2,5-dichlorohydroquinone (Pfaltz and Bauer), and 2,5-dichlorobenzoquinone (Pfaltz and Bauer). 2-Chlorophenol (Chemical Service Co.), 2,4-dichlorophenol (Eastman), and sodium hypochlorite (5%, Baker) were used as received. 2,6-Dichlorobenzoquinone was prepared from 2,4,6-trichlorophenol (*10*), and 2,3-dichlorobenzoquinone from 2,3-dichlorophenol (*11*) by CrO_3/acetic acid oxidation. 2,6- and 2,3-dichlorohydroquinones were prepared by reduction of the respective dichlorobenzoquinones with $NaBH_4$ in ethanol. Acetic acid, sodium acetate, NaH_2PO_4, Na_2HPO_4, and $NaClO_4$, used in preparing buffer solutions (*12*), were all reagent grade chemicals. The concentration of $NaClO_4$ in these solutions was 0.1 M, while those of phosphate and acetate were usually 0.01 and 0.02 M, respectively. A Markson Science Inc.

† National Research Council Postdoctoral Associate 1980–1981.

Model 884 micro pH electrode and a Corning Scientific Instruments Model 12 pH meter were used to measure pH.

Solutions of oxychlorine species were analyzed iodometrically with a Fischer-Porter amperometric titrator. The concentration of ClO_2 + HOCl was determined at pH 7 by adding a sample to 200 mL of water containing phosphate buffer (2 mL) and 5% KI (1 mL) and titrating immediately with 0.005 64 N phenylarsine oxide (Fisher Scientific Co.). Chlorite was determined subsequently in this solution at pH 2 by adding 2 mL of 6 N H_2SO_4 and titrating with phenylarsine oxide after 6 min.

Kinetic Analysis. Kinetic studies were performed in a Durrum (Dionex Corp., Sunnyvale, CA) Model 110 stopped-flow spectrophotometer in which 0.075-mL solutions of ClO_2 and the phenol were mixed in a 2-cm path length, 0.066-mL cuvette with a deadtime of 1.6 ms. The reaction temperature was 25.0 ± 0.1 °C. Reactions were followed by measurement of light absorbance, done by monitoring the disappearance of ClO_2 at 359 nm with a Biomation (Gould, Inc., Santa Clara, CA) 805 waveform recorder and a Tektronix 7613 oscilliscope. The data from the least noisy of similar curves of absorbance vs. time, spanning 95–99% of the reaction, were stored in a Data Graphics Datos 305 interface and then transferred to a digital computer. The pH of the reacted solution was determined.

As will be shown, the stoichiometry of the reaction can be represented by eq 1. The reaction was found to be first

$$\text{phenol} + 2ClO_2 \xrightarrow{k_2} \text{products} \tag{1}$$

order with respect to each reactant on the basis of the initial rates of reaction, which were determined by fitting a straight line through the first 1–2% of the absorbance–time data by linear regression. The applicable rate expression is

$$-d[ClO_2]/dt = 2k_2[P_T][ClO_2] \tag{2}$$

where $[P_T]$ = total concentration of the phenol and k_2 = observed second-order rate constant. Kinetic studies were carried out both with a molar excess of ClO_2 and a molar excess of the phenol.

When the phenol was in excess, it was present in at least a 5-fold and up to a 120-fold stoichiometric excess. Equation 2 thus becomes

$$-d[ClO_2] = 2k_{obsd}[ClO_2] \tag{3}$$

where

$$k_{obsd} = k_2[P_T] \tag{4}$$

and k_{obsd} is the pseudo-first-order rate constant. Upon integration and use of Guggenheim's method (*13*), this can be expressed as

$$\ln (A - A') = -2k_{obsd}t + \ln (A_\infty - A_0) + \ln e^{-k_{obsd}\Delta} - 1 \tag{5}$$

where A = absorbance at time t, A' = absorbance at time $t + \Delta$, A_0 = absorbance at time $t = 0$, A_∞ = absorbance at time $t = \infty$, and Δ is a time interval greater than the half-life of the reaction. Pseudo-first-order rate constants (k_{obsd}) were determined by plotting the function $\ln (A - A')$ vs. time for the initial 25–50% of the absorbance–time data by using the linear regression model RLONE (International Mathematical and Statistical Libraries Inc., Houston, TX).

If phenol is in stoichiometric excess, eq 2 can also be expressed as (*14*)

$$kt = \frac{1}{b_0 - 2a_0} \ln \frac{(a_0/b_0)(A_\infty - A)}{(a_0/b_0)(A_\infty - A_0) - \frac{1}{2}(A - A_0)} \tag{6}$$

which can be written

$$t = \frac{1}{X} \ln \frac{B(A_\infty - A)}{D - A/2} \tag{7}$$

where a_0 = total initial concentration of phenol, b_0 = initial concentration of ClO_2, $X = (b_0 - 2a_0)k$, $B = a_0/b_0$, $C = (A_\infty - A_0)$, and $D = BC + {}^1/_2A_0$. Rearranged and expressed exponentially, eq 7 becomes

$$A = \frac{De^{Xt} - BA_\infty}{e^{Xt}/2 - B} \tag{8}$$

If phenol is not in stoichiometric excess, eq 2 becomes

$$kt = \frac{1}{2a_0 - b_0} \ln \frac{(b_0/a_0)(A_\infty - A)}{(b_0/a_0)(A_\infty - A_0) - 2(A - A_0)} \tag{9}$$

Making the substitutions $X = (2a_0 - b_0)k$, $B = b_0/a_0$, $C = (A_\infty - A_0)$, and $D = BC + 2A_0$ and rearranging as before, we get

$$A = \frac{De^{Xt} - BA_\infty}{2e^{Xt} - B} \tag{10}$$

Second-order rate constants, k, were determined directly by fitting either eq 8 or eq 10 to the initial 25–50% of the absorbance–time data by using the curve fitting simulation, analysis, and modeling (SAM) program (*15*). The parameters X, C, and A_∞ were adjustable.

Product Analysis. A solution of ClO_2, $NaClO_2$, or HOCl was mixed rapidly and uniformly with a phenol solution by forcing the two together in the junction of two 1-mm diameter glass tubes. Mixing of 20-mL solutions was achieved within 10 s. The mixtures were kept at 25 ± 0.3 °C and were sampled for analysis of residual oxidants and organic compounds. The first samples were taken 45 s after mixing.

Residual oxidants were measured at pH 7 and 2 as described above. In solutions where it had been shown that all the ClO_2 was consumed within several seconds, any titer of a pH 7 sample was presumed to be due to HOCl alone. However, no satisfactory method was found to determine the concentrations of ClO_2 and HOCl when they were both present. All published titrimetric methods (*16–23*) were found to be inconsistent. The concentration of ClO_2^- determined after either all the ClO_2 or all the HOCl had dissipated was presumed to be the same as that present initially. In cases where it was likely that neither HOCl nor ClO_2 had completely disappeared, we assumed that the pH 7 titration formed ClO_2^-, which appeared as "excess" ClO_2^- on titration at pH 2. Any portion of the pH 7 titer not accounted for as ClO_2 via the pH 2 titration was presumed to be HOCl.

Organic compounds were analyzed by HPLC. Acetylation followed by GC analysis (*24*) was found unsatisfactory because the acetylation procedure produced chlorinated hydroquinones and benzoquinones. The liquid chromatographic system consisted of the following: (1) two Model 6000A pumps and Model M660 solvent programmer (Waters Assoc.); (2) SF-770 variable wavelength detector (Schoeffel Instrument Corp.) set at 220 nm; (3) Sigma 10 Data Station (Perkin-Elmer Corp.); (4) 300 × 3.9 mm 10 μm μBondapak C_{18} reversed-phase column (Waters Assoc.). A linear gradient elution program was used in which the eluent changed from 100% 0.02 M KH_2PO_4 pH 2.8 to 50% acetonitrile–water (80/20) in 30 min at 1.5 mL/min and 1200 psi. Under these conditions, phenol, mono- and dichlorophenols, hydroquinone, mono- and dichlorohydroquinones, *p*-benzoquinone, and mono- and dichloro-*p*-

Table I. Stoichiometry of the Reaction of ClO_2 with Phenols

$[ClO_2]/10^{-4}$, M	[reductant]/10^{-4}, M	pH	$\frac{\Delta ClO_2}{\Delta phenol}$	$\frac{\Delta benzoquinone}{\Delta phenol}$	$\frac{\Delta ClO_2^-}{\Delta ClO_2}$
(1) Phenol + ClO_2			(a) Phenol in Excess		
5.25	12.62	6.89	1.96	0.82	0.62
6.40	5.00	6.93	1.72	1.00	0.52
3.15	5.00	6.83	3.33	1.00	0.50
0.94	5.00	6.90	2.94	1.09	0.62
2.90	2.32	6.84	2.00	0.65	0.44
0.94	2.32	6.88	2.86	1.06	0.52
0.94	0.91	6.87	1.85	0.72	0.51
			av 2.4 ± 0.6	0.9 ± 0.2	0.5 ± 0.1
			(b) ClO_2 in Excess		
3.09	0.91	6.84	1.52	0.61	0.30
2.78	0.91	6.90	1.47	0.63	0.46
3.09	0.43	6.87	2.08	0.67	0.38
			av 1.7 ± 0.3	0.6 ± 0.1	0.4 ± 0.1
(2) Hydroquinone + ClO_2					
2.70	3.80	6.98	1.6	0.84	1.00
3.09	0.48	6.92	1.2	0.61	0.68

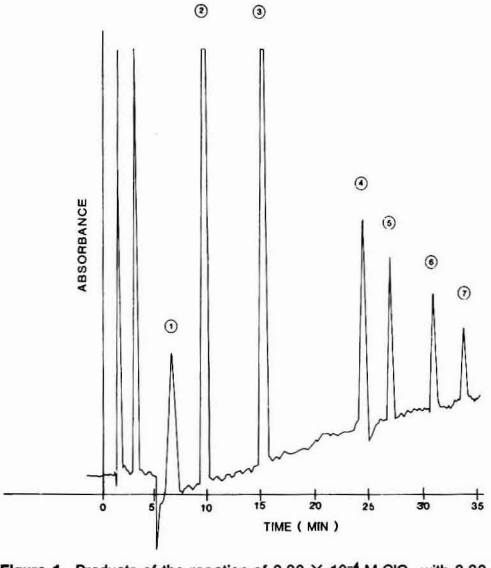

Figure 1. Products of the reaction of 2.90×10^{-4} M ClO_2 with 2.32×10^{-4} M phenol at pH 6.84 after 4.0 min: (1) hydroquinone; (2) benzoquinone; (3) phenol; (4) 2-chlorophenol; (5) 4-chlorophenol; (6) 2,6-dichlorophenol; (7) 2,4-dichlorophenol.

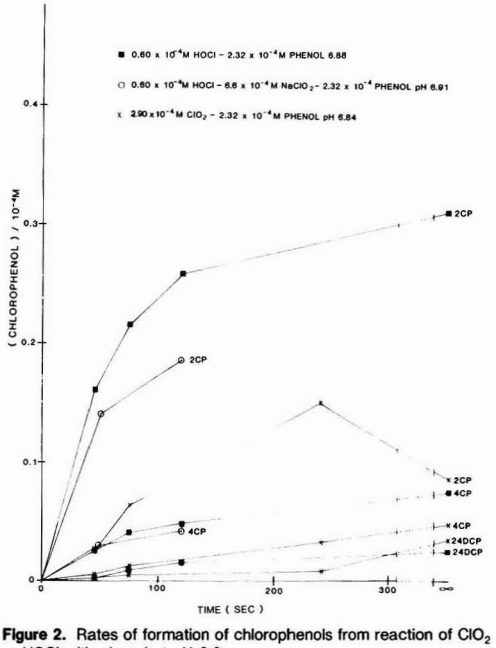

Figure 2. Rates of formation of chlorophenols from reaction of ClO_2 or HOCl with phenol at pH 6.9.

benzoquinones at concentrations $\geq 5 \times 10^{-6}$ M were eluted within 35 min.

Results

Products and Stoichiometry. When $1\text{–}7 \times 10^{-4}$ M solutions of ClO_2 (5–45 mg/L) were mixed with phenol in a phenol to chlorine dioxide mole ratio ≥0.75 at pH 6.85–6.95, ClO_2 disappeared within seconds, although an oxidizing titer at pH 7, presumed to be due to HOCl, remained for periods up to about 10 min. The products detected within 1 min were *p*-benzoquinone, 2-chlorophenol, 4-chlorophenol, 2,4-dichlorophenol, and 2,6-dichlorophenol. After 10 min, no oxidant titer was present, the concentration of the four chlorophenols had increased substantially, hydroquinone had also formed, and the concentration of *p*-benzoquinone had decreased slightly.

Figure 1 presents a typical chromatogram, and Figure 2 shows the rates of formation of the chlorophenols. Over the next 2 h, the concentration of hydroquinone increased rapidly while the concentration of benzoquinone decreased in almost a 1:1 correspondence (see Figure 3). Chlorinated hydroquinones or chlorinated benzoquinones were not detected at any time. From the results of seven experiments (see Table I), the ratio of ClO_2 consumed to phenol oxidized was found to be 2.4 ± 0.6, and of the phenol oxidized, 90 ± 20% was oxidized to *p*-benzoquinone. The ratio of ClO_2^- formed to ClO_2 consumed was found to be 0.5 ± 0.1.

When 3×10^{-4} M ClO_2 solutions (20 mg/L of ClO_2) were mixed with phenol in a ClO_2/phenol molar ratio >3, all the phenol was consumed within seconds. *p*-Benzoquinone

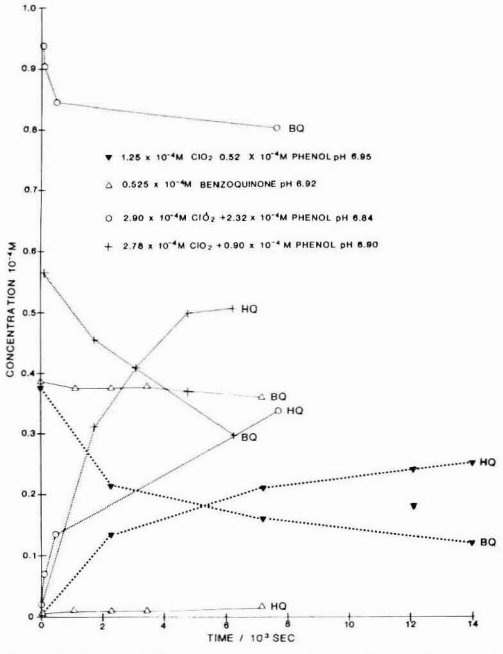

Figure 3. Rates of change of concentrations of hydroquinone and benzoquinone during the reaction of ClO_2 with phenol at pH 6.9.

was the only organic product detected, but the yield was only 64 ± 3% (Table I). The ratio of ClO_2 consumed to phenol oxidized was 1.7 ± 0.3, and the ratio of ClO_2^- formed to ClO_2 consumed was 0.4 ± 0.1. Over the next 2 h, the concentration of benzoquinone decreased steadily while that of hydroquinone increased (Figure 3). No chlorinated products were detected even though the presence of HOCl was suspected (on the basis of oxidant titer) for periods up to 10 min.

When 3×10^{-4} M ClO_2 solutions, either in molar excess or molar deficiency, were mixed with hydroquinone, the sole products detected were *p*-benzoquinone and ClO_2^-, whose concentrations remained unchanged for many hours. There was no evidence for the presence of HOCl at any time. The ratio of ClO_2 consumed to hydroquinone oxidized was 1.6 when hydroquinone was in excess and 1.2 when ClO_2 was in excess. The ratio of ClO_2^- formed to ClO_2 consumed was 1.0 when hydroquinone was in excess and 0.7 when ClO_2 was in excess.

While the accuracy of the oxidant analyses may be suspect, especially in solutions containing excess ClO_2, due to the simultaneous presence of several oxychlorine species that could not be determined separately, it nevertheless appears that 1 mol of hydroquinone consumes 2 mol of ClO_2, forming 2 mol of ClO_2^-, while 1 mol of phenol also consumes 2 mol of ClO_2 but forms only 1 mol of ClO_2^-. (Note added in proof: This stoichiometry was later confirmed in each case through ion chromatographic measurement of ClO_2^- formed.)

Kinetics. Reaction kinetics of ClO_2 and phenol and of ClO_2 and hydroquinone were observed in the pH range 4.5–8.0 at 25.0 °C. Absorbance–time data for three reactions at pH 7 are shown in Figure 4. In solutions with stoichiometric excesses of phenol or hydroquinone, plots of ln $(A - A')$ as a function of time, in accord with eq 5, were linear for at least 5 half-lives of the reaction, consistent with the assumption of pseudo-first-order behavior. A typical plot, from which the value of k_{obsd} was calculated, is shown in Figure 5. Rate constants (k_2), calculated from k_{obsd} by means of eq 4, were constant with varying initial phenol or hydroquinone concentrations, as shown in Table

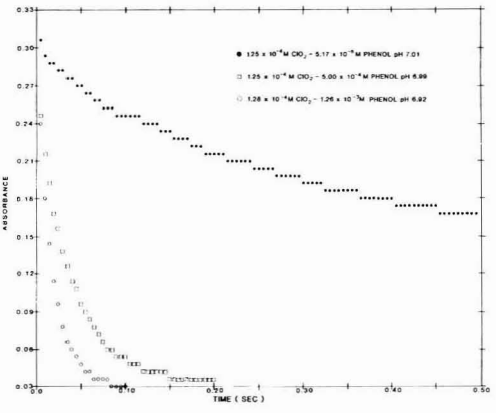

Figure 4. Absorbance–time plots for the reaction of ClO_2 with phenol at pH 7.0.

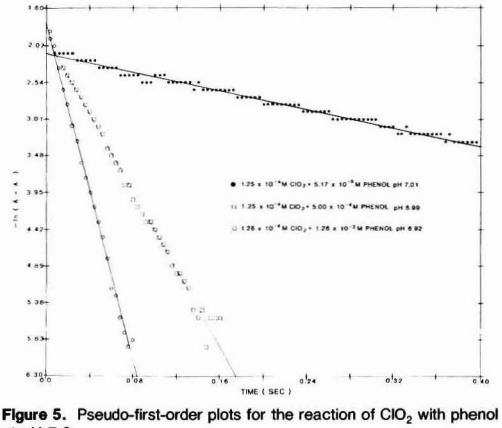

Figure 5. Pseudo-first-order plots for the reaction of ClO_2 with phenol at pH 7.0.

Table II. Second-Order Rate Constants at 25.0 °C for the Disappearance of ClO_2

pH	$[ClO_2]_0$/ 10^{-5}, M	$[phenol]_0$/ 10^{-5}, M	k_{obsd},[a] s^{-1}	$k_2/10^4$, $M^{-1}\ s^{-1}$
7.05	2.28	5.17	1.14	2.22
7.05	2.28	5.17		2.46
7.01	12.5	5.17		2.56
7.01	12.5	5.17		2.65
6.92	2.14	50.0	13.4	2.69
6.92	2.14	50.0	13.0	2.61
6.99	12.5	50.0	13.2	2.65
6.99	12.5	50.0		2.84
6.89	2.14	126.0	34.2	2.70
6.89	2.14	126.0	34.6	2.74
6.92	12.8	126.0	28.6	2.26
6.92	12.8	126.0		2.34
6.91	23.0	126.0	32.0	2.54
6.91	23.0	126.0		2.81

[a] When no value is listed for k_{obsd}, k_2 was obtained directly by fitting a second-order kinetic expression to the data.

Table III. Second-Order Rate Constants at 25.0 °C for the Oxidation of Phenol by ClO_2

pH	ionic strength, M	γ	k_2, M^{-1} s^{-1}	k_2^{calcd}, M^{-1} s^{-1} [a]
7.99	0.129	0.763	$(3.5 \pm 0.2) \times 10^5$	3.2×10^5
7.05	0.200	0.736	$(2.3 \pm 0.1) \times 10^4$	3.8×10^4
7.00	0.200	0.736	$(2.6 \pm 0.1) \times 10^4$	3.4×10^4
6.90	0.200	0.736	$(2.6 \pm 0.1) \times 10^4$	2.7×10^4
6.90	0.120	0.767	$(2.6 \pm 0.1) \times 10^4$	2.6×10^4
5.81	0.111	0.772	$(1.8 \pm 0.05) \times 10^3$	2.1×10^3
5.78	0.111	0.772	$(1.8 \pm 0.1) \times 10^3$	2.0×10^3
5.76	0.111	0.772	$(1.8 \pm 0.05) \times 10^3$	1.9×10^3
4.60	0.110	0.773	$(1.2 \pm 0.05) \times 10^2$	1.3×10^2
4.58	0.110	0.773	$(1.3 \pm 0.05) \times 10^2$	1.2×10^2
4.52	0.110	0.773	$(1.3 \pm 0.05) \times 10^2$	1.1×10^2
2.18	1.00	0.683	0.80 [b]	0.80
1.75	1.00	0.683	0.44 [b]	0.44
1.45	1.00	0.683	0.34 [b]	0.34
1.06	1.00	0.683	0.29 [b]	0.29
0.17	1.00	0.683	0.24 [b]	0.24

[a] Predicted on the basis of the proposed mechanism. [b] Data from Grimley and Gordon.

Table IV. Second-Order Rate Constants at 25.0 °C for the Oxidation of Hydroquinone by ClO_2

pH	ionic strength, M	γ	k_2, M^{-1} s^{-1}	k_2^{calcd}, M^{-1} s^{-1} [a]
8.02	0.129	0.763	$(4.6 \pm 0.6) \times 10^6$	1.1×10^7
7.28	0.120	0.767	$(1.8 \pm 0.2) \times 10^6$	2.1×10^6
7.25	0.120	0.767	$(1.4 \pm 0.05) \times 10^6$	1.9×10^6
6.93	0.120	0.767	$(8.8 \pm 0.4) \times 10^5$	9.4×10^5
6.91	0.120	0.767	$(9.5 \pm 1.0) \times 10^5$	9.0×10^5
6.89	0.120	0.767	$(9.0 \pm 0.1) \times 10^5$	8.6×10^5
5.81	0.111	0.772	$(1.1 \pm 0.05) \times 10^5$	1.1×10^5
5.78	0.111	0.772	$(1.0 \pm 0.05) \times 10^5$	1.0×10^5
5.76	0.111	0.772	$(1.0 \pm 0.05) \times 10^5$	1.0×10^5
4.61	0.110	0.773	$(4.2 \pm 0.2) \times 10^4$	4.3×10^4
4.58	0.110	0.773	$(4.3 \pm 0.1) \times 10^4$	4.3×10^4
4.16	0.106	0.775	$(4.1 \pm 0.05) \times 10^4$	4.1×10^4
4.13	0.106	0.775	$(4.0 \pm 0.05) \times 10^4$	4.0×10^4
4.11	0.106	0.775	$(4.0 \pm 0.05) \times 10^4$	4.0×10^4

[a] Predicted on the basis of the proposed mechanism.

II, thus confirming overall second-order behavior. For several of these reactions, the absorbance–time data were also fitted to eq 8, and values of k_2 so obtained directly were equal to the values obtained with eq 4 and 5 (see Table II). Values of k_2 for solutions with ClO_2 in excess, obtained by means of eq 10, were equal to those for solutions with phenol or hydroquinone in excess (see Table II).

Second-order rate constants (k_2) decreased with decrease in pH. In the case of phenol, k_2 decreased 10-fold for each unit pH decrease above pH 4 (see Table III), and began to level off at pH <3 (*7*). In the case of hydroquinone, k_2 decreased 10-fold for each unit pH decrease at pH >6 and began to level off at pH <6 (see Table IV). Such a variation of rate with pH can be attributed to the reaction of ClO_2 with both the free phenol and the phenoxide anion. That is, there are two simultaneous reactions (eq 11 and 12), where P represents either C_6H_5OH or HOC_6H_4OH, P^-

$$ClO_2 + P^- \xrightarrow{k_a} [X^-] \rightarrow \text{intermediate} \qquad (11)$$

$$ClO_2 + P \xrightarrow{k_b} [X] \rightarrow \text{intermediate} \qquad (12)$$

represents either $C_6H_5O^-$ or $HOC_6H_4O^-$, and X^- and X represent the activated complexes of reactions 11 and 12, respectively. The expression for the overall rate of disappearance of ClO_2 is thus

$$-d[ClO_2]/dt = 2k_2[P_T][ClO_2] \qquad (13)$$

$$= 2\left(\frac{k_a[P^-]\gamma_{P^-}}{\gamma_{X^-}} + \frac{k_b[P]\gamma_P}{\gamma_X}\right)[ClO_2]\gamma_{ClO_2} \qquad (14)$$

where γ_i is the activity coefficient of species i. When expressions for the acid dissociation constants (K_a) of C_6H_5OH and HOC_6H_4OH are substituted in eq 14 and when it is assumed that in dilute aqueous solution the activity coefficients of neutral molecules and neutral activated complexes are equal to unity and those of ions are given by the extended Debye–Hückel equation (*12*), eq 15 results.

$$-\frac{d[ClO_2]}{dt} = 2\frac{k_aK_a + k_b(H^+)\gamma_{\pm 1}}{K_a + (H^+)\gamma_{\pm 1}}[P_T][ClO_2] \qquad (15)$$

Equating (15) and (13) gives

$$k_2 = \frac{k_aK_a + k_b(H^+)\gamma_{\pm 1}}{K_a + (H^+)\gamma_{\pm 1}} \qquad (16)$$

At pH ≤8, with $pK_a = 9.98$ for phenol and $pK_a = 10.9$ for hydroquinone at 25.0 °C (*25*), eq 16 approximates to

$$k_2 = \frac{k_aK_a + k_b(H^+)\gamma_{\pm 1}}{(H^+)\gamma_{\pm 1}} = k_b + \frac{k_aK_a}{(H^+)\gamma_{\pm 1}} \qquad (17)$$

Thus, at pH ≤8

$$\frac{-d[ClO_2]}{dt} = 2\left(k_b + \frac{k_aK_a}{(H^+)\gamma_{\pm 1}}\right)[P_T][ClO_2] \qquad (18)$$

For hydroquinone, the plot of $k_2(H^+)\gamma_{\pm 1}$ vs. $(H^+)\gamma_{\pm 1}$ was linear in the pH range 4.0–7.0. Values of k_2 determined at pH >7.0 were considered unreliable since the reaction was so rapid. The value of the slope, k_b, determined by linear regression was 3.90 (±0.01) × 10^4 M^{-1} s^{-1} (r = 1.000). The plot of k_2 vs. $K_a/(H^+)\gamma_{\pm 1}$ was linear in the pH range 4.0–7.0, and the slope, equal to k_a, was 6.5 (±0.2) × 10^9 M^{-1} s^{-1} (r = 0.997). The values of k_2 calculated from these values of k_a and k_b by using eq 17 are shown in the last column of Table IV.

For phenol at pH >4, the value of $k_2(H^+)\gamma_{\pm 1}$ was independent of $(H^+)\gamma_{\pm 1}$ so that k_a was evaluated from the average value of $k_2(H^+)\gamma_{\pm 1}/K_a$ in the pH range 4.5–6.9. Values of k_2 determined at pH >6.9 were considered unreliable since the reaction was so rapid. The value of k_a obtained was 2.4 (±0.2) × 10^7 M^{-1} s^{-1}. The value of k_b could not be determined accurately in this pH range, so the data of Grimley and Gordon (*7*) were reevaluated in accordance with eq 17. The plot of k_2 vs. $K_a/(H^+)\gamma_{\pm 1}$ was linear in the pH range 0–2, and the value of the intercept, k_b, was 0.24 M^{-1} s^{-1}; the value of the slope, k_a, was 2.43 × 10^7 M^{-1} s^{-1} (r = 1.000). These differ from the original values published by Grimley and Gordon only in the stoichiometric factor 2, which they did not include. The values of k_2 calculated from values of k_a = 2.4 (±0.2) × 10^7 M^{-1} s^{-1} and k_b = 0.24 ± 0.01 M^{-1} s^{-1} by using eq 17 are shown in the last column of Table III.

Discussion

Any mechanism for the oxidation of phenol by chlorine dioxide in dilute, neutral solution needs to account for the following observations: (1) the very rapid disappearance of ClO_2; (2) the slow formation of chlorophenols but not of chlorinated quinones, only in solutions containing excess phenol; (3) the presence of *p*-benzoquinone but not of

Scheme I

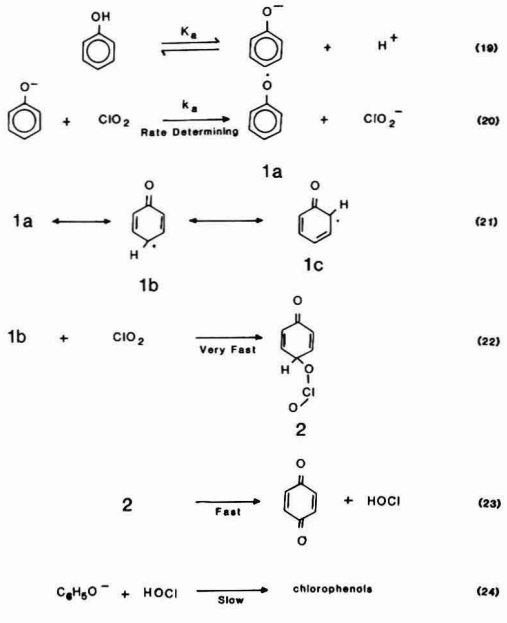

Scheme II

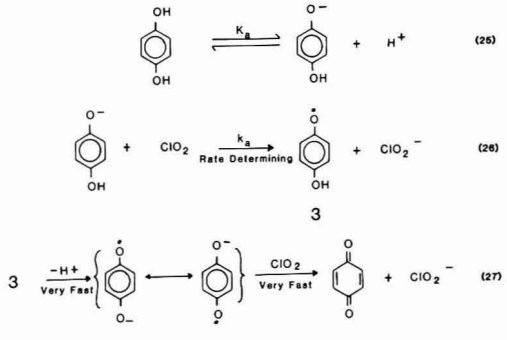

hydroquinone within seconds of mixing; (4) the presence of oxidant for several minutes after mixing; (5) the production of 0.5 mol of ClO_2^-/mol of ClO_2 consumed. The oxidation of hydroquinone to *p*-benzoquinone by ClO_2 would seem at first sight to be similar to the oxidation of phenol to *p*-benzoquinone. In both cases, the first step is most likely the removal of an electron from the phenoxide anion by ClO_2, forming a phenoxide radical and ClO_2^-. Yet, there is no chlorination in solutions of hydroquinone and ClO_2, and conversion of ClO_2 to ClO_2^- is quantitative. Schemes I and II account for these observations.

Scheme I is analogous to that proposed to account for the formation of HOCl from the reaction of ClO_2^- with aldehydes (*26*). It differs from the similar mechanism proposed by Strumilla in the attachment of the second molecule of ClO_2, which is here proposed to be para to the phenoxy group rather than ortho (*8*). An ortho attack would be expected to result in *o*-quinone, which was not detected in the oxidation of phenol itself but may be formed from guaiacols (*8*).

In Scheme I, *p*-benzoquinone is formed directly from phenol, and HOCl is released; 0.5 mol of ClO_2^- is formed/mol of ClO_2 reduced. If ClO_2 is in excess there is no chlorination, since phenol is oxidized before any HOCl is formed. But HOCl may react with excess phenol. The rate of formation of chlorophenols (Figure 2) and the disappearance of oxidant after 10 min are consistent with the known rates of reaction of HOCl and phenol (*1*). Furthermore, the distribution of chlorophenols is similar to that found when HOCl and phenol are mixed under the same conditions (Figure 2), and the distribution is not changed when up to 0.1 M $NaClO_2$ is added to reacting solutions of either ClO_2 or HOCl (see Figure 2). If Cl_2O_2, a postulated chlorinating agent (*7*), were present, its concentration should have increased via reaction 28 (*27*), and

$$HOCl + ClO_2^- \rightleftharpoons Cl_2O_2 + OH^- \qquad (28)$$

both the rate of formation of chlorophenols and their relative concentrations should have changed.

p-Benzoquinone was the only organic oxidation product—other than chlorinated phenols, which are oxidation products in a formal sense—detected from the reaction of phenol with ClO_2, but it was not always formed in 100% yield. Products of further oxidation such as maleic and oxalic acids may have formed, especially when ClO_2 was in excess (*4*, *28*), but were not sought. It is still unclear, however, how benzoquinone is reduced to hydroquinone in these solutions. Chlorite alone does not react with benzoquinone, but some uncharacterized or supposedly unreactive product may.

It is anticipated that Scheme I is equally applicable to other monohydric phenols (*4*, *8*, *28*, *29*) including para-substituted ones. The formation of either *p*-quinones or *o*-quinones can be expected. The relative rate of each step in Scheme I is likely to be different for each phenol and will vary with concentration and pH, so chlorinated benzoquinones could be formed (*4*, *8*, *28*) if reaction 24 were fast compared to reaction 20. Furthermore, if the phenoxyl radical **1b** were sufficiently stable and reaction 22 relatively slow, *p,p'*- and *o,p'*-hydroxybiphenyls could be formed as a result of dimerization of **1b** (*30*).

In Scheme II hydroquinone is oxidized to *p*-benzoquinone by ClO_2 in two successive one-electron transfers. No HOCl is formed, so no chlorination occurs, and 1 mol of ClO_2^- is formed/mol of ClO_2 consumed.

At pH 7, hydroquinone is oxidized 30 times more rapidly than phenol. The ratio of absolute reactivities of the anions is even greater (300:1) but is offset in part by the greater acidity of phenol. The difference in reactivity may be attributed to the stability of the resulting phenoxyl radical, suggesting **3** is more stable than **1b**. Phenols containing electron-withdrawing groups ortho or para to the phenoxy group are thus likely to be more reactive than phenol itself (*8*). Whether *o*- or *p*-quinones are formed depends on the relative stabilities of **1b** and **1c**.

The rapidity of the reaction of chlorine dioxide with phenol and the complete absence of chlorinated products (phenol is oxidized to *p*-benzoquinone within 2 s at pH 7) are advantageous for rapid, efficient removal of taste and odor at significantly lower doses (6 mg/L of ClO_2) than with the use of aqueous chlorine. A further advantage is that, although HOCl is a product of the ClO_2 treatment of phenols and probably also of guaiacol units of humic materials (*31*), trihalomethanes have not been found (*32*), and ClO_2-treated waters do not appear to be carcinogenic (*33*).

Against these advantages must be weighed the possible toxic effects of the products (*3*) which include ClO_2^-, ClO_3^-, and *p*-benzoquinone. Benzoquinone, for example, inhibited the growth of certain bacteria at 10 mg/L (*34*). Chlorite and ClO_3^- at 50 mg/L produced methemoglo-

binemia and hemolytic anemia in laboratory animals, and although 10 mg/L was without significant effect (*32*, *33*), it should be noted that in the human population certain groups highly susceptible to hemolytic anemia (*35*) may be affected by ClO_2^- levels as low as 5 mg/L (*33*). We have observed here a 2:1 stoichiometry of ClO_2/ClO_2^- in the reaction with phenol. If regeneration of ClO_2 from the reaction of HOCl with ClO_2^- (*8*, *27*) occurs to a significant extent under water-treatment conditions, then lower initial ClO_2 concentrations may be effective, giving rise to even lower ClO_2^- levels.

Literature Cited

(1) Lee, G. F.; Morris, J. C. *Int. J. Water Pollut.* **1962**, *6*, 419–431.
(2) Wallwork, J. F.; Bentley, M.; Symonds, D. C. *Water Treat. Exam.* **1969**, *18*, 203–219.
(3) Thielemann, H. *Gesund.-Ing.* **1971**, *92*, 295–299.
(4) Paluch, K. *Rocz. Chem.* **1964**, *38*, 35–42.
(5) Simmon, V. F.; Spanggord, R. J.; Eckford, S. L.; McClurg, V. "The Effects of Reactions of Chlorine Dioxide in Water"; Final Report, EPA, Contract No. 68-01-2894, 1979, Vol. 2.
(6) Paluch, K. *Rocz. Chem.* **1964**, *38*, 43–46.
(7) Grimley, E.; Gordon, G. *J. Inorg. Nucl. Chem.* **1973**, *35*, 2383–2392.
(8) Strumilla, G. B.; Rapson, W. H. *Trans. Tech. Sect. (Can. Pulp Pap. Assoc.)* **1977**, *3*, 119–126.
(9) Granstrom, M. L.; Lee, G. F. *J. Am. Water Works Assoc.* **1958**, *50*, 1453–1466.
(10) Kerhmann, F.; Tiesler, W. *J. Prakt. Chem.* **1889**, *40*, 480–497.
(11) Conant, J. B.; Fieser, L. F. *J. Am. Chem. Soc.* **1923**, *45*, 2194–2217.
(12) Robinson, R. A.; Stokes, R. H. "Electrolyte Solutions", 2nd ed.; Butterworths: London, 1968; p 545.
(13) Swinbourne, E. S. "Analysis of Kinetic Data"; Appleton-Century-Crofts: New York, 1971; pp 79–81.
(14) Frost, A. A.; Pearson, R. G. "Kinetics and Mechanism", 2nd ed.; Wiley: New York, 1961; pp 12–17.
(15) Publication Number NIH 78-180, Division of Cancer Biology and Diagnosis, National Cancer Institute: Washington, D.C., 1978.
(16) Haller, J. F.; Listek, S. S. *Anal. Chem.* **1948**, *20*, 639–642.
(17) Palin, A. T. *J. Inst. Water Eng.* **1967**, *21*, 537–546.
(18) Yamasaki, S.; Ohura, H.; Nakamari, I. *Bunseki Kagaku* **1973**, *22*, 843–849.
(19) Yankauskas, Y. Y.; Norkus, P. K. *J. Anal. Chem. USSR (Engl. Transl.)* **1973**, *28*, 2009–2011.
(20) Palin, A. T. *J. Inst. Water Eng.* **1974**, *28*, 139–154.
(21) Taymaz, K.; Williams, D. T. *Int. J. Environ. Anal. Chem.* **1979**, *6*, 289–296.
(22) Masschelein, W. J. "Chlorine Dioxide"; Ann Arbor Science: Ann Arbor, MI, 1979; pp 91–97.
(23) Tang, T.-F.; Gordon, G. *Anal. Chem.* **1980**, *52*, 1430–1433.
(24) Coutts, R. T.; Hargesheimer, E. E.; Pasutto, F. M. *J. Chromatogr.* **1979**, *179*, 291–299.
(25) Aylward, G. H.; Findlay, T. J. V. "SI Chemical Data Book"; Wiley: Sydney, Australia, 1971; p 48.
(26) Lindgren, B. O.; Nilsson, T. *Acta Chem. Scand.* **1973**, *27*, 888–890.
(27) Gordon, G.; Kieffer, R. G.; Rosenblatt, D. H. *Prog. Inorg. Chem.* **1972**, *15*, 201–286.
(28) Dence, C. W.; Gupta, M. K.; Sarkenen, K. V. *Tappi* **1962**, *45*, 29–38.
(29) Lindgren, B. O.; Ericsson, B. *Acta Chem. Scand.* **1969**, *23*, 3451–3460.
(30) Wisser, K.; Bub, F. P. *Mikrochim. Acta* **1980**, *2*, 145–157.
(31) Hedberg, T.; Josefsson, B.; Roos, C.; Lindgren, B.; Nemeth, T. "Oxidation Techniques in Drinking Water Treatment"; EPA 570/9-79-020: Washington, D.C., 1979; pp 481–509.
(32) Katz, J. "Ozone and Chlorine Dioxide Technology for Disinfection of Drinking Water"; Noyes Data Corp.: Park Ridge, NJ, 1980; pp 35–43.
(33) Bull, R. J. *J. Am. Water Works Assoc.* **1980**, *72*, 299–303.
(34) Trevors, J. T.; Basaraka, J. *Bull. Environ. Contam. Toxicol.* **1980**, *25*, 672–675.
(35) Moore, G. S.; Calabrese, E. J. *J. Environ. Pathol. Toxicol.* **1980**, *4*, 271–279.

Received for review September 4, 1981. Accepted March 17, 1982.

Environ. Sci. Technol. 1982, 16, 403–410

Structural Characterization of Aquatic Humic Material

Wenta Liao, Russell F. Christman,* J. Donald Johnson, and David S. Millington

Department of Environmental Sciences and Engineering, School of Public Health, University of North Carolina, Chapel Hill, North Carolina 27514

J. Ronald Hass

National Institute for Environmental Health Science, Research Triangle Park, North Carolina 27709

■ Gas chromatography/mass spectrometry analysis of methylated degradation products of aquatic humic and fulvic acids resulted in the identification of compounds that were classified as (a) benzenecarboxylic acid methyl esters (29 compounds), (b) furancarboxylic acid methyl esters (5 compounds), (c) aliphatic monobasic acid methyl esters (14 compounds), (d) aliphatic dibasic acid methyl esters (14 compounds), (e) aliphatic tribasic acid methyl esters (5 compounds), and (f) (carboxyphenyl)glyoxylic acid methyl esters (8 compounds). The degradation products of fulvic and humic fractions from two water sources were qualitatively similar to each other, but some distinct quantitative differences were found. Identified products amounted to about 25 wt % of starting material. The results indicate that aquatic humic substances contain both aromatic and aliphatic components. The aromatic rings contain mainly three to six alkyl substituents, and polynuclear aromatic and fused-ring structures may also be present. The data suggest that the principal aliphatic segments of the original natural product are composed of relatively short saturated chains (two to four methylene units), and branched structures are apparently present.

Introduction

Humic substances account for significant but variable proportions of the organic matter in soils and sediments and of the soluble organic matter in fresh and sea waters (*1–3*). Despite extensive research concerning the formation and environmental impact of water-borne organics, the chemical structures of aquatic humic substances are still not known with a desirable level of certainty.

These natural products are apparently acidic, hydrophilic, complex materials that range in molecular weight from a few hundred to many thousands (*4, 5*). Humic materials isolated from soils have been extensively studied (*6–11*), but it is presumptive to conclude that aquatic humic materials are similar except for chemical complexity. Degradation studies of soil humic acid have produced evidence of both aromatic (*10*) and aliphatic (*6*) constituents, but few degradation studies have been conducted on aquatic humics. Further, it is not known whether humic and fulvic materials isolated from different sources exhibit chemical similarities.

Therefore, our objectives have been to isolate natural aquatic humic substances (humic and fulvic acids) from two different and geographically separated natural water sources, subject them to controlled chemical degradation, and identify their specific reaction products.

Experimental Section

Aquatic Humics Preparation. Aquatic humic materials were extracted from two surface waters: Black Lake, located on the North Carolina coastal plain near Elizabethtown, NC, and Lake Drummond (Great Dismal Swamp), in southeastern Virginia. A modification of Thurman and Malcolm's XAD-8 method (*12*) was used to obtain humic materials from the lake waters and it has been described previously (*13*). The aquatic humic sample isolated from each source was further separated into humic acid and fulvic acid fractions by precipitating the former at pH 2.

Potassium Permanganate Oxidation. A 1-g humic sample was suspended in 50 mL of NaOH solution (pH 10). While maintaining the temperature of the mixture at 60–65 °C, 0.5–3.0 g of potassium permanganate previously dissolved in a small amount of water was added slowly to the stirred mixture over a period of 0.5–2 h. The reaction was allowed to proceed (1–6 h) until no excess permanganate was present. The mixture was then adjusted to pH 12 with concentrated NaOH solution and filtered through a glass fiber filter. The filtrate was acidified with concentrated HCl to pH 5 and freeze-dried. The residue was suspended in 50 mL of methylene chloride, methylated with diazomethane, and filtered.

Sodium Hydroxide Hydrolysis. A 1-g humic sample was dissolved in 50 mL of 0.5 N NaOH solution, and the mixture was refluxed under N_2 at atmospheric pressure for 1.5 h. After being acidified with concentrated HCl to pH 5, the sample was freeze-dried, suspended in 50 mL of methylene chloride, methylated, and filtered.

Gas Chromatography and Gas Chromatography/Mass Spectrometry. A Perkin-Elmer 900 gas chromatograph employing a flame ionization detector was used to provide preliminary sample analyses before the sample was submitted for GC/MS analyses and to obtain GC retention times. The columns used were 6 ft × $^1/_8$ in. o.d. (2.16 mm i.d.) stainless steel tubes packed with (a) 3% SP-2100 and (b) 3% OV-17 on 100–120 mesh Supelcoport (Supelco, Inc.). The injector and manifold were maintained at temperatures of 300 and 290 °C, respectively. The temperatures of columns were programmed at (a) 6 °C/min for SP-2100 and (b) 8 °C/min for OV-17 after a 4-min delay from an initial temperature set at 55 °C to a final temperature of 280 °C. The flow of nitrogen carrier gas was 30 mL/min.

GC/MS analyses were performed on a VG-Micromass 7070F double-focusing mass spectrometer interfaced to a Hewlett-Packard 5710A gas chromatograph and operated under the control of a VG-Micromass 2035 F/B data system. Separations were performed by splitless injection on HP fused-silica capillary columns (SP-2100, 30 m). Full details of the techniques employed have been described previously (*13*).

Degradation Product Identifications. The products of the humic degradation experiments were identified by GC/MS. Sample mixtures were first separated through a capillary gas chromatographic column, and the mass spectrum of each product was recorded. The sequence of events followed for compound identification was as follows: (a) acquire the electron impact (EI) mass spectrum; (b) acquire the chemical ionization (CI) mass spectrum; (c) acquire EI accurate mass data; (d) identify the molecular ion from CI data; (e) determine elemental composition of the molecular ion (if present) and the major daughter ions from EI accurate mass data; (f) interpret the EI data; (g)

0013-936X/82/0916-0403$01.25/0

Table I. Classification of Degradation Products for Yield Measurement

group	representative standard	component (compound)
A	1,2-benzenedicarboxylic acid dimethyl ester	benzenemonocarboxylic acid methyl esters (1-4), benzenedicarboxylic acid methyl esters (5-12), furandicarboxylic acid dimethyl ester (30), phthalonic acid dimethyl ester (68).
B	1,2,4,5-benzenetetracarboxylic acid tetramethyl ester	benzenetricarboxylic acid methyl esters (13-20), benzenetetracarboxylic acid methyl esters (21-26), benzenepentacarboxylic acid methyl esters (27-28), benzenehexacarboxylic acid hexamethyl ester (29), furantricarboxylic acid trimethyl esters (31-33), furantetracarboxylic acid tetramethyl ester (34), (dicarboxyphenyl)glyoxylic acid tetramethyl esters (69-70), (tricarboxyphenyl)glyoxylic acid tetramethyl esters (71-73), (tetracarboxyphenyl)glyoxylic acid pentamethyl esters (74-75)
C	octanoic acid methyl ester	C_4-C_{10} aliphatic monobasic acid methyl esters (35-41)
D	tridecanoic acid methyl ester	C_{11}-C_{16} aliphatic monobasic acid methyl esters (42-47)
E	malonic acid dimethyl ester	C_2-C_6 aliphatic dibasic acid dimethyl esters (48-55)
F	sebacic acid dimethyl ester	C_7-C_{13} aliphatic dibasic acid dimethyl esters (56-62)
G	tricarballylic acid trimethyl ester	C_5-C_8 aliphatic tribasic acid trimethyl esters (63-66), decanetrioic acid trimethyl ester (67)

Table II. Detector Response Factor and Analytical Recovery for a Standard Compound Mixture

std mixture compd	wt injected, ng	GC peak area,[a] counts	rel detector response factor	analyt procedure recovery,[b] %
1,2-benzenedicarboxylic acid dimethyl ester	304	914	1.22	94 ± 5
1,2,4,5-benzenetetracarboxylic acid tetramethyl ester	366	902	1.00	98 ± 4
octanoic acid methyl ester	170	623	1.48	41 ± 10
tridecanoic acid methyl ester	118	476	1.63	69 ± 5
malonic acid dimethyl ester	134	163	0.49	36 ± 11
sebacic acid dimethyl ester	114	313	1.11	81 ± 6
tricarballylic acid trimethyl ester	343	616	0.73	93 ± 8

[a] Average of three measurements. [b] Average of three determinations; averaged mean deviation was 7%.

deduce possible structural assignments; (h) confirm structural assignment by comparing GC retention indices (two columns) and the EI mass spectrum with a standard compound.

After the field of possible structural formulas was narrowed by using the accurate mass data, the general format for the examination of mass spectra involved standard interpretation procedures (*14–16*), consideration of sample history and relationship to similar compounds, and mass spectral library searches.

Kovats retention indices (*17*) were calculated for each compound from the retention times measured in two different packed GC columns (SP-2100 and OV-17) using the corresponding temperature programs described above.

Quantitative Analysis of Degradation Products. Semiquantitative estimates of the yield of each degradation product were made by measuring peak areas on the gas chromatogram by triangulation and by comparing these with the peak areas of reference compounds injected in known amounts.

The standard mixture consisted of the following seven compounds: 1,2-benzenedicarboxylic acid, 1,2,4,5-benzenetetracarboxylic acid, octanoic acid, tridecanoic acid, malonic acid, sebacic acid, and tricarballylic acid. These compounds were selected as representative of classes of compounds present in the humic degradation samples (Table I) and were completely separated by the GC procedure. The standard mixture containing each of the standard compounds in known concentrations was methylated in ether/methylene chloride, and the volume was adjusted to appropriate values before use. An average of three replicate injections of the standard methylated mixture yielded the relative flame ionization detector response factors given in Table II. A relative detector response value of 1.00 was then assigned to 1,2,4,5-benzenetetracarboxylic acid tetramethyl ester. A similar series of GC analyses on the standard solution with 100–2,000 ng of each of these seven compounds yielded

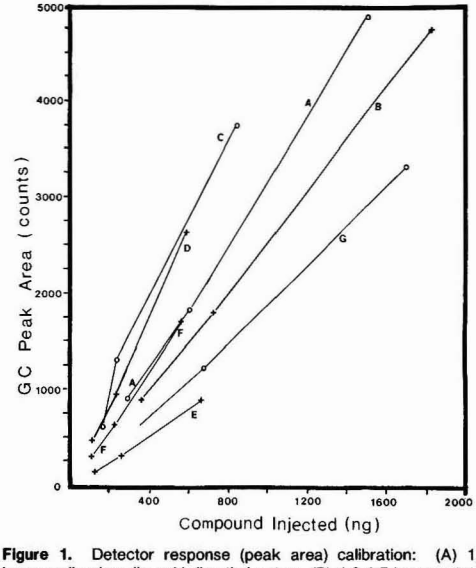

Figure 1. Detector response (peak area) calibration: (A) 1,2-benzenedicarboxylic acid dimethyl ester; (B) 1,2,4,5-benzenetetracarboxylic acid tetramethyl ester; (C) octanoic acid methyl ester; (D) tridecanoic acid methyl ester; (E) malonic acid dimethyl ester; (F) sebacic acid dimethyl ester; (G) tricarballylic acid trimethyl ester.

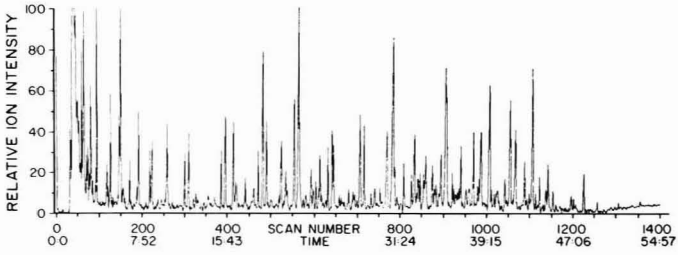

Figure 2. GC/MS total ion chromatogram of Black Lake humic acid/$KMnO_4$ degradation products.

calibration curves (Figure 1) for sample concentration determination. Detector response was assumed linear between consecutive concentration ranges.

For estimation of the product recoveries from sample cleanup procedures, another standard aqueous solution was prepared, which contained known quantities of the seven compounds mentioned above, and processed through the same procedures (filtration, freeze-drying, methylation, extraction) for analyzing the degradation samples. From Figure 1, compound recovery for each of the standards was then calculated from GC peak areas. The results of the percentage recoveries are shown in the last column of Table II. The mean deviation of three recovery experiments was found to be ±7%.

The amount (A_1) of each gas chromatographable degradation product injected into the GC column was obtained by reference to Figure 1 after peak area measurement. The amount (A_2) of each product in the total degraded sample after cleanup was then calculated with knowledge of the ratio of volume injected to total volume after cleanup. Finally, the amount (A_3) of each product produced by degradation of original sample (reported in Table III) was obtained by dividing A_2 by the appropriate recovery efficiency.

Results and Discussion

Chemical Degradation of Aquatic Humics. A typical total ion chromatogram from a permanganate oxidation of aquatic humic acid is shown in Figure 2. The chemical structures and yields of all products identified from all degradation experiments in this study are presented in Table III. These identifications account for 60–90% (among all experiments) of the total chromatographable products typified in Figure 2.

As an example of how the identifications were made, Figure 3 shows EI, CI, accurate mass measurement, and GC retention index data on one of the (carboxyphenyl)-glyoxylic acid methyl esters. The EI molecular ion peak of the methyl ester derivative is absent, but the M + 1 peak (m/z 223) is prominent in the CI spectrum. Cleavages at the CO–CO_2CH_3 and Ph–$COCO_2CH_3$ bonds give a base peak at M − 59 (m/z 163) and another prominent peak at M − 87 (m/z 135), respectively. The mass measurement obtained on the base peak is correct to within 15 ppm of its true value. Finally, the EI spectrum and GC retention indices were compared with those of the corresponding standard compound, and the agreement between the two sets of data confirmed the structural identification (similar data for each compound listed in Table III are available from the author).

Table IV summarizes the overall results, in which the identified products were classified according to structural similarity into six groups (benzenecarboxylic acid methyl esters, furancarboxylic acid methyl esters, (carboxyphenyl)glyoxylic acid methyl esters, aliphatic monobasic acid methyl esters, aliphatic dibasic acid methyl esters, and

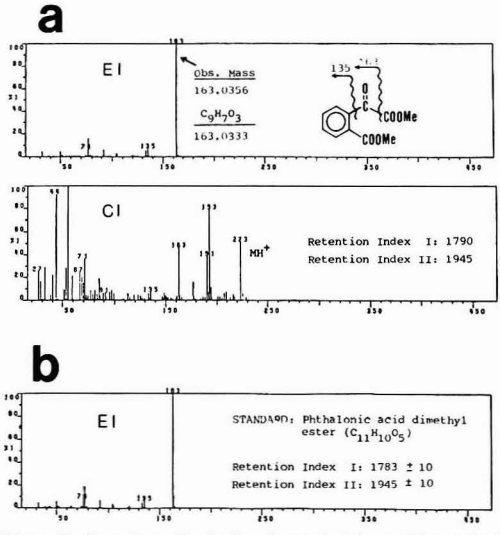

Figure 3. Example of structural assignment of degradation product: (a) EI, CI mass spectrum, accurate mass measurement, and GC retention index data of degradation product; (b) EI mass spectrum and GC retention index data of standard compound.

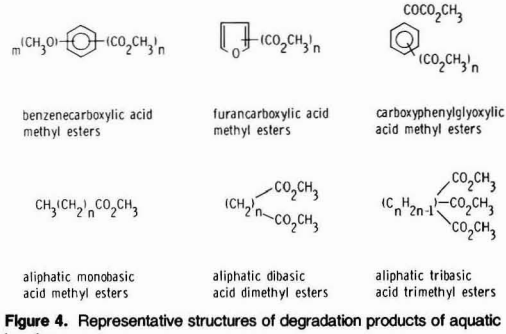

Figure 4. Representative structures of degradation products of aquatic humics.

aliphatic tribasic acid methyl esters) (see Figure 4). The yield of total permanganate oxidation products identified from Black Lake humic acid was 21.3%, from Black Lake fulvic acid 20.1%, from Lake Drummond humic acid 25.5%, and from Lake Drummond fulvic acid 24.5%. The total yields of base hydrolysis products from Black Lake humic acid, Black Lake fulvic acid, Lake Drummond humic acid, and Lake Drummond fulvic acid were 1.7%, 1.3%, 1.6%, and 1.3%, respectively.

The maximum yield of GC (or GC/MS) detectable degradation products was therefore about 25 wt % of

Table III. Identification and Yield of Degradation Products of Aquatic Humic Acids and Fulvic Acids from Black Lake and Lake Drummond. Yields (mg) Resulted from 1.0 g of Starting Humic Samples[a]

		Black Lake				Lake Drummond			
		$KMnO_4$ oxid		NaOH hydr		$KMnO_4$ oxid		NaOH hydr	
no.	compound	HA	FA	HA	FA	HA	FA	HA	FA
1	benzoic acid methyl ester[b]	0.54		0.11		0.75		0.21	
2	unidentified aromatic ester, mol wt 152[c]	0.14							
3	*p*-methoxybenzoic acid methyl ester[b]	0.68	0.66	0.19	0.11	2.90	0.67	0.29	0.08
4	unidentified heterocyclic methyl ester, $C_8H_{10}N_2O_4$[c]	0.37	0.40		0.03	1.31	1.03		0.06
5	1,2-benzenedicarboxylic acid dimethyl ester[b]	1.03	4.92	0.48	1.54	1.40	1.17	0.28	0.55
6	1,4-benzenedicarboxylic acid dimethyl ester[b]	0.27	0.11	0.02	0.08	0.98	0.76		
7	1,3-benzenedicarboxylic acid dimethyl ester[b]	0.58	2.08	0.10	0.10	1.82	0.48		
8	3,4-dimethoxybenzoic acid methyl ester[b]		0.66	0.17		2.15	0.69		
9	unidentified aromatic ester, possibly of a phenol dicarboxylic acid isomer, $C_{10}H_{10}O_5$[c]	3.56	3.79	0.07	0.47	6.74	6.89		1.61
10	unidentified isomer of **9**, $C_{10}H_{10}O_5$[c]	0.89	0.97		0.14		2.04		
11	methoxybenzenedicarboxylic acid dimethyl ester (isomer)[c]	0.43	0.51		0.10				
12	methoxybenzenedicarboxylic acid dimethyl ester (isomer)[c]	1.92	1.42		0.05	1.17	1.38	0.16	
13	1,2,3-benzenetricarboxylic acid trimethyl ester[b]	6.16	5.47	1.01	1.10	2.01	2.18	0.41	0.39
14	1,2,4-benzenetricarboxylic acid trimethyl ester[b]	13.42	12.53	0.09	0.06	8.44	8.75	0.05	
15	1,3,5-benzenetricarboxylic acid trimethyl ester[b]		0.08	0.24	0.57	0.08	0.48		0.09
16	methoxybenzenetricarboxylic acid trimethyl ester (isomer)[c]	9.14	4.47	0.42	0.05	4.30	4.96	0.19	0.11
17	methoxybenzenetricarboxylic acid trimethyl ester (isomer)[c]	2.11	3.41	0.44	0.03	1.38	1.70	0.17	0.23
18	methoxybenzenetricarboxylic acid trimethyl ester (isomer)[c]	1.55	0.95	0.72	0.09	3.23	3.35	0.63	0.13
19	methoxybenzenetricarboxylic acid trimethyl ester (isomer)[c]	6.76	4.83			1.31	2.78		0.04
20	unidentified aromatic methyl ester, $C_{12}H_{12}O_7$	2.21	4.88		0.05	1.33	1.45		
21	benzenetetracarboxylic acid tetramethyl ester (isomer)[c]	13.67	10.79	0.18	0.12	5.22	4.34	0.13	0.11
22	1,2,4,5-benzenetetracarboxylic acid tetramethyl ester[b]	10.90	11.21	0.02	0.16	5.38	5.70	0.06	0.11
23	benzenetetracarboxylic acid tetramethyl ester (isomer)[c]	14.66	14.99	0.19	0.21	8.82	9.30	0.09	0.20
24	methoxybenzenetetracarboxylic acid tetramethyl ester (isomer)[c]	2.92	1.48	0.16	0.03	5.57	5.74	0.10	
25	methoxybenzenetetracarboxylic acid tetramethyl ester (isomer)[c]	9.97	8.06	0.21	0.03	5.66	5.99	0.05	0.06
26	methoxybenzenetetracarboxylic acid tetramethyl ester (isomer)[c]	4.30	2.48			2.90	3.81		0.05
27	benzenepentacarboxylic acid pentamethyl ester[b]	16.17	19.63	0.36	0.11	29.36	18.28	0.14	0.15
28	methoxybenzenepentacarboxylic acid	5.56	1.61			2.87	4.18		
29	benzenehexacarboxylic acid hexamethyl ester[c]	12.28	5.38		0.33	3.63	6.04		0.06
30	furandicarboxylic acid dimethyl ester (isomer)[c]	0.33				0.08		0.36	
31	furantricarboxylic acid trimethyl ester (isomer)[c]	0.31	0.08	0.14	0.16	0.51	0.55		0.30
32	furantricarboxylic acid trimethyl ester (isomer)[c]	2.67	3.29			6.92	7.35		
33	unidentified, $C_{10}H_{10}O_8$, possibly hydroxyfurantricarboxylic acid trimethyl ester (isomer)[c]					1.12	3.47		0.08
34	furantetracarboxylic acid tetramethyl ester[c]	10.33	6.61			12.47	15.27		
35	butyric acid methyl ester[c]	0.08			0.88				
36	valeric acid methyl ester[c]	0.08					0.08		
37	hexanoic acid methyl ester[b]	1.03	0.66		0.97	9.24	5.96	0.34	1.64
38	heptanoic acid methyl ester[b]	0.35			0.51	1.52			0.35
39	octanoic acid methyl ester[b]	0.33	0.08		0.13	0.51			
40	nonanoic acid methyl ester[b]	0.33				0.47			
41	decanoic acid methyl ester[b]	0.08		0.03		0.14			
42	undecanoic acid methyl ester[b]	0.35				0.08			
43	lauric acid methyl ester[b]	0.48		0.09		2.22		0.02	
44	tridecanoic acid methyl ester[b]	0.39				0.58			
45	myristic acid methyl ester[b]	0.39							
46	pentadecanoic acid methyl ester[b]	0.08							
47	palmitic acid methyl ester[b]	0.10	0.08	0.60		0.08		0.18	
48	oxalic acid dimethyl ester[b]	13.77	18.59	3.44	1.21	27.96	29.08	4.89	1.51
49	malonic acid dimethyl ester[b]	16.27	17.26	2.17	1.39	29.38	30.32	1.44	1.67
50	succinic acid dimethyl ester[b]	14.83	17.39	2.43	1.37	29.45	30.48	4.09	1.68
51	glutaric acid dimethyl ester[b]	0.22	2.08	1.22	0.90	0.82	3.90	0.28	0.35
52	glutaric acid dimethyl ester (isomer)[c]	0.23	0.08		0.12	3.30	1.70	0.09	0.09

Table III (*Continued*)

		Black Lake				Lake Drummond			
		$KMnO_4$ oxid		NaOH hydr		$KMnO_4$ oxid		NaOH hydr	
no.	compound	HA	FA	HA	FA	HA	FA	HA	FA
53	adipic acid dimethyl ester[b]	0.25	0.62	0.18	0.06	0.68	0.76	0.07	0.06
54	adipic acid dimethyl ester (isomer)[c]		0.19		0.04	1.87	1.15		0.01
55	adipic acid dimethyl ester (isomer)[c]		0.08		0.04	0.82	0.10		
56	pimelic acid dimethyl ester[b]	0.25	0.19	0.09	0.04	0.08	0.09	0.03	0.02
57	suberic acid dimethyl ester[b]	0.29				2.88	0.18	0.06	
58	azelaic acid dimethyl ester[b]	0.47				0.26	0.08	0.35	0.27
59	sebacic acid dimethyl ester[b]	0.37				0.30			
60	undecanedioic acid dimethyl ester[b]	0.17				0.26	0.23		
61	dodecanedioic acid dimethyl ester[b]	0.37		0.08					
62	tridecanedioic acid dimethyl ester[b]	0.08							
63	pentanetrioic acid trimethyl ester (isomer)[c]		0.53	0.11	0.16		1.81	0.22	0.29
64	tricarballylic acid trimethyl ester[b]	0.43	0.51	0.18	0.20	4.94	2.71	0.23	0.22
65	heptanetrioic acid trimethyl ester (isomer)[c]	0.10	0.15		0.03				
66	octanetrioic acid trimethyl ester (isomer)[c]	0.09	0.28						
67	decanetrioic acid trimethyl ester (isomer)[c]	0.08							
68	phthalonic acid dimethyl ester[b]	2.40	3.29			3.15	2.41		
69	(dicarboxyphenyl)glyoxylic acid trimethyl ester (isomer)[c]	0.82				0.25			
70	(dicarboxyphenyl)glyoxylic acid trimethyl ester (isomer)[c]	0.16	0.25						
71	(tricarboxyphenyl)glyoxylic acid tetramethyl ester (isomer)[c]	0.11							
72	(tricarboxyphenyl)glyoxylic acid tetramethyl ester (isomer)[c]	0.29	0.71			0.47	1.61		
73	(tricarboxyphenyl)glyoxylic acid tetramethyl ester (isomer)[c]	0.09	0.14			0.26	0.77		
74	(tetracarboxyphenyl)glyoxylic acid pentamethyl ester (isomer)[c]	0.23				0.21			
75	(tetracarboxyphenyl)glyoxylic acid pentamethyl	0.39	0.31			1.43	0.82		
76	unidentified, $C_{11}H_{13}NO_6$, possibly dimethoxypyridinedicarboxylic acid dimethyl ester (isomer)[c]	0.08							

[a] Abbreviations: FA, fulvic acid; HA, humic acid. [b] Identified by EI and CI MS, exact measurement, by matching standard MS and GC retention indices. [c] Identified by EI and CI MS, exact mass measurement, but standard compound not available. [d] Identified by EI MS, exact mass measurement, but standard compound not available.

Table IV. Summary Results of $KMnO_4$ Oxidation and NaOH Hydrolysis of Aquatic Humic Acids and Fulvic Acids from Black Lake and Lake Drummond. Yields (mg) Resulted from 1.0 g of Starting Humic Samples[a]

	Black Lake				Lake Drummond			
	$KMnO_4$ oxid		NaOH hydr		$KMnO_4$ oxid		NaOH hydr	
components	HA	FA	HA	FA	HA	FA	HA	FA
benzenecarboxylic acid methyl esters	142.71	127.77	5.36	5.56	110.71	104.14	2.96	4.03
furancarboxylic acid methyl esters	13.61	9.98	0.14	0.16	21.10	26.64	0.36	0.38
(carboxyphenyl)glyoxylic acid methyl esters	4.49	4.70	0.00	0.00	5.77	5.61	0.00	0.00
aliphatic monobasic acid methyl esters	4.07	0.82	0.72	2.49	14.84	6.14	0.54	1.99
aliphatic dibasic acid methyl esters	47.57	56.48	10.62	4.57	98.06	98.07	11.30	5.66
aliphatic tribasic acid methyl esters	0.62	1.47	0.29	0.39	4.94	4.52	0.45	0.51
sum	213.07	201.22	17.13	13.17	255.42	245.12	15.61	12.57
identified percentage of total GC peak area	88%	91%	71%	73%	86%	88%	63%	69%

[a] Abbreviations: FA, fulvic acid; HA, humic acid.

starting material. The fact that approximately 60–90% of the $KMnO_4$ products were identified means that over two-thirds of the total chromatographable products had structures assigned to them. Most of the extracted and methylated reaction product was chromatographable, as judged from direct insertion probe analysis of the total product mixtures, which showed no significant ions above m/z 337, corresponding to the base peak of benzenehexacarboxylic acid methyl ester. Some organic materials were lost in the oxidative reaction by conversion to carbon dioxide or other very volatile products. By comparison of the total organic carbon concentration of the aqueous humic solution before and after permanganate oxidation, the loss was estimated at about 20–25% of the original TOC. If these volatile molecules are assumed to be carbon dioxide, then the overall accountability of degradation products is 35% of the original TOC prior to degradation, assuming that the identified products average 50% C.

Table IV shows that the dominant products produced from permanganate oxidation are benzenecarboxylic acids, followed by aliphatic dibasic acids, furancarboxylic acids, aliphatic monobasic acids, and (carboxyphenyl)glyoxylic acids. Aliphatic tribasic acids are present in relatively low yield.

Except for Black Lake fulvic acid, aliphatic dibasic acids were found to be the major base hydrolysis products for all the humic acid and fulvic acid samples. All of the base hydrolysis products identified were also present in permanganate oxidation products, but (carboxyphenyl)glyoxylic acids were not found in the hydrolyzed samples.

Comparison of $KMnO_4$ Oxidation Products of Aquatic Humic and Fulvic Acid Samples. From Table III it is evident that oxidation of both humic acids and fulvic acids yielded mostly similar product distributions. Both produced benzenecarboxylic acids as the dominant products, in which the benzene ring with three carboxyl groups (compounds **13–20**), four carboxyl groups (compounds **21–26**), five carboxyl groups (compounds **27–28**), or six carboxyl groups (compound **29**) represents the major substitution patterns. In addition, humic acids and fulvic acids also produced high relative yields of oxalic acid, malonic acid, and succinic acid.

A significant difference was found among the aliphatic acid products. Most of the monobasic acids (C_7–C_{15}, compounds **38–46**) and the long-chain dibasic acids (C_8–C_{15}, compounds **57–62**, data available on Black Lake samples only) that were identified among the humic acid oxidation products were not detected among those of fulvic acid samples. This difference may indicate that the long-chain acids were associated with the less soluble, hydrophobic humic acid macromolecules and were released as the humic acid macromolecules were degraded.

The permanganate oxidation, under the conditions conducted in this study, is believed to serve the function of oxidizing the alkyl side chains of arenes (aliphatic–aromatic compounds) and results in the formation of aromatic acids and saturated aliphatic acids. The permanganate oxidation data indicate that the principal number of alkyl constituents on the aromatic rings in the humic molecule is in the range of three to six to account for the predominance of the benzenepolycarboxylic acid derivatives. The principal length of saturated alkyl side chain must be relatively short to account for the predominance of C_2–C_4 aliphatic dibasic acids.

It is attractive to assume that most of the carboxyl groups observed among these products constitute sites of carbon to carbon linkages in the undegraded macromolecule. This is supported by the data in Tables III and IV, which show that the total yield of acids produced by base hydrolysis is much lower. Some of the acid groups must be bound originally in ester linkages probably with other aromatic moieties (to account for base hydrolysis yields), but most of the alkyl constituents of aromatic rings must be carbon chains, which resist sodium hydroxide hydrolysis. In addition, some of the carboxylic acids must be present as free groups in the undegraded macromolecule to account for the acidity of aquatic humics.

Comparison of NaOH Hydrolysis Products of Aquatic Humic Samples from Two Different Sources. Qualitatively, the degradation products of aquatic humic samples obtained from two sources are quite similar as seen from Table III. Inspection of the relative abundance data in Table IV reveals that the most striking effect of source difference on product distribution is that Lake Drummond samples produced higher total yields, which included significantly greater amounts of aliphatic acid products and slightly lower amounts of aromatic acid derivatives (benzenecarboxylic acids, furancarboxylic acids, and (carboxyphenyl)glyoxylic acids) from permanganate oxidation. The differences found between humic and fulvic fractions isolated from each source were smaller than the differences found between the two fractions isolated from each source.

In general, the predominant products found in Black Lake samples are also the predominant products in Lake Drummond samples. Based on the results of this study, it is believed that aquatic humic materials from different sources have a close relationship in their molecular structures, yet quantitatively there are variations in the structural composition of humics from different sources. Whether these variations are related to seasonal changes, various stages of the humification process, or vegetative conditions indigenous to the source is not known.

Chemical Composition of Aquatic Humics. 1. Aromatic Components. As discussed earlier, benzenecarboxylic acids are the most predominant permanganate oxidation products, and some of them are probably derived from oxidative cleavage of carbon side chains of alkyl-substituted aromatic rings. Some of these acids may as well be derived from polycyclic aromatic structures. Methoxybenzenecarboxylic acid methyl esters were also found in significant quantities among the aromatic products, but whether the methoxyl groups were originally present in the undegraded humic molecule in a free hydroxyl form or in a methylated form is not known. Nearly all the possible benzenecarboxylic acid isomers were identified. Tri-, tetra-, penta-, and hexacarboxylic acids are the major ring substitution patterns. This indicates that the aromatic rings of a humic molecule are highly substituted by functional groups other than hydrogen.

2. Polycyclic Aromatic Components. The finding of the (carboxyphenyl)glyoxylic acid derivatives (compounds **68–75**) in the permanganate oxidation products provides evidence that the aquatic humic macromolecule contains polycyclic aromatic structures. (Carboxyphenyl)glyoxylic acids are well-known as aqueous permanganate oxidation products of polynuclear aromatic compounds (*18–20*). Eight different (carboxyphenyl)glyoxylic acid isomers were identified in the methylated aquatic humic oxidation products (but not in base hydrolysis products). Except for phthalonic acid dimethyl ester, the exact structures of these isomers have not been determined.

Since these compounds have not previously been reported as degradation products of soil humics, it is interesting to note that a sample of commercial terrestrial humic acid (Aldrich Chemical Co.), when oxidized with $KMnO_4$ (*25*), produced a similar distribution of (carboxyphenyl)glyoxylic acids. They appear therefore to be general humic degradation products, missed by previous studies presumably through use of low-resolution GC columns and by the similarity of their EI mass spectra to the corresponding benzenecarboxylic acid esters.

The exact polycyclic aromatic structure of aquatic humics cannot be elucidated based on the present data. Further study is needed to establish the relationship between the polycyclic patterns and all possible reaction products. Nevertheless, the results show that the polynuclear aromatic components may be present in the humic molecule.

3. Fused-Ring Components. Five derivatives of furancarboxylic acid (compounds **30–34**) were identified. Tri- and tetracarboxylic acids are among the most predominant products. This is the first experimental evidence of the existence of these structures in aquatic humic materials. The relative-yield data (Tables III and IV) suggest that they are significant structural components. Various substituted furan derivatives are known in nature (*21*) and have been reported as degradation products of soil organic matter (*10*). It is reasonable to assume that the permanganate oxidation produced the furancarboxylic acids from polycyclic fused-ring structures or from single-ring structures with aliphatic side chains.

In addition to furancarboxylic acids another heteroaromatic product was tentatively identified (trace amounts) as dimethoxypyridinedicarboxylic acid dimethyl

Table V. Summary of Degradation Products and Their Possible Sources in Humic Macromolecules.

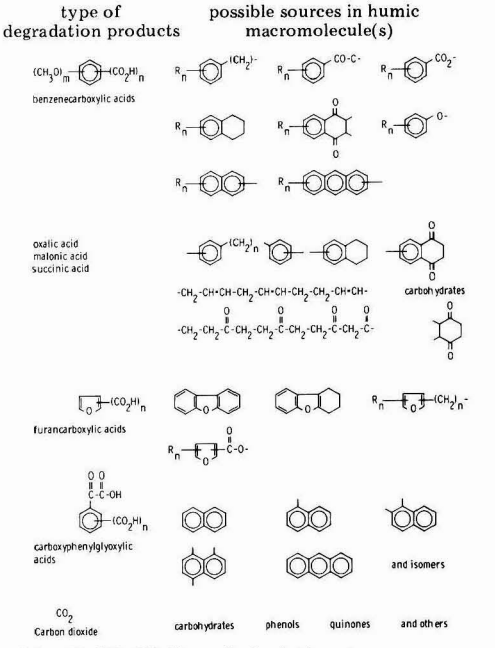

[a] R = H, OH, CO_2H, or alkyl substituents.

ester (compound **76**). Apart from compound **4**, which may be a diazomethane artifact, it was the only nitrogen-containing compound found.

4. Aliphatic Components. One group of the most abundant products found in this study is the methylated derivatives of three aliphatic dibasic acids: oxalic acid, malonic acid, and succinic acid (compounds **48–50**). The identification of these three acids demonstrates that aliphatic components are significant components of aquatic humic substances. An unknown portion of the oxalic acid may have resulted from permanganate oxidation of activated aromatic rings in the undegraded molecule, but it is likely that these short chain dibasic acids are derived from the main aliphatic constituents of the humic molecule. Permanganate oxidation of the humic molecular model proposed by Christman and Ghassemi (*22*) would be expected to produce similar short-chain dibasic acids from the intermonomeric bridges. This model is closely related to lignin, where phenylpropane derivatives are the basic building blocks of the macromolecule (*23*), but it does not explain the formation of the benzenepolycarboxylic acid products.

Short-chain dibasic acids could also be produced from polycyclic aliphatic–aromatic compounds or similar kinds of structures. The aliphatic tribasic acids, especially the abundant tricarballylic acid (compound **64**), are worthy of notice. It is attractive to assume that these tribasic acids were derived from branched intermonomeric linkages or brached aliphatic structures. Lack of information regarding the interaromatic carbon linkages in humic macromolecules is unfortunately a weakness of an oxidative experimental approach.

5. Summary. Other workers (Christman and Ghassemi (*22*); Wershaw, Pinckney, and Booker (*24*)) have hypothesized macromolecular structures for aquatic humic material based upon substantially less chemical evidence than obtained in the study reported here. In our opinion little purpose would be served by hypothesizing an additional structure based upon the present findings. It is possible to indicate those types of macromolecular carbon to carbon linkages that may account for the degradation products observed. These are summarized in Table V. With the exception of CO_2 the degradation products listed in Table V are listed in order of decreasing relative abundance.

The degradation products of fulvic and humic fractions from two water sources were qualitatively similar to each other but some quantitative differences were found. The difference found between fulvic and humic fractions isolated from each source are smaller than the differences between the fractions isolated from the different sources.

The general molecular structure of aquatic humics, inferred from the nature of the degradation products, may consist of (a) single-ring aromatics with mainly three to six substituents as alkyl side chain, carboxylic acid, ketone, or hydroxyl groups, (b) short aliphatic carbon chains, and (c) polycyclic ring structures including polynuclear aromatics, polycyclic aromatic–aliphatics, and fused rings involving furan and possibly pyridine. Although the structural relationships between these fragments could not be established, it is believed that these fragments are associated with humic macromolecules through carbon–carbon linkages.

It should be noted that these structural features are presented in rather generalized forms and are not exclusive. For example, the aromatic segments may include a variety of isomers in different substitution patterns, or the polycyclic structures may not be limited to two- or three-ring systems. The overall-yield data suggest that the structural information derived from this study accounts for a significant part of the humic macromolecule, and the specific substitution patterns observed may be useful in the design of future studies.

Acknowledgments

We express our appreciation to Alan A. Stevens, Daniel L. Norwood, William Glaze, and Werner Strumm for valuable discussions of the experimental approach and to Theodore Walters for preparation of the humic and fulvic acid samples.

Literature Cited

(1) Garrels, R. M.; MacKenzie, F. T.; Hunt, C. "Chemical Cycles and the Global Environment"; William Kautmann, Inc.: Los Altos, CA, 1973; Chapter 6.
(2) Steelink, C. *J. Chem. Educ.* **1977**, *54*, 599–603.
(3) Black, A. P.; Christman, R. F. *J. Am. Water Works Assoc.* **1963**, *55*, 897–912.
(4) Ghassemi, M.; Christman, R. F. *Limnol. Oceanogr.* **1968**, *13*, 583–597.
(5) Hall, K. J.; Lee, G. F. *Water Res.* **1974**, *8*, 239–251.
(6) Barron, P. F. *Nature (London)* **1981**, *289*, 275–276.
(7) Felbeck, G. T., Jr. *Soil Sci.* **1971**, *3*, 42–48.
(8) Kononova, M. M. "Soil Organic Matter", 2nd ed.; Pergamon: New York, 1976; pp 73–75.
(9) Ogner, G. *Acta Chem. Scand.* **1973**, *27*, 1601–1612.
(10) Schnitzer, M.; Khan, S. U. "Soil Organic Matter"; Elsevier: New York, 1978.
(11) Steelink, C. *J. Chem. Educ.* **1963**, *40*, 379.
(12) Thurman, E. M.; Malcolm, R. L. *Environ. Sci. Technol.* **1981**, *15*, 463–466.
(13) Christman, R. F.; Liao, W. T.; Millington, D. S.; Johnson, J. D. In "Advances in the Identification and Analysis of Organic Pollutants in Water"; Keith, L. H., Ed.; Ann Arbor Science: Ann Arbor, MI, 1981; Vol. 2, Chapter 49.
(14) McLafferty, F. W. "Interpretation of Mass Spectra", 3rd ed.; W. A. Benjamin: New York, 1980; p 209.

(15) Shrader, S. R. "Introductory Mass Spectrometry"; Allyn and Bacon: Boston, 1971.
(16) Silverstein, R. M.; Bassler, G. C. "Spectrometric Identification of Organic Compounds"; Wiley: New York, 1974.
(17) Kovats, E. *Adv. Chromatogr.* **1965**, *1*, 229.
(18) Fieser, M.; Fieser, L. "Reagents for Organic Synthesis"; Wiley Interscience: New York, 1967; Vol. 1.
(19) Graebe, C.; Trumpy, F. *Chem. Ber.* **1898**, *31*, 369–375.
(20) Elderfield, R. C.; Wythe, S. L. *J. Org. Chem.* **1954**, *19*, 683–692.
(21) Acheson, R. M. "An Introduction to the Chemistry of Heterocyclic Compounds"; Interscience: New York, 1967; p 93.
(22) Christman, R. F.; Ghassemi, M. *J. Am. Water Works Assoc.* **1966**, *58*, 723–741.
(23) Sarkanen, K. V. In "The Chemistry of Wood"; Browning, B. L., Ed.; Interscience: New York, 1963; Chapter 6.
(24) Wershaw, R. L.; Pinckney, D. J.; Booker, S. E. *J. Res. U.S. Geol. Surv.* **1977**, *5*, 565–569.
(25) Stevens, A. A.; Millington, D. S., unpublished data.

Received September 8, 1981. Accepted March 15, 1982. This research was supported in part by EPA Research Grant No. R804430 from the Municipal Environmental Research Laboratory, Cincinnati, OH, Alan A. Stevens, Project Officer.

Applicability of Passive Dosimeters for Ambient Air Monitoring of Toxic Organic Compounds

Robert W. Coutant*

Battelle Columbus Laboratories, Columbus, Ohio 43201

Donald R. Scott

Environmental Monitoring Systems Laboratory, U.S. Environmental Protection Agency, Research Triangle Park, North Carolina 27711

■ Three commercially available (3M, DuPont, Abcor) diffusion-based personal monitors were evaluated for possible use for toxic organics in ambient air. Test compounds were benzene, chlorobenzene, and six chlorinated hydrocarbons. An in-series EC-PID GC method was used to quantitate pollutants collected on the charcoal collectors. Tests of detection limits, blank levels, and desorption efficiencies were performed. All three badges were contaminated with several chlorinated hydrocarbons at levels that could impair their use for ambient sampling. Comparison of calculated lower useful limits for the DuPont device with ambient concentrations showed that only benzene, carbon tetrachloride, 1,1,1-trichloroethane, and trichloroethylene could be detected at representative ambient levels in a 24-h sampling time. Reasonable improvements in blank levels and detection limits would allow the detection of all other tested compounds except 1,2-dichloroethane and chlorobenzene.

Introduction

Over the past decade, pollutant sampling methodology has undergone a natural development from generalized stationary-source monitoring procedures to specialized techniques for mobile and stationary monitoring of large areas or regions to the use of portable monitoring equipment. While all phases of pollution monitoring remain important, there has recently been increased emphasis on the need for direct determination of personal exposure to toxic pollutants in different environments. Portable, pump-based (active) systems have been used for monitoring toxic organic compounds in industrial environments for some time. More recently, several more convenient, passive (no pump) personal monitors have become available commercially and have been evaluated for specialized applications in the workplace (*1–7*). These passive devices depend upon well-characterized diffusion or permeation-limited sampling of the air rather than pump sampling. The pollutants are collected on a suitable sorbent, normally charcoal. Because of their small size (generally less than 30 cm^3), low weight, low cost, and the absence of pumps, batteries, and tubing, they should be ideally suited for considerations as personal monitors for toxic organic compounds in ambient air.

Although these devices have been tested to a limited extent for monitoring of relatively high organic pollutant concentrations (ppm/V) in the workplace, there has been no evaluation of their applicability to sampling at much lower concentrations (ppt–ppb/V) in ambient air. The purpose of the current work was to examine this applicability with respect to a selected group of toxic hydrocarbons and chlorinated hydrocarbons. The compounds chosen were benzene, chlorobenzene, carbon tetrachloride, chloroform, 1,2-dichloroethane, 1,1,1-trichloroethane, trichloroethylene, and tetrachloroethylene. The devices investigated were manufactured by DuPont (Pro Tek organic vapor air monitoring badge), 3M (3500 organic vapor monitor), and Abcor (Gasbadge organic vapor dosimeter). The REAL personal monitor (*7*), which was designed for vinyl chloride, was not considered since each individual device must be calibrated for each compound. Critical laboratory tests were applied to the devices to determine potential analytical problems in ambient air applications, e.g., detection limitations, low desorption efficiencies, and high and variable blanks. Significant differences in blank levels were found among the various personal monitors. A gas chromatographic technique using an in-series combination of electron-capture and photoionization detectors was developed to determine the test compounds at the low concentrations required.

Experimental Section

Analytical Methods. The target compounds were desorbed from the charcoal strips and quantitated by gas chromatography with an in-series electron-capture (ECD) photoionization detection (PID) system. A Varian 3700 GC equipped with Hewlett-Packard 3380 integrators was used. The analytical column was a commerical 8 ft × $^1/_8$ in. o.d. stainless steel column packed with Carbopack-B and 1% SP-1000. Nitrogen at a flow rate of 30 mL/min was used as the carrier gas. A temperature program of 10

 0013-936X/82/0916-0410$01.25/0

Table I. GC Detection Limits and Relative Sensitivities[a]

compound	electron capture RS[b]	electron capture DL,[c] ng/badge	photoionization[b] RS[b]	photoionization DL,[c] ng/badge
chloroform	1.0	5.0	0.0	
1,2-dichloroethane	0.030	170	0.0	
1,1,1-trichloroethane	3.1	1.6	0.05	200
carbon tetrachloride	14	0.36	0.0	
trichloroethylene	1.4	3.6	0.34	29
benzene	0.0		1.0	10
tetrachloroethylene	7.0	0.71	0.30	33
chlorobenzene	0.0		0.55	18

[a] Mass basis; measured under conditions for detection of the complete list of chemicals, not optimized for particular compounds. [b] Sensitivity relative to chloroform (ECD) or benzene (PID). [c] Approximate detection limits in ng/badge with 0.1% of sample extract for analysis. Division by 1000 gives absolute mass limits. [d] 10.2-eV lamp.

min at 100 °C followed by a ramp of 4 °C/min to 180 °C was used. The photoionization detector was a HNU 10.2-eV system.

Desorption. Carbon disulfide, which is usually used as the desorbing solvent, cannot be used in pure form with electron-capture detection because of the excessive response of the detector and appreciable solvent tailing on most columns. Also, even the best grade of carbon disulfide that was examined (Baker Instra-Analyzed reagent) contains appreciable impurities that are evident by both ECD and PID. Methanol yields minimal response with both ECD and PID, and there are several commercially available grades that are "clean" enough for use. The current work was performed with a mixture of 5% (V/V) carbon disulfide in Baker Resi-Analyzed methanol. Charcoal collectors were taken from the badges, placed in a glass vial with 1 mL (DuPont) or 2 mL (Abcor and 3M) of the desorbing solution, and allowed to sit overnight, and then 1 μL of the resulting solution was used for GC analysis. Solvent blank corrections for this solvent mixture were found to be 2 pg/μL for 1,1,1-trichloroethane, 5 pg/μL for carbon tetrachloride, and 10 pg/μL for tetrachloroethylene.

Desorption Efficiencies. Preliminary experiments with chloroform were performed with a 1.9-L stainless steel canister coupled to the GC via a gas-sampling valve with graphite seats. This canister was flushed with nitrogen and then loaded to the desired concentration level. A stainless steel vial containing a test charcoal strip was then attached to the canister and allowed to adsorb the test compound for periods of time ranging from a few hours to a day. The change in concentration and the known volume of the canister were used to calculate the amount adsorbed by the charcoal strip. Comparison of this value with the results of analysis of the strip yielded apparent desorption efficiencies.

Final data were obtained by the phase-equilibrium method (*8*). Charcoal collectors were placed in sealed glass vials with 1 mL of the desorbing solvent containing a known loading of the test compounds and were allowed to equilibrate overnight. A similar vial containing 1 mL of the same solution was used as a reference. Comparison of the analysis data for the badge solution with those from the reference solution then gave the desorption efficiencies at each concentration level tested.

Results and Discussion

Detection Limits. Conventional analysis of the charcoal sorbents used in passive devices in industrial environments involves the use of a polar solvent, usually carbon disulfide, for desorption of the pollutants, followed by gas chromatographic (GC) analysis of an aliquot (ca. 0.1%) using flame ionization detection (FID). With use of these devices at typical ambient concentractions, however, the absolute amounts of pollutants collected over an 8–24 h period would be expected to be of the order of tens of nanograms. The amount of material presented to the detector would thus be of the order of tens of picograms, which is much less than that detectable by a FID detector. Therefore, in the current work a series combination of electron-capture (ECD) and photoionization (PID) (10.2-eV source) detectors was used to obtain the required detection limits.

The detection limits and relative sensitivities of the ECD–PID detector system for the various compounds evaluated are shown in Table I. No attempt was made to optimize for particular compounds. The detection limits are given in units of ng/badge and are defined as the concentration that corresponds to a signal 2 standard deviations above the apparent zero level. To obtain absolute mass detection limits the values in ng/badge should be divided by 1000. The ECD responses for benzene and chlorobenzene are effectively zero, and the PID is required for these compounds. For those compounds that responded to both detectors, the ECD gave better detection limits. Even with ECD, however, the response for 1,2-dichloroethane was very low in comparison to responses for other chlorinated hydrocarbons. These detection limits are representative of the particular methodology used, and modification of this methodology by the use of larger aliquots or the use of capillary column chromatography could improve the detection limits.

Badge Blanks. Contamination of unused charcoal collectors was determined for each of the three types of badges. Three to seven badges were selected at random from supplies purchased from the manufacturers and were analyzed in the same manner as exposed badges. The results expressed as range and median values are shown

Table II. Badge Blanks[a] (ng/badge)

compound	Abcor[b] median	Abcor[b] range	DuPont[c] median	DuPont[c] range	3M[d] median	3M[d] range
chloroform	<5.0	<5.0	<5.0	<5.0-108	15	<5.0-16.2
1,2-dichloroethane	<170	<170	<170	<170	<170	<170
1,1,1-trichloroethane	440	400-670	22	<1.6-68	240	180-290
carbon tetrachloride	230	220-170	6.0	<0.36-14	5.3	4.8-7.4
trichloroethylene	120	110-430	4.0	<3.6-45	230	190-310
tetrachloroethylene	44	20-50	24	<0.7-41	15	9.6-140
benzene	<10	<10	<10	<10	<10	<10
chlorobenzene	<18	<18	<18	<18	<18	<18

[a] Uncorrected for desorption efficiencies. Expected analytical error ±5%. [b] Three badges were extracted and analyzed. [c] Seven badges were extracted and analyzed. [d] Four badges were extracted and analyzed.

Table III. Desorption Efficiencies[a]

compound	N^b	median,[c] %	range, %
chloroform	7	79	71-100
1,2-dichloroethane	3	52	51-78
1,1,1-trichloroethane	5	81	69-89
carbon tetrachloride	7	81	55-94
trichloroethylene	7	60	50-71
tetrachloroethylene	7	32	30-52
benzene	6	47	32-58
chlorobenzene	4	16	14-29

[a] Compounds were added at seven different levels in the 0.05–120 μg/badge range. [b] Number of individual badges spiked. [c] Precision is ±10%.

in Table II, in units of ng/badge. These data are uncorrected for desorption efficiencies. None of the badges had sufficiently low blank levels to be useful for monitoring all of the target compounds. The blank levels for most compounds were so variable for all badges that use of an average or median value in correcting apparent collection values would be of dubious value. All three badges showed evidence of chlorinated hydrocarbons, which are common solvents, but little benzene or chlorobenzene. This suggests a specific primary source for these blanks rather than a generalized contamination. It is quite possible that the source of this contamination can be identified and eliminated.

Desorption Efficiencies. Only the DuPont collectors were used in the determination of desorption efficiencies. Initial results with chloroform obtained with the canister technique yielded consistent desorption efficiences (DE's) for chloroform of 70 ± 2% at loadings of from 100 to several thousand ng/badge. However, attempts to apply this method at lower loadings expected in ambient air sampling were unsuccessful due to erratic results, probably due to adsorption on the metal surfaces.

Results from the phase-equilibrium method at seven different concentrations of 50–120 μg per badge for three to seven different badges are presented in Table III. The median values for chloroform, carbon tetrachloride, and 1,1,1-trichloroethane were 80 ± 1%. However, the other compounds had median DE's of 60% (trichloroethylene) to 16% (chlorobenzene). All of the DE's were lower than those reported at workplace concentrations, i.e., 90–100%. Furthermore, the DE's for any given compound were much more variable than expected from the analytical errors of ± 10%. This variation is undoubtedly due to the variablility in the contamination level of the unused charcoal collectors as shown in Table II. No trend of DE's with concentration level was found in this study. The use of other desorption solvents may yield higher DE's. However, the use of carbon disulfide in the mixture must be limited if an EC detector is employed.

Applicability of Tested Devices to Ambient Monitoring. The significance of the analytical detection limits and blank levels in determining the potential utility of these badges for ambient air sampling must be considered relative to the limitations of air sampling that are achieved and the expected ambient levels of the particular compounds. Each of the devices considered is diffusion-limited in its sampling rate, and the mass (m in grams) of each substance collected over a given time period is given by

$$m = D(A/L)Ct \tag{1}$$

where D (cm^2/min) is the diffusion coefficient for the substance in air, A/L (cm) is the ratio of the total sampling area to the length of the diffusion channels, C is the concentration (g/cm^3) of species sampled in the air, and t is the sampling time (min). The values of A/L for the different badges differ according to the physical design of the system, but sampling rates of the order of tens of cm^3/min are normally achieved. Tabulations of sampling rates (DA/L) for individual compounds are normally available from the manufacturers. The concentration of a given species sampled in ppb/V is obtained by rearranging eq 1 and calculating the volume corresponding to the mass via the ideal gas law:

$$C\ (\text{ppb/V}) = \frac{10^9 mRT}{Mt(DA/L)P} \tag{2}$$

where M is the molecular weight of the compound, R (cm^3 atm deg^{-1} mol^{-1}) is the gas constant, P (atm) is the atmospheric pressure, and T is the temperature (K).

Because of the variability of the blanks and the fact that analyses performed near the detection limits are inaccurate, the lower useful limit for the devices was defined as 10 times the median blank level or 10 times the detection limit, whichever was greater. After correction of the actually measured values of desorption efficiencies and selection of a sampling time of 24 h at 1 atm and a temperature of 298 K, eq 2 becomes

$$C_{LL}\ (\text{ppb/V}) = \frac{17 \times 10^9 M_{B\text{-}DL}}{DE(DA/L)M} \tag{3}$$

where C_{LL} is the lower limit of concentration for which the badge is useful due to blank and/or detection limitations. The limiting mass ($M_{B\text{-}DL}$) is given in Table I or II. As an example of the application of eq 3, sampling rates and C_{LL} values calculated by eq 3 for the DuPont device are shown in Table IV. With some variation qualitatively similar results are obtained with reference to the other two types of badges. Both blank problems and detection limitations are responsible for the 0.1–7.0 ppb/V lower useful limits for the tested compounds.

Table IV. Lower Useful Exposure Levels for DuPont Badge[a]

compound	sampling rate,[b] cm^3/min	C_{LL},[c] ppb/V	limiting factor
chloroform	79	0.11	detection
1,2-dichloroethane	81	7.0	detection
1,1,1-trichloroethane	60	0.58	blank
carbon tetrachloride	74	0.11	blank
trichloroethylene	65	0.13	blank/ detection
benzene	71	0.65	detection
tetrachloroethylene	51	1.5	blank
chlorobenzene	66	2.5	detection

[a] 24-h sampling period. [b] As cited by DuPont brochure, May 1981. Rate is with both covers removed. [c] As defined by eq 3.

The important criterion for determining the potential utility of the tested devices in ambient air applications is the ratio of the expected ambient concentrations to the lower useful concentration limits listed in Table IV. Singh et al. (9) recently reported ambient air levels of some 33 organic compounds found in three western cities (Oakland, Phoenix, Los Angeles), including the compounds investigated in this study. The mean values for Los Angeles, which are usually higher than those for the other cities, are listed in Table V along with the ratios of these ambient concentrations (C_A) to the C_{LL} values from Table IV. C_A/C_{LL} values of 1 or less indicate no potential ambient utility unless the ambient levels for a potential location are much higher than those in Table V. Inasmuch as the

Table V. Comparison of Lower Useful Limits of DuPont Badge with Ambient Conditions

compound	mean ambient concn,[a] ppb/V	C_A/C_{LL}[b]
chloroform	0.088	0.80
1,2-dichloroethane	0.52	0.074
1,1,1-trichloroethane	1.0	1.8
carbon tetrachloride	0.21	1.9
trichloroethylene	0.40	3.1
benzene	6.0	9.2
tetrachloroethylene	1.5	1.0
chlorobenzene	~0.2	~0.08

[a] Reference 9, Los Angeles data. [b] Ratio of mean ambient to lower useful limit.

standard deviations of the cited mean ambient levels are generally of the order of 50–75%, even ratios of 1.5–2 can be considered of marginal usefulness. Ratios greater than 2 indicate good potential. For the ambient concentrations cited, chloroform, chlorobenzene, tetrachloroethylene, and 1,2-dichloroethane will not be detected in a 24-h sampling period. Carbon tetrachloride and 1,1,1-trichloroethane fall into the somewhat marginal classification. However, benzene and trichloroethylene could be monitored in a 24-h period with the present DuPont badge.

Obviously, there are a number of possible improvements that could be made. Lower and more consistent blanks, i.e., better quality control by the manufacturers, would permit analysis at lower levels. Also some improvements in the analytical methodology (capillary chromatography, larger aliquots) are possible which could improve the detection limits by at least a factor 2. These two improvements alone would yield an excellent potential rating for all compounds except 1,2-dichloroethane and chlorobenzene on all three badges.

Conclusions

It is concluded that none of these three currently available passive devices is entirely acceptable, within the current state of the art, for general organic vapor sampling at ambient levels due to detection or blank limitations. This is not unexpected since they were designed for industrial hygiene applications. However, these devices may be useful for particular compounds. For example, the DuPont device could presently be used to monitor benzene and trichloroethylene and perhaps carbon tetrachloride and 1,1,1-trichloroethane; the badges could be potentially useful for the other organic compounds if lower detection limits and blank levels can be achieved (*10*). Even with such improvement, there are some compounds such as 1,2-dichloroethane and chlorobenzene for which the badges will not be useful because of poor detectability of the compounds. In any case, considerably more laboratory evaluation of the devices for interferences, accuracy, humidity, and temperature effects is required before they can be used for routine monitoring of ambient level organic vapors.

Note added in proof: lower and more consistent blank levels in commercially prepared badges have recently been demonstrated (*10*).

Literature Cited

(1) Lutz, G. "Critical Literature Review of Active and Passive Air Pollution Monitors for Organic Compounds"; Final Report from Battelle Columbus Laboratories to the U.S. Environmental Protection Agency, Contract 68-02-2686, Task 127, 1981.
(2) "Proceedings of the Symposium on the Development and Usage of Personal Monitors for Exposure and Health Effect Studies"; EPA-600/9-79-032, June, 1979.
(3) "Dosimetry for Chemical and Physical Agents"; Kelley, W. D., Ed.; American Conference of Governmental Industrial Hygienists: Cincinnati, Ohio, 1981; Vol. I.
(4) Lautenberger, W. J.; Kring, E. V.; Morello, J. A. *Am. Ind. Hyg. Assoc. J.* **1980**, *41*, 737.
(5) Gosoelink, D. W.; Brown, D. L.; Mullins, H. G.; Rodrigue, S. T., paper presented at AIHA National Meeting, San Francisco, May, 1978.
(6) Tompkins, F. C.; Goldsmith, R. L. *Am. Ind. Hyg. Assoc. J.* **1977**, *38*, 371.
(7) Nelms, L. H.; Reizner, D. D.; West, P. W. *Anal. Chem.* **1977**, *49*, 944.
(8) Dommer, R. A.; Melcher, R. G. *Am. Ind. Hyg. Assoc. J.* **1978**, *39*, 240.
(9) Singh, H. B.; Salas, L. J.; Smith, A. J.; Shigeishi, H. *Atmos. Environ.* **1981**, *15*, 601.
(10) Coutant, R. W., paper presented at National Symposium on Recent Advances in Pollutant Monitoring of Ambient Air and Stationary Sources, Raleigh, NC, May 4–7, 1982.

Received for review September 21, 1981. Accepted March 18, 1982. This work was performed under U.S. Environmental Protection Agency Contract 68-02-2686, Task 128. Mention of commercially available devices in this paper does not constitute endorsement by EPA or BCL.

Environ. Sci. Technol. **1982**, *16*, 414–419

Observations of Nitrous Acid in the Los Angeles Atmosphere and Implications for Predictions of Ozone–Precursor Relationships

Geoffrey W. Harris, William P. L. Carter, Arthur M. Winer, and James N. Pitts, Jr.*

Statewide Air Pollution Research Center and Department of Chemistry, University of California, Riverside, California 92521

Ulrich Platt and Dieter Perner

Institut für Chemie 3, Atmosphärische Chemie, D-5170 Jülich, West Germany

■ Direct measurements of nitrous acid (HONO) were made in downtown Los Angeles and Riverside, CA, during night and early morning hours of July/August 1980 using a long-path differential optical absorption spectrometer. Up to 8 ppb of HONO were observed in Los Angeles, approximately twice the maximum levels previously measured in Riverside during the summer of 1979. Possible sources of the observed HONO are discussed. If the observed HONO levels are included in initial NO_x concentration, EKMA isopleth calculations predict that more rigorous control of NO_x emissions (especially at low HC/NO_x levels) or of hydrocarbons emissions is necessary to reduce ozone maxima by a given amount compared with predictions based on calculations neglecting initial HONO. Moreover, including HONO in the starting NO_x leads to predictions of accelerated rates of oxidant production which results in much larger predicted O_3 doses at elevated O_3 levels. For example, the predicted O_3 dosage at levels above 0.3 ppm ozone in the case of NMHC = 1 ppm and $[NO_x]_0$ = 0.12 ppm is increased by over 250% when 10 ppb of HONO is taken to be initially present.

Introduction

The critical role of hydroxyl radicals in the initiation of photochemical oxidant formation has been recognized for many years (*1–4*). The main photolytic steps in the primary production of the chain-initiating OH radical involve aldehydes, especially formaldehyde, ozone, and nitrous acid (HONO). Of these, ozone is generally not present prior to irradiation of the real or of simulated polluted atmospheres and hence does not contribute significantly as a radical source in the early morning or during the first stages of simulations. Measurements of aldehydes in the early morning atmosphere are sparse, though aldehyde concentrations appear to be relatively low during that time of the day (*5, 6*); moreover, the rate of radical production from formaldehyde by photolysis is much less than that from nitrous acid for equal concentrations (*7, 8*). Knowledge of levels of nitrous acid in polluted air has been limited to our previously reported studies in which we performed measurements of the nighttime buildup of HONO in Julich, Germany (*9*), and at a downwind receptor site (Riverside) and a midbasin site (Claremont) in the California South-Coast Air Basin (*10*).

Current airshed models differ in the concentrations of HONO assumed to be present at the start of their simulations. Certain models assume HONO is initially present, in some cases (*11*) up to the maximum value determined by the NO–NO_2–H_2O equilibrium (*12*). On the other hand, the standard conditions used in the EPA kinetic model (EKMA) (*13–15*) and isopleth programs (OZIPP) (*16*) recommended by the U.S. Environmental Protection Agency (EPA) for predicting O_3–precursor relations omit HONO completely from the starting conditions. Indeed, the OZIPP programs presently do not even allow for its optimal inclusion.

In the present study, carried out in July and August 1980, we set out to perform further HONO measurements at Riverside and at a heavily polluted site, the California State University, Los Angeles (CSLA), a central Los Angeles location near the intersection of two heavily traveled highways, the Santa Monica Freeway (US 10) and the Long Beach Freeway (CA 7). The results of the monitoring study are discussed in terms of their implications for possible modes of atmospheric HONO formation. The impact of the observed levels of HONO incorporated into EKMA-type calculations are considered in terms of predictions of O_3 formation rates and oxidant–precursor relationships by such airshed model calculations.

Experimental Methods

Nitrous acid was monitored by using the long-path differential UV absorption technique which has been discussed previously (*7, 9, 10*). The light source employed was a 500-W xenon high-pressure lamp whose output was collimated into a parallel beam by a spherical mirror. The light beam was transmitted ~1–2.3 km and received by another spherical mirror (30-cm diameter, 1.8-m focal length) focused on the entrance slit of a 0.3-m spectrograph. The spectrograph was equipped with a rotating metal disc carrying radial slits (100 μm wide, 10 mm spacing) across the focal plane. A 38-nm segment of the spectrum was scanned repetitively in a chosen spectral region. The light intensity passing through the slits was monitored by a photomultiplier tube (EMI 9659Q) and the analog signal was averaged for ~40 μs, then digitized, and stored by a DEC MINC 11/23 computer. The computer averaged the scans and was also used to manipulate the data in spectral deconvolution and in the calculation of optical densities. Absorption bands with optical densities as low as 10^{-4} (base 10) could be detected.

The HONO absorption bands employed were at 354.1 and 368.1 nm, which have a differential absorption cross section (*9*) of 4.7×10^{-19} and 3.8×10^{-19} cm^2 molecule^{-1} (base *e*), respectively. Before the optical density of the HONO bands were measured, nearby and overlapping bands arising from NO_2 were eliminated by subtraction of a suitably weighted NO_2 reference spectrum. For the HONO band at 354.1 nm the minimum optical density detectable over a 1-km light path corresponded to 0.2 ppb of HONO.

At Riverside the path length was 0.86 km and ran 2–20 m above the ground, while at the CSLA site two different light paths were used: path I was 2.26 km long and 50–100 m high; path II was shorter (0.96 km) and lower (2–50 m high) but in the same direction as path I. Both paths were over the same major freeway interchange.

The differential absorption technique was also used to monitor NO_2 and occasionally formaldehyde and SO_2. NO

 0013-936X/82/0916-0414$01.25/0

was measured by chemiluminescence, aerosol by a nephelometer, O_3 by UV absorption, and insolation by an Eppley radiometer.

Calculation Methods

The general physical approach utilized in the calculations performed to evaluate the significance of our measurements is based on a simplified trajectory model (*17*). A column of air containing the initial precursors is allowed to have negligible exchange with air outside the column other than dilution with pure air at a constant rate, simulating the raising of the inversion layer. Thus the column is treated like a large smog chamber for the purpose of model calculations. Although this approach completely ignores the complexities introduced by transport and diffusion processes occurring in actual airsheds, the same simplifications are implicit in the OZIPP programs and the EKMA isopleth technique and seem appropriate for the purpose of determining the effect of initial HONO.

The input data used are essentially the same as in standard EPA isopleth calculations (*13, 18, 19*), except for the inclusion of HONO at the start and the detailed kinetic mechanism employed (see below). Full pollutant loading was assumed to occur at 0700 local standard time, and the simulation was terminated at 1800. As used in the standard EPA calculations, a constant dilution rate of 3% h^{-1} and a starting NO/NO_2 ratio of 3 were assumed. All calculations were done for a latitude of 34.1° N and a solar declination of 23.5°, which is appropriate for Los Angeles in the summer. Photolysis rates were calculated by using the actinic irradiances as a function of zenith angle derived by Peterson (*20*) using his best estimate surface albedos.

The kinetic mechanism in these calculations was a slightly simplified version of the SAPRC propene–butane–NO_x–air model (*4*) with some minor updating of rate constants as given elsewhere (*21*). The mechanism given in the standard EPA isopleth model and included in the OZIPP program was not used since the latter is known to be incorrect in a number of details and gives significantly different predictions of O_3 dependence on initial NO_x levels compared to current mechanisms (*17*).

The representation of the hydrocarbon mixture for the calculations is based on the "surrogate" hydrocarbon mixture used in the UC Riverside smog chamber runs (*22, 23*) and was designed to represent hydrocarbon emissions from all sources in the Los Angeles basin (*24*).

In those present calculations for which initial HONO was included, HONO was counted as a component of the initial NO_x because it rapidly forms NO upon photolysis. Thus, for example, a calculation assuming 0.1 ppm of initial NO_x with 10 ppb of HONO used initial NO + NO_2 = 90 ppb.

Results and Discussion

Experimental Measurements. Table I gives the maximum predawn HONO concentrations observed in this study and gives values of related parameters measured around the time of the HONO maxima. As can be seen, the HONO maxima are highly variable, but in general the values measured at Riverside are within the range we have previously reported for that location (*10*), while the values observed at CSLA are considerably higher, particularly when the shorter, lower path II was employed. The highest predawn HONO observed by using path II was 8 ppb, compared with 4.5 ppb with path I and 4 ppb for the previous work at Riverside (*10*). Representative morning concentration–time profiles for HONO and NO_2 in Riverside and at CSLA using path II are shown in Figures 1 and 2, respectively. In general, the nighttime concentration–time behavior of HONO in Riverside tended to follow

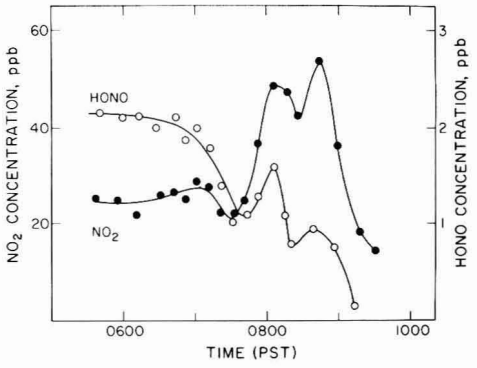

Figure 1. Time–concentration profiles of NO_2 (●) (left-hand scale) and HONO (O) (right-hand scale), Riverside, July 6, 1980.

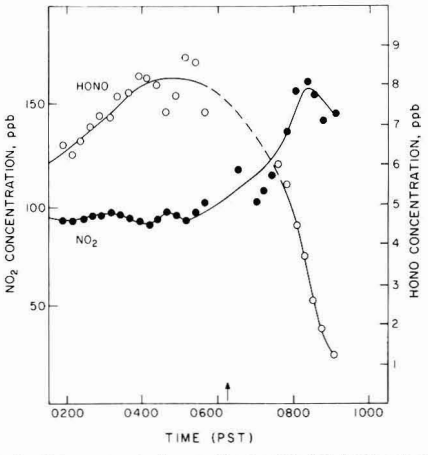

Figure 2. Time–concentration profiles for NO_2 (●) (left-hand scale) and HONO (O) (right-hand scale), CSLA, August 8, 1980; arrow marks time of sunrise.

that of NO_2, with temporary HONO minima and maxima occurring at the same time as NO_2 minima and maxima (Figure 1). This suggests that most of the HONO has been formed previously and is being transported along with NO_2 (and other pollutants) to Riverside. On the other hand, at CSLA, the HONO levels increased steadily throughout the night, with no close correspondence in concentration–time profile with that of NO_2 (Figure 2). This suggests that HONO is either formed or emitted at the site rather than being transported to it.

The mechanism for the observed nighttime buildup of HONO is presently unknown. The HONO levels observed using the shorter path II, with a larger relative contribution from the air mass directly over the freeway, were generally higher than observed with path I. This suggests the presence of higher HONO levels very near the freeway, either due to direct emission of HONO by vehicles or quite rapid formation from emitted NO_x before great dilution occurs. If HONO is not emitted its most probable known pathways of formation are

$$OH + NO \xrightarrow{M} HONO \qquad (1)$$

$$NO + NO_2 + H_2O \xrightarrow{het} 2HONO \qquad (2, -2)$$

$$2NO_2 + H_2O \xrightarrow{het} HONO + HONO_2 \qquad (3)$$

Table I. Maximum Concentrations of HONO in the Los Angeles Basin and Related Parameters

date	location	time, PST	[HONO], ppb	[NO_2], ppb	[NO], ppb	T,[a] K	RH,[a] %	B_{scat}, rel units	$[HONO]_{eq}$,[b] ppb	$\frac{[HONO]}{[HONO]_{eq}}$
5 Jul 80	Riverside	5:00	2.9	22	~1	289	78	56	~1	2.9
6 Jul 80	Riverside	5:00	2.1	25	~1	289	72	29	~1	2.1
7 Jul 80	Riverside	6:00	1.4	57	~6	291	63		~2	0.70
10 Jul 80	LA, path I	3:00	2.4	65		292	45			
11 Jul 80	LA, path I	3:00	2.1	87		294	55			
12 Jul 80	LA, path I	3:00	1.1	49		291	65			
16 Jul 80	LA, path I	3:00	4.2	94	~100	296	50		16	0.26
17 Jul 80	LA, path I	3:00	1.4	44	40	292	66	8	7	0.20
18 Jul 80	LA, path I	3:00	1.8	50	25	292	70	8	6	0.30
19 Jul 80	LA, path I	5:30	1.2	40	~5	291	78	21	~3	0.24
20 Jul 80	LA, path I	2:00		66	~6	290	73	27	~3	
21 Jul 80	LA, path I	5:30	1.5	49	~5	290	78	30	~3	0.50
22 Jul 80	LA, path I	3:00	2.8	76	6	291	78	36	4	0.70
23 Jul 80	LA, path I	3:00	3.6	66	35	293	71	12	8	0.45
24 Jul 80	LA, path I	5:30	3.2	57	22	293	73	18	6	0.53
25 Jul 80	LA, path I	3:00	2.6	70	15	293	71	16	6	0.43
26 Jul 80	LA, path I	3:00	4.1	80	45	293	71	20	10	0.41
27 Jul 80	LA, path I	3:00	4.2	57	44	292	76	22	9	0.47
28 Jul 80	LA, path I	3:00	4.4	83	44	294	66	14	10	0.44
29 Jul 80	LA, path II	6:00	6.0	80	100	295	64	16	15	0.40
1 Aug 80	LA, path II	5:30	7.5	120	90	298	54	17	16	0.47
5 Aug 80	LA, path II	4:30	0.4	28	0	295	69	15	0	
6 Aug 80	LA, path II	4:00	3.6	57	12	292	78	14	5	0.72
7 Aug 80	LA , path II	5:30	7.0	65	58	293	73	19	11	0.64
8 Aug 80	LA, path II	6:00	8.0	105	100	295	57	20	16	0.50

[a] Given for 0600 PST. [b] Calculated equilibrium value for the reaction $NO + NO_2 + H_2O \rightarrow 2HONO$.

Other reactions have been considered but can be shown to be of negligible importance (*10*).

If reaction 1 is the nighttime source of HONO, then the hydroxyl radicals must be formed from some nonphotolytic source. One possible dark source of OH radicals is intiated by the reaction of peroxyacetyl radicals ($CH_3C(O)O_2\cdot$) with NO, which may occur when NO is emitted into an air mass containing PAN formed photochemically on the previous day. Subsequent reactions involving NO and O_2 are known to result in the formation of hydroxyl radicals (*25–27*). Unfortunately, available data are not sufficient to assess the importance of this reaction system on our measurement days.

If reaction 2 is the source of HONO, it must proceed heterogeneously, since (2) has been shown (*12, 28*) to be slow in the gas phase. The possible role of reaction 2 as a source of HONO can be examined by comparing the observed HONO maxima with equilibrium values calculated on the basis of the known equilibrium constant (*12*) for reactions 2, –2 and our measurements of NO_x and relative humidity. It can be seen from Table I that at the CSLA site the observed HONO levels are 25–70% of the equilibrium concentrations, while at Riverside they can even exceed the calculated equilibrium levels. There is no simple correlation between $[HONO]/[HONO]_{eq}$ and aerosol levels as measured by nephelometry. However, since the reactions 2, –2 are slow (*12, 28*), the yield of HONO formed after emission of NO_x may reflect competition between dilution, approach to equilibrium, and thermal oxidation of NO to NO_2. Moreover, the distribution of HONO between the gas and aerosol phases may, in general, be a complex function of aerosol size, composition (especially pH), and temperature; it may thus be unreasonable to expect simple overall correlations and numerical relationships to hold.

The possibility of NO_2 hydrolysis, reaction 3, contributing to HONO formation is considered since we observed HONO buildup on several occasions in the evening at Riverside when NO concentrations are strongly suppressed by ozone. If a heterogeneous reaction 3 is important, the nitric acid coproduct in (3) would, in part, determine the pH of the droplet and in turn affect the distribution of HONO, formed in both reactions 2 and 3, between the solution and the gas phase. However, reported studies on the rate of reaction 3 in pure water (*29–32*), which are in agreement with each other, indicate that the process is much too slow to explain the observed HONO formation. Even under favorable assumptions (10^{-2} g m^{-3} liquid water and equilibrium distribution of NO_2 between phases) application of the literature rate data leads to predicted HONO formation rates about 4 orders of magnitude lower than those observed.

Effect of Initial HONO on Calculated Concentration–Time Profiles and Predicted Ozone Doses. Photolysis of HONO after dawn produces hydroxyl radicals. For the condition of CSLA on the morning of August 8, 1980, when the highest predawn levels of HONO were observed, we calculate an effective OH radical production rate of 2–3 × 10^7 cm^{-3} s^{-1} between 0630 and 0800 PST. This figure is based on the observed HONO disappearance rate and hence takes account of HONO reformation in reaction 1. For comparison, the radical production from formaldehyde photolysis can be estimated from the measured formaldehyde concentration and light intensity on that morning. Using the differential UV absorption spectrometer (*7*) at CSLA on August 8, 1980, we measured formaldehyde levels of 11 ppb at 0630 PST rising to 26 ppb at 1000 PST. This leads to calculated radical production rates for the measured light intensities increasing from zero at dawn to ~1 × 10^7 cm^{-3} s^{-1} by 0800 PST. Later in the day, radical production from ozone photolysis becomes the strongest calculated source. The effects of the strong additional early morning radical source due to HONO photolysis on O_3 production rates, maxima, and precursor relationships have been investigated and are discussed below.

Figure 3 shows plots of O_3 concentration–time profiles calculated for NMHC = 1 ppm C and three different NO_x levels with 0, 5, and 10 ppb of HONO present at the beginning of the simulation. It can be seen that except in

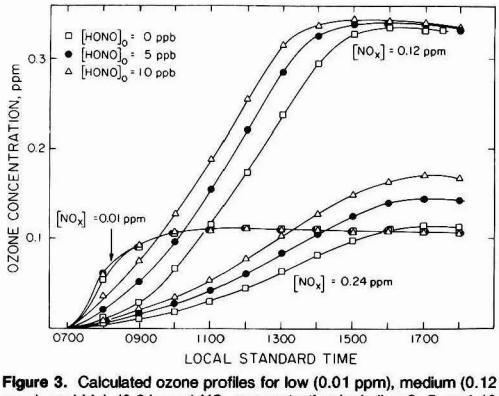

Figure 3. Calculated ozone profiles for low (0.01 ppm), medium (0.12 ppm), and high (0.24 ppm) NO_x concentration including 0, 5, and 10 ppb of HONO.

the very low NO_x case where O_3 formation is rapid anyway, initial HONO markedly increases the rate of O_3 formation. Thus a given level of O_3 occurs roughly 45 min earlier if 5 ppb of HONO was included and 75 min earlier when 10 ppb of HONO was present. These higher O_3 formation rates are clearly the result of the additional radical initiation caused by HONO photolysis and show that even 5 ppb of HONO can have a noticeable effect.

It can also be seen from Figure 3 that, except in the high NO_x case, the HONO does not greatly affect the maximum O_3 yield; this is because O_3 formation can only occur to a significant extent when NO_x is present (NO_2 photolysis is the only atmospheric source of $O(^3P)$ atoms other than photolysis of O_3 itself). Thus, the maximum O_3 yield is limited by the amount of NO_x available in the system, and if the system has higher rates of radical initiation, the rate of NO_x consumption is increased along with the rate of O_3 formation. However, the enhancements of final O_3 yields due to HONO are greater in the high NO_x case because the simulation ends before all of the NO_x is consumed and thus before the ultimate maximum O_3 yield is attained.

Even though the ultimate ozone yield is not strongly governed by the amount of initial HONO, the predicted integral under the ozone profile (i.e., the dose, in ppm min, received by a population) is quite strongly dependent on how much HONO is included in the starting NO_x. Thus, for the case of $[NO_x]_0 = 0.12$ ppm shown in Figure 3, the ozone dosage at levels of O_3 above 0.12 ppm (the federal air quality standard) is calculated to be increased by 44% when 10 ppb of initial HONO is considered compared to $[HONO]_0 = 0$. The increases in dose above higher ozone levels are even greater; the predicted dose at ozone levels above 0.2 ppm of O_3 increased by 62% and above 0.3 ppm by almost a factor of 3 according to our model when 10 ppb of HONO is included.

It should be restated that our modeling technique neglects transport effects and the effects of fresh emissions after 0700; however, within the limitations of the calculational method these predicted ozone dosage increases, especially above higher ozone levels, may be considered very significant.

Oxidant–Precursor Relations and Control Strategy Predictions Made by Using the EKMA Isopleth Technique. Isopleth hydrocarbon and NO_x levels that give maximum O_3 yields of 0.12 and 0.3 ppm were calculated by assuming 0, 5, and 10 ppb of initial HONO and are shown in Figure 4. A low ozone level of 0.12 ppm was chosen because it is the current federal air quality standard, while a high value of 0.3 ppm is representative of O_3

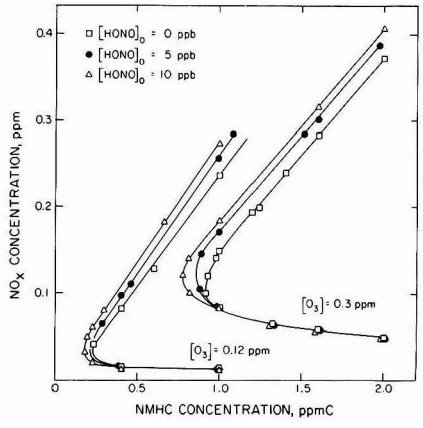

Figure 4. Ozone isopleths at 0.12 and 0.3 ppm for cases where HONO = 0, 5, and 10 ppb.

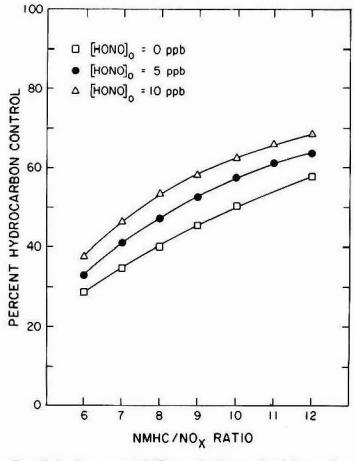

Figure 5. Predicted percent HC control required to reduce O_3 from 0.3 to 0.12 ppm for a range of HC/NO_x ratios in cases where HONO = 0, 5, and 10 ppb.

levels frequently reached or exceeded in the Los Angeles basin during air pollution episodes. It can be seen from Figure 4 that the major effect of initial HONO occurs at the higher NO_x levels, as discussed above, but that the overall shape of the isopleths are not dramatically changed.

In order to determine whether the predicted changes in the isopleths caused by including initial HONO have significant impacts on predictions of hydrocarbon control strategies, these isopleths were analyzed with the standard EPA-recommended "relative" isopleth analysis technique (*13, 33*) to determine the amount of hydrocarbon control required to reduce O_3 from 0.3 to 0.12 ppm, assuming NO_x levels remain the same. This technique is described in detail elsewhere (*13, 18, 33*) and involves assuming a representative hydrocarbon/NO_x ratio, determining the point on the $O_3 = 0.3$ ppm isopleth that corresponds to this ratio, and then determining the amount the hydrocarbon must be reduced to get the $O_3 = 0.12$ isopleth at the same NO_x level. Thus, the predicted amount of hydrocarbon control required depends on the initial hydrocarbon/NO_x ratio assumed as well as the isopleths used. The HC/NO_x ratio most appropriate for the Los Angeles basin remains the subject of controversy (*34*), and hence required hydro-

carbon controls were calculated for a range of HC/NO_x ratios from 6 to 12.

The results are shown in Figure 5. It can be seen that, regardless of the HC/NO_x ratio assumed, the percentage of hydrocarbon control projected to be required increases consistently as the amount of initial HONO assumed to be present increases, with ~6% more control required for 5 ppb of HONO and ~12% more control required with 10 ppb. This change in the predicted required hydrocarbon control is comparable to and in the same direction as that calculated by Carter et al. (*17*), resulting from the inclusion of initially present aldehydes as part of the NMHC. The effects due to HONO and aldehydes are expected to be partially additive.

The importance of the presence of initial HONO on predictions of the effect of NO_x control (assuming constant hydrocarbon) is quite dependent on the HC/NO_x ratio chosen. If the HC/NO_x ratio is high, including HONO in the NO_x input does not affect predictions of O_3 maxima and therefore does not affect predictions of the degree of NO_x control required to produce a given reduction in ozone levels. On the other hand, if the HC/NO_x ratio is low, the isopleths calculated for the HONO-included case predict that a greater reduction of NO_x is required to reduce O_3 a given amount at a constant hydrocarbon level. For example, assuming NMHC = 1 ppm C, a reduction in O_3 from 0.3 to 0.12 ppm requires that NO_x must be reduced by 0.17 ppm if 10 ppb of initial HONO is present, compared to a calculated required reduction of NO_x of 0.14 ppm when no initial HONO is included.

While the relationship between total NO_x levels and early morning HONO concentrations in the urban atmosphere is, as discussed above, not fully understood, it seems likely that application of NO_x controls would have an effect on HONO levels. From Figure 3 it can be seen that although the fraction of the initial NO_x that is taken to be present as HONO has a significant effect on predicted O_3 formation rates (compare [HONO] = 0 ppb with [HONO] = 10 ppb for $[NO_x]$ = 0.12 ppm), the effect of varying the total NO_x burden containing a constant fraction of HONO (compare $[NO_x]$ = 0.24 ppm, [HONO] = 10 ppb with $[NO_x]$ = 0.12 ppm, [HONO] = 5 ppb) is, as would be expected, much larger.

The observation of ambient HONO, an inhalable nitrite (which is a precursor to nitrosamines in simulated atmospheres (*35*, *36*)) has potential health implications that are beyond the scope of this paper, but which should be considered.

Acknowledgments

We thank Nicholas J. Miller and William D. Long for their assistance in acquiring the atmospheric spectra. The cooperation of Professor Joseph Bragin of the California State University, Los Angeles, and Nels Palm of the City of Monterey Park Water District in siting the spectrometer and the light source was appreciated.

Literature Cited

(1) Leighton, P. A. "Photochemistry of Air Pollution"; Academic Press: New York, 1961.
(2) Demerjian, K. L.; Kerr, J. A.; Calvert, J. G. *Adv. Environ. Sci. Technol.* **1974**, *4*, 1.
(3) Finlayson-Pitts, B. J.; Pitts, J. N., Jr. *Adv. Environ. Sci. Technol.* **1977**, *7*, 75.
(4) Carter, W. P. L.; Lloyd, A. C.; Sprung, J. L.; Pitts, J. N., Jr. *Int. J. Chem. Kinet.* **1979**, *11*, 45.
(5) Tuazon, E. C.; Winer, A. M.; Graham, R. A.; Pitts, J. N., Jr. *Adv. Environ. Sci. Technol.* **1980**, *10*, 259.
(6) Cleveland, W. S.; Graedel, T. E.; Kleiner, B. **1980**, *Atmos. Environ.* **1977**, *11*, 357.
(7) Platt, U.; Perner, D.; Patz, H. W. *J. Geophys. Res.* **1979**, *84*, 6329.
(8) Atkinson, R.; Lloyd, A. C. *J. Phys. Chem. Ref. Data*, in press.
(9) Perner, D.; Platt, U. *Geophys. Res. Lett.* **1979**, *6*, 917.
(10) Platt, U.; Perner, D.; Harris, G. W.; Winer, A. M.; Pitts, J. N., Jr. *Nature (London)* **1980**, *285*, 312.
(11) Lloyd, A. C., unpublished results, 1980.
(12) Chan, W. J.; Nordstrom, R. J.; Calvert, J. G.; Shaw, J. H. *Environ. Sci. Technol.* **1976**, *10*, 674.
(13) U. S. Environmental Protection Agency, "Uses, Limitations and Technical Basis of Procedures for Quantifying Relationships Between Photochemical Oxidants and Precursors"; EPA 450/2-77-021a, Research Triangle Park, NC, November 1977.
(14) U. S. Environmental Protection Agency, "Air Quality Criteria for Ozone and Other Photochemical Oxidants"; EPA 600/8-78-004, Washington, DC, April 1978.
(15) U. S. Environmental Protection Agency, *Fed. Reg.* **1980**, *45*, 64 856. September 30, 1980.
(16) Whitten, G. Z.; Hogo, H. "Users Manual for Kinetics, Model and Ozone Isopleth Plotting Package"; EPA 600/8-76-014a, July 1978.
(17) Carter, W. P. L.; Winer, A. M.; Pitts, J. N., Jr. *Atmos. Environ.* **1982**, *16*, 113.
(18) Dodge, M. C. In "Proceedings, International Conference on Photochemical Oxidant Pollution and Its Control"; EPA 600/3-77-001, Research Triangle Park, NC, January 1977.
(19) Dodge, M. C. "Effect of Selected Parameters on Predictions of a Photochemical Model"; EPA 600/3-77-048, Research Triangle Park, NC, June 1977.
(20) Peterson, J. T., "Calculated Actinic Fluxes (290-700 nm) for Air Pollution Photochemistry Application"; EPA 600/4-76-025, Research Triangle Park, NC, 1976.
(21) Atkinson, R.; Carter, W. P. L.; Darnall, K. R.; Winer, A. M.; Pitts, J. N., Jr. *Int. J. Chem. Kinet.* **1980**, *12*, 779.
(22) Pitts, J. N., Jr.; Winer, A. M.; Darnall, K. R.; Doyle, G. J.; McAfee, J. M. "Chemical Consequences of Air Quality Standards and of Control Implementation Programs: Roles of Hydrocarbons, Oxides of Nitrogen and Aged Smog in the Production of Photochemical Oxidant"; Final Report, California Air Resources Board Contract No. 3-017, July 1975.
(23) Pitts, J. N., Jr.; Winer, A. M.; Darnall, K. R.; Doyle, G. J.; McAfee, J. M. "Chemical Consequences of Air Quality Standards and of Control Implementation Programs: Roles of Hydrocarbons, Oxides of Nitrogen and Aged Smog in the Production of Photochemical Oxidant"; Final Report, California Air Resources Board Contract No. 4-214, May 1976.
(24) Pitts, J. N., Jr.; Winer, A. M.; Bekowies, P. J.; Doyle, G. J.; McAfee, J. M.; Wendschuh, P. H. "Development and Smog Chamber Validation of a Synthetic Hydrocarbon Oxides of Nitrogen Surrogate for California South Coast Air Basin Ambient Pollutants"; Final Report, California Air Resources Board Contract No. 2-377, September 1976.
(25) Hendry, D. G.; Kenley, R. A. Presented at the 173rd National ACS Meeting, New Orleans, LA, March 20–25, 1977.
(26) Hendry, D. G.; Kenley, R. A. In "Nitrogenous Air Pollutants: Chemical and Biological Implications"; Grosjean, D., Ed.: Ann Arbor Press: Ann Arbor, MI, 1979; p 137.
(27) Carter, W. P. L.; Winer, A. M.; Pitts, J. N., Jr. *Environ. Sci. Technol.* **1981**, *15*, 831.
(28) Kaiser, E. W.; Wu, C. H. *J. Phys. Chem.* **1977**, *81*, 1701.
(29) Ottolenghi, M.; Rabani, J. *J. Phys. Chem.* **1968**, *72*, 593.
(30) Sada, E.; Kumazawa, H.; Butt, M. A. *J. Chem. Eng.* **1979**, *12*, 111.
(31) Komiyana, H.; Inoue, H. *Chem. Eng. Sci.* **1980**, *35*, 154.
(32) Lee, Y. N.; Schwartz, S. E. *J. Phys. Chem.* **1981**, *85*, 840.

(33) Dimitriades, B. In "Proceedings, International Conference on Photochemical Oxidant Pollution and Its Control"; EPA 600/3-77-001, Research Triangle Park, NC, January 1977.
(34) Conference on Air Quality Trends in the South Coast Air Basin, California Institute of Technology, February 21–22, 1980.
(35) Hanst, P. L.; Spence, J. W.; Miller, S. M. *Environ. Sci. Technol.* **1977**, *11*, 403.
(36) Pitts, J. N., Jr.; Grosjean, D.; Van Cauwenberghe, K.; Schmid, J. P.; Fitz, D. R. *Environ. Sci. Technol.* **1978**, *12*, 946.

Received for review September 25, 1981. Accepted February 22, 1982. This work was supported by the National Science Foundation (Grant No. ATM-8001634).

Collection of Radon with Solid Oxidizing Reagents

Lawrence Stein* and Frederick A. Hohorst†

Chemistry Division, Argonne National Laboratory, Argonne, Illinois 60439

■ Although it is generally considered to be inert, radon reacts spontaneously at ambient temperature with a number of fluorine-containing compounds, including dioxygenyl salts, fluoronitrogen salts, and halogen fluoride–metal fluoride complexes. A method for the collection of radon from air, using either dioxygenyl hexafluoroantimonate ($O_2^+SbF_6^-$) or hexafluoroiodine hexafluoroantimonate ($IF_6^+SbF_6^-$) reagent, is described. The air is passed though a drying tube and then through a bed of the reagent, which captures radon as a nonvolatile product. In tests with radon–air mixtures containing 45–210 000 pCi/L of radon-222, more than 99% of the radon was retained by beds of powders (2.3–3.0 g of compound/cm^2) and pellets (7.5–10.9 g of compound/cm^2). The gas mixtures were designed to simulate radon-contaminated atmospheres in underground uranium mines. No dependence of collection efficiency upon radon concentration was observed. The method can be used for the analysis of radon-222 (by measurement of the γ emissions of the short-lived daughters, lead-214 and bismuth-214) and the purification of small volumes of air.

Introduction

Radon-222, a radioactive noble gas (half-life 3.823 days), is frequently collected for analysis by adsorption on charcoal at −80 °C (*1*, *2*) or condensation at −195 °C (*3*, *4*). It is then transferred with a carrier gas into a counting device such as a Lucas flask (*5*), ionization chamber, or proportional counter. Because of the widespread belief that radon is inert, chemical methods have been used in only a few instances for the collection of the gas. However, a number of tracer studies have shown tht radon can be trapped by means of strong oxidizing reagents (*6*–*9*).

Complexes of halogen fluorides and metal fluorides are among the compounds that can be used for this purpose. The complexes $ClF_2^+SbF_6^-$, $BrF_2^+SbF_6^-$, $BrF_2^+BiF_6^-$, and $IF_6^+SbF_6^-$ are typical examples. These are solids that have low vapor pressures (dissociation pressures) in the vicinity of room temperature. The last complex, hexafluoroiodine hexafluoroantimonate (*9*), is particularly well-suited for this application. Fluoronitrogen and dioxygenyl salts such as $N_2F^+SbF_6^-$, $N_2F_3^+Sb_2F_{11}^-$, $O_2^+SbF_6^-$, and $O_2^+Sb_2F_{11}^-$ can also be used to collect radon. All of these compounds react spontaneously with the gas to form nonvolatile products at 25 °C. The products have not been analyzed, because they have been prepared with only trace quantities of radon-222, but they are believed to be complex salts containing RnF^+ cation. Some examples of such reactions, inferred from known reactions of krypton and xenon, are shown in eq 1–5.

$$Rn + ClF_2^+SbF_6^- \rightarrow RnF^+SbF_6^- + ClF \quad (1)$$

$$Rn + BrF_2^+BiF_6^- \rightarrow RnF^+BiF_6^- + BrF \quad (2)$$

$$Rn + IF_6^+SbF_6^- \rightarrow RnF^+SbF_6^- + IF_5 \quad (3)$$

$$Rn + N_2F^+SbF_6^- \rightarrow RnF^+SbF_6^- + N_2 \quad (4)$$

$$Rn + 2O_2^+SbF_6^- \rightarrow RnF^+Sb_2F_{11}^- + 2O_2 \quad (5)$$

The results of tests of the collection of radon by two of the compounds, dioxygenyl hexafluoroantimonate and hexafluoroiodine hexafluoroantimonate, are reported in this article.

Experimental Section

Dioxygenyl hexafluoroantimonate was prepared by the photochemical reaction of antimony pentafluoride with a 2:1 molar mixture of oxygen and fluorine (*10*, *11*). The initial product was white, amorphous $O_2^+Sb_2F_{11}^-$ powder, which was gradually converted to microcrystalline $O_2^+SbF_6^-$ powder by prolonged reaction with the gases over a period of 3–4 days. Figure 1 shows the Raman spectra of the two compounds. The second compound is the preferred oxidant because of its higher content of dioxygenyl cation, O_2^+, per unit weight.

Hexafluoroiodine hexafluoroantimonate was prepared by the reaction of iodine heptafluoride with antimony pentafluoride (*9*). The product was a dense, white crystalline powder with a melting point of 175–180 °C.

Pyrex glass U-tubes of approximately 1.06 cm^2 internal cross-sectional area were loaded with weighed amounts of the powders and 3.2-mm diameter pellets, which were prepared by compressing the powders in a die. Glass beads and plugs of Kel-F plastic wool were added to the tubes to keep the compounds in place. Halocarbon lubricant was used on stopcocks, because ordinary lubricants are attacked by the chemicals. All of the loading and pellet-preparation steps were carried out in a drybox to prevent hydrolysis of the compounds.

Radon retention was measured with the apparatus shown in Figure 2. Radon–air mixtures were prepared in cylinder B with radon-222, collected from a radium chloride solution containing 61 μCi of radium-226. Each mixture was made up to approximately the desired concentration by expanding portions of the gas above the radium solution into the small "dosing" volume between valves V_1 and V_2, freezing the radon in trap T_1 with liquid nitrogen, transferring it into cylinder B with a stream of compressed air at room temperature, and filling the cyl-

†Present address: Exxon Nuclear Idaho Company, Inc., Idaho Falls, Idaho 83401.

0013-936X/82/0916-0419$01.25/0

Table I. Radon Retention of $O_2^+SbF_6^-$ and $IF_6^+SbF_6^-$ Powders

temp, °C	flow rate, std cm³/min	face veloc. m/min	radon concn in influent air, pCi/L	av radon concn in effluent air, pCi/L	radon retained, %
	Bed No. 1 (2.42 g of $O_2^+SbF_6^-$ Powder)				
25.2	138	1.30	229.0	0.075	99.967
25.4	229	2.16	163.9	0.110	99.933
25.4	490	4.63	163.5	0.136	99.917
26.8	1116	10.54	46.07	0.033	99.928
26.8	860	8.12	45.95	0.018	99.961
26.5	676	6.38	45.76	0.030	99.934
26.1	974	9.20	45.02	0.024	99.947
	Bed No. 6 (3.21 g of $IF_6^+SbF_6^-$ Powder)				
25.0	126	1.19	255.8	0.039	99.985
25.0	262	2.47	254.9	0.237	99.907
25.0	599	5.65	254.5	0.150	99.941
25.0	1185	11.18	253.4	0.715	99.718
25.0	32	0.30	251.1	0.037	99.985

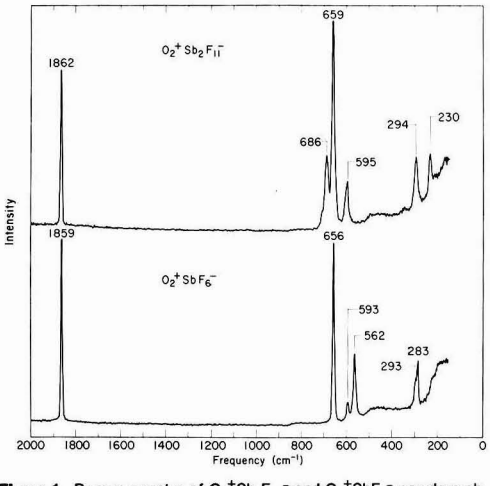

Figure 1. Raman spectra of $O_2^+Sb_2F_{11}^-$ and $O_2^+SbF_6^-$ powders obtained with 514.5-nm excitation and a Spex Model 1401 double spectrometer.

inder to 50–100 psig pressure with air. After a period of 12–36 h, the mixture was analyzed by the charcoal adsorption–scintillation counting method, using standard

Table II. Radon Retention of $O_2^+SbF_6^-$ Pellets

temp, °C	flow rate, std cm³/min	face veloc, m/min	radon concn in influent air, pCi/L	av radon concn in effluent air, pCi/L	radon retained, %
	Bed No. 2 (11.51 g of Pellets)				
10.0	484	4.57	149.8	0.058	99.961
10.0	810	7.65	149.2	0.027	99.982
10.0	229	2.16	146.0	0.023	99.984
25.0	509	4.81	620.2	0.301	99.952
25.0	252	2.38	534.7	0.121	99.977
25.0	1206	11.39	33 620	10.56	99.969
25.0	34	0.32	33 310	0.050	100.000
25.0	269	2.54	139 500	0.031	100.000
25.0	1215	11.47	139 100	40.92	99.971
25.0	33	0.31	137 800	0.193	100.000
40.0	1254	11.84	442.4	0.155	99.965
40.0	51	0.48	436.5	0.024	99.994
40.0	113	1.07	430.6	0.044	99.990
	Bed No. 5 (6.12 g of Pellets)				
10.0	1183	11.17	752.7	6.212	99.175
10.0	38	0.36	739.6	0.025	99.997
10.0	844	7.97	728.2	3.051	99.581
25.0	1245	11.76	363.5	2.933	99.193
25.0	127	1.20	361.9	0.044	99.988
25.0	41	0.39	357.8	0.028	99.992
25.0	876	8.27	354.5	1.060	99.701
25.0	258	2.44	353.6	0.048	99.986
40.0	1321	12.47	210.2	2.089	99.006
40.0	178	1.68	204.7	0.036	99.982
40.0	902	8.52	204.0	0.501	99.954

Lucas Flasks (*5*). It was then used for a series of measurements, with corrections for radon decay.

In a typical experiment, the radon–air mixture was passed through a bed of Drierite, through the test sample of oxidant immersed in a constant-temperature bath, and through a bed of charcoal at −80 °C, for a measured period of time. The volume of air was measured with a wet-test meter. Any radon that passed completely through the oxidant was captured by the charcoal and was analyzed, as before, by the α-scintillation counting method. Radon retention was calculated from the concentration of radon entering the oxidant bed and the time-averaged concentration of radon leaving the bed, determined by the analysis and the volume of air.

Measurements were made at ambient temperature (25–27 °C), 10.0, 25.0, and 40.0 °C with radon–air mixtures containing 45–210 000 pCi/L of radon-222. The face velocity of the impinging air ranged from 0.28 to 12.47 m/

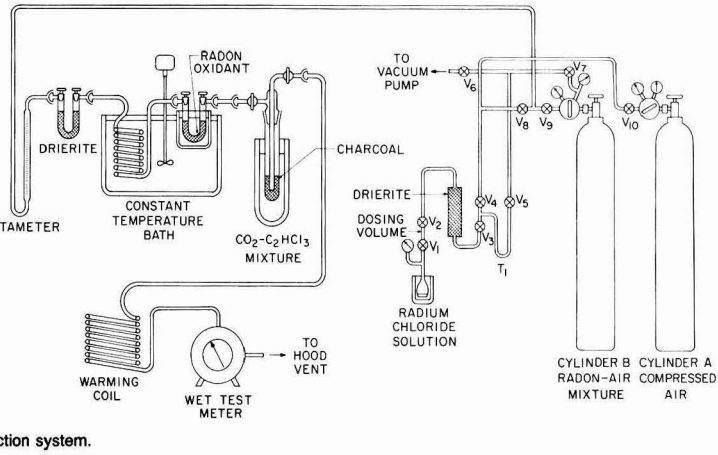

Figure 2. Radon collection system.

Table III. Radon Retention of $O_2^+SbF_6^-$ Pellets

temp, °C	flow rate, std cm³/min	face veloc, m/min	contact time, s	radon concn in influent air, pCi/L	av radon concn in effluent air, pCi/L	radon retained, %
			Bed No. 4 (3.23 g of Pellets)			
10.0	494	4.66	0.149	571.3	64.74	88.67
10.0	1172	11.07	0.063	570.2	194.65	65.86
10.0	42	0.40	1.757	564.4	0.43	99.92
25.0	518	4.89	0.142	398.3	67.44	83.07
25.0	1254	11.84	0.059	397.3	172.21	56.66
25.0	122	1.15	0.605	395.5	7.33	98.15
25.0	283	2.67	0.261	34 680	2049	94.09
25.0	40	0.38	1.845	34 240	5.25	99.98
25.0	271	2.56	0.272	144 800	8743	93.96
25.0	1206	11.39	0.061	144 700	63 890	55.83
40.0	538	5.08	0.137	190.2	39.86	79.04
40.0	1276	12.05	0.058	189.8	93.14	50.92
40.0	136	1.28	0.543	189.0	5.48	97.10
			Bed No. 3 (1.78 g of Pellets)			
10.0	517	4.88	0.064	347.9	86.88	75.26
10.0	1250	11.80	0.026	347.0	193.8	44.15
10.0	42	0.40	0.788	339.2	1.51	99.56
25.0	489	4.62	0.068	244.0	69.59	71.48
25.0	255	2.41	0.130	243.1	35.27	85.49
25.0	1178	11.12	0.028	242.3	149.4	38.34
25.0	34	0.32	0.974	238.0	0.64	99.73
25.0	115	1.09	0.288	235.2	11.58	95.08
25.0	819	7.73	0.040	234.1	124.6	46.77
25.0	533	5.03	0.062	521.0	138.7	73.37
40.0	547	5.16	0.060	200.7	82.78	58.75
40.0	1284	12.12	0.026	194.9	133.8	31.35
40.0	121	1.14	0.274	194.1	17.28	91.10

Table IV. Radon Retention of $IF_6^+SbF_6^-$ Pellets

temp, °C	flow rate, std cm³/min	face vel, m/min	radon concn in influent air, pCi/L	av radon concn in effluent air, pCi/L	radon retained, %
		Bed No. 7 (4.01 g of Pellets)			
10.0	32	0.30	482.9	0.008	99.998
10.0	249	2.35	477.3	5.822	98.780
10.0	1176	11.09	476.4	66.92	85.951
25.0	264	2.49	472.3	7.217	98.472
25.0	1231	11.61	471.5	67.68	85.645
25.0	32	0.30	402.5	0.089	99.978
25.0	37	0.35	123.5	0.014	99.988
25.0	278	2.62	122.4	1.271	98.962
25.0	1237	11.67	122.1	12.96	89.390
40.0	35	0.33	698.9	0.034	99.995
40.0	293	2.76	693.4	13.81	98.009
40.0	1298	12.24	692.1	110.6	84.015
		Bed No. 8 (8.02 g of Pellets)			
25.0	35	0.33	1139	0.021	99.998
25.0	271	2.56	1125	0.041	99.996
25.0	1203	11.35	1123	0.988	99.912
25.0	35	0.33	19 290	0.017	100.000
25.0	267	2.52	19 140	0.036	100.000
25.0	1205	11.37	19 100	15.15	99.921
25.0	32	0.30	210 700	0.047	100.000
25.0	257	2.42	208 700	0.051	100.000
25.0	1235	11.65	208 100	214.8	99.897

min, corresponding to time–average flow rates of 30–1321 standard cm³/min.

Results and Discussion

Tables I–IV show some representative results; more tables of data are contained in the supplementary material.

Both $O_2^+SbF_6^-$ powder and $IF_6^+SbF_6^-$ powder removed radon from air efficiently at all flow rates. Deep beds of pellets also removed the gas efficiently, whereas shallow beds passed about 15–70% of the radon at the highest flow rates. The shallow beds were most useful for determining the dependence of radon removal upon flow rate and temperature, because the residual radon-222 in the effluent from these beds could be measured most readily.

The percentage of radon that passed through 1.78 and 3.23 g beds of $O_2^+SbF_6^-$ pellets was approximately inversely proportional to the square root of contact time, as shown in Figure 3. The contact time was calculated from the cross-sectional area, length, and void space of each bed, and the flow rate. Changes of radon retention with temperature were imperceptible in the measurements with $IF_6^+SbF_6^-$ but were noted in those with $O_2^+SbF_6^-$. The retention decreased from 66% at 10.0 °C to 51% at 40.0 °C for the 3.23-g bed of $O_2^+SbF_6^-$ pellets, for example, at

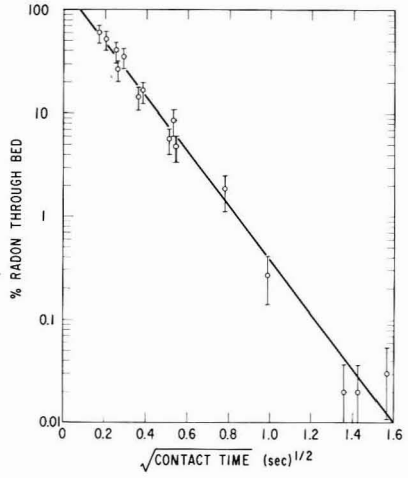

Figure 3. Percentage of radon passing through 1.78- and 3.23-g beds of $O_2^+SbF_6^-$ pellets as a function of the square root of contact time at 25.0 °C.

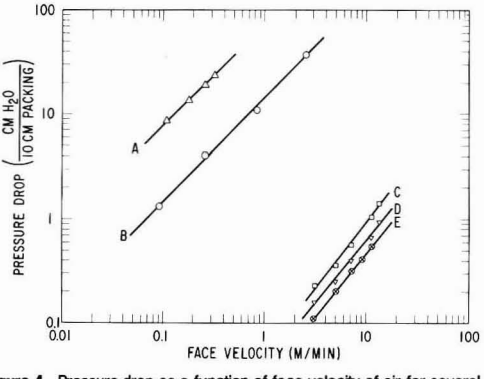

Figure 4. Pressure drop as a function of face velocity of air for several types of reagents: (A) $O_2^+SbF_6^-$ powder; (B) $IF_6^+SbF_6^-$ powder; (C) $O_2^+SbF_6^-$ pellets containing 10% fines; (D) $IF_6^+SbF_6^-$ pellets; (E) $O_2^+SbF_6^-$ pellets (diameter of pellets = 3.2 mm).

flow rates of 1170–1280 standard cm^3/min. No dependence of retention upon radon concentration was observed.

The tests showed that these reagents can be used instead of charcoal or cold traps to collect radon from air. A principal advantage of the method is that no refrigerant is required. In one application that has been tested for the U.S. Bureau of Mines (*12*), radon-222 is collected for analysis in a plastic cartridge containing 0.5–2.0 g of $O_2^+SbF_6^-$ powder. After radioactive equilibrium has been established beteen the radon and its short-lived daughters (approximately 4 h), the γ emission of the cartridge is measured with a scintillation counter. With the most favorable geometry, 2.74 counts/(min pCi) of radon-222 are observed (all energies).

Both reagents, $O_2^+SbF_6^-$ and $IF_6^+SbF_6^-$, are stable and can be stored at room temperature in sealed Teflon containers. They are decomposed by moisture, hence must be used in conjunction with desiccants in humid atmospheres. Many radon oxidants such as $ClF_2^+SbF_6^-$, $BrF_2^+SbF_6^-$, and $BrF_4^+Sb_2F_{11}^-$, react violently with liquid water, but $O_2^+SbF_6^-$ and $IF_6^+SbF_6^-$ have been shown to hydrolyze smoothly and exothermically (*9*, *11*). They are therefore considered to be the safest oxidants available at present. Reactions of the compounds with carbon monoxide, methane, sulfur dioxide, nitric oxide, and other components of diesel exhausts have been reported (*9*, *11*, *12*). The pellets have lower flow resistance than the powders (Figure 4) and may be more suitable for some applications (*9*, *12*). However, the highest radon retention per unit weight is obtained with $O_2^+SbF_6^-$ powder.

Acknowledgments

We thank F. Markun for radon analyses and I. M. Fox for chemical analyses.

Supplementary Material Available

Listings of radon retention results (7 pages) will appear following these pages in the microfilm edition of this volume of the journal. Photocopies of the supplementary material from this paper or microfiche (105 × 148 mm, 24× reduction, negatives) may be obtained from the Distribution Office, Books and Journals Division, American Chemical Society, 1155 16th St., N.W., Washington, D.C. 20036. Full bibliographic citation (journal, title of article, author) and prepayment, check or money order for $7.00 for photocopy ($8.50 foreign) or $4.00 for microfiche ($5.00 foreign), are required.

Literature Cited

(1) Stehney, A. F.; Norris, W. P.; Lucas, H. F., Jr.; Johnston, W. H. *Am. J. Roentgenol., Radium Ther. Nucl. Med.* **1955**, *73*, 774.
(2) Moses, H.; Stehney, A. F.; Lucas, H. F., Jr. *J. Geophys. Res.* **1960**, *65*, 1223.
(3) Conlan, B.; Henderson, P.; Walton, A. *Analyst* **1969**, *94*, 15.
(4) Kobal, I.; Kristan, J. *Radiochem. Radioanal. Lett.* **1972**, *10*, 291.
(5) Lucas, H. F. *Rev. Sci. Instr.* **1957**, *28*, 680.
(6) Stein, L. *Science (Washington, D.C.)* **1972**, *175* 1463.
(7) Stein, L. *Nature (London)* **1973**, *243*, 30.
(8) Stein, L. *Chemistry* **1974**, *47*, No. 9, 15.
(9) Hohorst, F. A.; Stein, L.; Gebert, E. *Inorg. Chem.* **1975**, *14*, 2233.
(10) Shamir, J.; Binenboym, J. *Inorg. Chim. Acta* **1968**, *2*, 37.
(11) Stein, L.; Hohorst, F. A. *J. Inorg. Nucl. Chem., Supp.* **1976**, 73.
(12) Stein, L.; Shearer, J. A.; Hohorst, F. A.; Markun, F. "Development of a Radiochemical Method for Analyzing Radon Gas in Uranium Mine Atmospheres"; Report USBM-H0252019, U.S. Bureau of Mines, Washington, D.C., 1977.

Received for review October 1, 1981. Accepted March 15, 1982. This work was performed under the auspices of the Office of Basic Energy Sciences, Division of Chemical Sciences, U.S. Department of Energy, and was supported by the Bureau of Mines, U.S. Department of the Interior, under contract H0252019.

Environ. Sci. Technol. 1982, 16, 423–427

Studies of Surface Layers on Single Particles of In-Stack Coal Fly Ash

Jeffrey L. Hock* and David Lichtman

Department of Physics and Laboratory for Surface Studies, University of Wisconsin—Milwaukee, Milwaukee, Wisconsin 53201

■ Surface and bulk analytical techniques have been used to study individual fly-ash particles collected in a defined manner and particle size range from within a power plant stack. A sampling system using collection on a dry, soft-metal substrate (e.g., indium), which meets the needs of both high-temperature sampling and analysis under clean vacuum conditions, has been employed. Scanning electron microscopy (SEM) and energy-dispersive X-ray fluorescence (EDX) measurements provide morphological and quasi-bulk composition of individual particles, after which the samples are then transferred to another system for single-particle Auger electron spectroscopy (AES) and ion beam depth profiling. The results obtained show clearly a wide chemical and physical disparity between different particles even in this limited sample range. However, there is no evidence of either an organic layer or a surface layer containing high (>1%) concentrations of high atomic number elements in the sample studied. In addition we find 90–95% of the particles are spherical and 10% are electrically conducting. SEM/EDX shows Al, Si, Fe, Ca, S, Cu, Cl, Mg, Cr, I, Ni, Zn, Na, Co, P, Mn, Sn, W, Ta, As, Pd, and V in decreasing abundance, whereas AES shows Si, Al, O, Fe, Ca, K, Na, and Mg.

Introduction

When coal is burned at high temperatures, the inorganic material it contains becomes molten. The majority of this material is removed either as slag from the bottom of the furnace or by cyclone filters, electrostatic precipitators, or bag filters. Nevertheless, small quantities of μm-size particles escape in the flue gas and are exhausted from the stack. Previously, a great deal of work has been performed on fly-ash particles which has employed a wide range of analytical techniques; see, for example, ref *1–10*. Most of these studies, other than electron microscopy measurements, have used collections of particles, thus obtaining bulk properties averaged over the many particles in the sample. Many questions such as surface chemical segregation, bulk chemical distributions, and surface morphological implications are still unanswered. Thus it seems there may be additional value in obtaining comparative data on individual particles by using surface-sensitive and bulk-sensitive techniques. The surface-sensitive techniques, in conjunction with ion bombardment surface erosion, have potential to provide elemental and chemical depth-profile information. Toward this end we have employed a number of modern surface-analysis techniques in an attempt to obtain detailed information about the physical and chemical characteristics of individual air particulates in the size range 5–30 μm. The fly-ash particles studied have been collected under defined conditions inside the stack of a power plant, at a temperature of 151 °C, in a manner designed to minimize the number of experimental artifacts.

Experimental Section

The procedures used to study individual fly-ash particles start with the collection of individual particles under controlled and well-documented conditions. The services of Meteorology Research, Inc. (MRI), were engaged to perform the collection activities under the Plume Validation Study contracted by the Electric Power Research Institute (EPRI). Particles were collected within one of the smokestacks of the Kincaid Generating Station of Commonwealth Edison near Springfield, IL. The collections were performed on dry indium foil, which has the advantage over other substrates of being a very soft metal that is compatible with the ultra-high-vacuum studies discussed below. Impact collectors were employed that used dry indium foils as the collecting stages. These were operated for 2.2 min at an elevation of 405 ft (123.4 m) in the stack. The flue-gas temperature at this elevation was 151 °C, whereas the melting temperature of indium is 156 °C. The impactors were run for 2 min. After collection, the indium foils (which were annular rings of 2.7 cm i.d. and 4.5 cm o.d.) were sectioned, and orientation markings were pressed into the soft metal by using a scalpel (see Figure 1). Following this preparation, the substrates were placed in a JEOL Model JSM U3 scanning electron microscope (SEM), during which surface morphology was determined and energy-dispersive X-ray analysis (EDX) data were obtained from individual isolated particles by using a Nuclear Diodes 605-X detector and an EDAX Model 504 energy analyzer. Following the initial SEM studies, the samples were then transferred to a Varian 10-keV scanning Auger electron spectroscopy system (AES). The scanning mode of the AES is used for locating the particles of interest. This is done in conjunction with the orientation markings on the indium substrates along with low-magnification photographs produced during the SEM work. Typical AES is performed by using beam currents from 0.2 to 1 μA at a beam energy of 8 keV. The spot diameter attainable under these conditions is approximately 15 μm at full width at half maximum. AES, which has a predicted sampling depth of 0.5–3 nm, is used to obtain data that upon sensitivity factor corrections, provide the elemental composition of the exposed surface of the particles, which had previously been characterized in the SEM.

In addition to the AES system, the vacuum chamber is equipped with a rasterable sputter ion gun (Varian Model 981-2043). This is used in conjunction with the AES system to obtain depth-profile data on individual particles (see Figure 2 for the relative beam orientations and beam size). It is to be noted that the electron beam overlaps the edge of the particle and interacts with some of the background substrate material. This results in some component of indium in the Auger spectra obtained from single particles. The method used to center the particle under the electron beam is to move the particle by using a precision manipulator in such a manner as to minimize the residual indium signal. Another aspect of this arrangement is the size of the sputtering beam. The sputter ion beam has a fwhm of approximately $^1/_2$ cm, much larger than the particle. This results in a significant fraction of the substrate being sputtered and a possibility for substrate material to be deposited onto the particle being studied. This problem has been observed by others (*10, 11*) and is discussed in detail elsewhere (*12*). So that accurate depth-profile information can be obtained, the sputtering rate

0013-936X/82/0916-0423$01.25/0

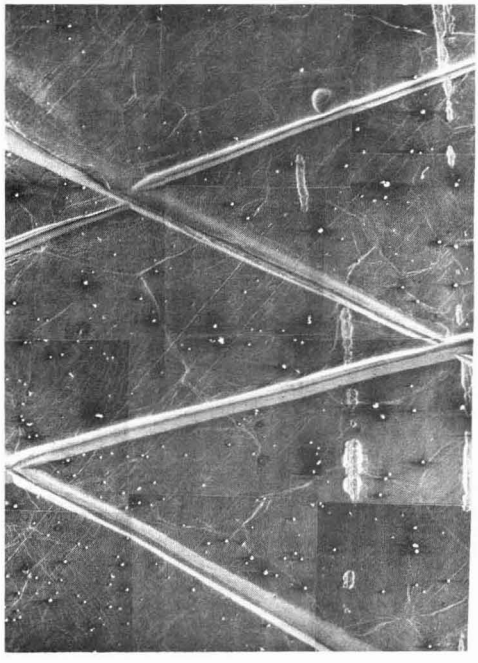

Figure 1. Section of indium foil showing orientation markings and several individual isolated particles of the type discussed in this work.

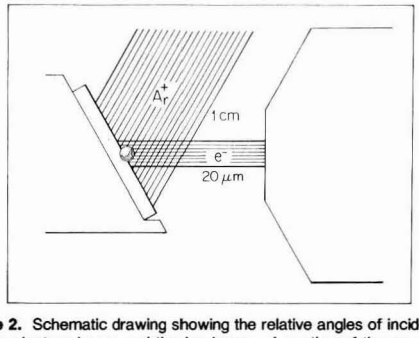

Figure 2. Schematic drawing showing the relative angles of incidence for the electron beam and the ion beam. A portion of the carousel with an indium substrate and particle mounted to it is shown along with a section of the cylindrical mirror analyzer (note: the particle size is greatly exaggerated for clarity).

of the ion gun must be known for the particle being analyzed. This information is not available for each particle, so standards of known thickness that match the matrix composition of the particles must be used. Fly ash derived from the combustion of coal in a conventional power plant is composed primarily of an impure aluminosilicate glass together with small amounts of several crystalline minerals (*13*). Thus, a standard of a SiO_2 layer of known thickness on pure Si was used. (The SiO_2/Si samples were prepared by Bell Labs under part of Round Robin depth-profile study.) From operation of the sputter ion gun in 5×10^{-5} torr (1.3×10^{-3} Pa) of argon and at an ion energy of 3 keV, a sputtering rate of 2.8 ± 0.2 nm/min is obtained for this standard. This sputtering rate is used as a calibration for the depth-profile data. Limitations to the accuracy of this sputtering rate include the influence of particle geometry, porosity, indium deposition, and nonuniform sputtering.

Table I. SEM Particle Data

element	av atomic % comp	population std dev	% particles with this element at concn > 1%
Fe	35	46	84
Si	20	27	90
Al	18	22	97
Ca	6.4	10	71
Cl	5.2	13	41
S	4.5	8.7	55
Cu	4.5	10	43
Cr	1.1	4.7	20
I	1.1	4.3	14
Mg	0.68	1.6	26
Zn	0.55	2.1	8.7
Ta	0.49	4.1	1.5
P	0.43	2.8	5.8
Na	0.39	1.7	8.7
Ni	0.36	1.1	12
Co	0.25	1.1	7.3
W	0.16	0.98	2.9
Mn	0.13	0.65	4.4
Sn	0.10	0.61	2.9
As	0.10	0.85	1.5
Pd	0.06	0.48	1.5
V	0.03	0.24	1.5

Results

Optics. In addition to the SEM and AES work to be discussed below, preliminary work has been performed by using visible light microscopy. Similar work has been performed by others (*14*), and our investigations have also revealed a range of colors for the particles from clear to black, the predominant colors seen being yellow, red, and orange. These colors are undoubtedly related to chemical composition and trace impurities in the glassy material. However, to date no correlations between color and chemical composition have been made. In addition to the variety of colors present, it has been observed that a large fraction, ~95%, of the particles are spherically shaped and lie on the top of the indium foil, imbedded less than 20% of their diameter.

Scanning Electron Microscopy. The studies performed in the SEM verified the usefulness of the collecting techniques employed. In the size range of interest for these studies (5–15 μm) many single isolated particles have been found on the sections of foil examined, along with clusters of smaller single particles (see Figure 1). The general nature of the particles that have been collected is that they are 90–95% spherical with surface morphology that varies from glassy smooth to rough surfaces (this is as viewed with the secondary electron image and does not necessarily infer optical morphology).

EDX analysis shows a large variety of elements, which are listed in Table I in the order of decreasing average abundance (EDX is not routinely sensitive to elements of atomic number less than 11). As can be seen from examining the population standard deviation shown in Table I, the percent abundance of a particular element varies widely from particle to particle. Four of the particles in the group of 69 studied had iron concentration (by EDX) of over 90%, whereas ten particles contained no measurable iron. It is to be noted that, due to the limitation in detecting low atomic number elements by EDX, it is possible that the particles that indicated large iron content may actually have been largely composed of lighter atomic number elements (atomic number <11) with relatively small amounts of iron. A further representation of the data is shown in the bar graphs of Figure 3. These show the relative occurrence of these various elements from a ran-

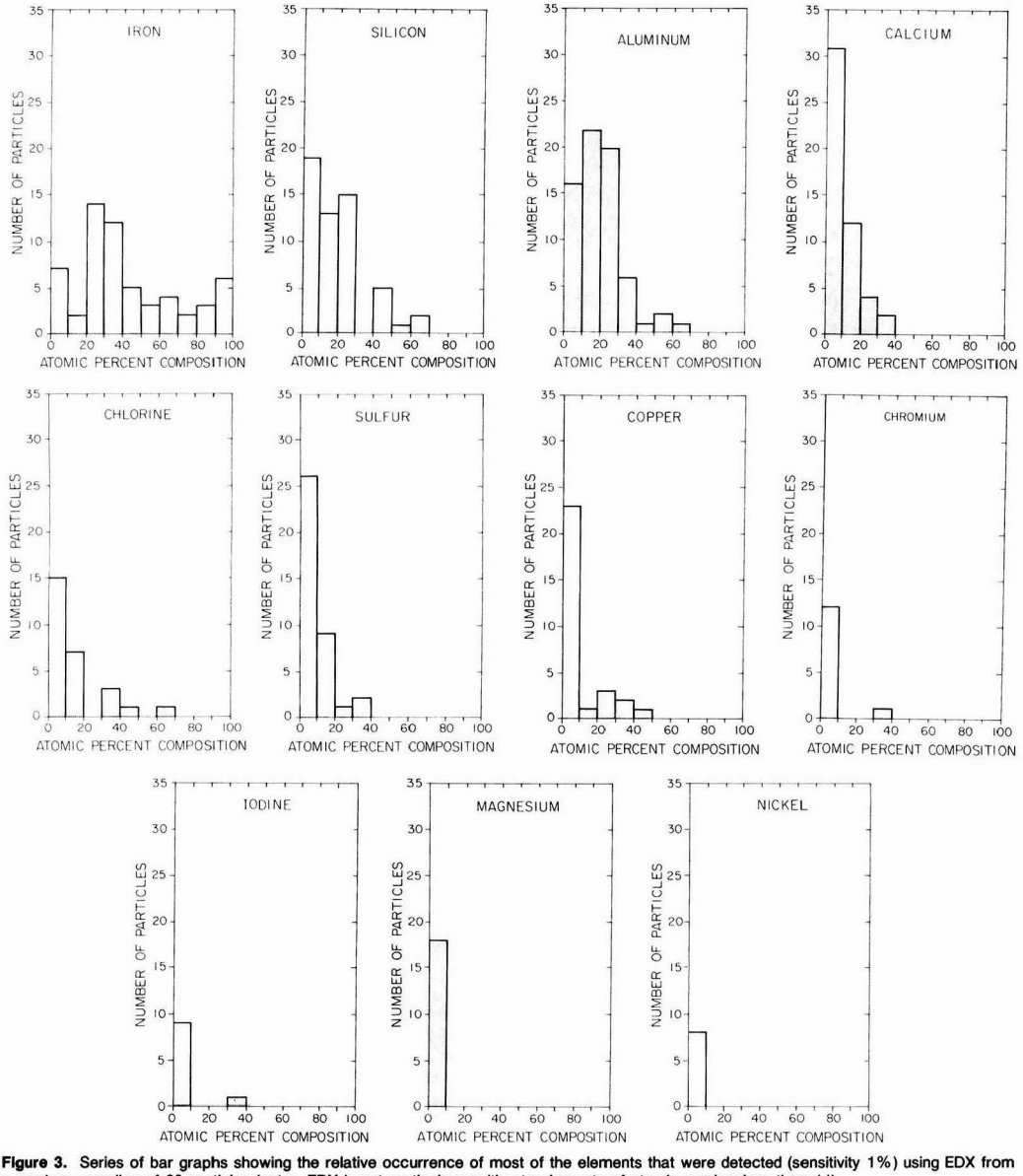

Figure 3. Series of bar graphs showing the relative occurrence of most of the elements that were detected (sensitivity 1%) using EDX from a random sampling of 69 particles (note: EDX is not routinely sensitive to elements of atomic number less than 11).

dom sampling of 69 particles. An examination of these graphs (and Table I) reveals that Fe occurs in 85% of these particles, while Si and Al occur in 90% and 97%, respectively.

In an attempt to examine the data for correlation of occurrence between elements, a correlation coefficient was determined between all possible pairs of elemental data. The correlation coefficient was defined as

$$r = \frac{\sum xy - (1/n)\sum x \sum y}{[(\sum x^2 - (1/n)(\sum x)^2)(\sum y^2 - (1/n)(\sum y)^2)]^{1/2}}$$

Application of this equation to the EDX data resulted in only one statistically significant correlation, which was between aluminum and iron and had a value of −0.63 (69 particles). This may suggest a competition between aluminum and iron in filling particular sites in the silica matrix or the presence of iron-rich particles low in aluminum (*15*).

Auger Electron Spectroscopy. The collection of individual particles on dry, soft-metal substrates, while desirable for the high-vacuum environment of the SEM, is a necessity for the ultra-high-vacuum (UHV) conditions needed to perform meaningful AES. A variety of tests were performed to ensure that the samples were not contaminated by pump oil used in the SEM. The indium

Table II. Auger Depth Profile Data[a]

element	virgin surface $\bar{x}$	virgin surface s	virgin surface %	1 nm below virgin surface $\bar{x}$	1 nm below virgin surface s	1 nm below virgin surface %	3 nm below virgin surface $\bar{x}$	3 nm below virgin surface s	3 nm below virgin surface %
Be	0.81	3.25	6			0			0
C	29	14	100	5.1	11.6	27	3.8	10.4	13
O	46	10	100	74	12	100	75	13	100
Na	0.19	0.40	19	0.33	0.82	20	0.38	1.0	19
Mg	0.06	0.25	6	0.13	0.35	13	0.19	0.40	19
Al	1.2	1.8	44	1.5	1.9	53	2.4	2.1	75
Si	1.6	1.9	63	2.0	2.5	67	2.6	2.6	75
P	0.25	1	6			0			0
S	10.3	7.0	100	6.4	5.6	100	4.3	3.2	100
Cl	5.4	3.8	100	3.7	3.3	73	3.1	3.0	75
K	1.4	2.9	38	1.7	2.0	13	2.0	2.5	56
Ca	2	3.6	31	1.4	3.7	13	2.1	4.6	25
Fe	1.1	1.7	44	3.2	4.2	73	4.6	5.9	69

[a] $\bar{x}$, the percent composition of an element averaged over all particles; s, the population standard deviation; %, the percentage of particles that contained this element at concentrations greater than 1%.

Table III. Auger Data

at. range, %	virgin surface C	O	Al	Si	S	Cl	K	Ca	Fe	1 nm below virgin surface C	O	Al	Si	S	Cl	K	Ca	Fe	3 nm below virgin surface C	O	Al	Si	S	Cl	K	Ca	Fe
1-10			7	10	9	13	5	4	7	2		8	10	12	12	7	1	9			12	12	15	11	9	3	8
10-20	5				4	3	1							4			1	2					1			3	3
20-30	5	2			3					2				3					1								
30-40	3	1																	1								
40-50	2	6								1										1							
50-60		7																		2							
60-70	1									4										2							
70-80										4										5							
80-90										5										4							
90-100										1										2							

substrates, having been examined in the SEM, were then transferred to the scanning Auger system where, using the orientation markings on the foils, the same previously characterized particles could be examined with AES. These studies revealed a separation of the particles into two main groups: particles that are electrically conductive and consist mostly of carbon, and those which are electrically insulating and consist of a variety of elements (again, it is to be noted that EDX analysis cannot routinely detect elements of atomic number less than 11 and, hence, carbon cannot normally be detected by using EDX). The carbon particles are most likely soot (which is often intentionally produced in the furnace to improve radiative heat transfer (*16*)), while the insulating particles are the residue after combustion of the coal. The fly-ash particles that we studied in detail are the electrically insulating ones and, although such materials pose numerous problems for AES (as discussed elsewhere (*17*)), useful data can be obtained.

AES coupled with ion sputtering allowed depth profiling of the near-surface region (0–3 nm). Auger spectra were obtained at three different depths corresponding to (a) virgin surface, (b) 1 nm of surface material removed, and (c) 3 nm of surface removed. Results of these runs are shown in Tables II and III. As can be seen from an examination of these data, the particles were partially covered with a very thin (<1 nm) layer of carbon, probably in the form of hydrocarbon (AES cannot detect hydrogen), which was readily removed by ion sputtering. Also present in the virgin layer were S and Cl, which were removed to varying degrees as deeper depths were obtained. Even with the presence of this surface layer, the basic structural elements, Si, Al, and O were detected, thus indicating that these particles were not covered by a thick (>1 nm) layer of hydrocarbons. Also to be noted is the lack of heavy trace metals present on these particles (at the 1% level), which is consistent with results obtained by others (*18*). This is not to say that there are not trace metals on the surface of these particles but that, at the limited sensitivity of AES ($\simeq$1%), none could be detected. Figure 4 shows a sequence of histograms for the various elements found by Auger analysis at three different depths analyzed. Again, as with the EDX results, there is a wide variation in the elemental concentration from one particle to the next. The AES data were subjected to correlation examination between all possible pairs of elements for each sputtering depth. The only correlation of significance was between carbon and oxygen on the virgin surface, for which the correlation coefficient was $r = -0.93$. this large negative correlation indicates that on those particles that have a large surface-carbon overlayer, the surface oxygen is in very low concentration. The oxygen present on the virgin surface may be due to the adsorption of water vapor, which is ubiquitous in the vacuum chamber. The negative correlation may be an indication that surface carbon inhibits the coadsorption of water vapor and thus the presence of surface oxygen. (It is to be noted that AES is not capable of detecting the presence of hydrogen.)

Conclusions

The results of these experiments performed on single isolated fly-ash particles, collected within a smokestack, can be summarized as follows (some of the SEM measurements simply duplicate what has been done before, e.g., ref *1–10*).

I. SEM Studies. (a) 90–95% of the particles were spherical.

(b) Surface roughness varied from glassy smooth to quite rough.

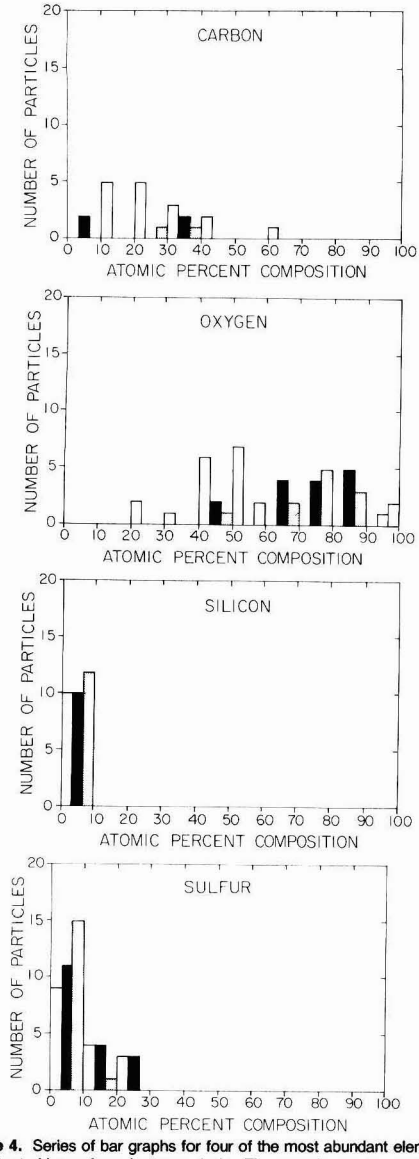

Figure 4. Series of bar graphs for four of the most abundant elements as detected by surface Auger analysis. The open bars represent data for the virgin surface while the solid bars and dotted bars are for 1 and 3 nm below the virgin surface, respectively.

(c) Approximately 60% of the particles showed indications of charging under the influence of the electron beam.

(d) A correlation of –0.63 existed between aluminum and iron in the bulk of the particles.

(e) The following elements were detected (detection limit ≃1%) and are presented in order of decreasing appearance in the particles: Al, Si, Fe, Ca, S, Cu, Cl, Mg, Cr, I, Ni, Zn, Na, Co, P, Mn, Sn, W, Ta, As, Pd, V.

II. AES Studies. (a) Charging particles accounted for approximately 90% of the particulates. (This percentage is different from that noted above for the SEM data due to differences in electron beam operating conditions of the SEM and the AES systems.)

(b) The electrically conductive particles consisted of carbon to at least the 30-nm depth and perhaps were solid carbon.

(c) The electrically insulating particles (1) contained many elements on the surface, (2) had a very thin layer of surface carbon (<1.0 nm), and (3) had a thicker layer of sulfur and chlorine (~3.0 nm). These elements were also present to approximately the same depth on the indium substrate. They are possibly due to gases present in the smokestack or from the adsorption of compounds containing these materials subsequent to the collection. The presence of these elements on the substrate as well as on the particles must be taken into account when attempting to draw conclusions from this data. And, in addition to carbon, sulfur, and chlorine in the near surface region, the insulating particles (4) contained the following elements (in decreasing abundance): Si, Al, O, Fe, Ca, K, Na, Mg. (It is to be remembered that AES is a very surface-sensitive technique and thus can only detect the elements present in the first few atomic layers.)

The elements detected showed large variation from particle to particle both for bulk X-ray analysis and for surface Auger analysis. In addition, very few high atomic number elements were detected (at concentrations >1%), and they showed no preferential surface segregation.

Acknowledgments

We thank Professor Dale Snider for help in accumulating and interpreting data and for help in the preparation of the manuscript and Dr. Roger Ford of Imperial Chemical Ind., Ltd., Cheshire, England, for help in preparing the manuscript.

Literature Cited

(1) Craig, N. L.; Harker, A. B.; Novakov, T. *Atmos. Environ.* **1973**, *8*, 15.
(2) Gutenmann, W. H. et al. *Science (Washington, D.C.)* **1976**, *191*, 966.
(3) Linton, R. W. et al. *Science (Washington, D.C.)* **1976**, *191*, 852.
(4) Eatoush, D. J. et al. *Atmos Environ.* **1978**, *12*, 263.
(5) Miller, S. S. *Environ. Sci. Technol.* **1978**, *12*, 1353.
(6) Lee, M. L. et al. *Science (Washington, D.C.)* **1980**, *207*, 186.
(7) Powell, C. J. *NBS Spec. Publ. No. 535*, February, 1980.
(8) Davison, D. L.; Gause, E. M. *NBS Spec. Publ. No. 533*, February 1980.
(9) Rothenberg, S. J.; Denee, P.; Holloway, P. *Appl. Spectrosc.* **1980**, *34*, 549.
(10) Lindfors, P. A.; Hovland, C. T. *Environ. Sci. Res.* **1978**, *13*, 349.
(11) Hosaka, S.; Kawamoto, Y.; Hashimoto, S. *J. Vac. Sci. Technol.* **1981**, *18*, 17.
(12) Hock, J. L.; Snider, D.; Ford, R.; Lichtman, D. *J. Vac. Sci. Technol.*, in press.
(13) Perera, F. P.; Ahmed, A. K. "Respirable Particles"; Ballinger: Cambridge, MA, 1979.
(14) Fisher, G. L. et al. *Environ. Sci. Technol.* **1978**, *12*, 447.
(15) Loh, A. Ph.D. Thesis, University of Illinois, 1976.
(16) Hart, A. B.; Lawn, C. J. *CEGB Res.* **1977**, *5*, 4.
(17) Hock, J. L.; Snider, D.; Kovacich, J.; Lichtman, D. *Appl. Surf. Sci.*, in press.
(18) Keyser, T. R.; Natusch, D. F. S.; Evans, C. A., Jr.; Linton, R. W. *Environ. Sci. Technol.* **1978**, *12*, 769.

Received for review October 13, 1981. Accepted February 19, 1982. Support for this work was given by the Electric Power Research Institute (Contract RP 1625-1).

Environ. Sci. Technol. 1982, 16, 428–432

Adsorption of Phthalic Acid Esters from Seawater

Kevin F. Sullivan, Elliot L. Atlas, and Choo-Seng Giam*

Department of Chemistry, Texas A&M University, College Station, Texas 77843

■ Controlled laboratory experiments have shown the influence of several factors on the adsorption of two phthalic acid esters. Di-*n*-butyl phthalate and bis(2-ethylhexyl) phthalate dissolved in seawater rapidly adsorb onto and desorb from three clay minerals, calcite, a sediment sample, and glass test tubes. The adsorption of phthalates is inversely related to the aqueous solubility of the two phthalates studied. An increase in the lipophilic character of the adsorbent or the salinity of the solution increases the amount of phthalate bound. The probable binding mechanisms include van der Waals forces and hydrophobic interactions.

Introduction

Phthalic acid esters (PAEs) are prevalent industrial chemicals that have been found in a variety of environmental samples. The annual production of PAEs in the United States more than doubled from 1960 to 1970 and has since remained in excess of one billion pounds (*1*). Bis(2-ethylhexyl) phthalate (BEHP), which accounts for nearly one-third of the production, and di-*n*-butyl phthalate (DBP) are the most frequently identified PAEs in diverse environmental samples. These environmental samples include ground water (*2*), river water (*3*), drinking water (*4*), open ocean water (*5*), urban and suburban air (*6*), marine air (*7*), fish (*8, 9*), crustaceans (*10*), seal (*11*), soil humates (*12*), lake sediments (*8*), and marine sediments (*5*). Of particular importance is the fact that these compounds are being transported to the oceans where their fate is largely unknown.

The distribution and fate of a compound in the oceans is largely controlled by transport mechanisms within phases and across phase boundaries. Adsorption of a compound from solution is one mechanism that can significantly influence the transport and distribution in the ocean environment. To our knowledge, however, no studies have been reported on the adsorption of the ubiquitous phthalate esters. Several studies have been done concerning the adsorption from aqueous solutions of various pesticides onto clay minerals (*13–16*), humates (*16, 17*), and sediments (*17–19*). Weber (*20*) reviewed the factors affecting adsorption and the mechanisms of adsorption for numerous classes of pesticides. The adsorption reactions of the persistent polychlorinated biphenyls also have been studied experimentally (*21, 22*) and theoretically (*22*). Representative biogenic compounds demonstrate adsorption behavior that is similar to that of the synthetic organics (*23–25*). In particular, the adsorption of different classes of compounds is influenced by the mineralogy of the adsorbing particle and by the presence of other naturally occurring organics.

The desorption process is as important as adsorption in understanding the distribution of organic compounds. The desorption of DDE and lindane from settling particles once they were below a freshwater thermocline caused the pesticides to reach uniform aqueous concentrations prior to the autumn breakdown of the thermal stratification (*26*). Sediments contaminated with DDT and polychlorinated biphenyls by a submarine outfall acted as a source of the pollutants to the surrounding water and biota well after the abatement of the initial source (*27*). Whether sediments act as a final repository or as a secondary source of pollutant is determined by the adsorption and desorption reactions. For help in understanding the fate of phthalic acid esters in the marine environment, an investigation of their adsorption and desorption reactions was done. To examine these reactions, we chose to first characterize the adsorption/desorption behavior of phthalates on common inorganic components of marine sediments. This behavior is then compared to adsorption reactions on a natural marine sediment.

Methods

Apparatus. Two electron-capture gas chromatographs were used for quantitation of the nonradioactive phthalates and for checking the cleanliness of the glassware. A Tracor MT-220 gas chromatograph was fitted with 6-ft glass columns packed with 3% SE-30 on Gas-chrom Q (100–120 mesh) or 1.95% QF-1/1.5% OV-17 on Supelcoport (100–120 mesh). A Hewlett-Packard 5700 A gas chromatograph was fitted with a 6-ft glass column packed with 1.5% SP-2250/1.95% SP-2401 on Supelcoport (100–120 mesh). The carrier gases for the instruments were nitrogen at 60 mL/min and 95% argon/5% methane at 40 mL/min, respectively. External standards of the phthalates were injected along with the samples and formed a linear calibration curve for the quantitation of samples.

The radioactive phthalates were quantitated on one of three liquid scintillation counters: a Beckman LS-100C, a Beckman LS-7000, or a Beckman LS-9000. The samples were counted for a minimum of 20 min or until enough data had been accumulated so that there was only a 2.0% probability that the actual counts per minute (cpm) were greater than twice the sample standard deviation away from the measured cpm. All the samples for the adsorption studies had negligible and constant quench.

Other apparatus included a centrifuge and a constant temperature bath. The centrifuge was an Adams analytical angle-head centrifuge with a specified speed of 3400 rpm (1550*g*). The constant-temperature bath consisted of a Haake heat bath and circulator regulated against a Polyscience KR-30 refrigerated chiller.

Glassware. The glass containers for the adsorption experiments and for the analysis of phthalates were made of borosilicate glass and had Teflon-lined caps. The vessels for the adsorption experiments were 16 × 125 mm screw-cap culture tubes. The extracts of the various phases for nonradioactive phthalates were stored in 3-dram vials.

Meticulous cleaning of glassware was required to reduce the background contamination by the ubiquitous phthalates. The test tubes and vials were placed in a 300 °C oven overnight and, once cool, were rinsed twice with acetone and repeatedly with petroleum ether. The glassware was acceptable when contamination corresponding to less than 1 ng of phthalate per piece of glassware was measured, which corresponds to <0.5% of the nonradioactive phthalate used in an experiment per test tube.

The liquid scintillation vials of borosilicate glass were cleaned of contaminating radiation by sequential rinses of methanol and acetone. The final rinse was evaporated to dryness, dissolved in 10 mL of scintillation cocktail, and counted along with a vial containing only cocktail. A

 0013-936X/82/0916-0428$01.25/0

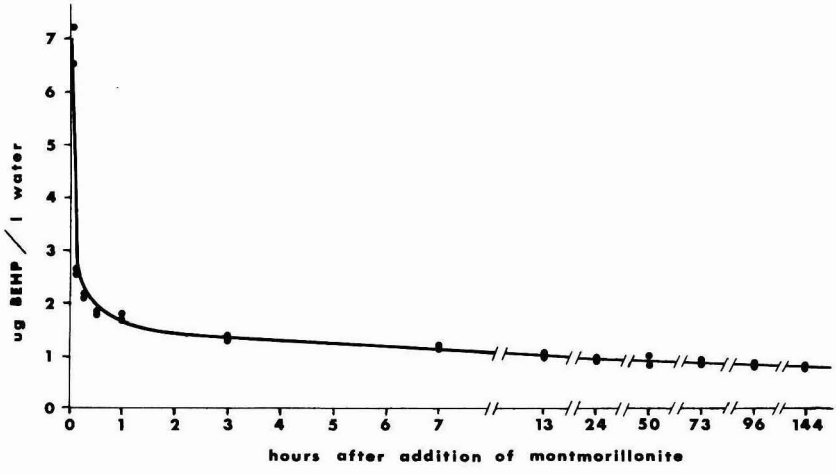

Figure 1. Rate of removal of BEHP from seawater by montmorillonite.

difference between the vials' cpm no greater than the counting error was necessary before the rinsed vials were used.

Adsorbate Solutions. The seawater was natural seawater that had most of its organic compounds removed before being spiked with phthalates. The seawater was cleaned by passing it through a small glass column containing Amberlite XAD-2 and charcoal. The removal of the organic solutes by the Amberlite-charcoal column did not change the pH (8.10 ± 0.02) or salinity (36.0 ± 0.5‰) of the seawater. The distilled water used in one of the experiments was preextracted with petroleum ether to remove background contamination. Subsequent experiments showed no effect of residual solvent on the adsorption of phthalate esters.

The seawater was spiked with phthalate esters in acetone solution. Small amounts of sodium azide were added to the aqueous solutions to prevent microbial degradation of the phthalates.

Adsorbents. The solid adsorbents used in the adsorption experiments were montmorillonite, calcium montmorillonite, kaolinite, calcite, and a marine sediment sample. The mineralogical purity of the clay minerals and calcite were determined by X-ray diffraction. Dry slide mounts of the kaolinite and calcium montmorillonite showed both to be >90% pure. A slide mount of the montmorillonite adsorbent indicated that >75% of the material was a smectite, while the remainder was kaolinite and quartz. The calcite was reagent grade calcium carbonate, and its mineralogy was confirmed by a powder diffraction analysis.

The sediment sample was collected on the continental shelf off Texas at 28°10.4' N and 96°24.3' W. This position has been sampled regularly and the following sediment texture of the area determined: 43.7% sand, 25.8% silt, and 30.4% clay. Sediments in the area typically contain 1% organic matter or less (Brooks, private communication). The sediment sample was dried in a 60 °C oven, and the large clumps were broken up before the sediment was used.

The adsorbents were cleaned by sequential solvent extraction prior to the adsorption studies so that the effect of the clay mineralogy on adsorption could be studied separate from the effect of the organic content of the adsorbent.

Adsorption Studies. For the adsorption experiments, varying amounts of the solid adsorbent were dispersed in seawater to which known amounts of phthalate had been added (Table I). Each experiment consisted of two blanks and from 5 to 11 sample test tubes. The sample test tubes contained phthalate-spiked seawater and various amounts of the solid adsorbent. One of the blanks contained only phthalate-spiked water (no-solid blank) and would show any loss of phthalate from the aqueous phase not caused by adsorption onto the solid adsorbent. The other blank contained unspiked water plus solid adsorbent (no-phthalate blank); background contamination in the analyses would be evident in this blank.

Time was allowed for the solid adsorbent to reach equilibrium before and after the addition of the phthalate-spiked solutions. After the aliquots of the solid adsorbent were weighed and placed in the test tubes, 2 mL of unspiked seawater was added to each test tube. After several hours, 10 mL of spiked seawater was added to the no-solid blank and the sample test tubes, while 10 mL of unspiked water was added to the no-phthalate blank test tube. The test tubes were kept in a 25 °C water bath and were inverted repeatedly to disperse the solids. A kinetic study of phthalate adsorption on montmorillonite clay demonstrated that after 12 h the phthalate adsorption reached at least 90% of the equilibrium value (Figure 1).

After at least 12 h, the test tubes were removed from the water bath and centrifuged for 10 min. The aqueous phases were extracted twice with 2-mL aliquots of isooctane. The combined extracts were evaporated to dryness under a stream of nitrogen and were redissolved in isooctane or liquid scintillation cocktail depending on the method of quantitation.

The desorption of phthalates from the solids was studied by replacing the phthalate-spiked aqueous phases with unspiked seawater. After the initial aqueous phases had been removed from the test tubes containing the centrifuged solids, 10 mL of unspiked seawater was added to each test tube. Then the test tubes and aqueous phases were treated the same as during the adsorption process. The addition of unspiked seawater to the test tubes was repeated as many times as desired to yield several desorption steps.

After all the desorption steps, the amount of phthalate bound to the solid adsorbents was determined by extrac-

Table I. Amount of Adsorbent and Phthalate Used in Adsorption Experiments

adsorbate	adsorbent	range of adsorbent, mg	initial concn of phthalate, μg/L
BEHP	montmorillonite	6–80	377
[^{14}C]BEHP	montmorillonite	5–77	13
[^{14}C]BEHP	kaolinite	6–126	13
BEHP	calcite	23–178	208
[^{14}C]BEHP	calcite	3–210	7
[^{14}C]BEHP	calcium montmorillonite	6–80	16
[^{14}C]BEHP	sediment	11–83	6
[^{14}C]BEHP	montmorillonite (distilled water)	6–80	9
DBP	montmorillonite	55–687	3930
[^{14}C]DBP	montmorillonite	6–58	22
DBP	kaolinite	25–621	3840
[^{14}C]DBP	kaolinite	4–64	19
DBP	calcite	30–435	3710
[^{14}C]DBP	calcite	8–94	25
DBP	calcium montmorillonite	26–542	3440
[^{14}C]DBP	calcium montmorillonite	7–90	27
DBP	sediment	9–79	19

tion with acetonitrile and quantitation by gas chromatography or liquid scintillation counting. An analogous experiment for BEHP adsorption on montmorillonite was also performed with solvent-extracted distilled water.

Results and Discussion

In order to compare the results among experiments, a mathematical description of the adsorption behavior that is independent of the amount of solid adsorbent and of the aqueous concentration of phthalate is needed. A linear relationship between the amount of adsorbate bound per gram of solid adsorbent and the aqueous concentration of adsorbate adequately described the adsorptive behavior of biogenic materials (*23*) and chlorinated hydrocarbons (*22*) and was checked for its suitability with phthalates. A partition coefficient, K, is defined as S/C, where S is the ng of phthalate/mg of adsorbent and C is the ng of phthalate/mL of water. This coefficient was determined for each of the sample aqueous phases involved in adsorption (K_a) or desorption (K_d) and for the no-solid blanks (K_b).

The K_b values represent adsorption onto the test tube, which amounted to as much as 45% of the total BEHP in the test tubes, and they were used to refine the K_a and K_d values. The uncorrected K_a and K_d values involved the adsorption onto and desorption from the solid adsorbents plus the test tubes. The average K_b values, 0.52 for DBP and 10.3 for BEHP, were multiplied by the aqueous concentration to estimate the amount of phthalate bound to the glass test tube in contact with each aqueous phase. Partition coefficients were corrected for the phthalate bound to the glass test tubes by using the equation

$$\frac{P - (K_b C)}{A} C^{-1} = K \text{ (corrected)}$$

where P is the nanograms of phthalate extracted from the solid adsorbent and test tube and A is the milligrams of solid adsorbent.

The corrected K_a and K_d values were averaged and are presented with the standard error of the mean in Table II. The relative standard errors for corrected K_a values for most of the adsorbate–adsorbent combinations were smaller than the corresponding values for the uncorrected K_a values. This increased agreement of the partition coefficients for phthalate adsorption within a set of test tubes verifies that the correction for adsorption onto the glass is reasonable, which is in contrast to results reported for DDT adsorption by Picer (*28*). The unrealistic results for DDT adsorption when the data were corrected for adsorption by the glass vessels caused Picer to use the uncorrected data.

An agreement between the adsorption partition coefficients for experiments using the same adsorbent and phthalate, but at different aqueous concentrations, would indicate that the linear relationship adequately describes the adsorption behavior over the concentration range studied. Even for aqueous solutions of BEHP differing by orders of magnitude in concentration there is no statistically significant difference in the adsorption partition coefficients. For the calcite experiments with [^{14}C]BEHP and BEHP, the original aqueous concentrations are 7.3 and 208 μg/L and their K_a values are 1.8 ± 0.4 and 1.8 ± 0.8, respectively. For the montmorillonite experiments with [^{14}C]BEHP and BEHP, the original aqueous concentrations are 13 and 377 μg/L and the K_a values are 12.7 ± 0.8 and 11.4 ± 1.1, respectively. The linear relationship is adequate for the BEHP data, which show extensive adsorption.

Experiments using [^{14}C]DBP and DBP with the same adsorbent are significantly different, which could be due to the small adsorption of DBP and the relatively large

Table II. Average Corrected Partition Coefficients for the Adsorption and Desorption of Phthalates

adsorbate	adsorbent	adsorption step	first desorption step	second desorption step	third desorption step
BEHP	montmorillonite	11.4 ± 1.1	13.0 ± 1.8	11.3 ± 1.3	
[^{14}C]BEHP	montmorillonite	12.7 ± 0.8	9.0 ± 0.8	7.5 ± 0.9	9.2 ± 1.4
[^{14}C]BEHP	kaolinite	12.1 ± 1.8	15.3 ± 3.0	10.3 ± 1.5	
BEHP	calcite	1.8 ± 0.8	2.3 ± 0.7		
[^{14}C]BEHP	calcite	1.8 ± 0.4	3.5 ± 1.5	4.4 ± 2.0	3.9 ± 2.0
[^{14}C]BEHP	calcium montmorillonite	1.3 ± 0.3	6.2 ± 2.5	8.1 ± 3.6	7.1 ± 3.4
[^{14}C]BEHP	sediment	5.1 ± 1.0	13.9 ± 2.2		
[^{14}C]BEHP	montmorillonite (distilled water)	4.6 ± 0.3	9.8 ± 1.1		
DBP	montmorillonite	0.044 ± 0.005	0.078 ± 0.021		
[^{14}C]DBP	montmorillonite	0.019 ± 0.002	0.040 ± 0.010	0.396 ± 0.167	4.29 ± 2.54
DBP	kaolinite	0.020 ± 0.003	0.131 ± 0.052		
[^{14}C]DBP	kaolinite	0.004 ± 0.001	0.105 ± 0.016	0.641 ± 0.344	4.11 ± 1.92
DBP	calcite	0.005 ± 0.001			
[^{14}C]DBP	calcite	0.010 ± 0.002	0.029 ± 0.009	0.071 ± 0.022	
DBP	calcium montmorillonite	0.004 ± 0.001			
[^{14}C]DBP	calcium montmorillonite	0.036 ± 0.017	0.058 ± 0.020	0.096 ± 0.036	
[^{14}C]DBP	sediment	0.149 ± 0.017	0.198 ± 0.023		

correction for adsorption of DBP onto the glass test tubes. For the experiments using the cleaned adsorbents, no more than 11% of the total DBP added to the test tubes was adsorbed, which can be compared to a minimum 78% of the total BEHP. The correction for adsorption onto the glass test tubes decreases the partition coefficients since less phthalate is considered to be on the solid adsorbent. The uncorrected K_a values for DBP are an average 2.8 ± 1.8 times larger than the corrected partition coefficient. This relatively large correction and the insubstantial adsorption of DBP could cause some of the discrepancies between the partition coefficients for the DBP and [^{14}C]DBP studies. Even though the partition coefficients for DBP are not independent of the aqueous concentration, the K_a values for DBP can be compared to the K_a values for BEHP.

The smaller adsorption of DBP vs. BEHP on all the adsorbents correlates with the greater water solubility of DBP. The solubilities of DBP and BEHP have been reported to be 28 and 18 mg/L of distilled water, respectively, by Morita (*3*) and to be 3.2 and 1.2 mg/L of artificial seawater, respectively, by Kakareka (*29*). The most concentrated solutions used in the adsorption experiments were 4.4 mg of DBP/L, 0.6 mg of BEHP/L, 0.04 mg of [^{14}C]DBP/L, and 0.02 mg of [^{14}C]BEHP/L. Even with the solutions of radioactive phthalates whose concentrations were well below the phthalates' solubility limits, the partition coefficients for BEHP are several orders of magnitude greater than the coefficients for DBP. If this inverse relationship is true then one might expect less adsorption of BEHP from fresh water.

Our experiments confirmed that the adsorption of BEHP onto montmorillonite is less from a distilled water solution than from seawater. The greater ionic strength of the seawater likely decreases the solubility of the nonionic phthalate and results in a greater adsorption partition coefficient for the seawater solution, 12.7 ± 0.84, than for the distilled water solution, 5.10 ± 1.04. The structural features of the phthalates responsible for their different solubilities could also be responsible for their different adsorptivities.

The structural difference between BEHP and DBP is the size of the alkyl chains; the longer alkyl chains of BEHP seem to be responsible for its greater adsorption via van der Waals forces and hydrophobic interactions. Phthalic acid esters are nonionic molecules that do not contain hydrogen atoms attached to electronegative atoms; therefore, electrostatic attraction and hydrogen bonding can be eliminated as major binding mechanisms. Hydrophobic interactions were postulated as the mechanisms for the adsorption of aromatic compounds on aluminosilicates (*3*) and soils (*31*), although the extent of adsorption was small. The negligible adsorption due to an aromatic ring is evident in the small adsorption of DBP. BEHP can be bound not only by the aromatic ring but also by the eight-carbon alkyl chains, which are longer than the five-carbon length found to be the minimal size necessary for significant adsorption of various classes of compounds (*32*). For hydrophobic interactions and van der Waals attraction, the extent of adsorption should depend upon available surface area.

The ranking of the K_a values for BEHP on the cleaned adsorbents (montmorillonite ≃ kaolinite > calcite ≃ calcium montmorillonite) could be due to differences in the surface areas for the first three adsorbents. The K_a values for montmorillonite, 12.7 ± 0.8, and kaolinite, 12.1 ± 1.8, are not statistically different; however, the K_a value for calcite, 1.8 ± 0.4, is significantly smaller. The specific surface area for calcite particles was estimated to be 2.5 m^2/g by treating the particles as spheres with a minimum diameter of 0.1 μm, which was determined via microscopic examination. This estimate of the surface area of the calcite particles is considerably less than characteristic surface areas of clay minerals (50–750 m^2/g (*20*)). The relatively small adsorption onto calcium montmorillonite could be explained if the interlamellar surfaces of the calcium montmorillonite were inaccessible to BEHP. Experiments have shown that the extent of adsorption correlated with the available surface area (*15*, *33*), while other researchers have found the correlation to be poor (*14*, *23*).

In our experiments the organic content of the adsorbent also influences the extent of adsorption, which substantiates hydrophobic interactions as an adsorption mechanism. Solvent-extracted montmorillonite adsorbed 3% less DBP than the unextracted montmorillonite, while cleaned calcium montmorillonite adsorbed 14% less BEHP than the unextracted calcium montmorillonite. The greatest difference in adsorption behavior was seen with the actual sediment sample and DBP. The sediment sample is predominantly sand-size particles and so has less surface area per gram than the clay minerals; however, the natural organic component of the sediment was left intact. The lipophilic character of the sediment contributed to the K_a for DBP (0.149 ± 0.017), which is an order of magnitude greater than for DBP on any other adsorbent. An increase in the lipophilicity of the solid adsorbent has been reported to increase the adsorption of polychlorinated biphenyls (*21*), DDT (*17*), 2,4-D (*16*), and lindane (*19*).

Hydrophobic and van der Waals adsorption on clay minerals involves nonspecific interactions that should allow mass transfer to and from the surface of the clay minerals. For the BEHP studies, between 2% and 7% of the total phthalate desorbed into the unspiked seawater that replaced the phthalate-spiked seawater solutions. After equilibrium with the solid adsorbents, the spike solutions retained between 3% and 22% of the total BEHP with five of the seven studies falling between 2% and 7%. The aqueous phases accommodated comparable amounts of BEHP regardless of the direction of mass transfer.

All of the studies with BEHP exhibit extensive desorption, and most of the studies show completely reversible adsorption. If adsorption is completely reversible, one would expect the K_a and K_d values to be the same. There is no statistically significant difference between the K_a and K_d values for the BEHP studies with calcium montmorillonite, kaolinite, and calcite. Substantial irreversibility is observed with the sediment sample, whose K_a, 5.1 ± 1.0, is notably smaller than its K_d, 13.9 ± 2.2. The larger K_d value indicates that the sediment is retaining proportionately more BEHP than expected for a reversible equilibrium. However, we do not know if this apparent irreversible behavior would be smaller if the sediment/water mixture were allowed more time to equilibrate. It is evident though, that the adsorption of BEHP by the sediment involves factors other than merely equilibrium with clay minerals. The long-term significance of such factors on sorption processes in the marine environment has yet to be determined. These factors might include the extensive van der Waals forces and hydrophobic interactions of an organic complex. Varying degrees of irreversibility for the adsorption of DDT (*17*, *18*) and polychlorinated biphenyls (*21*) also have been attributed to the organic material in the adsorbents.

To determine how representative of environmental processes the partition coefficients for the phthalates are,

we calculated partition coefficients for environmental samples and then compared them to the laboratory partition coefficients. By division of the average phthalate contents of sediment samples by the average concentrations of phthalates in surface water for the Mississippi Delta (5), approximate partition coefficients for DBP, 0.14, and for BEHP, 1.00, are obtained. Surprisingly these partition coefficients are close to the K_a values for the sediment adsorption studies with DBP, 0.149 ± 0.017, and BEHP, 5.1 ± 1.0, indicating that laboratory experiments can approximate environmental processes. However, caution should be used in applying laboratory-determined partition coefficients to field situations. Kinetic factors, as well as the quantity and character of the organic components in natural sediments, may significantly influence the long-term behavior of phthalates in marine sediments.

Conclusions

Adsorption experiments for di-*n*-butyl phthalates and bis(2-ethylhexyl) phthalate on three clay minerals, calcite, and a sediment sample were done to elucidate some of the factors and mechanisms controlling the transfer of the phthalic acid esters between the aqueous and particulate phases in the oceans. A kinetic study showed that most of the adsorption of BEHP occurred within the first hour and that after 12 h the solid adsorbent and aqueous phase were essentially at equilibrium. The adsorptive behavior was described adequately by partition coefficients relating the amount of phthalate in the aqueous phase to the amount of phthalate bound to the solids at equilibrium. Both phthalates adsorbed onto the solid adsorbents and the glass test tubes.

The effect on adsorption of the solubility of the phthalates, salinity, the surface area of the adsorbent, and the organic content of the adsorbent were studied. The extent of adsorption increased with an increase in salinity or a decrease in the solubility of the phthalate. The expected positive correlation between the adsorption of BEHP and the surface area of the adsorbent was apparent for calcite in comparison to some of the clay minerals but not for comparison among the clay minerals. An increase in the lipophilicity of the adsorbent increased the adsorption of both phthalates.

Extensive desorption of BEHP occurred for all the adsorbents, and most of the adsorbents exhibited completely reversible adsorption. Comparable amounts of BEHP were extracted from adsorption and desorption aqueous phases for all the adsorbents. For kaolinite, calcite, and calcium montmorillonite the adsorption and desorption partition coefficients for BEHP were statistically identical, indicating complete reversibility. The sediment sample showed significant irreversibility of adsorption, which suggests that marine sediment may act as a final repository of phthalic acid esters.

Acknowledgments

We would like to express our appreciation to J. B. Dixon and M. V. Fey for the X-ray analyses.

Literature Cited

(1) U.S. International Trade Commission, "Synthetic Organic Chemicals"; U.S. Production and Sales, 1960–1978.
(2) Robertson, James M. *Water Sewage Works* **1976**, *123*, 58.
(3) Morita, M.; Nakamura, H.; Mimura, S. *Water Res.* **1974**, *8*, 781.
(4) Keith, L. H.; Garrison, A. W.; Allen, F. R.; Carter, M. H.; Floyd, T. L.; Pope, J. D.; Thurston, A. D., Jr. "Identification and Analysis of Organic Pollutants in Water"; Ann Arbor Science: New York, 1976.
(5) Giam, C. S.; Chan, H. S.; Neff, Grace S.; Atlas, Elliot L. *Science (Washington, D.C.)* **1978**, *199*, 419.
(6) Bove, John L.; Daven, Paul; Kukreja, Ved P. *Int. J. Environ. Anal.* **1978**, *5*, 189.
(7) Giam, C. S.; Atlas, Elliot; Chan, H. S.; Neff, Grace S. *Rev. Int. Oceanogr. Med.* **1977**, *47*, 79.
(8) Mayer, Foster L., Jr.; Stallings, David L.; Johnson, James L. *Nature (London)* **1972**, *238*, 411.
(9) Williams, David T. *J. Agric. Food Chem.* **1973**, *21*, 1128.
(10) Chan, H. S. Ph.D. Dissertation, Texas A&M University, College Station, TX, 1975.
(11) Zitko, V. *Int. J. Environ. Chem.* **1973**, *2*, 241.
(12) Kahn, S. U.; Schnitzer, Morris *Geochim. Cosmochim. Acta* **1972**, *36*, 745.
(13) Bowman, B. T.; Sans, W. W. *J. Soil Sci. Soc. Am.* **1977**, *41*, 514.
(14) Huang, Ju-Chuang; Liao, Cheng-Lun *J. Sanit. Eng. Div., Am. Soc. Civ. Eng.* **1970**, *96*, 1057.
(15) Aly, Osman M.; Faust, Samual D. *J. Agric. Food Chem.* **1964**, *12*, 541.
(16) Khan, Shahamat *Environ. Sci. Technol.* **1974**, *8*, 236.
(17) Pierce, Richard H., Jr.; Olney, Charles E.; Felbeck, George T., Jr. *Geochim. Cosmochim. Acta* **1974**, *28*, 1061.
(18) Picer, N.; Picer, M.; Strohal, P. *Water Air Soil Pollut.* **1977**, *8*, 429.
(19) Lotse, Erik G.; Graetz, Donald A.; Chesters, Gordon; Lee, Gerherd B.; Newland, Leo W. *Environ. Sci. Technol.* **1968**, *2*, 353.
(20) Weber, J. B. "Fate of Organic Pesticides in the Aquatic Environment"; Symposium, American Chemical Society Division of Pesticide Chemistry, Los Angeles, CA, 1971.
(21) Hague, R.; Schmedding, D. W.; Freed, V. H. *Environ. Sci. Technol.* **1974**, *8*, 139.
(22) Dexter, R. N.; Pavlou, S. P. *Mar. Chem.* **1978**, *7*, 67.
(23) Hedges, John I. *Geochim. Cosmochim. Acta* **1977**, *41*, 1119.
(24) Meyers, P. A.; Quinn, J. G. *Geochim. Cosmochim. Acta* **1973**, *37*, 1745.
(25) Muller, Peter J.; Suess, Erwin *Geochim. Cosmochim. Acta* **1977**, *41*, 941.
(26) Hamelink, J. L.; Waybrant, R. C. Tech. Rep. No. 44, Purdue University Water Resource Center, West Lafayette, IN, 1973.
(27) Young, David R.; McDermott-Ehrlich, Diedre; Heesen, Theodore *Mar. Pollut. Bull.* **1977**, *8*, 254.
(28) Picer, M.; Picer, N.; Strohal, P. *Sci. Total Environ.* **1977**, *8*, 159.
(29) Kakareka, J. P. M.S. Thesis, Texas A&M University, College Station, TX, 1974.
(30) Healy, Thomas W. "Organic Compounds in Aquatic Environments"; Marcel Dekker: New York, 1971.
(31) McBride, M. B.; Pinnavaia, T. J.; Mortland, M. M. "Fate of Pollutants in the Air and Water Environments"; Wiley: New York, 1977.
(32) Hoffman, R. W.; Brindley, G. W. *Geochim. Cosmochim. Acta* **1960**, *20*, 15.
(33) Boucher, F. R.; Lee, G. F. *Environ. Sci. Technol.* **1972**, *6*, 538.

Received for review June 23, 1981. Revised manuscript received March 5, 1982. Accepted March 14, 1982. This work was supported by the National Science Foundation, Grant Nos. OCE76-14148 and OCE77-12482, and in part by the Robert A. Welch Foundation.

Environ. Sci. Technol. 1982, 16, 433–436

Mineralization of Linear Alcohol Ethoxylates and Linear Alcohol Ethoxy Sulfates at Trace Concentrations in Estuarine Water

Robert D. Vashon* and Burney S. Schwab

Environmental Safety Department, The Procter & Gamble Company, Ivorydale Technical Center, Cincinnati, Ohio 45217

■ The rate and extent of mineralization (ultimate biodegradation) of linear alcohol ethoxylates (LAE), a class of nonionic surfactants, and of linear alcohol ethoxy sulfates (LAES), a class of anionic surfactants, were measured in water from Escambia Bay, FL (EBW). Results indicate that mineralization of LAE and LAES trace concentrations in estuarine water is rapid and extensive. Studies were conducted on four pure chain length materials ($*C_{16}E_3$, $C_{12}*E_9$, $C_{16}E_9S$, $C_{16}*E_3S$) labeled with ^{14}C either at the α-alkyl carbon or uniformly in the ethoxylate chain. The sulfate moiety had no effect on the rate or extent of mineralization of either the alkyl or the ethoxylate chains of LAES. Kinetics of mineralization of α-alkyl carbon were exponential (first order) over a concentration range 850 ng/L to 140 μg/L with a half-life for α-alkyl carbon of 2.1 days. Kinetics of mineralization of ethoxylate carbon were exponential at an initial concentration of 1 μg/L or less of LAE or LAES, with a half-life of 6.3 days, but linear or sigmoidal at higher concentrations.

Introduction

Primary biodegradation of linear alcohol ethoxylates (LAE), a class of nonionic surfactants, has been demonstrated in both fresh water and sea water (*1*). Mineralization (ultimate biodegradation) of the carbon in these compounds to CO_2 by bacteria in synthetic media occurs as well (*2, 3*). While both the ethoxylate and alkyl moieties are biodegradable, there is evidence that the rate of ethoxylate degradation is somewhat slower (*4, 5*). The anionic surfactants, linear alcohol ethoxy sulfates (LAES), have been shown to degrade in laboratory media (*6, 7*). Ultimate biodegradation of LAE or LAES in estuarine water by indigenous microorganisms has not been reported.

The initial concentration of LAE or LAES used in previous reported studies was 10 mg/L or greater. This is considerably higher than the concentrations expected to be present in estuarine water (*8*). Recent reports suggest that xenobiotic chemicals may not degrade at concentrations below a certain "threshold" (*9, 10*). However, saturation-kinetic models of enzyme activity (*11*) suggest that mineralization rates should be proportional to concentration at concentrations below those supporting microbial growth. The objective of this study was to measure the rate and extent of mineralization of LAE and LAES at environmentally relevant trace concentrations in estuarine water.

Experimental Section

Chemicals. The LAE's used in this study were pure (both alkyl and ethoxylate) chain length $CH_3(CH_2)_{10}CH_2(OCH_2CH_2)_9OH$ [$C_{12}*E_9$] uniformly labeled with ^{14}C in the ethoxylate chain and $CH_3(CH_2)_{14}CH_2(OCH_2CH_2)_3OH$ [$*C_{16}E_3$] ^{14}C labeled at the α carbon in the alkyl chain. The LAES's studied were pure chain length $CH_3(CH_2)_{14}CH_2(OCH_2CH_2)_9OSO_3^-$ [$*C_{16}E_9S$] ^{14}C labeled at the α-alkyl carbon and $CH_3(CH_2)_{14}CH_2(OCH_2CH_2)_3OSO_3^-$ [$C_{16}*E_3S$] uniformly ^{14}C labeled in the ethoxylate chain.

Ethoxylate-labeled LAE was synthesized via condensation of [^{14}C]ethylene oxide with the appropriate alcohol. Alkyl-labeled LAE was prepared by reacting α-[^{14}C]alcohol with a previously synthesized ethoxylate chain. Purity was determined by radio TLC on silica gel and gas chromatography with FID and radiochemical detection. $*C_{16}E_3$ had a specific activity of 2.8 $\mu Ci/mg^{-1}$ and a radiochemical purity >98%. $C_{12}*E_9$ had a specific activity of 3.78 $\mu Ci/mg^{-1}$ and a radiochemical purity of 70–80%, with $C_{12}*E_8$ as the major contaminant. Further details on the synthesis and purification of these compounds can be found elsewhere (*12*).

Sulfation of LAE to form LAES was accomplished by reacting LAE with $ClSO_3H$. Following cleanup, the $*C_{16}E_9S$ had a specific activity of 1.4 $\mu Ci/mg$ and a radiochemical purity of >95%. $C_{16}*E_3S$ was 85% radiochemically pure and had a specific activity of 2.2 $\mu Ci/mg$.

Biodegradation Assays. Estuarine water for biodegradation assays was collected from Escambia Bay, Florida and shipped to our laboratory in Cincinnati, Ohio. Samples of Escambia Bay water (EBW) vary in salinity from 22‰ to 33‰ depending on the relative contributions from the Escambia River and from Pensacola Bay.

This proportion varies with tidal stage and river flow volume. The sample used in this work had a salinity of 28‰. Analyses showed the concentration of total organic carbon to be less than 1 mg/L, of total nitrogen to be less than 0.5 mg/L, and of total phosphate to be less than 20 μg/L. Asays began within 48 h of collection. EBW contained 5×10^4 colony forming units/mL able to grow on nutrient agar of the same salinity as the water.

Ultimate biodegradation was monitored by measurement of the $^{14}CO_2$ produced from the ^{14}C-labeled compound. Test compounds were added to 200 mL of EBW at the concentrations shown in Table I to give 5, 50, and 500 dpm/mL in stoppered 500-mL flasks. Periodically, the contents of the flasks were acidified (<pH 2) with 0.1 N HCl, the head space was flushed with N_2, and evolved $^{14}CO_2$ was trapped in 2 mL of 2-methoxyethanolamine. The trapping fluid was added quantitatively to 18 mL of liquid scintillation cocktail (Amersham spectrafluor PPO/POPOP in ethanol–toluene). Radioactivity was assayed in a ISOCAP 300 (Nuclear, Chicago) liquid scintillation counter with quench correction by the external standards method.

Kinetics and Data Analysis. The rate of biodegradation of an organic compound is a function of the level of necessary enzymatic activities present during biodegradation and of the rate of change of those levels resulting from microbial growth. The exact nature of this function is not known, but empirical saturation-kinetic models have been used to describe enzymatic activity (*11*) and microbial growth (*13*). The generalized models

$$R = R_{max}S/(K_m + S) \quad (1)$$

where R = reaction velocity (Michaelis (*11*) or specific growth constant (Monod (*13*)), R_{max} = asymptotic maximum value of R (at enzyme saturation, or when something other than substrate is growth-rate limiting), K_m = saturation coefficient numerically equal to S at $0.5R_{max}$, S = substrate concentration, reduce to

$$R \approx R_{max}S/K_m \quad (2)$$

when $K_m \gg S$.

0013-936X/82/0916-0433$01.25/0

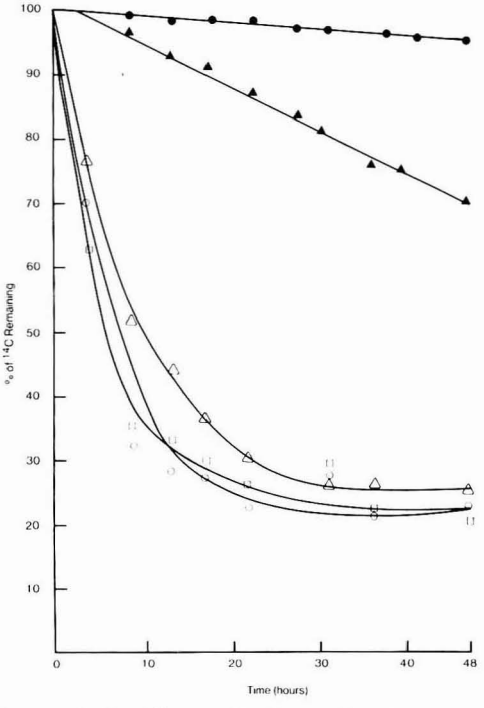

Figure 1. Kinetics of ^{14}C loss during biodegradation of glucose. D-[U-^{14}C]glucose was added to EBW. Periodically, radioactivity of the solution was assayed by LSC. Initial concentrations of glucose were 10 mg/L (●), 1 mg/L (▲), 100 μg/L (△), 10 μg/L (□), and 1 μg/L (○).

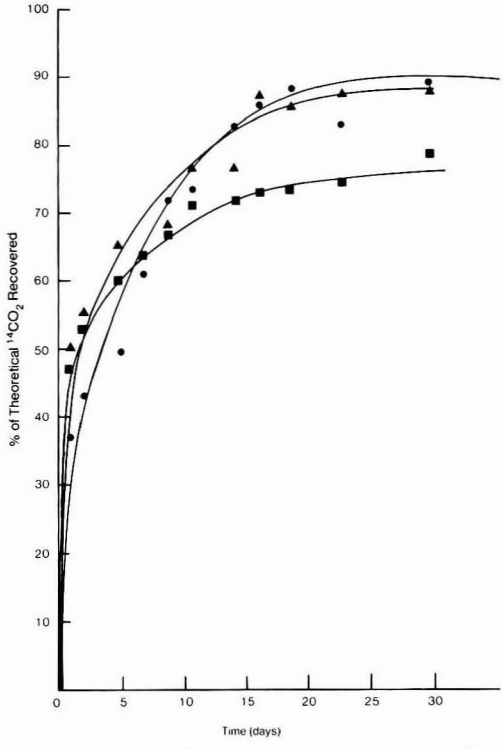

Figure 2. Kinetics of CO_2 evolution during biodegradation of $*C_{16}E_3$ α-alkyl carbon in EBW. Initial concentrations of LAE were 68 μg/L (●), 6.6 μg/L (▲), and 0.85 μg/L (■).

The models are not equivalent. For enzymatic activity, R_{max}/K_m has the dimension of time^{-1} and is analogous to a first-order rate constant, implying that R is proportional to S. For microbial growth, R_{max}/K_m has the dimensions of concentration^{-1} × time^{-1}, analogous to a second-order rate constant. (It is the rate of change of the rate of growth that is proportional to substrate concentration.) These models imply that in the presence of sufficient enzymatic activity the rate of biodegradation should be first order with respect to substrate concentration at concentrations below those supporting microbial growth and mixed order at concentrations that support microbial growth (and a net increase in enzymatic activity). They further imply that when $S \gg K_m$ for growth ($R \approx R_{max}$), the biodegradation rate is constant (zero order). Examples of first-order (exponential), mixed-order (sigmoidal), and zero-order (linear) kinetics are given in the present study. Where first-order kinetics were observed, the data were analyzed by nonlinear regression to an exponential model (*14*). Values in Table I were derived from this analysis. No attempt was made to fit obviously nonexponential data to a model or to differentiate linear from sigmoidal biodegradation curves.

Results and Discussion

Glucose Mineralization. In preliminary experiments with [U-^{14}C]glucose (Amersham) designed to measure the microbioal activity in EBW, we found that first-order (i.e., exponential) kinetics for loss of [^{14}C]glucose from solution occurred at initial concentrations ranging from 1 to 100 μg/L (Figure 1). At concentrations 1 mg/L and above, degradation kinetics were linear (i.e., zero order with respect to substrate). This activity is low compared to laboratory media inoculated with wastewater-treatment-plant bacteria or river water, where glucose degradation is exponential at 20 mg/L (*14*). Furthermore, the lack of any increase in biodegradation rates over the course of the experiment indicates that growth was not carbon limited. It was important, therefore, to measure biodegradation at concentrations well below the saturation level for LAE- or LAES-degrading activity in EBW in order to predict the half-life of these compounds in the estuarine environment.

LAE Mineralization. Rapid mineralization of the α-alkyl carbon of $*C_{16}E_3$ LAE occurred in Escambia Bay water (EBW) (Figure 2). The kinetics of $^{14}CO_2$ evolution were first order with respect to concentration. There were no significant differences among the rate constants for biodegradation at the initial concentrations tested (Table I). Based on the average rate constant for these three experiments, the half-life for ultimate biodegradation of the alkyl-chain carbon in EBW was 2.3 days.

The kinetics of ethoxylate-chain mineralization were more complex (Figure 3). At an initial concentration of 420 ng/L, $^{14}CO_2$ evolution with time was exponential (first order). However, at 3.9 μg/L the rate of mineralization increased with time until 30% of the theoretical $^{14}CO_2$ had been recovered and then decreased through the 30th day of the experiment. When the initial concentration was 31.2 μg/L, biodegradation was linear through day 30. These results indicate first that the available enzymatic activity is approaching saturation at 3.9 μg/L. Second, the increasing rate of degradation indicates an initial increase

Table I. Rate and Extent of Mineralization of LAE and LAES

compd (label position)	concn, nM	concn, ppb	rate constant, $days^{-1}$ + 1 sd	asymptote, % TCO_2
$*C_{16}E_3$ (C_1-alkyl)	182	68	0.22 ± 0.07	86.3
$*C_{16}E_3$ (C_1-alkyl)	17.5	6.6	0.34 ± 0.12	87.2
$*C_{16}E_3$ (C_1-alkyl)	2.3	0.850	0.33 ± 0.11	79.3
$C_{12}*E_9$ (U-ethoxylate)	53	31.2	linear[a]	
$C_{12}*E_9$ (U-ethoxylate)	6.7	3.9	linear	
$C_{12}*E_9$ (U-ethoxylate)	0.79	0.420	0.12 ± 0.03	82.4
$*C_{16}E_9S$ (C_1-alkyl)	199	140	0.39 ± 0.04	82.4
$*C_{16}E_9S$ (C_1-alkyl)	19.3	13.6	0.31 ± 0.03	96.7
$*C_{16}E_9S$ (C_1-alkyl)	2.0	1.43	0.32 ± 0.04	92.4
$C_{16}*E_3S$ (U-ethoxylate)	266	113	linear	
$C_{16}*E_3S$ (U-ethoxylate)	25.9	10.9	linear	
$C_{16}*E_3S$ (U-ethoxylate)	3.20	1.21	0.10 ± 0.02	74.5

[a] Rate constants were not evaluated for nonexponential curves. "Linear" is meant to include those curves that may in fact be sigmoidal.

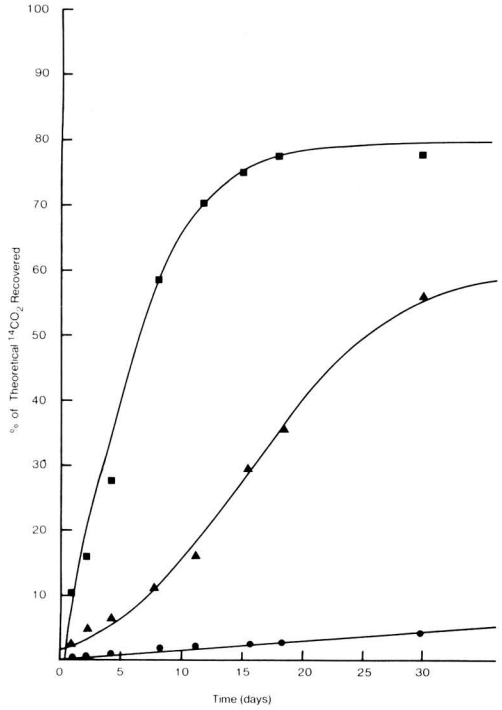

Figure 3. Kinetics of CO_2 evolution during biodegradation of $C_{12}*E_9$ ethoxylate carbon in EBW. Initial concentrations of LAE were 31.2 μg/L (●), 3.9 μg/L (▲), and 0.42 μg/L (■).

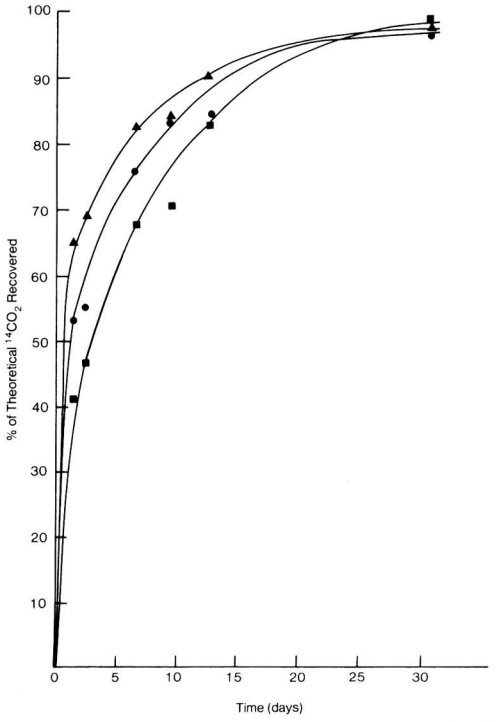

Figure 4. Kinetics of CO_2 evolution during biodegradation of $*C_{16}E_9S$ α-alkyl carbon in EBW. Initial concentrations of LAES were 140 μg/L (●), 13.6 μg/L (▲), and 1.43 μg/L (■).

in the enzymatic activity through growth or induction. Finally, the capacity to increase this activity is limited, as degradation at 31.2 μg/L is close to zero order. The rate of biodegradation in estuaries is known to be limited by the low concentration of available nitrogen (*15*). Based on the first-order rate constant for biodegradation at an environmentally relevant concentration (420 ng/L), the half-life for LAE ethoxylate carbon in EBW was 5.8 days.

Recovery of $^{14}CO_2$ from both the ethoxylate-labeled and the α-alkyl-labeled LAE was extensive (≈80% theoretical $^{14}CO_2$). Little carbon from these compounds was assimilated, therefore, by the microorganisms responsible for biodegradation of either moiety. This low ratio of assi-*milative to respiratory catabolism of LAE has been shown to occur in fresh water as well (12). Apparently the minimal energy requirement for cell maintenance is higher relative to the total energy available from sources at trace concentrations than from those in typical bacterial media. This was true for glucose in our preliminary experiments as well.*

The high rate of α-alkyl mineralization compared to ethoxylate chain mineralization supports the theory that hydrolysis of the ether linkage occurs prior to further degradation (*16*). That the pathways for biodegradation of these chains diverge after they are cleaved is further indicated by the lower concentration of LAE needed to

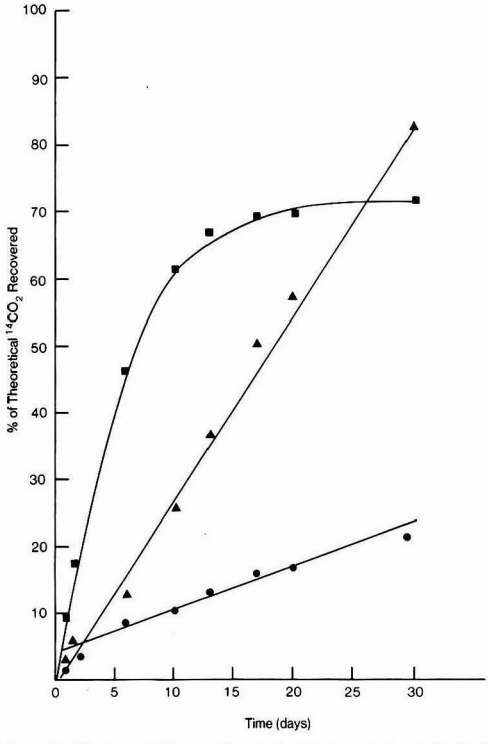

Figure 5. Kinetics of CO_2 evolution during biodegradation of C_{16}*E_9S ethoxylate carbon in EBW. Initial concentration of LAES were 113 μg/L (●), 10.9 μg/L (▲), and 1.21 μg/L (■).

saturate the ethoxylate-degrading activity than the alkyl-degrading activity.

Effect of OSO_3^-. The presence of sulfate had virtually no effect on the rate of extent of mineralization of the alkyl or ethoxylate chains of LAES. The rate of $^{14}CO_2$ evolution from *$C_{16}E_9S$ LAES was proportional to concentration over an inital concentration of 1.43–140 μg/L (Figure 4). The half-life for α-alkyl carbon in EBW was 2.1 days based on the average rate constant in these three experiments. Mineralization at the ethoxylate chain from C_{16}*E_9S LAES is remarkably similar to that of the ethoxylate chain from C_{12}*E_9 LAE (Figures 2 and 5). There is no significant difference in the rate constants for mineralization of these compounds at the lowest concentration tested, and ethoxylate-degrading activity was saturated at comparable concentrations. Thus, neither chain length (within the limits studied here) nor the presence of OSO_3^- affected the mineralization of ethoxylate chains in EBW.

It is not surprising that the alkyl chains from LAE and LAES degrade at the same rate, particularly if hydrolysis at the ether linkage of these compounds is the first step of the degradative pathway. However, the similarity in biodegradation of ethoxylate chains from LAE and LAES indicates either that the sulfate group is removed first or that the sulfate group simply does not affect the mechanism of ethoxylate chain degradation. The former explanation is most likely in view of the published mechanism of poly(ethylene glycol) degradation, which shows that both ends of this compound are degraded at the same time (*17*). If the sulfate group was not removed prior to degradation, one would expect ethoxylate chains from LAE to be mineralized at a somewhat higher rate than those from LAES.

Conclusion

Alkyl- and ethoxylate-chain carbon of LAE is rapidly and extensively mineralized at trace concentrations in estuarine water. The sulfate moiety of LAES has no effect on the mineralization of either alkyl or ethoxylate carbon. The relatively higher mineralization rate of α-alkyl carbon is consistent with hydrolysis of the ether linkage between alkyl and ethoxylate chains prior to mineralization of either chain. The rate of mineralization of LAE or LAES at concentrations below saturation for biodegradation activity and microbial growth is first order with respect to concentration. There is no evidence for a concentration threshold below which these compounds will not degrade, at initial concentrations as low as 7.9×10^{-10} M.

Literature Cited

(1) Schoberl, P.; Mann, H. *Arch. Fisch. Wiss.* **1976**, *29*, 149–158.
(2) Strum, R. N. *J. Am. Oil Chem. Soc.* **1973**, *50*, 154–167.
(3) Larson, R. J. *App. Environ. Microbiol.* **1979**, *38*, 1153–1161.
(4) Tobin, R. S.; Onuska, F. I.; Brownlee, B. G.; Anthony, D. H. J.; Comba, M. E. *Water Res.* **1976**, *10*, 529.
(5) Tobin, R. S.; Onuska, F. I.; Anthony, D. H. J.; Comba, M. E. *Ambio* **1976**, *5*, 30.
(6) Itoh, S.; Setsuda, S.; Utsunomiya, A.; Naito, S. *Yukagaku* **1979**, *29*, 199–204.
(7) Muira, K.; Yamanaka, K.; Sangai, T.; Yoshimura, K.; Hayashi, N. *Yukagu* **1979**, *28*, 351–355.
(8) Maki, A. W. *Proc. 14, Int. Marine Biol. Symp.*, in press.
(9) Boethling, R. S.; Alexander, M. *Environ. Sci. Technol.* **1979**, *13*, 989–991.
(10) Alexander, M. *ASM News* **1980**, *49*, 35–38.
(11) Michaelis, L.; Menten, M. L. *Biochem. Z.* **1913**, *49*, 333–369.
(12) Larson, R. J.; Games, L. M. *Environ. Sci. Technol.* **1981**, *15*, 1488–1492.
(13) Monod, J. *Ann. Rev. Microbiol.* **1949**, *3*, 371–394.
(14) Larson, R. J. *App. Environ. Microbiol.* **1979**, *38*, 1153–1161.
(15) Atlas, R. M.; Bartha, R. *Biotech. Bioeng.* **1972**, *14*, 309–317.
(16) Patterson, S. J.; Scott, C. C.; Tucker, K. B. E. *J. Am. Oil Chem. Soc.* **1970**, *47*, 37–41.
(17) Kravetz, L. *J. Am. Oil Chem. Soc.* **1981**, *58*, 58A–65A.
(18) Kawai, F.; Kimura, T.; Fukaya, M.; Tani, Y.; Koichi, O.; Ueno, T.; Fukami, T. *Appl. Environ. Microbiol.* **1978**, *35*, 679–684.

Received for review October 6, 1981. Accepted March 30, 1982.

Environ. Sci. Technol. 1982, 16, 437–439

NOTES

Characterization of Plutonium in Ground Water near the Idaho Chemical Processing Plant

Jess M. Cleveland* and Terry F. Rees

U.S. Geological Survey, MS 412, Lakewood, Colorado 80225

■ Plutonium is present in very low concentrations in ground water near the disposal well at the Idaho Chemical Processing Plant but was not detected in waters at greater distances. Because of the absence of strong complexing agents, the plutonium is present as an uncomplexed (perhaps hydrolyzed) tetravalent species, which is readily precipitated or sorbed by basalt or sediments along the ground-water flow path.

The mobility of plutonium in ground water is largely influenced by its chemical and physical form—oxidation state, charge, presence or absence of complexes, hydrolytic species, and colloids—which in turn depend on the chemistry of the ground water. In an effort to relate plutonium speciation to ground-water composition, we have sampled and analyzed plutonium-containing waters in and around several low-level radioactive-waste-disposal sites in the U.S. An earlier report (*1*) describes our results from a study of trench leachates from the Maxey Flats radioactive-waste-disposal site in Kentucky. In this report we present data obtained from ground water in the vicinity of a low-level waste-disposal well at the Chemical Processing Plant of the Idaho National Engineering Laboratory. This plant has been in operation since 1952 and is used almost entirely to process highly enriched uranium fuels. It is on the Snake River plain, approximately 80 km west of Idaho Falls, ID, in an area underlain principally by basaltic lava flows to a depth of 600–700 m (*2*), and receives 250–300 mm of annual precipitation. The site thus contrasts markedly with Maxey Flats in terms of geology, hydrology, and climate.

High-level liquid waste from the Chemical Processing Plant is converted to solid in an evaporator and stored as granules. Condensate from the evaporator, containing measurable amounts of radioactivity, is diluted with a large excess of other waste streams such as cooling water and ion-exchange regenerating solutions and discharged into the ground through a disposal well at depths ranging from 135 to 180 m. So that ground-water quality could be monitored, a series of wells has been drilled to similar depths. Selected for sampling in this study were four wells at varying distances from the disposal well, whose ground-water compositions were known to be especially sensitive to waste discharges. A map of the area is shown in Figure 1, with the sampled wells indicated by number. For indication of the direction of ground-water flow, isopleths of sodium concentration as reported by Barraclough and Jensen (*3*) are superimposed on this map.

Selected solute concentrations in waters from the four wells are shown in Table I. Because there is considerable nitrate in the discharged waste, it is not surprising that this anion is present in relatively high concentrations in the ground water, particularly that from well 40, the closest to the disposal well. Dissolved organic carbon contents are low because organic species are destroyed in the evaporation process, suggesting the absence of strong organic complexing agents. This conclusion was confirmed by analyses indicating the absence of detectable (25 μg/L) concentrations of ethylenediaminetetraacetic acid (EDTA), the compound shown to be largely responsible for plutonium mobilization in Maxey Flats waters (*1*).

Table I. Ground-Water Solute Concentrations (mg/L)

well	DOC[a]	NO_3	SO_4	alkalinity (as $CaCO_3$)
40	3.9	102	58	150
43	5.0	53	33	112
67	5.5	66	41	132
37	7.6	36	35	135

[a] DOC = Dissolved organic carbon.

Solute concentrations in both the waste solution and the ground waters vary with time, thus making it difficult to obtain an exact dilution factor. However, on the basis of data presented in ref 2, it is estimated that waste solution has been diluted through hydrodynamic dispersion by a factor of approximately 2 when it reaches well 40.

Experimental Section

Sampling and analysis procedures were the same as those employed at Maxey Flats (*1*). Water from each well was filtered sequentially through 5-, 0.4-, and 0.05-μm Nuclepore (the use of brand names in this report is for information purposes only and does not imply endorsement by the U.S. Geological Survey) membrane filters, with samples taken of the unfiltered water and each of the filtrates. The samples were collected in bottles containing enough HNO_3 to render the final volume 1 M in HNO_3. In addition, unacidified samples of the 0.05-μm filtrates were collected under argon in Teflon bottles for oxidation-state analyses. Two separate sampling runs, using clean equipment, were made on each well except well 40, which was sampled three times. Analysis for plutonium, described in detail elsewhere (*4*), consisted of anion-exchange separation of plutonium from 8 M HNO_3 followed by electrodeposition and counting on an α spectrometer. Three replicate 300-mL samples of each fraction were analyzed.

Within a matter of minutes after collection, separate 100-mL samples of the unacidified 0.05-μm filtrates were subjected, in an inert atmosphere, to a series of carrier-precipitation and solvent-extraction procedures (*5*) to determine the oxidation-state distribution of the plutonium. After separation, the extracted phases were heated to evaporate the organic solvent, and the residue was dissolved in HNO_3 and analyzed by the usual anion-ex-

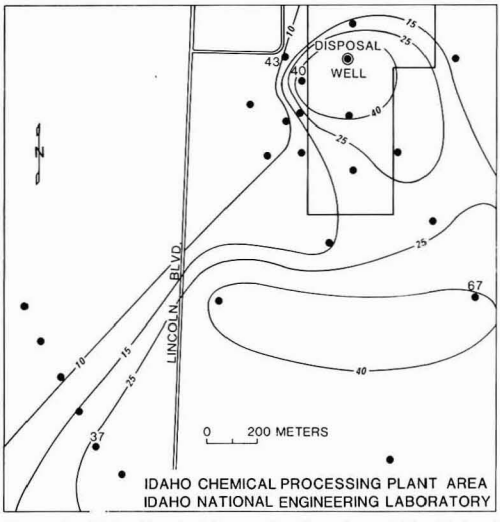

Figure 1. Idaho Chemical Processing Plant Area, Idaho National Engineering Laboratory: closed circles identify locations of monitoring wells; those that are numbered refer to wells sampled in this study. Isopleths indicate ground-water sodium concentrations (mg/L) resulting from waste discharges into the disposal well.

Table II. ^{238}Pu Concentrations[a] in Ground Water

well	^{238}Pu concn, fCi/L unfiltered	0.05-μm filtrate
40	78 (10)	59 (13)
	55 (10)	35 (3)
	64 (17)	54 (20)
43	14 (2)	<10
	12 (4)	<10
67	<10	<10
	12 (2)	12 (1)
37	<10	<10
	<10	11 (2)

[a] Values in parentheses are standard deviations.

change procedure. The carrier precipitates were dissolved in HNO_3 and analyzed in the same manner.

Results and Discussion

Sequential filtration results are shown in Table II, where each value is the average of three replicates. (The plutonium concentrations are for ^{238}Pu; ^{239}Pu, because of its lower specific activity, was not detectable. Consequently, this discussion refers to ^{238}Pu, although all plutonium isotopes should exhibit similar behavior.) More than 75% of the plutonium in well 40 water is in true solution or present in fine colloidal particles smaller than 0.05 μm. Because of the small differences in values for the unfiltered water of the 0.05-μm filtrate, we deemed it unnecessary to analyze the intermediate filtrates.

The plutonium concentrations in all the well waters were very low, being statistically above our detection limit of 10 fCi/L only in well 40. It is instructive to compare the plutonium concentration in well 40 water to that in the waste liquid discharged into the disposal well. Careful records are kept of the amount of radionuclides discharged, and each month a weighted average concentration of each radionuclide in the waste is computed for the total volume of waste discharged for that month. The composite concentrations of ^{238}Pu were 1790, 810, and 510 fCi/L for the month during which we sampled, and 1 and 2 months preceding, respectively, giving an average of 1037 fCi/L. (Since ground-water velocities in the area are several m/day (*6*), only waste discharged during these 3 months would be expected to influence our well 40 water samples). Comparison of this average concentration with that for well 40 as shown in Table II indicates that the diminution of plutonium concentration between the disposal well and well 40 is by a factor of approximately 16. Because this is considerably greater than the expected dilution factor of 2, we conclude that, in the absence of strong organic complexes, the majority (>80%) of the plutonium has been removed by precipitation or sorption along the ground-water flow path.

Table III. Oxidation-State Results of Well 40 (0.05-μm Filtrate)[a]

separation	Pu separated, fCi/L
thenoyltrifluoroacetone (TTA) extraction [Pu(IV)]	44 (7)
methyl isobutyl ketone (hexone) extraction [Pu(IV), (VI)]	54 (8)
$Zr(IO_3)_4$ precipitation [Pu(III), (IV)]	55 (13)
PrF_3 precipitation [Pu(III), (IV)]	59 (23)
PrF_3 (after reduction) [Pu(III), (IV), (V), (VI)]	57 (16)
$NaUO_2(C_2H_3O_2)_3$ precipitation [Pu(VI)]	not detected

[a] Species separated are indicated in brackets.

Oxidation-state analyses of well 40 water are shown in Table III, in which each value is the average of three samples, one from each of the three samplings. Comparison of these results with the average value for the 0.05-μm filtrate from well 40 (49 fCi/L) from Table II indicates that essentially all the plutonium was present in tetravalent form. (Results in Table III are actually higher than 49 fCi/L, but do not differ statistically from this value). However, because of the relatively high uncertainties—resulting from low activity levels—the presence of a minor fraction of plutonium(III) or -(VI) or colloidal species cannot be totally excluded.

In summary, these results indicate that concentrations of plutonium in the well waters were low, primarily because of the absence of organic complexing agents to stabilize it against precipitation or sorption. In the one well water in which plutonium was present at a detectable concentration, it existed as the uncomplexed (perhaps hydrolyzed) tetravalent ion. The Idaho well waters are in marked contrast to the Maxey Flats trench leachates, where the presence of strong organic complexes has resulted in relatively high concentrations of plutonium that is resistant to removal by sorption and precipitation processes. In the Maxey Flats paper (*1*) the ability of strong complexes to solubilize plutonium was stressed; results of the present study reinforce that conclusion. Hence the need for isolating plutonium-containing wastes from dissolved organic species in ground water is further emphasized.

Acknowledgments

We thank R. G. Jensen, J. T. Barraclough, T. J. Bodnar, B. D. Lewis, G. R. Chapman, and J. C. Bagby of the U.S. Geological Survey Idaho Falls Project Office for invaluable aid in collecting and processing samples and Dr. J. L. Means of Battelle Columbus Laboratories for the EDTA analyses. The nonradioactive solute analyses were performed by the U.S. Geological Survey's National Water

Quality Laboratory in Denver.

Literature Cited

(1) Cleveland, J. M.; Rees, T. F. *Science (Washington, D.C.)* **1981**, *212*, 1506.
(2) Robertson, J. B.; Schoen, R.; Barraclough, J. T. "The Influence of Liquid Waste Disposal on the Geochemistry of Water at the National Reactor Testing Station, Idaho, 1952-70"; U.S. Geological Survey Open-File Report published by U.S. Department of Energy as IDO-22053, February 1974.
(3) Barraclough, J. T.; Jensen, R. G. "Hydrologic Data for the Idaho National Engineering Laboratory Site, Idaho, 1971 to 1973", U.S. Geological Survey Open-File Report published by U.S. Department of Energy as IDO-22055, January 1976.
(4) Rees, T. F. In Lyon, W. S., Ed. "Radioelement Analysis Progress and Problems"; Ann Arbor Science: Ann Arbor, MI, 1980; pp 199–206.
(5) Bondietti, E. A.; Reynolds, S. A. In Ames, L. L., Ed. "Proceedings of Actinide-Sediments Reactions Working Meeting, Seattle, WA, February 10–11, 1976", Report BNWL-2117, Battelle Northwest Laboratories, Richland, WA; pp 505–530.
(6) Morris, D. A. "Hydrology of Waste Disposal—National Reactor Testing Station, Idaho, Annual Progress Report, 1962", U.S. Geological Survey Open-File Report issued by U.S. Department of Energy as IDO-22044, April 1963.

Received for review September 8, 1981. Accepted February 25, 1982.

CORRESPONDENCE

Comment on "Automobile Traffic and Lung Cancer. An Update on Blumer's Report"

SIR: The article by Polissar and Warren, in spite of extensive use of scientific survey language, did not really demonstrate any proofs for the claimed results, which appears to be in marked contrast to the Blumer study.

To a considerable extent the different findings are attributable to the entirely different character of the survey areas used in the two studies.

Being familiar with the conditions prevailing in both the Seattle and the Swiss locations (the latter happens to be the place where many decades ago I was born), I should like to point out that the study in the Swiss region took place at a location that is singularly suitable to studies of automotive exhausts and its consequencies.

To understand this statement, it is necessary to describe the particular geographical and topographical features of the test area. The Swiss area under study was a stretch of highway in a narrow mountain valley, flanked on both sides by high mountains.

The principal highway at the time of the survey was the only possible automotive communication between towns of that valley. All traffic had to use it. At the time of the survey rows of buildings on both sides of the highway were abutting that artery, with only 50 to 60 feet of space between the front walls of the structures on either side of the highway.

Traffic at all other locations in that area was of strictly local character, with traffic of only a minute percentage of that of the main artery. It was a combination of circumstances that lent itself ideally to the kind of study Dr. Blumer et al. carried out; circumstances that would indeed be difficult to duplicate even in present-day Switzerland and practically impossible in U.S. cities, with their wider traffic arteries, less cluttered and wider spaced residential building patterns, and a much greater choice of routes—instead of the *one* main artery with no alternatives.

Seattle, on the other hand, is entirely different. It is hilly and windy, and buildings generally are widely spaced, providing for no concentration of exhaust gases, with consequent entirely different results. It also does not provide, as the Swiss community did, a sharp contrast between very heavily travelled roads and others with absolutely minimal or no automotive traffic at all.

The small scope of the Swiss survey made it possible to obtain very detailed information on the length of time the various residents were exposed to exhaust gases. The Seattle report does not give that sort of information—at least not in the published excerpts.

Because of the ideal natural configuration, the Swiss study can lay greater claim for demonstrating the differences between heavily travelled and lightly travelled locations, and its findings may indeed be more significant than those of the Seattle study. The Swiss town where Dr. Blumer et al. made their studies almost had the character of a laboratory situation, while Seattle was not favored by nature and traffic pattern with such ideal conditions.

It would appear that the results of the Swiss survey can hardly be dismissed by a mere comparison with the results of the Seattle study.

A detailed analysis of the basic conditions under which the Blumer study was made might easily explain the drastic difference between the findings at the two survey locations.

Alphonse A. Kubly

777 Beach Road
Sarasota, Florida 33581

SIR: Thank your for the opportunity to respond to Alphonse Kubly's letter concerning our study (*1*), which was an investigation of the findings of Blumer et al. (*2*, *3*). We would like to discuss Kubly's main points in turn.

First, we take Kubly's comment on our use of "scientific survey language" as his concern that Blumer's findings might be disregarded or discredited due to our study. Such should not be the case. When we read Blumer's first paper (*2*) in translation, we felt that it was an excellent scientific study. We feel that our finding of an excess (but nonsignificant) risk for females partially supports Blumer's results. The extent of reported risk is certainly different in the two studies, and it would be worthwhile finding out why this is so.

0013-936X/82/0916-0439$01.25/0

Kubly suggests that a radical difference between the physical settings in Switzerland and Seattle accounts for the difference in findings. In our original paper we also pointed out that the two locations may have dissimilar rates of automobile exhaust dilution. Kubly has amplified on the character of the Swiss town in his letter, and it is possible, as he suggests, that the Swiss results are due to an extreme type of setting. What is missing from both of the studies is an accurate measurement of exposure to automobile exhaust or fractions of it in the vicinity of the study subjects. Both studies used average daily traffic (ADT) as a surrogate for exposure. We would agree with Kubly that there is almost surely less exhaust dilution in the Swiss town than in Seattle.

Another of Kubly's points is that Seattle does not provide a sharp contrast between heavily travelled and less travelled roads. It is probably true that Seattle does not have many streets as quiet as some of those in the Swiss town. However, there was a wider range of exposures to traffic found among our study subjects than in the Swiss town. 74% of our 1330 subjects lived on streets with less than 2000 ADT, 16% lived on streets with 2000–15000 ADT, and 9% lived on streets with over 15000 ADT. The busy Swiss road carried 5000–6000 ADT, and the outer quarter of the town had, presumably, close to zero traffic.

Kubly notes that Blumer was able to obtain very detailed information on the length of residence of the Swiss subjects. Indeed, our use of current residence to imply past exposure is a less powerful and less certain approach than use of length-of-residence data, which was available to Blumer. In our study only residence at diagnosis was available to us. We pointed out our lack of migration data and the potential importance of such data. If our subjects had been highly migratory, which is a possibility, then the imputed exposures could be in error. We have commented at length on the migration problem in environmental studies in another publication (*4*).

A point not discussed by Kubly is that excessive cancer deaths occurred for *all* sites combined in the Swiss study. The 75 cancer deaths along the busy road involved breast, uterus, ovaries, intestines, prostate, and other sites. It is unusual that an environmental insult has that general an effect. Would not the auto exhaust be expected to mimic the effects of smoking? Of the 75 cancer deaths along the busy road, only 11 were of the respiratory type. Is it possible that another mechanism—possibly stress—might play a role in the Swiss town? From Kubly's description, the main road is an unpleasant place to live, and an unusual set of risk factors might be operating.

By this time, the Swiss town has experienced an additional 11 years (1971–1981) of mortality that could be compared to the 12 years (1959–1970) reported on earlier. A replication study with very specific information on a variety of risk factors could possibly be carried out at this time. Other locations in the world may also have ideal settings for studying the effects of concentrated automobile exhaust.

We thank A. A. Kubly and the editor for bringing some important points to our attention and providing us with the opportunity to comment on them.

Literature Cited

(1) Polissar, L.; Warner, H., Jr. *Environ. Sci. Technol.* **1981**, *15*, 713–714.
(2) Blumer, W.; Jauman, T.; Reich, T. Schweiz. *Rundsch. Med. (Praxis)* **1972**, *61*, 514–518.
(3) Blumer, M.; Blumer, W.; Reich, T. *Environ. Sci. Technol.* **1977**, *11*, 1082–1084.
(4) Polissar, L. *Am. J. Epidemiol.* **1980**, *111*, 175–182.

Lincoln Polissar*
Fred Hutchinson Cancer Research Center
Program in Epidemiology and Biostatistics
Seattle, Washington 98104

Homer Warner, Jr.
1841 East 900 South
Salt Lake City, Utah 84108

Comment on "Nature of Bonding between Metallic Ions and Algal Cell Walls"

SIR: The article by Crist and co-workers on the "Nature of Bonding between Metallic Ions and Algal Cell Walls" (*Environ. Sci. Technol.* **1981**, *15*, 1212) raises some questions that we would like to address at this time.

1. The authors mention that the ZPC of algal cells is approximately at pH 3 (*1*). This is consistent with our observations of *Chlorella*. Electrophoretic mobility (EM) values decrease from pH 3 to pH 5. No further decrease is observed in EM with increases in pH to pH 9. Christ et al. observed significant proton dissociation at high pH values (Figure 1). This might suggest a higher ZPC than observed by other investigators.

2. The authors suggest that the response of intact cells and fragmented cells to cationic additions is similar. This is in contrast to our work. We have observed profound differences between active and inactive cells. Hydroxide titration curves (Figures 1 and 3) appear to exhibit a different response for intact and fragmented cells. Fragmented cells (Figure 3) have a low pH buffering capacity at pH 4 and a high buffering at pH 7, while intact cells (Figure 1) have a high buffering capacity at pH and a minimum buffering capacity at pH 7. These figures seem to contradict the authors contention that the ionic equilibria of intact and lysed cells is similar.

3. Our studies suggest that cell age and equilibration time are important when quantifying cationic adsorption/uptake by algal cells. Other studies have also reported similar results (*2–4*). The authors make no mention of equilibration times over which their cells were incubated.

4. Finally, we object to eq 2.

$$Na^+ + (ZnA) = (NaA) + Zn^{2+} \qquad (2)$$

An electroneutrality balance is a prerequisite to all aqueous transformations. We are at a loss to understand why it is not valid here.

Literature Cited

(1) Stumm, W.; Morgan, J. J. "Aquatic Chemistry"; Wiley-Interscience: New York, 1970; p 455.
(2) Hassett, J. M.; Jennett, J. C.; Smith, J. E. *Appl. Environ. Microbiol.* **1981**, *41*, 1097–1106.
(3) Fujita, M; Hashizumie, K. *Water Res.* **1975**, *9*, 889–894.
(4) Button, K. S. Hostetter, H. P. *J. Phycol.* **1977**, *13*, 198–202.

William D. Schecher, James M. Hassett
Charles T. Driscoll*
Department of Civil Engineering
Syracuse University
Syracuse, New York 13210

0013-936X/82/0916-0440$01.25/0

SIR: We are pleased to have the opportunity of responding to the questions raised by Schecher et al. concerning the article on the "Nature of the Bonding between Metallic Ions and Algal Cell Walls" (*1*).

1. We welcome their observations on the ZPC of *Chlorella*. Recent work here with the ΔpH effect on addition of $NaNO_3$ (2) using the alga *Tribonema* indicates a ZPC around pH 3.5.

The data on *Vancheria* shown in Figure 1 represent an early attempt to show reversibility in the pH titration that would indicate a degree of structural integrity during the process. The figure demonstrates this point. The data were not corrected, however, for a water blank; this would bring Figure 1 more in line with Figure 3.

2. The use of fragmented cells raises the question of applicability to cells that are intact but nonfunctional due to the experimental environment as well as to those that are fully viable. The technique was developed because early work was not sufficiently reproducible to establish physical–chemical relationships. Data on fragmented cells were more reproducible and at the same time were comparable to those obtained with intact cells. This is supported by present results. (Cell Wall Fragments vs. Intact Cells, p 1213 (*1*)).

Recently, *Tribonema* fragment preparations have been used for pH titration studies. This alga has a considerably smaller cross section than *Vaucheria*, and though the fibers are broken up by the Thomas tissue grinder the cells appear quite intact. Results here are in line with those reported for the *Vaucheria* fragments. Also with a water blank correction as noted above, Figure 1 would be more like the corresponding curve of Figure 3, suggesting comparable buffering capacities.

3. The adsorption of metallic ions was relatively fast, being complete in 5–10 min, with a half hour generally allowed for equilibration. Since the pH decreases on adsorption, periodic adjustment to a stated pH gave a good indication of completeness of reaction.

4. The stochiometry of eq 2 represents the apparent first-power dependence that was obtained for both sodium and zinc. As for electroneutrality we have at present no basis for specifying species that would represent this, though obvious suggestions could be

$$Na^+ + (ZnA) = (NaA^-) + Zn^{2+}$$

or

$$Na^+ + H^+ + ZnA = (NaHA) + Zn^{2+}$$

where for the latter a pH change is indicated.

The data for *Tribonema* are from work in this laboratory by Joanna Lehman.

Literature Cited

(1) Crist, Ray H.; Oberholser, Karl; Shank, Norman; Nguyen, Ming *Environ. Sci. Technol.* **1981**, *15*, 1212.
(2) Davis, James A.; Leckie, James O. *J. Colloid Interface Sci.* **1978**, *67*, 90.

Ray H. Crist,* Karl Oberholser
Norman Shank, Ming Nguyen

Department of Natural Science
Messiah College
Grantham, Pennsylvania 17027

0013-936X/82/0916-0441$01.25/0

The Reaction is Purely Chemical

Subscribe to these outstanding AMERICAN CHEMICAL SOCIETY publications. Choose from 23 different titles.

ACS publications are designed for you. They're timely, authoritative, comprehensive. They give you the latest in research, news, and commentary — everything you need to know to keep you on top of every aspect of your professional life.

- Analytical Chemistry
- Chemical & Engineering News
- CHEMTECH
- Environmental Science & Technology
- SciQuest
- Accounts of Chemical Research
- Biochemistry
- Chemical Reviews
- Industrial & Engineering Chemistry — Process Design and Development
- Industrial & Engineering Chemistry — Product R&D
- Industrial & Engineering Chemistry — Fundamentals

CALL TOLL FREE 800-424-6747
Cable Address: JIECHEM
Telex: 440159 ACSP UI or 892582 ACSPUBS

AMERICAN CHEMICAL SOCIETY PUBLICATIONS
1155 Sixteenth Street, N.W.
Washington, D.C. 20036 U.S.A.

- Inorganic Chemistry
- Journal of Agricultural & Food Chemistry
- Journal of the American Chemical Society
- Journal of Chemical & Engineering Data
- Journal of Chemical Information and Computer Sciences
- Macromolecules
- Journal of Medicinal Chemistry
- The Journal of Organic Chemistry
- The Journal of Physical Chemistry
- ACS Single Article Announcement
- Journal of Physical and Chemical Reference Data
- plus the all new *Organometallics*

Trying to Track Down a Chemistry Professor?

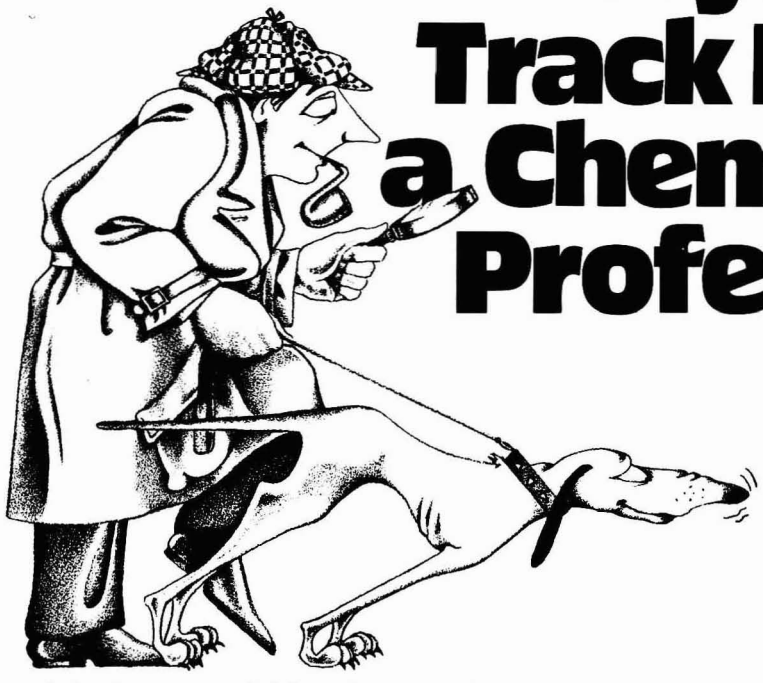

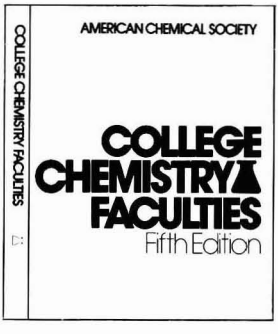

With the new fifth edition of COLLEGE CHEMISTRY FACULTIES you can be hot on the trail of any of the 17,000 faculty members in the chemical sciences in the U.S., Canada, and Mexico.

Have you heard about some interesting research that you'd like to learn more about, but don't know how to locate the researcher?

Do you have trouble reaching that special segment of the academic community that needs your products and services?

When the trail is cold and clues are hard to find, the solution is in the American Chemical Society's fifth edition of **College Chemistry Faculties.**

This thorough, up-to-date directory of college chemistry faculties is conveniently organized to quickly provide the information you need to find:

- Major field(s) of teaching for each faculty member: analytical, biochemistry, chemical engineering, inorganic, organic, physical, or polymer
- Faculty listed by college or university so you know at a glance who's who in any chemistry, biochemistry, chemical engineering, or medicinal chemistry department, including the present chair
- Alphabetical index of the 17,000 faculty members and their current affiliation
- Departmental telephone numbers and addresses to help make contacting professors easy
- Name, academic rank, and highest degree for all faculty members

Since institutions are listed by state, it's easy to see who's nearby when planning meetings or looking for a consultant. For marketers, it's ideal for planning sales and service territories.

Listings of over 17,000 chemistry, biochemistry, chemical engineering, and medicinal chemistry teachers at 2,000 two-year colleges, four-year colleges, and universities

College Chemistry Faculties, published by the American Chemical Society, is one of the major reference sources in the academic chemical world. If you move around in that world or want to contact people who do, you shouldn't be without it.

American Chemical Society Department 3D 1155 Sixteenth Street, N.W. Washington, D.C. 20036

Please send _____ **copies of COLLEGE CHEMISTRY FACULTIES @ $25.00.**

☐ Payment enclosed (payable to American Chemical Society)

☐ Bill me ☐ Bill company (add $1.50 billing costs) Charge my ☐ Master Card ☐ Visa

Card # _____ Interbank # _____ (Master Card Only)

Exp. Date _____ Signature _____

Name _____

Company _____

Address _____

Billing Address _____

City _____ **State** _____ **Zip** _____

Or ORDER BY CALLING TOLL FREE: (800) 424-6747

Find, identify, measure, count, record, and analyze pollutants with Zeiss

For all microscope techniques illustrated below and for many others used in pollution analysis, Zeiss has the instrument you need.

Fully automatic camera microscope Photomicroscope III with automatic flash and data recording system for 35mm photomicrography. **Circle #70**

Inverted camera microscope ICM 405. Fully automatic, inverted camera microscope for transmitted and reflected light with integrated 35mm and 4x5" cameras. Ultra-stable. **Circle #71**

Standard, WL, and Universal microscopes. For routine and research applications. Automatic attachment camera MC 63 takes 35mm or 4x5" film, provides highly resolved, exceptionally bright images. 137 Zeiss objectives. **Circle #72**

Stereo and dissecting microscopes. High resolution, flat field, long working distances. **Circle #73**

Specimen-saving transmission electron microscope EM-109. High-performance TEM (3.44Å.) Instantly ready for use. Outside-the-vacuum camera system. **Circle #74**

Zonax. Unique system for automated particle size analysis directly from the microscopic image. **Circle #75**

Videoplan. Operator-instrument interactive system for image analysis and measurement from the microscopic image or photomicrograph. **Circle #76**

Quality service—Expert dealers.

The great name in optics

ZEISS

West Germany

Carl Zeiss, Inc., One Zeiss Drive, Thornwood, N.Y. 10594 (914) 747-1800. Branches: Atlanta, Boston, Chicago, Houston, Los Angeles, San Francisco, Washington, D.C. In Canada: 45 Valleybrook Drive, Don Mills, Ontario, M3B 2S6. (416) 449-4660.

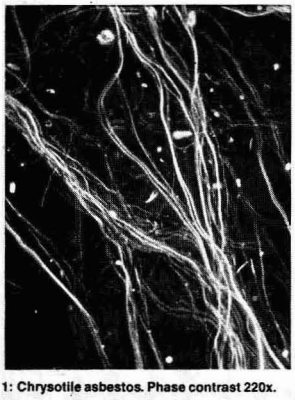

1: Chrysotile asbestos. Phase contrast 220x.

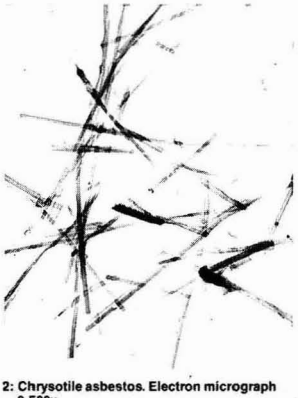

2: Chrysotile asbestos. Electron micrograph 9,500x.

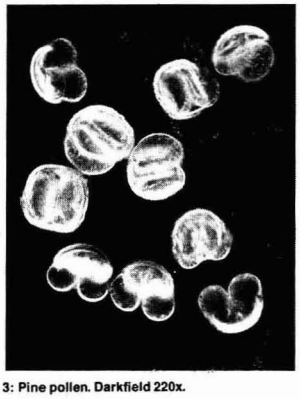

3: Pine pollen. Darkfield 220x.

4: Fly ash. Combination of slightly uncrossed polarizers and reflected light 35x.

5: Fly ash. Nomarski Differential Interference Contrast 620x.

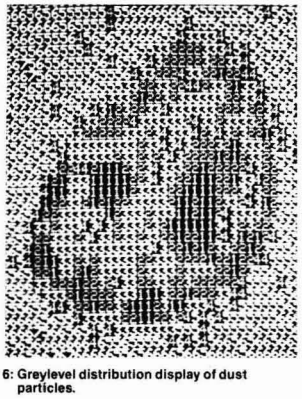

6: Greylevel distribution display of dust particles.

Photos 1, 2, 3 and 4 by John G. Delly, Senior Research Microscopist, McCrone Research Institute.
Photo 5 by Dr. Robert F. Smith, Director of Biomedical Communications, New York State College of Veterinary Medicine, Cornell University.
Photo 6 from Zonax screen.